Institut für Phytopathologie

der Justus-Liebig-Universität Gießen

The Role of RNA-interference in the pathogenesis of *Fusarium graminearum* on *Hordeum vulgare* and the evolutionary adaptation of *Arabidopsis thaliana* to *Hyaloperonospora arabidopsidis* derived small RNAs

INAUGURAL-DISSERTATION

zur Erlangung des Doktorgrades (Dr. rer. nat.)

im Fachbereich Agrarwissenschaften, Ökotrophologie und Umweltmanagement der Justus-Liebig-Universität Gießen

vorgelegt von

Bernhard Timo Werner

aus Herborn

Gießen, 2021

Mit Genehmigung des Fachbereichs Agrarwissenschaften,
Ökotrophologie und Umweltmanagement der
Justus-Liebig-Universität Gießen

Prüfungskommission:

1. Gutachter:	Prof. Karl-Heinz Kogel
2. Gutachter:	Prof. Patrick Schäfer
3. Gutachter:	Prof. Rod Snowdon
Prüfer:	Prof. Stefan Janssen
Prüfer:	Prof. Volker Wissemann
Vorsitzender:	Prof. Marc F. Schetelig

Tag der Disputation: 09.03.2022

Erklärung gemäß der Promotionsordnung des Fachbereichs 09 vom 07. Juli 2004 § 17 (2)

„Ich erkläre: Ich habe die vorgelegte Dissertation selbständig und ohne unerlaubte fremde Hilfe und nur mit den Hilfen angefertigt, die ich in der Dissertation angegeben habe.

Alle Textstellen, die wörtlich oder sinngemäß aus veröffentlichten Schriften entnommen sind, und alle Angaben, die auf mündlichen Auskünften beruhen, sind als solche kenntlich gemacht.

Bei den von mir durchgeführten und in der Dissertation erwähnten Untersuchungen habe ich die Grundsätze guter wissenschaftlicher Praxis, wie sie in der „Satzung der Justus-Liebig-Universität Gießen zur Sicherung guter wissenschaftlicher Praxis“ niedergelegt sind, eingehalten.“

_____

Bernhard Timo Werner

„That surely makes science central to a most interesting project, which is to invent, improve, and put to use an ideology that explains in a coherent and useful way as much of the blooming buzzing inrush of the world as possible. What one would hope for in an ideology is clarity and explanatory breadth, and power."

-Kim Stanley Robinson

Parts of this work already published or under consideration for publication

Werner, B. T., Gaffar, F. Y., Schuemann, J., Biedenkopf, D., & Koch, A. M. (2020). RNA-spray-mediated silencing of Fusarium graminearum AGO and DCL genes improve barley disease resistance. *Frontiers in plant science*, *11*, 476.

Werner, B. T., Koch, A., Šečić, E., Engelhardt, J., Jelonek, L., Steinbrenner, J., & Kogel, K. H. (2021). Fusarium graminearum DICER-like-dependent sRNAs are required for the suppression of host immune genes and full virulence. *Plos one*, *16*(8), e0252365.

Werner, B. T., Kopp-Schneider, A., Kogel, K. H. (2022). The impact on codon-usage emphasizes the biological significance and points to the double-edged nature of cross-kingdom RNAi. (unpublished).

Contents

List of tables

List of figures

Chapter I:

Chapter II:

Abbreviations

3'	nucleotide polymer end with 3rd C unbound
5'	nucleotide polymer end with 5th C unbound
95%-CI	95% confidence interval
A	adenine
AA	amino acid
ABCG	ABC transporter G
ABC	ATP-binding cassette
ACS	Aminocyclopropane-1-carboxylate synthases
AGO	Argonaute
ai	alignment index
ARF	Auxin response transcription factor
amiRNA	artificial microRNA
At / At / *Ath*	*Arabidopsis thaliana*
ATG	Autophagy-related
ATP	adenosine triphosphate
AVE	average
BAK	BRI1-associated receptor kinase
Bc	*Botrytis cinerea*
Bd / Bd / *Bdi*	*Brachypodium distachyon*
BGLU	Beta-D-glucopyranosyl abscisate beta-glucosidase
C	cytosine
CAI	codon adaptation index
cDNA	complementary DNA
CDS	coding sequence
ci	codon index
ck	cross-kingdom
ckRNAi	cross-kingdom RNAi
CME	clathrin-mediated endocytosis
CS	complementarity score
Ct	Cycle threshold
CTR	constitutive triple response

cv.	cultivar
CYP	cytochrome P450 monooxygenase
CYP51	cytochrome P450 lanosterol C-14α-demethylase
DCL	Dicer-like
DEPC	diethyl pyrocarbonate
DKO / dKO	double knockout
DMI	demethylation inhibitor
dpi	days post inoculation
DON	deoxynivalenol
ds	double stranded
dsRNA	double stranded RNA
e.g.	*exempli gratia*
EBF	EIN3-binding F-box
EBI	European Bioinformatics Institute
EDTA	Ethylenediaminetetraacetic acid
Ef-Tu	elongation factor thermo unstable
EF1-α / EF1-a	Elongation factor 1-α
EFR	Ef-Tu receptor
EIN	ET insensitive
emb	Embryo defective
EOL1	ethylene overproducer 1-like 1
ERF	ET response factor
ET	ethylene
EtBr	ethidium bromide
ETI	effector-triggered immunity
ETO	Ethylene overproducer
ETS	effector-triggered susceptibility
EV	extracellular vesicle
EXA	essential for potexvirus accumulation
f.sp.	*Forma specialis*
FDR	false discovery rate
Fg / Fg	*Fusarium graminearum*

Fig.	Figure
FHB	fusarium head blight
FLS	flagellin-sensitive
FOR	Research Unit
G	guanine
GDH	Glycine decarboxylase complex H
GFP	green fluorescent protein
Gg / Gg	*Gorilla gorilla*
Gly	glycine
GO	gene ontology
GO.ID	GO-term identifier
GOI	gene of interest
GP	Golden Promise
GSP	gene specific primer
GYF	glycine-tyrosine-phenylalanine
Ha / Ha / *Hpa*	*Hyaloperonospora arabidopsidis*
HIGS	host-induced gene silencing
Hv / Hv / *Hvu*	*Hordeum vulgare*
IP	immunopurification
IQR	interquartile range
JA	jasmonate
KO	knock-out
MAMP	microbe-associated molecular pattern
MCL	Maximum Composite Likelihood
MED	median
MEGA	Molecular Evolutionary Genetics Analysis
MFE	minimum free energy
MID	middle
miRNA	microRNA
miR***	microRNA ***
milR	microRNA-like RNA
MM	mismatch

mRNA	messenger RNA
msa	multiple sequence alignment
MVB	multivesicular body
MYB	myeloblastosis
MYB-TF	MYB-transcription factor
N_c	effective number of codons
NGS	next-generation sequencing
NLR	nucleotide-binding domain leucine-rich repeat receptor
NIV	nivalenol
nt	nucleotide
OE	overexpression
P	probability
PAZ	PIWI/Argonaute/Zwille
P_{CHS}	probability of complementarity is higher or the same
PCR	polymerase chain reaction
PGLP	Phosphoglycolate phosphatase
pi-miRNA	primary microRNA
Pi	*Phytophthora infestans*
PIWI	P-element-induced whimpy tested
PIX	Putative interactor of XopAC
Pol IV	nuclear RNA polymerase IV
PPR	Pentatricopeptide repeat
PR	pathogenesis-related
PRR	pattern recognition receptor
Pst	*Puccinia striiformis* f.sp. *tritici*
Pt	*Puccinia triticina*
PTGS	post-transcriptional gene silencing
qRT-PCR	quantitative reverse-transcription PCR
RART index	RSCU adaptation in RNAi targeted region
RDR	RNA-dependent RNA polymerase
RdRP	RNA-dependent RNA polymerase
RdDM	RNA-directed DNA methylation

RISC	RNA-induced silencing complex
RLM	RNA-ligase-mediated
RLM-RACE	RNA-ligase-mediated Rapid Amplification of cDNA Ends
RNAi	RNA interference / RNA-silencing
RNase	ribonuclease
ROS	reactive oxygen species
rpm	reads per million
rRNA	ribosomal RNA
RSCU	relative synonymous codon usage
rsRNA	analogous random sRNA
RST	Resurrection
RT	reverse transcription
RTG	Research Training Group
SA	salicylic acid
SD	standard deviation
SE	standard error
SEA	singular enrichment analysis
SERK	somatic embryogenesis receptor kinase
SGS3	suppressor of gene silencing 3
SID	*systemic RNA interference defective*
SIGS	spray-induced gene silencing
SL	stem loop
siRNA / siR	small interfering RNA
SNA	synthetic nutrient poor agar
sRNA	small RNAs (21-24 nt), not bacterial sRNAs (50-500 nt)
ss	single stranded
SUB	Short under blue light
SUVR	Su(var)3–9-related
T	thymine
Tab.	Table
tasiRNA	trans-acting small interfering RNA
TE	Tris-EDTA

TGS	transcriptional gene silencing
TPR	Topless-related
tRF	tRNA-derived fragment
tRNA	transfer RNA
U	uracil
UBQ	ubiquitin
UTR	untranslated region
vs.	versus
vsiRNA	virus-derived small interfering RNA
WSIP	WUSCHEL-interacting protein
wt	wild type

Summary

The outcome of interactions between plant pathogens and hosts are determined by the interplay of the multi-layered plant immune system and pathogen virulence system. These systems are the outcome of the evolutionary accumulation of counteracting innovations on both sides, often described as an ongoing “arms race”.

While plants perceive microbe-associated molecular patterns (MAMPs) via cell surface pattern recognition receptors (PRRs), which leads to the induction of defense mechanisms, pathogens interfere with this process of pattern-triggered immunity (PTI). This interference is mediated by specific proteins, called effectors, that modify, degrade or mask MAMPs, interfering with recognition or directly interfere with PRRs or the downstream signaling cascade. The outcome of this is effector-triggered susceptibility (ETS). Plants, as a response to this, have evolved means to perceive effectors or their activity via nucleotide-binding domain leucine-rich repeat receptors (NLRs), which leads to effector-triggered immunity (ETI).

In 2013 a new class of non-protein pathogen effector molecules, exploiting the plant RNA interference (RNAi) machinery, was discovered. These new effector molecules are small RNAs (sRNAs), which are produced in pathogens by molecules of the dicer-like (DCL) class and are loaded into a protein of the Argonaute (AGO) class in the plant. Here, the sRNA guides AGOs to a target mRNA, based on the complementarity between sRNA and mRNA, which silences the respective gene, leading to ETS. This process which is also utilized by hosts to defend against pathogens, is called cross-kingdom RNAi (ckRNAi).

In this work ckRNAi is investigated in the important plant pathogen *Fusarium graminearum* (Fg) on the host plant barley. As a first step barley plants were treated with long double-stranded RNAs (dsRNAs) to silence the fungal *AGO* and *DCL* genes (Chapter I). This silencing was effective and reduce disease symptoms in barley, showing that Fg*AGO*s and Fg*DCL*s are important for pathogenesis, which can be harnessed via spray-induced gene silencing (SIGS) in crop protection. Different manual and tool-based design approaches of the dsRNA trigger molecules and their silencing efficiency were compared, showing longer manually designed dsRNAs were more efficient in gene silencing and disease alleviation.

With the role of Fg*DCL*s and Fg*AGO*s shown, Fg*DCL* knock-out (KO) mutants were further investigated to show the involvement of ckRNAi in the pathogenesis of Fg (Chapter II). Due to the necessity of DCLs in the production of sRNAs, fungal ckRNAi should be prevented. This was reflected by reduced disease severity on the host plants barley and *Brachypodium distachyon*. Additionally, barley Fg-sRNA target genes were highly expressed during the interaction with KO-mutants. Degradation products of the targets of three fungal tRNA-derived sRNAs were present in plants infected with the wild type fungus, but were lacking in plants infected with DCL-KO mutants. Together, this shows the involvement of ckRNAi in the pathogenesis of Fg.

While the involvement of ckRNAi in the pathogenesis was shown, the biological significance of ckRNAi is debatable, due to the roles of *DCL* genes in the internal gene regulation of Fg. To address this issue, I formed the hypothesis, that target regions of ckRNAi-exerting sRNAs should be subject to an evolutionary pressure, which would alter the codon-usage in these regions (Chapter III). To this end a new bioinformatics workflow was developed to calculate the likelihood of observing the actual complementarity of an sRNA-mRNA interactions, under conservation of amino acid (AA) sequence and following the organisms' codon frequency. The calculation was performed for Fg sRNAs from chapter II, a set of *Hyaloperonospora arabidopsidis* (Ha) sRNAs and Arabidopsis thaliana (At) and Gorilla gorilla (Gg) miRNAs. Ha is another filamentous pathogen utilizing ckRNAi for full pathogenesis and the miRNA-sets served as positive and negative controls respectively.

While negative and positive controls behaved as expected, the results obtained for Fg and Ha sRNAs could show an unlikely high complementarity between pathogen sRNAs and host mRNAs. This observation demonstrated the biological significance of ckRNAi by proving an evolutionary pressure on hosts by ckRNAi-derived sRNAs. Intriguingly, this pressure pushes hosts to enable ckRNAi, while following the effector hypothesis one would expect hosts to prevent ckRNAi. To resolve this apparent contradiction, the hypothesis was formed, that plants utilize ckRNAi to perceive pathogen sRNAs and react accordingly. This resembles the way NLRs and PRRs perceive protein effectors and MAMPs, respectively, leading to Immunity, and would be a yet undescribed and new step in the arms race between pathogen and plant, bearing enormous potential for future applications in the generation of disease resistant crops.

Zusammenfassung

Der Ausgang von Interaktionen zwischen Pflanzenpathogen und Wirt wird durch das vielschichtige Zusammenspiel von pflanzlichem Immunsystem und pathogenem Virulenzsystem bestimmt. Diese Systeme sind das Produkt der beidseitigen evolutionären Akkumulation von gegeneinander arbeitender Neuerungen, oft beschrieben als anhaltendes „Wettrüsten“.

Während Pflanzen mikrobenassoziierte molekulare Muster (MAMPs) mittels zelloberflächlicher Mustererkennungsrezeptoren (PRRs) wahrnehmen, was zur Aktivierung von Abwehrmaßnahmen führt, stören Pathogene diesen Prozess der durch Muster angestoßenen Immunität (PTI). Diese Störung findet mittels speziellen Proteinen, so genannten Effektoren, statt, welche MAMPs modifizieren, degradieren oder maskieren, oder direkt PRRs und ihre nachgelagerte Signalkaskade stören. Der Ausgang dieses Prozesses ist effektorangestoßene Suszeptibilität (ETS). Als Reaktion darauf haben Pflanzen Mittel entwickelt, um Effektoren, oder ihre Aktivität mittels nucleotidbindenden leucinreichen Wiederholungsrezeptoren (NLRs) wahrzunehmen, was zur Effektor-angestoßener Immunität (ETI) führt.

2013 wurde eine neue Klasse von nichtproteinbasierten pathogenen Effektormolekülen entdeckt, welche die pflanzliche RNA-Interferenz (RNAi) Maschinerie ausnutzt. Diese neuen Effektoren sind kleine RNAs (sRNAs), welche im Pathogen durch Dicer-ähnliche (DCL) Proteine produziert werden, und in der Pflanze in Argonauten (AGO)-Proteine geladen werden. Dort leiten die sRNAs AGOs zu Ziel-mRNAs, auf der Basis der Komplementarität zwischen sRNA und mRNA, wodurch das entsprechende Gen stillgelegt und ETS herbeigeführt wird. Dieser Prozess, der auch von Wirten als Abwehrmechanismus genutzt werden kann, wird reichübergreifende RNAi (ckRNAi) genannt.

Diese Arbeit untersucht ckRNAi in dem wichtigen Pflanzenpathogen *Fusarium graminearum* (Fg) auf der Wirtspflanze Gerste. Als ersten Schritt, wurden Gerstepflanzen mit langer doppelsträngiger RNA (dsRNA) behandelt, um pilzliche *AGO*- und *DCL*-Gene auszuschalten (Kapitel I). Dieses Ausschalten war effektiv und reduzierte Krankheitssymptome in Gerste, was zeigt das Fg*AGO*s und Fg*DCL*s wichtig für die Pathogenese sind, was wiederum für den Pflanzenschutz genutzt werden kann. Verschiedene manuelle und maschinelle Designstrategien für die dsRNA-Moleküle wurden verglichen, wobei manuell designte dsRNAs effektiver in der Genstillegung und Krankheitsverhinderung waren.

Nachdem die Bedeutung von Fg*DCL*s und Fg*AGO*s gezeigt wurde, wurden Fg*DCL* knock-out (KO) Mutanten eingehender untersucht, um die Mitwirkung von ckRNAi in der Pathogenese von Fg zu zeigen (Kapitel II). Wegen der Notwendigkeit von DCLs in der Biogenese von sRNAs, sollte pilzliches ckRNAi in diesen aufgehoben sein. Dieses zeigte sich durch reduzierte Krankheitssymptome in den Wirtspflanzen Gerste und *Brachypodium distachyon*. Ergänzend dazu waren Zielgene der Fg-sRNAs, während der Infektion mit diesen KO-Mutanten, in Gerste stärker exprimiert. Abbauprodukte der Zielgene von drei pilzlichen tRNA-abgeleiteten sRNAs wurden in Pflanzen die mit dem Wildtyp-Pilz infiziert waren gefunden, und fehlten in Pflanzen die mit dem KO Mutanten infiziert wurden. Zusammen zeigt dies die Beteiligung von ckRNAi in der Fg-Pathogenese.

Die biologische Signifikanz hiervon bleibt jedoch fragwürdig, da *DCL* Gene auch an der internen Genregulation von Fg beteiligt sind. Um dieses Problem zu beheben, habe ich die Hypothese formuliert, dass Zielregionen von ckRNAi-ausübenden sRNAs einem evolutionären Druck unterworfen sind, welcher die Codonnutzung in diesen Regionen verändert (Kapitel III). Um dieses zu belegen wurden neue bioinformatische Arbeitsschritte entwickelt, welche die Wahrscheinlichkeit berechnen die tatsächliche Komplementarität der sRNA-mRNA Interaktionen zu beobachten, während die Aminosäure (AA)-sequenz unverändert bleibt und unter Berücksichtigung der organismustypischen Codonnutzung. Diese Kalkulation wurde für die Fg-sRNAs aus Kapitel II, für *Hyaloperonospora arabidopsidis* (Ha) sRNAs, sowie *Arabidopsis thaliana* (At) und *Gorilla gorilla* (Gg) miRNAs durchgeführt. Ha ist ein weiterer filamentöser Pathogen, der ckRNAi für die vollständige Pathogenese verwendet und die miRNA Sets dienten als positive und negative Kontrollen.

Die Ergebnisse für Fg- und Ha-sRNAs zeigten eine unwahrscheinlich starke Komplementarität zwischen Pathogen-sRNAs und Wirt-mRNAs. Diese Beobachtung demonstriert die biologische Bedeutung von ckRNAi. Verblüffender Weise begünstigt dieser Druck ckRNAi, während, der Effektor Hypothese folgend, eine Verhinderung dieser durch den Wirt zu erwarten gewesen wäre. Um diesen Wiederspruch aufzulösen, wird die Hypothese formuliert, dass Pflanzen ckRNAi nutzen, um pathogene sRNAs wahrzunehmen und angepasst zu reagieren. Dieses ähnelt der Wahrnehmung von Effektoren durch NLRs und MAMPS durch PRRs, und repräsentiert den nächsten Schritt im Wettrüsten zwischen Pathogen und Pflanze, was ein enormes Potenzial für die zukünftige Anwendungen in der Erstellung von krankheitsresistentem Saatgut hat.

Introduction

RNA interference

RNA interference (RNAi) is a conserved mechanism shared by most eukaryotic organisms where small RNAs (sRNAs) sequence specifically target messenger RNAs (mRNAs) in the case of post-transcriptional gene silencing (PTGS) or DNA in the case of transcriptional gene silencing (TGS). In the context of this work sRNA refers to all classes of short RNAs exerting a role in RNAi and not to bacterial small RNAs. With the many RNAi capable species including bacteria and archaea with some cases of DNA guided PTGS comes a huge variety of different mechanisms in terms of guide molecule biogenesis, participating proteins and functions (Kuzmenko et al. 2020).

The role of Dicer-like proteins and RNA-dependent RNA polymerases in RNAi

In *Arabidopsis thaliana* (*Ath*) RNAi-triggering sRNAs are generated through the action of four Dicer-like proteins (DCL1-4). These proteins cleave longer double stranded (ds) RNAs into mainly 21-24 nucleotide (nt) long RNAs which guide silencing (Fukudome & Fukuhara 2017). DCL1 is responsible for the generation of microRNAs (miRNAs) with a length of 21 nt which perform essential roles in plant development (Vazquez et al. 2004), responses to abiotic stresses such as drought and nutrient deficiency (Sunkar & Zhu 2004) and responses to biotic stresses (Jay et al. 2010). miRNAs are generated from endogenous primary miRNAs (pri-miRNA) with partial self-complementarity leading to the formation of a hairpin like structure (Wang et al. 2019). DCL2, DCL3 and DCL4 act partially redundant in the generation of small interfering RNAs (siRNAs). DCL2 and DCL4 act together in the generation of trans-acting siRNAs (tasiRNAs) from tasiRNA precursor RNA (TAS) genes whose transcripts are complemented through a pathway involving RNA-dependent RNA polymerase 6 (RDR6) and suppressor of gene silencing 3 (SGS3) to form long dsRNAs. These dsRNAs are subsequently cleaved into tasiRNA duplexes which leads to RNA-induced silencing complex (RISC) mediated gene silencing (Gasciolli et al. 2005). In a similar fashion DCL2 and DCL4 are also involved in antiviral RNAi (Garcia-Ruiz et al. 2017). DCL3 in contrast is involved in the generation of 24nt long siRNAs responsible for TGS via DNA methylation. In this process DNA is transcribed by nuclear RNA polymerase 4 (Pol IV) and this single stranded (ss) RNA transcript is complemented by RNA-dependent RNA polymerase 2 (RDR2) in to a dsRNA substrate for DCL3 (Singh et al. 2019).

Functions and clades of Argonaute proteins during RNAi

After the generation of small dsRNAs by the action of DCL proteins these duplexes are loaded into an Argonaute (AGO) protein where the passenger strand, also known as *miRNA, is separated and the so called guide strand remains associated with the protein. AGO proteins are usually part of a larger protein complex the so called RISC (Yuan et al. 2006). In this RISC AGO serves as guide to find a more or less complementary target of the PIWI/Argonaute/Zwille (PAZ) and middle (MID) domain associated sRNA and also as a slicer via its P-element-induced whimpy tested (PIWI) domain which cleaves the targeted mRNA (Song et al. 2004). Like the DCL proteins the *Ath*-AGOs can be divided into several distinct classes with various functions. In *Ath* AGO proteins can be grouped into three clades, Clade I (AGO1/5/10), Clade II (AGO2/3/7) and Clade III (AGO4/6/8/9) (Fang & Qi 2016). While in monocots an additional subclade is described (AGO18) with roles in antiviral defense, development and gametogenesis (Das et al. 2020). Clade I AGOs in *Ath* are responsible for miRNA mediated silencing in development and stress responses, Clade II AGOs are associated with the function of specific miRNAs (miR390), virus-derived siRNAs (vsiRNAs) and double-strand DNA break induced siRNAs and Clade III AGOs are mainly associated with RNA-directed DNA methylation, suppression of female gametogenesis and transposable element silencing (Zhang et al. 2015).

This separation of functions of the different clades is achieved via specific loading of sRNA-duplexes into AGO family members and also the localization of respective AGOs and sRNAs. One main separator is the identity of the first nucleotide (5') of the sRNA, where AGO1 predominantly loads 5' uracil (U) sRNAs, AGO2 and AGO4 5' adenine (A) sRNAs and AGO5 5' cytosine (C) sRNAs (Mi et al. 2008). Another factor is the presence of mismatches, especially at the 15th nt, in the sRNA duplex which are mostly present in miRNAs and lead to a loading into AGO1, whereas duplexes without a mismatch at the 15th nt are preferably loaded into AGO2 (Zhang et al. 2014).

Limitations of the *Ath* centered view in monocot crop species

While these different functions of AGOs and DCLs are well studied in the model organism *Ath*, much can only be inferred via homology for the roles and functions of these proteins in monocot model and crop species and in mycelial pathogens. The four classes of DCLs and three or four clades (AGO5 can be seen as own clade) of AGOs are the results of early duplication

events and are already present in the common ancestor of angiosperms (Borges & Martienssen 2015; Singh et al. 2015). In the monocotyledonous model species *Brachypodium distachyon* (*Bdi*) 16 AGOs and 6 DCLs were identified (Šečić et al. 2019). While the expansion of the AGO and DCL families in barley lead to the presence of just 11 AGOs and 5 DCLs (Hamar et al. 2020) and in the monocot crop species rice (*Oryza sativa*) (Kapoor et al. 2008) and foxtail millet (*Setaria italica*) (Yadav et al. 2015) the AGO and DCL families expanded even more to contain 19 AGOs and 8 DCLs and in the hexaploid crop species wheat (*Triticum aestivum*) this expansion led to the presence of 7 DCLs and 39 AGOs (Akond et al. 2020). While the forward and reverse genetic approaches that lead to the decipherment of AGO and DCL functions in *Ath* are only now becoming possible with libraries of KO-mutants for *Bdi* (Thole et al. 2012; Scholthof et al. 2018), and new comprehensive assemblies of monocot crop species genomes (Appels et al. 2018; Wang et al. 2018; Jayakodi et al. 2020).

Differences and commonalities of fungal RNAi vs. plant RNAi

In the kingdom “fungi” the mechanisms of RNAi are more diverse than in the plant kingdom and while functioning through the principal components of AGOs and DCLs as in plants and fulfilling similar functions such as viral defense, control of transposable elements and gene regulation, some fungal model species such as *Saccharomyces cerevisiae* and pathogens such as *Ustilago maydis* do not have a functional RNAi machinery (Lax et al. 2020). The class of oomycetes has many members of mycelial plant pathogens which were formerly falsely classified as fungi or lower fungi. Yet they are more closely related to algae and are classified today either in the kingdom stramenopila or chromista (Lamour & Kamoun 2009). The oomycetal order peronosporales contains the two agronomically important genera Phytophthora and Hyaloperonospora with the historically important pathogen, model organism, and causal agent of potato blight and the Great Irish Famine *Phytophthora infestans* (*Pi*) and causal agent of downy mildew and model organism *Hyaloperonospora arabidopsidis* (*Ha*) (Haas et al. 2009; Coates & Beynon 2010). Both *Pi* and *Ha* have functioning AGOs from both oomycetal AGO clades (Bollmann et al. 2018) and one DCL from each of the two oomycetal DCL clades (Bollmann et al. 2016).

Cross-kingdom RNAi

The challenge of understanding the diverse roles of mycelial pathogens RNAi machinery during pathogenesis lead to a surprising discovery for *Botrytis cinerea* (*Bc*) where fungal DCLs produced sRNAs that silenced specific genes in the host *Ath* via the plants AGO1 (Weiberg et al. 2013). This process is now known as cross-kingdom RNAi (ckRNAi) as genes are silenced across the borders between different kingdoms of life. This process was shown to take place during the pathogenic interaction of *Ha* on *Ath* (Dunker et al. 2020), from plant host to pathogenic fungus for cotton and *Verticillium dahliae* (Zhang et al. 2016), within kingdoms for parasitic plants and animals (Buck et al. 2014; Shahid et al. 2018) and during symbiotic interaction of plants and bacteria (Ren et al. 2019). During the pathogenic interaction these fungal sRNAs are thought of as sRNA-effectors similar to traditional protein effectors. These traditional protein effectors are thought of as pathogenesis factors which evolve in an arms race between plant and pathogen in which pathogens produce and secrete effectors targeting the plants immune responses. The plant evolves as reaction to these, means to recognize effectors by guarding its proteins, producing bait proteins or by direct recognition of these effectors via receptors to which the pathogen reacts in a back and forth manner. This model is the zig-zag model (Jones & Dangl 2006).

Applications of ckRNAi and RNAi in crop protection

The agronomical potential of this discovery was later shown by the application of dsRNA with sequence homology to the two fungal DCLs onto fruits and leaves of host plants or the transgenic expression of siRNAs targeting the fungal DCLs. These dsRNAs and siRNAs inhibited pathogenesis and were shown to be a feasible strategy in crop protection (Wang et al. 2016a). The foliar application of dsRNAs onto leaf surfaces is known as spray-induced gene silencing (SIGS) and the genetically modified organism (GMO) counterpart is known as host-induced gene silencing (HIGS). Both technologies were shown to be applicable on plant protection against *Fg* (Koch et al. 2013; Koch et al. 2016) and SIGS was shown to be effective against *Ha* (Bilir et al. 2019) by silencing essential genes for membrane or cell wall integrity in the case of *Fg* the three *cytochrome P450 monooxygenases / sterol 14α-demethylases* (*CYP51*) and in the case of *Ha* the *cellulose synthase A3*.

RNA mobility within plants

The movement of mRNA molecules between adjacent plant cells via plasmodesmata was the first discovery of moving RNA species within the plant kingdom (Lucas et al. 1995). The transport of the maize transcription factor KNOTTED1 via plasmodesmata was accompanied by its transcript. In *Ath*, miRNAs of the MIR165/165 family were shown to move via plasmodesmata, a movement which is essential for the cell differentiation in roots. This is achieved by the RNA-directed cleavage of specific transcription factors (Carlsbecker et al. 2010). Studies on the phloem sap of squash (*Cucurbita maxima*), where the collection of phloem samples is quite easy like in most plants of the Cucurbitaceae family, could show the long distance movement of mRNAs via the phloem by the association of mRNAs with RNA-binding proteins (Xoconostle-Cázares et al. 1999). Today, with the development of next-generation sequencing (NGS) technologies in combination with stylectomy, a technique using stylets of phloem sucking insects for the sampling of phloem sap from non-cucurbitaceae plants, and grafting studies, many long distance mobile mRNAs and sRNAs were discovered (Kehr & Kragler 2018).

Ribonucleases during host defense

The transport of different RNA species is only poorly understood and can vary between organisms of different kingdoms. With the central role of RNA, organisms unsurprisingly have developed a plethora of different ribonucleases (RNases), RNA modifying and degrading enzymes. *Escherichia coli*, a bacterial model species, produces at least 11 types of endo- and 8 types of exoribonucleases (Nicholson 1997). One of the most studied proteins mammalian RNase A and its family members are excreted from epithelial and immune cells and have antimicrobial, -viral and -fungal as well as RNA degrading properties (Koczera et al. 2016). Plants and fungi also facilitate extracellular RNases as part of their immune response (Galiana et al. 1997; Hugot et al. 2002; Olombrada et al. 2014).

Current understanding of RNA mobility between organisms

The omnipresence of RNases especially during defense responses renders the exchange of naked RNA species between organisms unlikely. Recent research unraveled some of the modes for RNA exchange between organisms. First investigations of the uptake of dsRNAs were done in invertebrates and two contrasting conclusions were found: *systemic RNA interference*

defective (*SID*) is necessary in *Caenorhabditis elegans* for silencing by dsRNA species independent of clathrin-mediated endocytosis (CME) (Tijsterman et al. 2004), while in the model insect *Drosophila melanogaster* the *clathrin heavy chain gene*, together with other components of CME-pathway, is necessary for RNAi by dsRNAs (Ulvila et al. 2006). The fungal pathogen *Sclerotinia sclerotiorum* is susceptible to SIGS (McLoughlin et al. 2018) and it was shown that the uptake of dsRNAs and subsequent RNAi are also dependent on the CME-pathway (Wytinck et al. 2020). With the observation of semi systemic RNAi via SIGS in plants (Koch et al. 2016) it is plausible for SIGS in other fungi being dependent on clathrin-mediated endocytosis as well.

RNAi via HIGS on the other hand is often mediated by long inverted repeats of sequences homolog to pathogen genes which form long dsRNA (Nowara et al. 2010). Yet it is unlikely for this dsRNA inside the plant cell to be excreted in an uncleaved form due to the presence of plant DCLs. The purification of plant derived extracellular vesicles (EVs) produced during pathogen challenge (Rutter & Innes 2017) gave rise to the idea that similar to mammalian systems RNAi signals could be transmitted via these vesicles (Mittelbrunn et al. 2011). This was confirmed by the verification of HIGS-derived siRNAs in plant EVs and the dependence of HIGS-mediated resistance on components of the plants EV pathways (Koch et al. 2020). However, for the transport of RNAi signals from fungi and other mycelial pathogens during ckRNAi no mechanism could be described up to date.

The problems of fungicide resistances and off-targeting

HIGS and SIGS are potential solutions to two of the major problems facing the control of fungal diseases via the application of chemical pesticides. Firstly, the development of resistances against commonly applied pesticides which rely on only a few effective modes of action (Baibakova et al. 2019). The fungicide class with the highest market share (Price et al. 2015), the triazoles, targets the ergosterol synthesis by interfering with the CYP51 function as previously described for HIGS and SIGS approaches in *Fg*. Emerging resistances against triazoles are not only of agronomical concern, exemplified by the reduced sensitivity of *Fg* against these (Anderson et al. 2020), but also of concern for the treatment of fungal diseases in humans (Bowyer & Denning 2014). An issue with increased importance during the COVID-19 pandemic illustrated by a case report of a patient with a secondary triazole resistant *Aspergillus fumigatus* infection (Ghelfenstein-Ferreira 2021). These problems are linked to the second major problem

of chemical fungicides mentioned earlier, the unintended targeting of non-target organisms. Fungicides are effective against many plant pathogens but also effect beneficial soil microbiota (Yang et al. 2011), reducing temporally soil function like the decomposition of organic matter and fungal toxins (e.g. deoxynivalenol (DON)) (Meyer et al. 2021) as well as aquatic species (Adams et al. 2021; Jiménez et al. 2021), pollinators (Belsky & Joshi 2020) and the effectiveness of medical antifungal compounds (Fisher et al. 2018).

Computational prediction of RNAi target genes

HIGS and SIGS bear the potential to solve these problems due to their specificity and, in the case of HIGS, due to the confinement of the RNAi trigger molecules within the plant. Yet, for these technologies to be specific on the species level the prediction of siRNA targets within the fungal pathogen needs to be precisely predicted. For this process of target prediction several different algorithms are available, either for plants where especially in *Ath* the guidance of the RISC by sRNAs is quite specific and a high degree of complementarity is necessary for efficient RNAi. For instance, the si-Fi21 algorithm (Lück et al. 2019) is designed to generate a dsRNA with effective silencing, due to a perfect complementarity of dsRNA and target, the selection of an mRNA region with a high accessibility of the target region based on the RNAplfold algorithm from the ViennaRNA Package (Lorenz et al. 2011) and thermodynamic parameters of the siRNA duplexes which can trigger the loading of the antisense strand relative to the mRNA and enabling efficient targeting (Lück et al. 2019). The off-target prediction within si-Fi21 is intended to prevent the targeting of other mRNAs of the plant. This is achieved with the short read aligner bowtie (Langmead 2010) where all possible siRNAs are aligned to the mRNA sequences of the plant and siRNAs with 0, 1, 2 or 3 mismatches (MM) to a non-target mRNA are reported. Of note, this short read aligner is not intended to be used for the purpose of siRNA target prediction. Another example of a RNAi trigger design tool is pssRNAit (Ahmed et al. 2020) which similarly to si-Fi21 assesses the target site accessibility via the ViennaRNA package and takes the RISC strand preference into account. Additionally, a support vector machine model was trained on data derived from a human cell culture experiment to select the most effective RNAi triggers. To identify off-targets the psRNATarget algorithm was applied (Dai et al. 2018). psRNATarget is an algorithm with the stated purpose to predict targets of sRNAs in plants, making it more suitable to predict off-targeting events in comparison to bowtie. There are several algorithms available to predict targets of plants and mammalian sRNAs. These

algorithms differ in their computational demands and the number of predicted targets per sRNA by several orders of magnitude (Srivastava et al. 2014). In plants there is a near perfect complementarity between sRNA and mRNA, especially in the seed region, necessary for effective silencing (Mallory et al. 2004). This makes the prediction of sRNA targets much more efficient and precise compared to animal systems, in which the degree of complementarity can be much lower (Rehmsmeier et al. 2004). It was also shown that at least in plants, these algorithms are less precise in non-model organisms with more false positives and negatives (Srivastava et al. 2014). For RNA target prediction in fungi and oomycetes no specific algorithms are available and researchers tend to utilize successfully algorithms intended for plants, e.g. psRNATarget (Zhang et al. 2016; Hu et al. 2019; Jin et al. 2019).

Considerations of specificity and resistance development in regard to RNAi-trigger length

These uncertainties in the reliability of off-target predictions call for shorter RNAi trigger sequences with less potential sRNAs, in order to reduce potential unpredicted off-targets. Some vectors expressing a single siRNA by mimicking the stem-loop structure of miRNA genes are available for plant systems (Qu et al. 2007; Liang et al. 2020). These single siRNA or artificial miRNA (amiRNA) expressing vectors can be used to confer resistances against insects (Guo et al. 2014; Yogindran et al. 2021), viruses (Wagaba et al. 2016; More et al. 2021) and, potentially, fungi (Jin et al. 2013). The downside of this short RNAi trigger is a high potential for the development of resistances where just a few or even one mutation can render the amiRNA ineffective. These mutations in miRNA target sites can even develop in the relatively conserved coding sequence (CDS) of a gene without changing the protein amino acid (AA) sequence (Mallory et al. 2004). The targeting of CDS by miRNAs is, with few exceptions (Forman et al. 2008), uncommon in animals, and miRNAs target in majority the 3' untranslated region (UTR) of mRNAs (Eulalio et al. 2008). In plants the targeting of CDS by miRNA is much more common and has a long evolutionary history, being already present in green algae (Chung et al. 2017).

Codon usage bias and natural selection

The CDS of an mRNA determines the AA sequence of the respective protein. In the genetic code an AA in a protein is coded as a codon of three nt length. This genetic code, which is conserved among most organisms, is of a degenerate nature (Crick et al. 1961), meaning that many AA can be coded with more than one codon. Codons coding for the same AA are called synonymous

codons. The usage of synonymous codons within an organisms' genome is neither random nor ubiquitous. Instead it is often highly biased to specific codons and differs greatly between species and clades (Murray et al. 1989; Sharp & Matassi 1994). Two major groups of biases can be distinguished, one is driven by a selective pressure and confers selective advantages, the other is driven by mutational biases. The latter stems from the uneven occurrence of transitions and transversions between nts (Zhao et al. 2006), leading to the accumulation of specific synonymous codons in the CDS, while selective pressure often favors different codons leading to a specific balance between both. There are several reasons known for the selection of specific synonymous codons. The most prominent among them is an increase of translational efficiency due to a higher abundance of respective transfer RNAs (tRNAs) (Moriyama & Powell 1997). Surprisingly, a correlation between codon usage and the evolution of miRNA or siRNA targeted sites has not been established yet.

F. graminearum related risks for food security

The development of resistances against fungicides (Talas & McDonald 2015), the impact of fungicide application on the degradation of mycotoxins, especially DON, in soils (Meyer et al. 2021), the possibility of crop protection via RNAi technology in the form of HIGS and SIGS (Koch et al. 2013; Koch et al. 2016) are highly relevant for *Fg*. *Fg* is one of the most important pathogens in modern crop production due to its broad host range encompassing all cereal staple crops, like wheat (Triticum), rice (Oryza), barley (Hordeum), oats (Avena) and maize (Zea) (Goswami & Kistler 2004). Wheat and rice alone account for nearly 50% of calorie intake worldwide (WHO 2009) as a results of growing importance of these crops in the 50 years' period predating the report (Khoury et al. 2014). *Fg* can reduce crop yields by nearly 50% in some areas and in local fields up to 80% of plants can be affected (McMullen et al. 1997). Affected fields not only suffer yield losses, but remaining yield is often contaminated with mycotoxins which can cause, in the case of DON, anorexia, gastroenteritis, growth retardation, immunotoxic and teratogenic effects (Pestka 2010). Contaminations with DON in the EU were found in more than half of the collected samples according to a EU report and the tolerable daily intake of some *Fg* associated toxins could exceed the recommended limits in some populations, emphasizing the need for new strategies to manage this pathogen (Gareis 2003). These risks for health and food security caused by *Fg*, in combination with developing resistances against fungicides urge the development of new management strategies.

The *Fusarium graminearum* species complex

Morphological classification of *Fg*, the causal agent of fusarium head blight (FHB), fusarium crown rot (FCR) and fusarium root rot (FRR) on wheat, rice, barley, oats and maize was unable to identify subtle differences between species which are now grouped under the term *Fusarium graminearum* species complex (FGSC). Methods to differentiate between these species observed isolates during specific growth conditions and light regiments (Nirenberg 1981) or the electrophoresis of certain isozymes (Laday et al. 2000). This classification is especially important due to the types of mycotoxins associated with the FGSC species. Up to date 16 distinct Fusarium species (*F. acacia-mearnsii*, *F. aethiopicum*, *F. asiaticum*, *F. austroamericanum*, *F. boothii*, *F. brasilicum*, *F. cortaderiae*, *F. gerlachii*, *F. graminearum sensu stricto*, *F. louisianense*, *F. meridionale*, *F. mesoamericanum*, *F. nepalense*, *F. ussurianum*, *F. vorosii* and U.S. Gulf Coast population of *F. graminearum*) were identified within the FGSC by modern sequencing methods (Amarasinghe et al. 2019).

The functions of AGO and DCL in *Fg*

Research in recent years could uncover some roles of the *Fg* RNAi machinery. Chen and colleagues (Chen et al. 2015) silenced genes by the expression of long hairpin-like RNAs targeting endogenous genes. This silencing was dependent on *FgAGO1* and *FgDCL2* shown by gene knockout (KO). *FgDCL2* was also involved in the generation of miRNA-like RNAs in *Fg*. The tested single and double KO (DKO) mutants did not show differences in colony morphology, pathogenesis and abiotic stress resilience. The roles of *FgAGO1* and *FgDCL2* were confirmed by a study of Son and colleagues (Son et al. 2017) which also showed that *FgAGO2* and *FgDCL1* are strongly expressed during ascospore formation and contribute to normal morphology of these spores. A more thorough investigation of single KO mutants of RNAi components by Gaffar and colleagues (Gaffar et al. 2019) found differences in pigmentation in liquid cultures (*FgDCL1*, *FgDCL2*, *FgAGO1*) and differences in conidial germination (*FgDCLs* and *FgAGOs*). Ascospore discharge was compromised in *FgDCL1* and *FgAGO2* single KO mutants, confirming the results of Son et al. Contrasting to the results from Chen et al., a reduced infection of wheat spikes 9 days post inoculation (dpi) was shown in this study, accompanied by reduced levels of DON for these and all other RNAi pathway KO mutants. Yu and colleagues (Yu et al. 2018) investigated the role during viral infections and found an increased expression of most components (*AGOs*, *DCLs* and *RdRPs*) in response to viral infection with three different mycovirus strains in *Fg*.

Single KO mutants of *FgAGO1*, *FgAGO2*, *FgDCL1*, *FgDCL2*, *FgRdRP1* and *FgRdRP4* did not show differences in colony morphology. Over expression (OE) of the respective genes could show an antiviral effect of *FgAGO1*-OE on one of the three tested viruses. Double knockout (DKO) mutants of both *DCLs* or *AGOs* had normal colony morphology until infection, when the DKOs had reduced growth in comparison to the infected wild type (wt) and increased viral RNA accumulation, indicating a redundancy of *AGOs* and *DCLs* during mycovirus infection.

Research question

The aim of this work is (i) to further elucidate the importance of *FgAGOs* and *FgDCLs* genes during pathogenesis, (ii) to evaluate these genes as potential targets for crop protection via SIGS, (iii) to investigate a possible involvement of ckRNAi during *Fg* pathogenesis and (iv) to develop an assessment method for the biological significance of ckRNAi.

Chapter I: RNA-spray-mediated silencing of *Fusarium graminearum AGO* and *DCL* genes improve barley disease resistance.

This chapter is published in the journal Frontiers in Plant Science, in Volume 11, Article 476, on the April 29th 2020. DOI: https://doi.org/10.3389/fpls.2020.00476

Chapter I: Introduction

This chapter answers the research questions i and ii by the application of SIGS against *FgAGOs* and *FgDCLs*.

frontiers in Plant Science

ORIGINAL RESEARCH
published: 29 April 2020
doi: 10.3389/fpls.2020.00476

RNA-Spray-Mediated Silencing of *Fusarium graminearum AGO* and *DCL* Genes Improve Barley Disease Resistance

Bernhard Timo Werner[1†], *Fatima Yousiff Gaffar*[2†], *Johannes Schuemann*[1†], *Dagmar Biedenkopf*[1] *and Aline Michaela Koch*[1*]

[1] Centre for BioSystems, Land Use and Nutrition, Institute of Phytopathology, Justus Liebig University Giessen, Giessen, Germany, [2] Botany and Agricultural Biotechnology, University of Khartoum, Khartoum, Sudan

Over the last decade, several studies have revealed the enormous potential of RNA-silencing strategies as a potential alternative to conventional pesticides for plant protection. We have previously shown that targeted gene silencing mediated by an *in planta* expression of non-coding inhibitory double-stranded RNAs (dsRNAs) can protect host plants against various diseases with unprecedented efficiency. In addition to the generation of RNA-silencing (RNAi) signals *in planta*, plants can be protected from pathogens, and pests by spray-applied RNA-based biopesticides. Despite the striking efficiency of RNA-silencing-based technologies holds for agriculture, the molecular mechanisms underlying spray-induced gene silencing (SIGS) strategies are virtually unresolved, a requirement for successful future application in the field. Based on our previous work, we predict that the molecular mechanism of SIGS is controlled by the fungal-silencing machinery. In this study, we used SIGS to compare the silencing efficiencies of computationally-designed vs. manually-designed dsRNA constructs targeting *ARGONAUTE* and *DICER* genes of *Fusarium graminearum* (*Fg*). We found that targeting key components of the fungal RNAi machinery via SIGS could protect barley leaves from *Fg* infection and that the manual design of dsRNAs resulted in higher gene-silencing efficiencies than the tool-based design. Moreover, our results indicate the possibility of cross-kingdom RNA silencing in the *Fg*-barley interaction, a phenomenon in which sRNAs operate as effector molecules to induce gene silencing between species from different kingdoms, such as a plant host and their interacting pathogens.

Keywords: RNA spraying, RNA silencing, spray-induced gene silencing, *Fusarium graminearium*, AGO and DCL

OPEN ACCESS

Edited by:
Azeddine Si Ammour, Fondazione Edmund Mach, Italy

Reviewed by:
Andrew Leigh Eamens, University of Newcastle, Australia
Andreas Voloudakis, Agricultural University of Athens, Greece

***Correspondence:**
Aline Michaela Koch
aline.koch@agrar.uni-giessen.de

† These authors have contributed equally to this work

Specialty section:
This article was submitted to Plant Microbe Interactions, a section of the journal Frontiers in Plant Science

Received: *09 July 2019*
Accepted: *30 March 2020*
Published: *29 April 2020*

Citation:
Werner BT, Gaffar FY, Schuemann J, Biedenkopf D and Koch AM (2020) RNA-Spray-Mediated Silencing of Fusarium graminearum AGO and DCL Genes Improve Barley Disease Resistance. Front. Plant Sci. 11:476. doi: 10.3389/fpls.2020.00476

INTRODUCTION

Diseases of cereal crops, such as Fusarium head blight caused by phytopathogenic fungi of the genus *Fusarium* and primarily by the ascomycete *Fusarium graminearum* (*Fg*), exert great economic and agronomic impacts on global grain production and the grain industry (Goswami and Kistler, 2004; Kazan et al., 2012; McMullen et al., 2012). In addition to significant yield losses, food quality is adversely affected by grain contamination with mycotoxins, representing a serious threat

to human and animal health (Ismaiel and Papenbrock, 2015). Plant-protection and toxin-reduction strategies are presently mediated by chemical treatments. Currently, the application of systemic fungicides, such as sterol demethylation inhibitors (DMIs), is essential for controlling Fusarium diseases and to assist in reaching the maximum attainable production level of high-yield cultivars. DMI fungicides act as ergosterol biosynthesis inhibitors because of cytochrome P450 lanosterol C-14α-demethylase (CYP51) binding, which subsequently disturbs fungal membrane integrity (Kuck et al., 2012). Because of a shortage of alternative chemicals, DMIs have been used extensively in the field since their discovery in the 1970s. Therefore, it is hardly surprising that reduced sensitivity, or even resistance to DMI fungicides, has begun to develop in many plant pathogenic fungi (Yin et al., 2009; Spolti et al., 2014). These alarming developments demonstrate that novel strategies in pathogen and pest control are urgently needed.

RNAi is known as a conserved and integral part of the gene regulation processes present in all eukaryotes and is mediated by small RNAs (sRNAs) that direct gene silencing at the post-transcriptional level. Post-transcriptional gene silencing (PTGS) starts with the initial processing or cleavage of a precursor double-stranded (ds)RNA into short 21–24 nucleotide (nt) small-interfering RNA (siRNA) duplexes by an RNaseIII-like enzyme called Dicer (Baulcombe, 2004; Ketting, 2011). Double-stranded siRNAs are incorporated into an RNA-induced silencing complex (RISC) that initially unwinds the siRNA, thereby generating an antisense (or guide) strand which base-pairs with complementary mRNA target sequences. Subsequent degradation of the targeted mRNA mediated by an RNase protein called Argonaute (AGO) prevents translation of the target transcript (Vaucheret et al., 2004; Borges and Martienssen, 2015) ideally resulting in a loss of function phenotype. Therefore, RNAi has emerged as a powerful genetic tool not only in fundamental research for the assessment of gene function but also in various fields of applied research, such as agriculture. In plants, RNAi strategies have the potential to protect host plants against infection by pathogens or predation by pests mediated by lethal RNAi signals generated *in planta,* a strategy known as 'host-induced gene silencing' (HIGS; Nowara et al., 2010) (for review, see Koch and Kogel, 2014; Yin and Hulbert, 2015; Guo et al., 2016; Zhang et al., 2017; Gaffar and Koch, 2019; Qi et al., 2019). In addition to the generation of RNA-silencing signals *in planta*, plants can be protected from pathogens and pests by spray-applied RNA biopesticides designated as spray-induced gene silencing (SIGS) (Koch et al., 2016; Wang et al., 2016; Konakalla et al., 2016; Mitter et al., 2017a; Kaldis et al., 2018; Koch et al., 2019). Regardless of how target-specific inhibitory RNAs are applied (i.e., endogenously or exogenously), the use of HIGS and SIGS technologies to control *Fusarium* species have been shown to be a potential alternative to conventional pesticides (Koch et al., 2013; Ghag et al., 2014; Cheng et al., 2015; Hu et al., 2015; Chen et al., 2016; Pareek and Rajam, 2017; Bharti et al., 2017; Baldwin et al., 2018; Koch et al., 2018, 2019) supporting the notion that RNAi strategies may improve food safety by controlling the growth of phytopathogenic, mycotoxin-producing fungi (reviewed by Majumdar et al., 2017; Machado et al., 2018).

Despite the notable efficiency the RNAi-based technology holds for agriculture, the mechanisms underlying HIGS and SIGS technologies are inadequately understood. There is little information regarding the contribution of either plant- or fungal-silencing machinery in cross-species RNA silencing (i.e., plant and fungus) or how inhibitory RNAs translocate from the plant to the fungus after its transgenic expression or spray application. Whereas HIGS is virtually based on the plant's ability to produce mobile siRNAs (through plant Dicers [DCLs]), the mechanism of gene silencing by exogenously delivered dsRNA depends primarily on the fungal RNAi machinery, mainly fungal DCLs (Koch et al., 2016; Gaffar et al., 2019). Interestingly, recent studies revealed that AGO and DCL proteins of *Fg* contribute to fungal vegetative and generative growth, mycotoxin production, antiviral response, sensitivity to environmental RNAi, and plant disease development (Kim et al., 2015; Son et al., 2017; Yu et al., 2018; Gaffar et al., 2019). In *Fg*, two Dicer proteins (*Fg*DCL1 and *Fg*DCL2) and two AGO proteins (*Fg*AGO1 and *Fg*AGO2) were identified (Chen et al., 2015). Characterization of those RNAi core components revealed functional diversification, as *Fg*AGO1 and *Fg*DCL2 were shown to play important role in hairpin-RNA-induced gene silencing (Chen et al., 2015). In addition, we recently demonstrated that *Fg*AGO2 and *Fg*DCL1 are required for sex-specific RNAi (Gaffar et al., 2019). Moreover, *Fg*AGO2 and *Fg*DCL1 participate in the biogenesis of perithecium-specific microRNAs (Zeng et al., 2018).

Notably, we previously demonstrated that *Fg*DCL1 is required for SIGS-mediated *Fg* disease resistance (Koch et al., 2016). However, further analysis of *Fg* RNAi KO mutants revealed that all tested mutants were slightly or strongly compromised in SIGS, whereas *FgCYP51* target gene expression was completely abolished *in* Δ*dcl2* and Δ*qip1* mutants (Gaffar et al., 2019).

Together, these studies indicate a central role of RNAi pathways in regulating *Fg* development, pathogenicity, and immunity. Consistent with this notion, we assume that *Fg* RNAi components represent suitable targets for RNA spray-mediated disease control. To determine this, we generated different dsRNA constructs targeting *FgAGO* and *FgDCL* genes that were sprayed onto barley leaves. We also compared two different dsRNA design strategies; in particular, we used a tool-based prediction of suitable dsRNA construct sequences vs. a manual construct design related to current dsRNA design principles and experiences. The tool-designed dsRNA molecules, which target specific and easily accessible regions are shorter, while the manually-designed dsRNA molecules are longer and target non-overlapping regions.

MATERIALS AND METHODS

Construction of AGO1, AGO2, DCL1, and DCL2 Templates and Synthesis of dsRNA

Primers were designed to generate PCR amplicons of 658–912 bp in length for the manually-designed construct or of 173–193 bp in length for the tool-designed construct (Zhao Bioinformatics

Laboratory tool)[1], corresponding to exons of selected target genes, in which *Fg* represents *Fusarium graminearum*: *FgAGO1* (FGSG_08752), *FgAGO2* (FGSG_00348), *FgDCL1* (FGSG_09025), and *FgDCL2* (FGSG_04408) (**Supplementary Figures S1–S4**). The target gene sequences were amplified from *Fg* wt strain IFA65 cDNA using target-specific primers (**Supplementary Table S1**). The length of manually selected sequences were 658 bp for *FgAGO1*, 871 bp for *FgAGO2*, 912 bp for *FgDCL1*, and 870 bp for *FgDCL2*, while the respective tool-designed sequences were 173, 192, 182, and 193 bp in length, respectively. The respective sequences of tool- and manually-designed constructs did not overlap.

The construction of pGEMT plasmids comprised of the tool- and manually-designed target sequences was performed using restriction enzyme-cloning strategies. The first step in constructing pGEMT plasmids containing manually-designed double targets was to amplify target sequences of *AGO1*, *AGO2*, *DCL1*, and *DCL2* from the confirmed plasmids with primers containing restriction sites (**Supplementary Table S1**). The manually-designed dsRNA targeting *FgAGO1* and *FgAGO2* had a length of 1,529 bp and was therefore named ago1/ago2_1529nt. According to this scheme the other manually-designed dsRNAs were named ago1/dcl1_1570nt, ago1/dcl2_1528nt, ago2/dcl1_1783nt, ago2/dcl2_1741nt, and dcl1/dcl2_1782nt. Briefly, an *AGO2* PCR fragment was inserted between NotI and NdeI restriction sites of pGEMT plasmids containing *AGO1* or *DCL1* target sequences to generate ago1/ago2_1529nt and ago2/dcl1_1583nt constructs. The PCR fragment of *AGO1* was inserted between NotI and NdeI restriction sites of pGEMT plasmids containing the *DCL1* target sequence to construct ago1/dcl1_1570nt target plasmid. The other manually designed constructs (ago1/dcl2_1528nt, ago2/dcl2_1741nt and dcl1/dcl2_1782nt) were generated following the same procedure as described above: DCL2 PCR fragments were inserted in the AGO1 background (using NotI and NdeI), in AGO2 (using NotI and BstXI) and in DCL1 (using NotI and SalI). To construct pGEMT plasmids containing tool-designed target sequences (ago1/ago2_365nt, ago1/dcl1_355nt, ago2/dcl1_374nt, ago1/dcl2_366nt), the single targets were amplified using primers containing a restriction site (**Supplementary Table S1**), as described above. A tool-designed sequence of *DCL1* was inserted between NotI and SalI restriction sites of the pGEMT plasmid containing *AGO1* and *AGO2* targets to generate ago1/dcl1_355nt and ago2/dcl1_374nt constructs, respectively. The *DCL2* fragment was inserted between the NotI and SalI restriction sites of the pGEMT plasmid containing the *AGO1* sequence to construct ago1/dcl2_366nt. Finally, *AGO2* was inserted between the NotI and SalI restriction sites of the pGEMT plasmid containing the *AGO1* target sequence to generate an ago1/ago2_365nt construct. As a negative control a previously described dsRNA corresponding to a 720 nt long fragment of the jellyfish green fluorescent protein (GFP) was used (Koch et al., 2016).

MEGAscript Kit High Yield Transcription Kit (Ambion) was used for dsRNA synthesis by following the manufacturers' instructions using primers containing a T7 promoter sequence at the 5' end of both forward and reverse primers (**Supplementary Table S1**).

[1]http://plantgrn.noble.org/pssRNAit/

Spray Application of dsRNA on Barley Leaves

The second leaves of 2- to 3 week old barley cultivar (cv.) Golden Promise were detached and transferred to square Petri plates containing 1% water-agar. The dsRNA was diluted in 500 µl of water to a final concentration of 20 ng μl^{-1}. For the Tris-EDTA (TE) control, TE buffer was diluted in 500 µl of water, corresponding to the amount used for dilution of the dsRNA. The typical dsRNA concentration after elution was 500 ng μl^{-1}, representing a buffer concentration of 400 µM of Tris-HCL and 40 µM of EDTA in the final dilution. Leaves were sprayed using a spray flask as described earlier (Koch et al., 2016). The upper half of each plate containing ten detached leaves was evenly sprayed (3–4 puffs) with the different tool- and manually-designed dsRNAs or TE buffer and subsequently kept at room temperature. Forty-eight hours after spraying, leaves were drop-inoculated with three 20 µl drops of *Fg* suspension containing 5×10^4 conidia ml^{-1} water. After inoculation, plates were closed and incubated for 5 days at room temperature. The relative infection of the leaves was recorded as the infection area (**Supplementary Figure S5**) (by determining the size of the chlorotic lesions) relative to the total leaf area using ImageJ software (Schneider et al., 2012). We produced four biological replicates for independent sample collection. Each treatment group was compared to the TE-Buffer control using students *t*-test.

Fungal Transcript Analysis

To assess the silencing of the *FgAGO* and *FgDCL* genes, mRNA expression analysis was performed using quantitative reverse-transcription PCR (qRT-PCR). RNA extraction from the diseased leaves was performed with TRIzol (Invitrogen) following the manufacturer's instructions. Freshly extracted mRNA was used for cDNA synthesis using a qScript™ cDNA kit (Quantabio). For qRT-PCR, 10 ng of cDNA was used as a template with the reactions run in a QuantStudio 5 Real-Time PCR system (Applied Biosystems). Amplifications were performed in 7.5 µl of SYBR® Green JumpStart Taq ReadyMix (Sigma-Aldrich) with 5 pmol of oligonucleotides. Each sample had three technical repetitions. Primers were used for studying expressions of *FgAGO* and *FgDCL* genes with reference to the *Elongation factor 1-alpha* (*EF1-a*) gene (FGSG_08811) and *ß-tubulin* (**Supplementary Table S1**). After an initial activation step at 95°C for 5 min, 40 cycles (95°C for 30 s, 57°C for 30 s, 72°C for 30 s) were performed. Cycle threshold (Ct) values were determined using the 7,500 Fast software supplied with the instrument. Levels of *FgAGO* and *FgDCL* transcripts were determined via the $2^{-\Delta\Delta Ct}$ method (Livak and Schmittgen, 2001) by normalizing the amount of target transcript to the amount of the reference transcripts of the *EF1-a (translation elongation-factor 1α)* and *ß-tubulin*.

siRNA Prediction

Sequences of the single manually- and tool-designed dsRNA constructs for each gene, *FgAGO1*, *FgAGO2*, *FgDCL1*, and *FgDCL2*, were split into k-mers of 21 bases and mapped to the coding sequences of the four *FgAGO* and *FgDCL* genes. The efficient siRNAs were calculated on the basis of the thermodynamic properties of the siRNA-duplex, the 5'-nucleotide of the guide strand and the target site accessibility based on the default parameters of the SI-FI software tool[2]. These parameters were: no mismatches to the target sequence, a 5'-A or -U on the potential guide strand, a higher minimum free energy (MFE) on the 5'-end of the guide strand compared to the passenger strand and good target site accessibility; the default parameters were used.

RESULTS

Spray-Induced Gene Silencing by AGO- and DCL-dsRNAs Reduces *Fg* Infection

We assessed whether *FgAGO* and *FgDCL* genes are suitable targets for SIGS-mediated plant protection strategies. Detached barley leaves were sprayed with 20 ng μl^{-1} dsRNA and drop-inoculated 48 h later with a suspension of *Fg* conidia. After 5 dpi, necrotic lesions were visible at the inoculation sites of leaves sprayed with TE buffer or non-homologous GFP-dsRNA as negative controls. All homologous dsRNAs reduced the Fg-induced symptoms, as revealed by significantly smaller lesions in detached barley leaves (**Figure 1**). Infected areas were reduced on the average by 50% compared to the control (**Figure 1**). The highest infection reduction of 60% was reached with dsRNAs targeting ago1/ago2_365nt and ago1/dcl1_1570nt (**Figure 1**). The lowest disease resistance efficiencies of 31% were shown for the ago2/dcl1_1783nt dsRNA construct (**Figure 1**).

DCL-dsRNAs Exhibited Higher Target Gene Silencing Than AGO-dsRNAs

To analyze whether the observed resistance phenotypes were provoked by target gene silencing, we measured the transcript levels of *FgAGO* and *FgDCL* genes of *Fg* grown in the infected leaf tissue by qRT-PCR. As anticipated, the relative transcript levels of targeted genes *FgAGO1*, *FgAGO2, FgDCL1,* and *FgDCL2* were reduced after the inoculation of leaves sprayed with the respective dsRNA constructs (**Figures 2A,B**), except for *FgAGO1*, if targeted with tool-designed constructs ago1/dcl1_355nt, ago1/dcl2_366nt, and ago1/ago2_365nt (**Figure 2A**). However, regarding those three constructs, we detected silencing effects for the second target gene, as the *FgDCL1* expression was reduced by 47%, *FgDCL2* by 44%, and *FgAGO2* by 52% (**Figure 2A**). The most efficient construct in terms of overall target gene silencing was ago2/dcl1_374nt, which reduced the transcripts of *FgAGO2* and *FgDCL1* by 40 and 74%, respectively, compared to the TE control (**Figures 2A,B**).

Notably, if we compared the results for the tool-designed dsRNA constructs with the manually-designed dsRNAs we observed similar results for the *FgAGO1* target-silencing

[2]http://labtools.ipk-gatersleben.de/

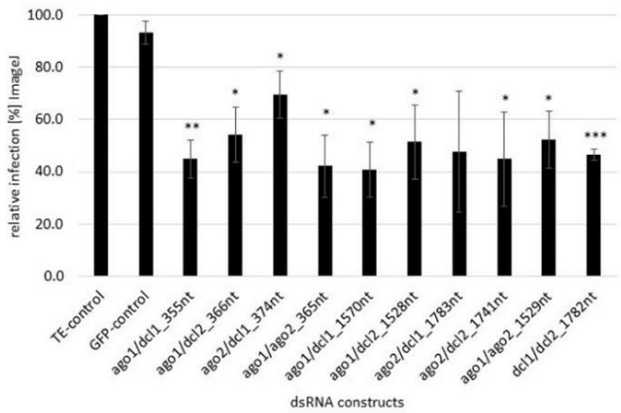

FIGURE 1 | Quantification of infection symptoms of *Fg* on barley leaves sprayed with AGO/DCL-targeting dsRNAs. Detached leaves of 3 week-old barley plants were sprayed with AGO/DCL-targeting dsRNAs or TE buffer. After 48 h, leaves were drop inoculated with 5×10^4 ml^{-1} of macroconidia and evaluated for infection symptoms at 5 dpi. Infection area, shown as the percent of the total leaf area for 10 leaves for each dsRNA and the TE control relative to the infected leaf area. Bars represent mean values ± SDs of three independent experiments. Asterisks indicate statistical significance (*$p < 0.05$, **$p < 0.01$, ***$p < 0.001$, students *t*-test).

(**Figures 2A,B**). The constructs ago1/dcl1_1570nt and ago1/dcl2_1528nt reduced *FgAGO1* transcripts by only 17 and 29%, respectively (**Figure 2B**). Analyzing the transcript levels of *FgAGO2* revealed that: (a) the silencing efficiencies of ago2/dcl1_1783nt and ago2/dcl2_1741nt were higher than *FgAGO1* target silencing and (b) targeting both *FgAGO* genes with the ago1/ago2_1529nt construct resulted in 50% reduction for *FgAGO1* and 62% for *FgAGO*2. This, therefore, showed the highest overall *FgAGOs* gene silencing (**Figure 2B**).

Interestingly and consistent with the tool-designed target gene silencing results, we detected the strongest reduction of >70% for *FgDCL1* (**Figure 2B**). For example, ago2/dcl1_1783nt-dsRNA provoked a 79% reduction of *FgDCL1* transcripts. Target gene silencing for *FgDCL2* was also highly efficient, as use of all three constructs, ago1/dcl2_1528nt, ago2/dcl2_1741nt and dcl1/dcl2_1782nt, resulted in an ˜60% silencing efficiency (**Figure 2B**). The most efficient construct in terms of overall target gene silencing was dcl1/dcl2_1782nt, which reduced the transcripts of *FgDCL1* and *FgDCL2* by 78 and 58%, respectively, compared to control. Overall, these results suggest that silencing conferred by AGO- and DCL-dsRNAs exhibited the highest efficiency for silencing of *FgDCL1* (AVE: 70%), followed by *FgDCL2* (AVE: 58%), *FgAGO2* (AVE: 48%) and *FgAGO1* (AVE: 26%) (**Table 1**).

Manually-Designed dsRNAs Exhibit Higher Gene-Silencing Efficiencies Than Tool-Designed dsRNAs

To assess whether tool-designed dsRNA is more efficient than manually designed constructs, we directly compared target gene-silencing efficiencies of both design approaches (**Figure 3**). We observed that target gene silencing of manually-designed

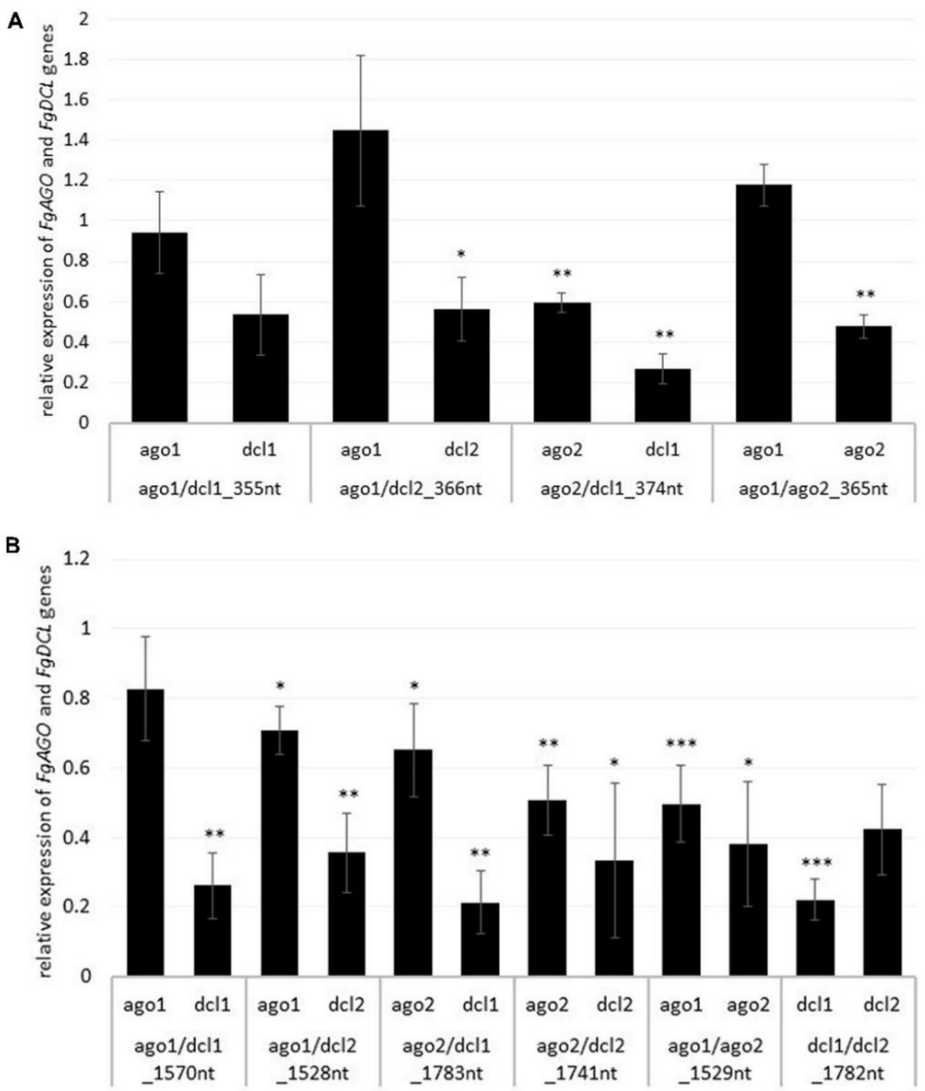

FIGURE 2 | Relative expression of the respective fungal *DCLs* and *AGOs* 5 dpi on **(A)** tool- and **(B)** manually-designed-dsRNA-sprayed leaves. The expression was measured via the $2^{-\Delta\Delta Ct}$ method in which the expression of the respective *AGOs* and *DCLs* was normalized against the fungal reference genes *EF1α (translation elongation-factor 1 α)* and *ß-tubulin*, and this Δ-Ct value was then normalized against the Δ-Ct of the GFP control. Error bars represent the SE of the four independent experiments, each using 10 leaves of 10 different plants for each transgenic line. Asterisks indicate statistical significance (*$p < 0.05$, **$p < 0.01$, ***$p < 0.001$, students *t*-test).

constructs was superior to tool-designed dsRNA (**Figure 3**), except for *FgAGO2*, for which we found no differences between tool- or manually-designed dsRNA. Based on these findings and considering previous results, we anticipated that larger dsRNA constructs resulted in higher numbers of efficient siRNAs (Höfle et al., 2019; Koch et al., 2019). As the tool-designed constructs were <200 nt in length compared to >650 nt for the manually-designed dsRNA (**Table 2** and **Supplementary Figures S1–S4**), we calculated bioinformatically the possible siRNA hits in the *FgAGO and FgDCL* target genes for all tested dsRNA constructs (**Table 2**).

For the manually-designed dsRNA, which target different regions of the respective genes, we calculated siRNAs that were 4- to 10-fold more efficient compared to the tool-designed constructs (**Table 2**), confirming that the dsRNA precursor length probably plays a role in determining the number of derived siRNAs. For example, we predicted 49 efficient siRNAs deriving from the 912 nt manually-designed dsRNA, which targets *FgDCL1*, which is 10-fold >5 siRNA hits derived from the 182 nt tool-designed *FgDCL1*-dsRNA (**Table 2**). Notably, these differences resulted in only an overall 10% silencing efficiency decrease of the tool-designed dsRNA compared to the manually-designed constructs targeting *FgDCL1* (**Table 2**). Together, these data suggest that longer dsRNAs result in a higher number of efficient siRNAs, but there is no stringent correlation between the number of efficient siRNAs and the increase in target gene silencing (**Table 2**).

TABLE 1 | Overview of target gene-silencing efficiencies of different tested AGO- and DCL-dsRNA constructs.

		FgAGO1	*FgAGO2*	*FgDCL1*	*FgDCL2*
Tool	AGO1-DCL1	6	–	47	-
	AGO1-DCL2	No silencing	–	–	44
	AGO2-DCL1	–	41	73	–
	AGO1-AGO2	No silencing	52	-	–
	Average	6	46	60	44
Manual	AGO1-DCL1	17	–	74	–
	AGO1-DCL2	29	–	–	64
	AGO2-DCL1	–	35	79	–
	AGO2-DCL2	–	49	–	67
	AGO1-AGO2	50	62	–	–
	DCL1-DCL2	–	–	78	58
	Average	32	49	77	63

TABLE 2 | Number of efficient siRNAs and silencing efficiency of double dsRNA constructs.

Target gene	Length (nt)		Efficient siRNAs		AVE: silencing efficiency	
	Tool	Manual	Tool	Manual	Tool	Manual
FgAGO1	173	658	13	57	6	32
FgAGO2	192	871	12	58	46	49
FgDCL1	182	912	5	49	60	77
FgDCL2	193	870	9	92	44	63

These efficient sRNA are designated by the dsRNA design tool si-Fi (http://labtools.ipk-gatersleben.de).

DISCUSSION

Microbial pathogens and pests, unlike mammals, are amenable to environmental sRNAs, meaning that they can take up non-coding RNAs from the environment, and these RNAs maintain their RNAi activity (Winston et al., 2007; Whangbo and Hunter, 2008; McEwan et al., 2012). This knowledge raises the possibility that plants can be protected from pathogens/pests by exogenously supplied RNA biopesticides (for review, see Mitter et al., 2017b; Cai et al., 2018b; Dubrovina and Kiselev, 2019; Gaffar and Koch, 2019; Dalakouras et al., 2020). Possible agronomic application of environmental RNA is affirmed by the high sensitivity of *Fg* to dsRNAs and siRNAs (Koch et al., 2016). Here, we demonstrated that targeting, via SIGS, key components of the *Fg* RNAi machinery, such as *AGO* and *DCL* genes, could protect barley leaves from *Fg* infection. Our findings, together with other reports, underline that *Fg* RNAi pathways play a crucial role in regulating fungal development, growth, reproduction, mycotoxin production and pathogenicity (Kim et al., 2015; Son et al., 2017; Gaffar et al., 2019). However, the mechanistic role of *Fg* RNAi components in these processes are inadequately understood. Nevertheless, existing data suggest that there is a functional diversification of *Fg*AGO1/*Fg*DCL2- and *Fg*AGO2/*Fg*DCL1-regulated pathways (Chen et al., 2015; Son et al., 2017; Zeng et al., 2018; Gaffar et al., 2019).

Based on these findings, the dsRNAs tested in this study were designed to target *FgAGO* and *FgDCL* genes pairwise.

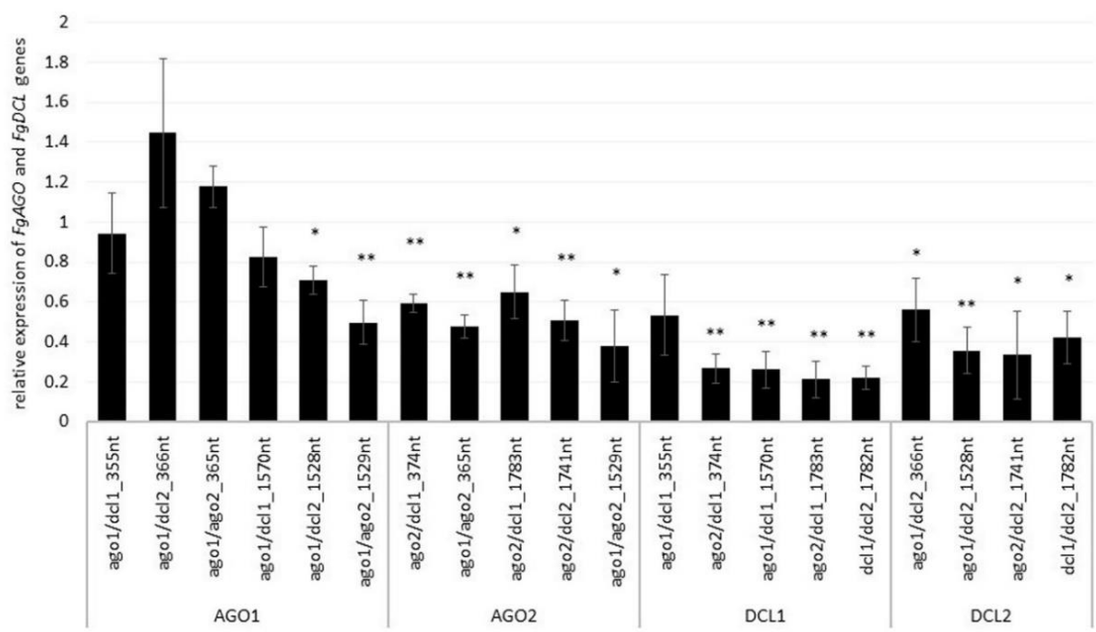

FIGURE 3 | Direct comparison of long (manual) and short (tool) constructs. Relative expression of the respective fungal *DCLs* and *AGOs* 5 dpi on dsRNA-sprayed leaves is grouped by the target gene. The expression was measured via the ΔΔ-Ct method in which the expression of the respective *AGOs* and *DCLs* was normalized against the fungal reference gene *EF1α (translation elongation-factor 1 α)* and *β*-tubulin, and this Δ-Ct value was then normalized against the Δ-Ct of the GFP control. The asterisks indicate a significant expression of the sprayed leaves in comparison to the mock-treated TE controls. Bars represent mean values ± SE of the four independent experiments.

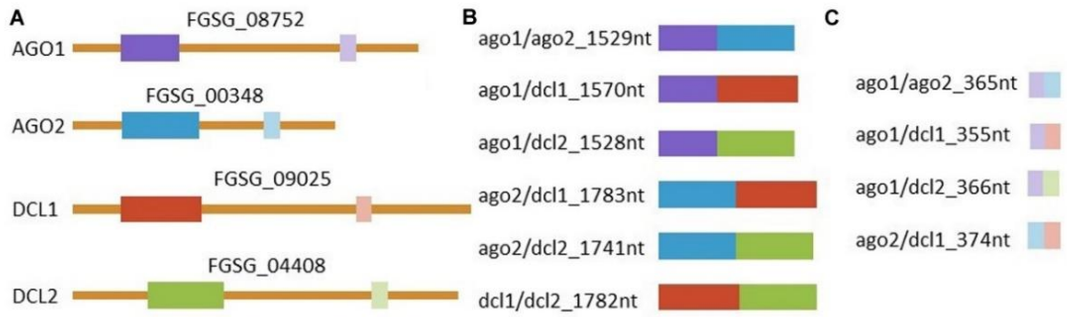

FIGURE 4 | Representation of dsRNAs and the complementary region in the corresponding genes. **(A)** Graphic representation of all four targeted mRNAs and their respective accessions with target regions marked in colors. Manually selected regions are marked in dark colors and regions selected by the pssRNAit tool[1] for better target accessibility are marked with light colors. All **(B)** manually and **(C)** tool designed dsRNAs triggers are shown. RNAs are represented correctly scaled to each other.

Thus, we generated six different dsRNA constructs covering all possible *AGO-DCL* combinations (**Figure 4**). Spraying the different dsRNAs onto barley leaves resulted in ∼50% inhibition of fungal infection for all constructs (**Figure 1**). By analyzing the silencing efficiencies of the different dsRNA constructs, we found that the expression of *FgDCLs* genes was more suppressed than *FgAGOs* genes (**Table 1**). More importantly, the expression of *FgAGO1* was completely unaffected, regardless of which dsRNA was sprayed. Based on this result, we could speculate that *Fg*AGO1 is required for binding of SIGS-associated siRNAs; thus, loss of function mediated by SIGS will not work. Of note, Δ*AGO1* mutants of *Fg* were only slightly compromised in SIGS and less sensitive to dsRNA treatments, indicating redundant functions of *Fg*AGO1 and *Fg*AGO2 in the binding of SIGS-derived siRNAs (Gaffar et al., 2019). However, further studies must explore the mechanistic role of *Fg*AGO1 in SIGS.

While our data showed that SIGS-mediated downregulation of *FgDCLs* gene expression resulted in inhibition of *Fg* infection, we cannot exclude the possibility of sprayed dsRNAs being processed by plant DCLs, which would explain the effective silencing even with silenced fungal DCLs. Consistent with this finding, previous studies demonstrated that spraying of siRNAs led to the induction of local and systemic RNAi in plants (e.g., Dalakouras et al., 2016; Koch et al., 2016). These findings are significant contributions to our mechanistic understanding of RNAi spray technology, as our previous data indicate that effective SIGS requires the processing of dsRNAs by the fungal RNAi machinery (Koch et al., 2016; Gaffar et al., 2019). Whereas HIGS mainly relies on the host plant's ability to produce mobile siRNAs (generated from transgene-derived dsRNAs), the mechanism of gene silencing by exogenously delivered dsRNA constitutes a more complex situation; for instance, the possible involvement of the silencing machinery of the host and/or pathogen (**Figure 5**). Our previous finding that unprocessed long dsRNA is absorbed from leaf tissue (Koch et al., 2016) has important implications for future disease control strategies based on dsRNA. It is very likely that the application of longer dsRNAs might be more efficient than the application of siRNAs, given their dsRNAs more efficient translocation (Koch et al., 2016). Moreover, in contrast to using only one specific siRNA, processing of long dsRNA into many different inhibitory siRNAs by the fungus may reduce the chance of pathogen resistance under field test conditions. However, RNAi-based plant protection technologies are limited by the uptake of RNAi-inducing trigger molecules, either siRNAs and/or dsRNAs; both RNA types have been shown to confer plant disease resistance independent of how they were applied/delivered (i.e., endogenously or exogenously).

Previously, we discovered that longer dsRNAs of 400–800 nt exhibited a higher gene-silencing efficiency and a stronger disease resistance than 200 nt dsRNAs (Koch et al., 2019) indicating that the quantity of siRNAs derived from a longer dsRNA precursor is simply higher. To test whether the length and/or the selected target gene sequence influences silencing efficiencies, we constructed 10 different dsRNA constructs

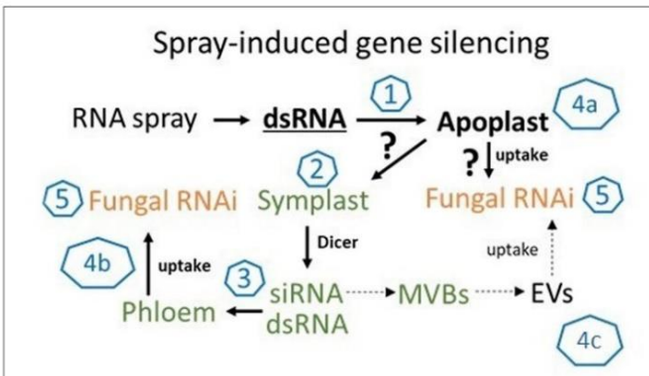

FIGURE 5 | The molecular mechanism of SIGS is controlled by the fungal silencing machinery. In summary, our findings support the model that SIGS involves: (1) uptake of sprayed dsRNA by the plant (via stomata); (2) transfer of apoplastic dsRNAs into the symplast (DCL processing into siRNAs); (3) systemic translocation of siRNA or unprocessed dsRNA via the vascular system (phloem/xylem); (4) uptake of apoplastic dsRNA (a) or symplastic dsRNA/siRNA by the fungus (b) or siRNAs from multivesicular body (MVBs) derived extracellular vesicles (EVs) (c); (5) processing into siRNA by fungal DCL.

targeting *FgAGO/FgDCL* pairs (**Figure 4**). For the design of the dsRNA constructs we used a dsRNA design tool[3] that generates dsRNAs of shorter lengths (173–197 nt), compared them to manually selected sequences (658–912 nt) and calculated the number of efficient siRNAs for each construct using si-Fi 2.1[4] *in silico* prediction tool (**Table 2**). These differences in length are inherent in the design methods and represent therefore the different design approaches. While the tool-designed RNA-trigger are designed to target a specific and well accessible region of the target mRNA the manual design approach pays little attention to these factors and is based on a more or less random selection of regions. Notably, we found that the number of efficient siRNAs derived from the longer, manually-designed dsRNAs was 4- to 5-fold higher for the constructs that target *FgAGO1* and *FgAGO2*. Moreover, the manually-designed constructs targeting *FgDCL1* and *FgDCL2* resulted in 10-fold more efficient siRNAs than the tool-designed versions (**Table 2**). However, such a correlation was only observed when we compared tool- vs. manually-designed dsRNA (<200 vs. >650 nt constructs). If we attempt to predict the number of efficient siRNAs of all the manually-designed dsRNAs, based on the length of their precursors, we obtained contrasting results. For example, the 912 nt precursor dsRNA that targets *FgDCL1* resulted in 49 efficient siRNA hits, which is approximately half of the 92 siRNA hits for the 870-nt dsRNA designed to target *FgDCL2* (**Table 2**). Importantly, the tested dsRNAs that target *FgDCL1*, which showed the lowest number of siRNAs, revealed the highest efficiencies compared to all other constructs (**Table 2**). Together, our data support the notion that longer dsRNAs tend to result in higher numbers of siRNA, although this can differ in particular cases. However, these data were obtained from *in silico* predictions; therefore, their accuracies remain unknown. Small RNA-sequencing must be performed to quantify, analyze and map the SIGS-derived siRNAs to their target genes as well as their dsRNA precursors. Besides siRNA concentration, the siRNA sequence represents a crucial determinant affecting silencing efficiency of its complementary target genes (Ossowski et al., 2008). In addition, mapping of siRNAs to their target sequence revealed processing patterns that might help to define principles for RNAi trigger design, producing effective siRNAs (Yang et al., 2013; Koch et al., 2016; Baldwin et al., 2018). Importantly, to construct our manually-designed dsRNAs, we performed a random selection of sequences complementary to the specific target genes. Moreover, to guarantee optimal silencing, we chose longer dsRNA sequences compared to the tool-designed dsRNAs. Thus, a random selection of longer target sequences, which are more effective in target silencing, tends to increase off-target effects *per se*, due to the increase in the number of different potential siRNAs (Roberts et al., 2015). Shorter target sequences, which are also specifically selected to produce potential siRNAs with a minimal potential to silence unintended targets, could greatly reduce these off-target effects. Therefore, based on our results obtained with the tool-designed dsRNAs and the work of others, we suggest using minimal-length dsRNA sequences carefully selected based on known design criteria requirements. Another possible way to achieve high silencing efficiencies while retaining high target specificity (less off-target effect) could be the construction of dsRNAs repeating a shorter tool- designed sequence several times.

Nevertheless, the number of efficient siRNAs that reach the fungus depends on the uptake efficiency of sprayed dsRNA molecules and that can differ depending on the parameters which determine the uptake efficiency, such as the stomata opening (Koch et al., 2016). Additionally, as we previously found in SIGS, the concentration of siRNAs in the target organism (i.e., fungus) can vary and mainly rely on the uptake of unprocessed dsRNA from the plant's apoplast and their processing by fungal DCLs (Koch et al., 2016; Gaffar et al., 2019). Finally, and even more important than quantities of target-specific siRNAs in determining silencing efficacy, is the target accessibility of a siRNA (Reynolds et al., 2004; Shao et al., 2007). Therefore, the design of RNAi triggers that likely mediate the efficient uptake of dsRNAs and/or siRNAs by the target pathogen is crucial in the success of SIGS as well as HIGS technologies.

Together, our results indicate that silencing fungal RNAi pathway genes, especially *DCL* genes, using SIGS efficiently increases plant disease resistance toward necrotrophic fungal pathogens, such as *Fg*. Moreover, our results support the notion that fungal RNAi-related genes in *Fg* play an essential, direct or indirect role in pathogenicity and/or virulence (Gaffar et al., 2019). These findings are consistent with other reports demonstrating that the two DCL proteins (DCL1 and DCL2) of the necrotrophic fungal pathogen *Botrytis cinerea* (*Bc*) play a central role in disease development (Wang et al., 2016). These authors showed that the application of sRNAs or dsRNAs on fruits, vegetables and flowers targeting *BcDCL1* and *BcDCL2* genes significantly inhibited gray mold disease. Of note, the same group previously discovered that *Bc* delivers sRNAs into plant cells to silence host immunity genes, a phenomenon called 'cross-kingdom RNAi (ckRNAi)' (Weiberg et al., 2013). Emerging data further suggest that some sRNA effectors can target multiple host defense genes to enhance *Bc* pathogenicity. For example, Bc-siR37 suppresses host immunity by targeting at least 15 *Arabidopsis* genes, including WRKY transcription factors, receptor-like kinases and cell wall-modifying enzymes (Wang B. et al., 2017). Moreover, one of the most destructive biotrophic pathogens of wheat *Puccinia striiformis* also delivers fungal sRNAs, such as microRNA-like RNA1 (milR1), into host cells and suppresses wheat *Pathogenesis-related 2* (*PR-2*) in the defense pathway (Wang M. et al., 2017). Notably, such ckRNAi-related sRNA effectors are produced by fungal DCL proteins, and thus SIGS of fungal DCLs abolishes sRNA production and attenuates fungal pathogenicity and growth. However, whether our findings suggest that *Fg* utilizes ckRNAi-related sRNAs to suppress host immunity needs further exploration.

More importantly, while several studies have demonstrated bidirectional ckRNAi and sRNA trafficking between plant hosts

[3]http://plantgrn.noble.org/pssRNAit/

[4]http://labtools.ipk-gatersleben.de/

and their interacting fungal pathogens (Zhang et al., 2012, 2016; Weiberg et al., 2015; Wang B. et al., 2017; Wang M. et al., 2017; Zhu et al., 2017; Cai et al., 2018a; Dubey et al., 2019; Zanini et al., 2019) the mechanisms underlying the transfer and uptake of transgene-derived artificial sRNAs (HIGS) as well as exogenously applied dsRNA (SIGS) remain elusive. Further research is needed to determine, for example: (a) how plant and fungal-silencing machinery contributes to HIGS and SIGS; (b) the nature of the inhibitory RNA that translocates from the plant to the fungus after its transgenic expression or spray application; (c) how that RNA crosses the plant-fungal interface; and (d) how dsRNA is transported at the apoplast-symplast interface. Therefore, addressing these questions is key for making RNAi-based strategies a realistic and sustainable approach in agriculture.

DATA AVAILABILITY STATEMENT

All datasets generated for this study are included in the article/**Supplementary Material**.

AUTHOR CONTRIBUTIONS

AK designed the study and wrote the manuscript. BW, FG, DB, and JS conducted the experiments. AK and BW analyzed all the data and drafted the figures. JS and DB conducted the RNA spray experiments. BW performed the bioinformatics analysis. All authors reviewed the final manuscript.

FUNDING

This work was supported by the Deutsche Forschungsgemeinschaft, Research Training Group (RTG) 2355 (project number 325443116) to AK.

ACKNOWLEDGMENTS

This work was supported by Deutsche Forschungsgemeinschaft to AK (RTG:2355) and Deutscher Akademischer Austauschdienst to FG.

SUPPLEMENTARY MATERIAL

The Supplementary Material for this article can be found online at: https://www.frontiersin.org/articles/10.3389/fpls.2020.00476/full#supplementary-material

FIGURES S1–S4 | Coding sequences (CDS) of the respective *Fg* target gene with the sequences of the dsRNA marked (blue, tool-designed; red, manually designed).

FIGURE S5 | Representative pictures of barley (golden promise) leaves sprayed with 10 μg (20 ng/μl) of respective dsRNA in TE-Buffer and the control without dsRNA. DsRNA was applied on the upper half of 10 leaves and 2 days after spraying the leaves were inoculated with three 20 μl droplets of *Fg* (50,000 spores/ml). The pictures were taken 5 dpi.

TABLE S1 | Primers used in this study.

REFERENCES

Baldwin, T., Islamovic, E., Klos, K., Schwartz, P., Gillespie, J., Hunter, S., et al. (2018). Silencing efficiency of dsRNA fragments targeting *Fusarium graminearum* TRI6 and patterns of small interfering RNA associated with reduced virulence and mycotoxin production. *PLoS One* 13:e0202798. doi: 10.1371/journal.pone.0202798

Baulcombe, D. (2004). RNA silencing in plants. *Nature* 431, 356–363.

Bharti, P., Jyoti, P., Kapoor, P., Sharma, V., Shanmugam, V., and Yadav, S. K. (2017). Host-induced silencing of pathogenicity genes enhances resistance to *Fusarium oxysporum* wilt in tomato. *Mol. Biotechnol.* 59, 343–352. doi: 10.1007/s12033-017-0022-y

Borges, F., and Martienssen, R. A. (2015). The expanding world of small RNAs in plants. *Nat. Rev. Mol. Cell Biol.* 16, 727–741. doi: 10.1038/nrm4085

Cai, Q., He, B., Kogel, K. H., and Jin, H. (2018a). Cross-kingdom RNA trafficking and environmental RNAi nature's blueprint for modern crop protection strategies. *Curr. Opin. Microbiol.* 46, 58–64. doi: 10.1016/j.mib.2018.02.003

Cai, Q., Qiaom, L., Wang, M., He, B., Lin, F. M., Palmquist, J., et al. (2018b). Plants send small RNAs in extracellular vesicles to fungal pathogen to silence virulence genes. *Science* 360, 1126–1129. doi: 10.1126/science.aar4142

Chen, W., Kastner, C., Nowara, D., Oliveira-Garcia, E., Rutten, T., Zhao, Y., et al. (2016). Host-induced silencing of *Fusarium culmorum* genes protects wheat from infection. *J. Exp. Bot.* 67, 4979–4991. doi: 10.1093/jxb/erw263

Chen, Y., Gao, Q., Huang, M., Liu, Y., Liu, Z., Liu, X., et al. (2015). Characterization of RNA silencing components in the plant pathogenic fungus *Fusarium graminearum*. *Sci. Rep.* 5:12500. doi: 10.1038/srep12500

Cheng, W., Song, X. S., Li, H. P., Cao, L. H., Sun, K., Qiu, X. L., et al. (2015). Host-induced gene silencing of an essential chitin synthase gene confers durable resistance to Fusarium head blight and seedling blight in wheat. *Plant Biotechnol. J.* 13, 1335–1345. doi: 10.1111/pbi.12352

Dalakouras, A., Wassenegger, M., Dadami, E., Ganopoulos, I., Pappas, M. L., and Papadopoulou, K. (2020). Genetically modified organism-free RNA interference: exogenous. *Plant Physiol.* 182, 38–50.

Dalakouras, A., Wassenegger, M., McMillan, J. N., Cardoza, V., Maegele, I., and Dadami, E., (2016). Induction of silencing in plants by high-pressure spraying of in vitro-synthesized small RNAs. *Front. Plant Sci.* 7:1327. doi: 10.3389/fpls.2016.01327

Dubey, H., Kiran, K., Jaswal, R., Jain, P., Kayastha, A. M., and Bhardwaj, S. C. (2019). Discovery and profiling of small RNAs from *Puccinia triticina* by deep sequencing and identification of their potential targets in wheat. *Funct. Integr. Genomics* 19, 391–407.

Dubrovina, A. S., and Kiselev, K. V. (2019). Exogenous RNAs for gene regulation and plant resistance. *Int. J. Mol. Sci.* 20:2282. doi: 10.3390/ijms20092282

Gaffar, F. Y., Imani, J., Karlovsky, J. P., Koch, A., and Kogel, K. H. (2019). Various components of the RNAi pathway are required for conidiation, ascosporogenesis, virulence, DON production and SIGS-mediated fungal inhibition by exogenous dsRNA in the Head Blight pathogen *Fusarium graminearum*. *Front. Microbiol.* 10:1662. doi: 10.3389/fmicb.2019.01662

Gaffar, F. Y., and Koch, A. (2019). Catch me if you can! RNA silencing-based improvement of antiviral plant immunity. *Viruses* 11:673.

Ghag, S. B., Shekhawat, U. K., and Ganapathi, T. R. (2014). Host-induced post-transcriptional hairpin RNA-mediated gene silencing of vital fungal genes confers efficient resistance against Fusarium wilt in banana. *Plant Biotechnol. J.* 12, 541–553. doi: 10.1111/pbi.12158

Goswami, R. S., and Kistler, H. C. (2004). Heading for disaster: *Fusarium graminearum* on cereal crops. *Mol. Plant Pathol.* 5, 515–525. doi: 10.1111/j.1364-3703.2004.00252.x

Guo, Q., Liu, Q., Smith, N. A., Liang, G., and Wang, M. B. (2016). RNA silencing in plants: mechanisms, technologies and applications in horticultural crops. *Curr. Genomics* 17, 476–489. doi: 10.2174/1389202917666160520103117

Höfle, L., Shrestha, A., Jelonek, L., and Koch, A. (2019). Study on the efficiency of dsRNAs with increasing length in RNA-based silencing of the *Fusarium CYP51* genes. *RNA Biol.* 17, 463–473.

Hu, Z., Parekh, U., Maruta, N., Trusov, Y., and Botella, J. R. (2015). Down-regulation of *Fusarium oxysporum* endogenous genes by host-delivered RNA interference enhances disease resistance. *Front. Chem.* 3:1. doi: 10.3389/fchem.2015.00001

Ismaiel, A., and Papenbrock, J. (2015). Mycotoxins: producing fungi and mechanisms of phytotoxicity. *Agriculture* 5, 492–537. doi: 10.3390/agriculture5030492

Kaldis, A., Berbati, M., Melita, O., Reppa, C., Holeva, M., Otten, P., et al. (2018). Exogenously applied dsRNA molecules deriving from the Zucchini yellow mosaic virus (ZYMV) genome move systemically and protect cucurbits against ZYMV. *Mol. Plant Pathol.* 19, 883–895. doi: 10.1111/mpp.12572

Kazan, K., Gardiner, D. M., and Manners, J. M. (2012). On the trail of a cereal killer: recent advances in *Fusarium graminearum* pathogenomics and host resistance. *Mol. Plant Pathol.* 13, 399–413. doi: 10.1111/j.1364-3703.2011.00762.x

Ketting, R. F. (2011). The many faces of RNAi. *Dev. Cell* 20, 148–161. doi: 10.1016/j.devcel.2011.01.012

Kim, H. K., Jo, S. M., Kim, G. Y., Kim, D. W., Kim, Y. K., and Yun, S. H. (2015). A large-scale functional analysis of putative target genes of mating-type loci provides insight into the regulation of sexual development of the cereal pathogen *Fusarium graminearum*. *PLoS Genet.* 11:e1005486. doi: 10.1371/journal.pgen.1005486

Koch, A., Biedenkopf, B., Furch, A. C. U., Abdellatef, E., Weber, L., Linicus, L., et al. (2016). An RNAi-based control of *Fusarium graminearum* infections through spraying of long dsRNAs involves a plant passage and is controlled by the fungal silencing machinery. *PLoS Pathog.* 12:e1005901.

Koch, A., and Kogel, K.-H. (2014). New wind in the sails: improving the agronomic value of crop plants through RNAi-mediated gene silencing. *Plant Biotechnol. J.* 12, 821–831. doi: 10.1111/pbi.12226

Koch, A., Kumar, N., Weber, L., Keller, H., Imani, J., and Kogel, K. H. (2013). Host-induced gene silencing of cytochrome P450 lanosterol C14α-demethylase-encoding genes confers strong resistance to *Fusarium* spec. *Proc. Natl. Acad. Sci. U.S.A.* 110, 19324–19329.

Koch, A., Stein, E., and Kogel, K. H. (2018). RNA-based disease control as a complementary measure to fight *Fusarium* fungi through silencing of the azole target cytochrome P450 lanosterol C-14 α-demethylase. *Eur. J. Plant Pathol.* 152, 1003–1010. doi: 10.1007/s10658-018-1518-4

Koch, A., Höfle, L., Werner, B. T., Imani, J., Schmidt, A., Jelonek, L., et al. (2019). SIGS vs HIGS: a study on the efficacy of two dsRNA delivery strategies to silence Fusarium FgCYP51 genes in infected host and non-host plants. *Mol. Plant Pathol.* 20, 1636–1644. doi: 10.1111/mpp.12866

Konakalla, N. C., Kaldis, A., Berbati, M., Masarapu, H., and Voloudakis, A. E. (2016). Exogenous application of double-stranded RNA molecules from TMV p126 and CP genes confers resistance against TMV in tobacco. *Planta* 244, 961–969.

Kuck, K. H., Stenzel, K., and Vors, J. P. (2012). Sterol biosynthesis inhibitors. *Mod. Crop Prot. Compd.* 1, 761–805.

Livak, K. J., and Schmittgen, T. D. (2001). Analysis of relative gene expression data using real-time quantitative PCR and the 2- ΔΔCT method. *Methods* 25, 402–408. doi: 10.1006/meth.2001.1262

Machado, A. K., Brown, N. A., Urban, M., Kanyuka, K., and Hammond-Kosack, K. E. (2018). RNAi as an emerging approach to control Fusarium head blight disease and mycotoxin contamination in cereals. *Pest Manag. Sci.*74, 790–799. doi: 10.1002/ps.4748

Majumdar, R., Rajasekaran, K., and Cary, J. W. (2017). RNA interference (RNAi) as a potential tool for control of mycotoxin contamination in crop plants: concepts and considerations. *Front. Plant Sci.* 8:200. doi: 10.3389/fpls.2017.00200

McEwan, D. L., Weisman, A. S., and Hunter, C. P. (2012). Uptake of extracellular double-stranded RNA by SID-2. *Mol. Cell* 47, 746–754. doi: 10.1016/j.molcel.2012.07.014

McMullen, M., Bergstrom, G., De Wolf, E., Dill-Macky, R., Hershman, D., Shaner, G., et al. (2012). A unified effort to fight an enemy of wheat and barley: Fusarium head blight. *Plant Dis.* 96, 1712–1728. doi: 10.1094/PDIS-03-12-0291-FE

Mitter, N., Worrall, E. A., Robinson, K. E., Li, P., Jain, R. G., Taochy, C., et al. (2017a). Clay nanosheets for topical delivery of RNAi for sustained protection against plant viruses. *Nat. Plants* 3:16207. doi: 10.1038/nplants.2016.207

Mitter, N., Worrall, E. A., Robinson, K. E., Xu, Z. P., and Carroll, B. J. (2017b). Induction of virus resistance by exogenous application of double-stranded RNA. *Curr. Opin. Virol.* 26, 49–55. doi: 10.1016/j.coviro.2017.07.009

Nowara, D., Gay, A., Lacomme, C., Shaw, J., Ridout, C., Douchkov, D., et al. (2010). HIGS: host-induced gene silencing in the obligate biotrophic fungal pathogen *Blumeria graminis*. *Plant Cell* 22, 3130–3141. doi: 10.1105/tpc.110.077040

Ossowski, S., Schwab, R., and Weigel, D. (2008). Gene silencing in plants using artificial microRNAs and other small RNAs. *Plant J.* 53, 674–690. doi: 10.1111/j.1365-313x.2007.03328.x

Pareek, M., and Rajam, M. V. (2017). RNAi-mediated silencing of MAP kinase signalling genes (Fmk1, Hog1, and Pbs2) in *Fusarium oxysporum* reduces pathogenesis on tomato plants. *Fungal Biol.* 121, 775–784. doi: 10.1016/j.funbio.2017.05.005

Qi, T., Guo, J., Peng, H., Liu, P., Kang, Z., and Guo, J. (2019). Host-induced gene silencing: a powerful strategy to control diseases of wheat and barley. *Int. J. Mol. Sci.* 20:206.

Reynolds, A., Leake, D., Boese, Q., Scaringe, S., Marshall, W. S., and Khvorova, A. (2004). Rational siRNA design for RNA interference. *Nat. Biotechnol.* 22, 326–330. doi: 10.1038/nbt936

Roberts, A. F., Devos, Y., Lemgo, G. N., and Zhou, X. (2015). Biosafety research for non-target organism risk assessment of RNAi-based GE plants. *Front. Plant Sci.* 6:958. doi: 10.3389/fpls.2015.00958

Schneider, C. A., Rasband, W. S., and Eliceiri, K. W. (2012). NIH image to ImageJ: 25 years of image analysis. *Nat. Methods* 9, 671–675. doi: 10.1038/nmeth.2089

Shao, Y., Chan, C. Y., Maliyekkel, A., Lawrence, C. E., Roninson, I. B., and Ding, Y. (2007). Effect of target secondary structure on RNAi efficiency. *RNA* 13, 1631–1640. doi: 10.1261/rna.546207

Son, H., Park, A. R., Lim, J. Y., Shin, C., and Lee, Y. W. (2017). Genome-wide exonic small interference RNA-mediated gene silencing regulates sexual reproduction in the homothallic fungus *Fusarium graminearum*. *PLoS Genet.* 13:e1006595. doi: 10.1371/journal.pgen.1006595

Spolti, P., Del Ponte, E. M., Dong, Y., Cummings, J. A., and Bergstrom, G. C. (2014). Triazole sensitivity in a contemporary population of *Fusarium graminearum* from New York wheat and competitiveness of a tebuconazole-resistant isolate. *Plant Dis.* 98, 607–613. doi: 10.1094/PDIS-10-13-1051-RE

Vaucheret, H., Vazquez, F., Crété, P., and Bartel, D. P. (2004). The action of *ARGONAUTE1* in the miRNA pathway and its regulation by the miRNA pathway are crucial for plant development. *Genes Dev.* 18, 1187–1197. doi: 10.1101/gad.1201404

Wang, B., Sun, Y. F., Song, N., Zhao, M. X., Liu, R., Feng, H., et al. (2017). *Puccinia striiformis* f. sp *tritici* microRNA-like RNA 1 (*Pst*-milR1), an important pathogenicity factor of *Pst*, impairs wheat resistance to *Pst* by suppressing the wheat pathogenesis-related 2 gene. *New Phytol.* 215, 338–350. doi: 10.1111/nph.14577

Wang, M., Weiberg, A., Dellota, E. Jr., Yamane, D., and Jin, H. (2017). Botrytis small RNA Bc-siR37 suppresses plant defense genes by cross-kingdom RNAi. *RNA Biol.* 14, 421–428. doi: 10.1080/15476286.2017

Wang, M., Weiberg, A., Lin, F.-M., Thomma, B. P. H. J., Huang, H. D., and Jin, H. (2016). Bidirectional cross-kingdom RNAi and fungal uptake of external RNAs confer plant protection. *Nat. Plants* 2:16151. doi: 10.1038/nplants.2016.151

Weiberg, A., Bellinger, M., and Jin, H. L. (2015). Conversations between kingdoms: small RNAs. *Curr. Opin. Biotechnol.* 32, 207–215. doi: 10.1016/j.copbio.2014

Weiberg, A., Wang, M., Lin, F. M., Zhao, H., Zhang, Z., Kaloshian, I., et al. (2013). Fungal small RNAs suppress plant immunity by hijacking host

RNA interference pathways. *Science* 342, 118–123. doi: 10.1126/science.1239705

Whangbo, J. S., and Hunter, C. P. (2008). Environmental RNA interference. *Trends Genet.* 24, 297–305. doi: 10.1016/j.tig.2008.03.007

Winston, W. M., Sutherlin, M., Wright, A. J., Feinberg, E. H., and Hunter, C. P. (2007). *Caenorhabditis elegans* SID-2 is required for environmental RNA interference. *Proc. Natl. Acad. Sci. U.S.A.* 104, 10565–10570. doi: 10.1073/pnas.0611282104

Yang, Y., Jittayasothorn, Y., Chronis, D., Wang, X., Cousins, P., and Zhong, G. Y. (2013). Molecular characteristics and efficacy of 16D10 siRNAs in inhibiting root-knot nematode infection in transgenic grape hairy roots. *PLoS One* 8:e69463. doi: 10.1371/journal.pone.0069463

Yin, C., and Hulbert, S. (2015). Host induced gene silencing (HIGS), a promising strategy for developing disease resistant crops. *Gene Technol.* 4:130. doi: 10.4172/2329-6682.1000130

Yin, Y., Liu, X., Li, B., and Ma, Z. (2009). Characterization of sterol demethylation inhibitor-resistant isolates of *Fusarium asiaticum* and *F. graminearum* collected from wheat in China. *Phytopathology* 99, 487–497. doi: 10.1094/PHYTO-99-5-0487

Yu, J., Lee, K. M., Cho, W. K., Park, J. Y., and Kim, K. H. (2018). Differential contribution of RNA interference components in response to distinct *Fusarium graminearum* virus infections. *J. Virol.* 92:e01756-17. doi: 10.1128/JVI.01756-17

Zanini, S., Šeèiæ, E., Busche, T., Kalinowski, J., and Kogel, K. H. (2019). Discovery of interaction-related sRNAs and their targets in the *Brachypodium distachyon* and *Magnaporthe oryzae* pathosystem. *BioRxiv [Preprint]*

Zeng, W., Wang, J., Wang, Y., Lin, J., Fu, Y., Xie, J., et al. (2018). Dicer-like proteins regulate sexual development via the biogenesis of perithecium-specific microRNAs in a plant pathogenic fungus *Fusarium graminearum*. *Front. Microbiol.* 9:818. doi: 10.3389/fmicb.2018.00818

Zhang, J., Khan, S. A., Heckel, D. G., and Bock, R. (2017). Next-generation insect-resistant plants: RNAi-mediated crop protection. *Trends Biotechnol.* 35, 871–882.

Zhang, L., Hu, D., Chen, X., Li, D., Zhu, L., and Zhang, Y. (2012). Exogenous plant MIR168a specifically targets mammalian LDLRAP1: evidence of cross-kingdom regulation by microRNA. *Cell Res.* 22, 107–126. doi: 10.1038/cr.2011.158

Zhang, T., Zhao, Y. L., Zhao, J. H., Wang, S., Jin, Y., Chen, Z. Q., et al. (2016). Cotton plants export microRNAs to inhibit virulence gene expression in a fungal pathogen *Nat. Plants* 2:16153. doi: 10.1038/nplants.2016.153

Zhu, K., Liu, M., Fu, Z., Zhou, Z., Kong, Y., Liang, H., et al. (2017). Plant microRNAs in larval food regulate honeybee caste development. *PLoS Genet.* 13:e1006946. doi: 10.1371/journal.pgen.1006946

Conflict of Interest: The authors declare that the research was conducted in the absence of any commercial or financial relationships that could be construed as a potential conflict of interest.

Supplementary materials

FgAGO1-FGSG_08752

ATGGCGGACAGAGGTGATCGAGGCGGCCGTGGAGGCCGTGGCCGTGGCGGACGCGGCGGCGGCTATCAAGATGGTCGAGGAGGCGGACGAGGTGGCGGAGATGGGAGAGGA
CGAGGTGATGGTGGTTTCCGTGGCGGCAGAGGACGAGGTGAGGGAGGACGTGGTGACTTCCGAGGCGGCTTCAGTGGTCCTAGAGGCGGCCGTGGAGGTTCTGATCGCGGGAG
AGGAGGATACAGGGGAGGCCGAGGTGGAGGGCAATTCTCAAACGAGCCGTCTTTCTTCAAGATCGAATCCGGTGTTCCTCAGCCCGATGCTGCTATTACCAAGCTCGAGGATGAG
GTGGTAAAGAATCAAAATAATTCTGTTGCCCAGCTTACATCGAAAATGTCCAAGTTGGGAGTAGAAGAAAAGGAGCATTTGAGCAAATTCCCTCCACGACCTGCATTTGGAAACAA
AGGCCGTCCAGTCACTTTATGGGCAAACTATTACCAGATCGACACCAATATTCCCATGCTTTTCAAATACACAATTTCTGTCAAAGAGATCGTAGCTGAATCAGAAGAAAAGACCGA
CAAGCCCACTGTCGCCCAGCCTAAGGGGAAAGGGAAAGGAAAAGGCAAGCCCGGAAAGCCTAAGAAGTCCGGTTCTGTCGAAGTCAAGGGACGTAAACTTTTCTTGGTCATCAAA
GAGACTCTAAACGAGCTCACCAAGAAGGACAAGAGCCTGCTTCTTGCGACCGAGTTCAAGTCTCAGCTTATCTCCTTGCGCAAGCTTGACCTTGGACTTGACAACTCATTTCGAGTAAA
CCTCCCGTCATCAGCAAACCCCGACAAGACCGAAGTCTTTGAAGTGACCTTAAATGGCCCTGAAGTAGCCCGAGTTGACGAGATGCTCAAGTACGTCAAATCGAATACCAGTGCTTCA
CATGACGCCCCAGGCAAACTTGCCGACGACGACGACGATGCAGCAAAAGCCCTGGCATTCCCAAAATTCCCTGATGTTGTTGATGCCCTGAATGTCATCTTTGGGTTTGGCCCGAGGT
CGAACGAAGACATTAGTGCTGTCGGAAACTCCCGATTCTTCTCTTTCAAGAACGGTGGTATCTGCAGGGATATGAGCATGCGTGGGAGACCCTTACAAGCTGTTCGTGGGACATTCCA
GTCTGTCCGCCTAGGTACCGGCCGACTTCTTTTAAACACAAACATCACTGTTGGCATTTTCAAGATATCCGGTAACTGTGCCAAGCTCTTCCAGGATCTCAATGTCTTTGAAGCACAGAA
GTCGGAATGGCGGAAAGTGAATAACGCGAAGTTGATGAACAAATTTCTCCCAAAAACCCGCGTACTGGCAACGATGAAGTTTGCCAATGACAAGAAAGTCCAACGACGGAAAGCAAT
TTACAGTCTGGCCTATGCACCTGAGATTGAACGAGCCTGTCGTGGCAACGATCATCCTCCCCGGTTCACGAAGGGTTATGAATACCCTGGACCAGGCAACGTGAGCTTCTACATGGTG
TCTGATTCTAAAGGGACCGGTGAATATATCACTGTCAGAGAATTCTACAAGCGGAAATACAACGACACTACGCTCAAAGACTACCCTCTTCTTAATCTCGGCACTGCCGCAAACCCGAA
CTTTACCCCAGCGGAGTATGTCGAGATCCTACCGGGACAGTCAGTCAAGGCGAAGTTGAATAGCCAAGAATCGACCGCGATGGTCGATTTTGCCTGTCGGTCACCTTACGCCAATGCT
TTATCCATTACGAAAGATGCGCGGGAAACTCTAGGTCTTGACGACGAGAAATTGGTGTACAAGCCCGGCAAAAGCATACAAAAATGGACCTATGTCAATGTCAAACCAGGAGGCAGG
TCTGGGCCGGTTCCAAAGCGCACTGTGATGGAATTTGCTCAGGTCATGAGACAAATGAATATTGGAATCAGCAGCAACCCTGTAGACCCTTGCACAGAGGTCATCACCCAAGAAGATT
ACGCTCAAGGACGTTCAGATGCTTTCTTCAAATGGGCGAAGCAGAATCGCATAGAGTTTATACTTGTGATTCTTGGTACATCAGAGTCCGAAACATACGGCAGGATCAAGACATTGGG
CGACTGCACCTATGGTATTCACACCTGCTGCGCCCAGGCCGAAAAGTTTGGATTCAACAGAAACCCTCTGCCATATTTCGCCAACTGTGCTCTCAAATGGAACCTGAAGGCAGGTGGTG
TAAACCACAAGCTCCACAACGAGTTCGGTCTCATTAAAGAGGGCAAAACGATGTTGGTAGGATATGACGTCACCCACCCAACCAACATGCCTTCAGGCCAGGGTGATGATGCTCCCAG
TTTGGTCGGATTGGTGGCCACCATTGACCGAGATATGGGACAATGGCCAGCCTACTCTTGGGAACAGTCGTCCAAACAGGAGATGTTGGACGAGACTTTGACTGAAGCATTCAAGTCA
CGACTTGCACTTTGGCAAATGCACAACCGACAGCAGCTGCCTGAGAACATCGTTATATTCCGTGATGGCGTGTCGGAGGGCCAGTTTGCCCAAGTTTTACAAAGAGAGCTACCACGC
ATTCGCATTGCCTGCAATGCCAAGTACCCCAAGAACAAGCCACCAAGAATTTCTCTGATCGTTTCCGTCAAGCGACATCAGACTCGCTTTTATCCTACTTCTTCCGAGAGCATGACGTC
CAAGAACAATATCGAAAACGGTACCATCGTCGATCGTGGTGTCACGCAGGCTCGATACTGGGACTTCTTTCTTACTGCACACTCCAGCATCAAAGGCACGGCTCGCCCTGCGCACTACA
CTGTGTTGCTGGACGAGGTCTTCCGAGCGAAGTACGGAGCCGAGGCAGCCAATGAATTGGAGAGATATGCCCACGAGCTCTGCTACTTGTTTGGCCGAGCCACCAAGGCTGTGAGCA
TTTGCCCCCCGGCATACTATGCAGACGTTGTGTGCACTCGAGCGAGATGTTACAGACCTGAGTTCTTCGAAATCAGTGACGTTGAAAGTGTCTCAACAGCTGGGCCGGGCTTAGGTGC
CAGTGACCCAAAGCAGGTCCATGCGGACCTCGCCAACTCGATGTACTATATCTAA

Fig. S1: CDS of *FgAGO1* with the sequences of the dsRNAs marked

Coding sequences (CDS) of the respective Fg target gene with the sequences of the dsRNA marked (blue, tool-designed; red, manually designed).

FgAGO2-FGSG_00348

ATGTCTGATAGAGGGCGCTCACCCTCTCCAGGGGGTCCCTCAGGGCCTGGGAGGCGACCTTCACAGTCCCCAGCCCGATCGGCAACTGGCTCTGGTAGTGGACCTGCTGGCGGCTAT
GCAAAGCCCCTGGGCTACGATCCTGCGAAGCCTCCAAAGCAGGAGGACCAGGGAAACACACGAATGGAACTACCTCCAGATGCGTACATTTCCGAGACCAAAAAGGATATGTTTACT
TTAAGAAACAATCGTTTCAACACTGAGGGAAAGCCTGAGCACATCGAGGTCAACCAGTACCGAATGACCAAGTTCGACTTCAACAAGAAGATCTACCAGTACGATGTAAGTATCTATC
GAATTCATTAGTGCTGGCCCATGCTAACAACAACTTCAGGTTGTACTTTCGCCTAGCCCTGACAAGATCGGTCCGGTCATGAAGAAGATTTGGGCTCATCCTGTTACCGTGAAGACCAT
GAAGCCCTACAAGCTTGAGATGTGGCTTTTCGACGGTAAGAAACTGGCATGGAGCCCCGCGCTTGTCGACCGTGGTGAACTTCGGTTCAGTGTCGATCTAGACGAAGGCCAACGTCCT
CCTGGAGCCAAGCCTCGGGATGGTGGCAAGTTCCTAGTCACTATTCGAAAGACCACCGAGATCCAAGTTGCTGCTCTGCAGGGCTATCTGTCTCACAAGATGTCCTTCAATAACAGT
GTTCAAGAGGCACTGAACTTCATTGATCACCTTGTTCGACAGTTCCCCTCCAGGAACCTACTTGCTATCAAGCGAAACTTTTACCAAACTGGTCGACCTGGAGCTCCTCTTCAAGACG
GAGCCATCGTTGAGGTCCACAAGGGAACCTACGCTTCAATCCGAATGAGTGACAACTTGAAGCAAGGTGGTGTCGGACTTGGCTACAACATTGATGTCGCCAACACCTGTTTCTGG
ATTGGCAACCAGCCATTGGACAGGATGGCCTGCAACTTTCTTGCTACCATTGACCCAAGCAAGTTCCGAGGACACACTCCTGCGACTCTCAATGAGATCCTGAAGCCAGTCAGGAAT
AGGAGTGGCGGGTGGGAGTCATCTGATGGCTTCAAGCAACTTCGCAAGTTGCGACGCCTCAAATTCAAGATCAAGCACAAGGGCCGCCCAAACGAGGACAAGCTGTACACGATCA
TGGACTTTGCATTCGATGCCAAGTTTGGTGAAGCTGGTCACACCTCCCGCACCCACACCTTTGAGAAGGATGGAAAGGACATCAGCGTCTATGACTACTACAAGAAAATGTACAAT
GTCACCCTGCGACTTTCCCACCTTCCTCTTATCAACGCTGGAAAGGGTGGCTTCATTCCCATGGAGCTTGCCTTCGTTGAGAGCATGCAACGATACCCATTCAAGCTCAACCCCGACC
AGACAGCTGCGATGATCAAGATCGCGGTCACCCGCCCTGCCGTACGCAAAGCCGACATCCAAAAGGGAGCTGCCGCTCTTCAGATCGGTCAAGATCCTTATCTGAGGGAGTATGGT
GTCAATTTCGAAGCCCAGTTTGCGAAGACCGAGGCTCGTATCTTGCCTCCCCCTACTGTCAGGTTTGGCCAGGGCACAGCGGAACCCAAGTTCGCTGGTCGCTGGGACTTGCGAGGAA
AGAAGTTCTTCAAGCAGAACACCGCCCCCCTCCAGAACTGGGGCTTTGTTGCCTGTGAAGCACCTGTCCCACAGGCTGTTCTTTCAGCATTCGCCACAACATTCAAGACCACTTTCCTTG
GTCATGGCGGCAAGGTGACTGGAGACCCCATGCTTCTCAATGCACCTAGCAACCTGCGTTTTGAACCCGGAAAGCTGGTTGAGTGGGCTCATGAGGAGATCACTCGCCGAAAAGGCT
ACACACAACTCTTGTTCATTGTCGTGTCCAAGAAGAACAGTGGTACCTACGAGCGCCTCAAGAAGTCTGCTGATTGCAGATACGGCATTCTCAGCCAGGTTGTCCTTGGTAGCCATGTG
CAGAAGAACAATGGCCAATACCACTCCAACGTTTGCATGAAGGTGAACGCCAAGCTTGGTGGTGCCACTGCCTGCACGCCTCCTCTGTGGAAGACTCCCACATTCTTCCCCGACAGCC
GCCCAACCATCATTGTAGGTTGCGATGTCTCCCACGCTGCTCCCGGTGGTGCGACTGCTTCAGTTGCTTCCATGACCATGTCTGTGGACCCCAATGCCACTCGATACGCCGCAGTCGCT
CAGACAAATGGATATCGCGTCGAGATGCTTACCCCCAGCAACATTCGACTCATGTTTGCAGAACTTCTTCCTCAGTGGCGACACAACCACCCAGGAAAGATACCTGCTCATCTGATC
TACATGCGAGATGGAGTTAGTGAAGGCCAGTTCGCTCATGTATTGGAGCAGGAGGTATCCGAAATCAAGAAATTCTTTGGAGGCAGCCTCCCCCCGACAAGATTCCCAAGATGACA
GTCATCATCGCTACGAAGCGTCACCATGTACGCTTCTTTCCACAGAGGGGTGACAAGAACGGAAATCCCTTGCCCGGTACTCTGGTTGAGAAGGAAGTTACCCACCCTTTCATGTTTGA
CTTCTACCTCAACTCCCATGTTGCTATCCAGGGAACTGCACGCCCCGTGCACTACTCAGTGATTCTGGATGAGATGGCTATGCCAGTGAATGATCTGCAGAAGATGATTTACCAGCAGT
GCTATTCCTACGCCCGCTCAACCACCCCCGTCTCCCTTCACCCGGCGGTCTACTACGCGCATCTCGCTAGCAACCGAGCTCGTGCACACGAGAACGTCGCAACCAGTGATGGATTTAGA
ACCGGTGCCAAGGGGCATGAGATTATTCGGGAGAAGCAAGCCCATGGCATCACCTCGGACGCTCCTAACAGGACCGCTGATGCACCCCCCCTGATCCGTCTAGGAGGCCCTTGTGGA
CAGACTCCTGCTGATGGCGAGAAGCGCCAACGAGATTTTTTCCGCAGTACCATGTGGTACATCTAA

Fig. S2: CDS of *FgAGO2* with the sequences of the dsRNAs marked

Coding sequences (CDS) of the respective Fg target gene with the sequences of the dsRNA marked (blue, tool-designed; red, manually designed).

FgDCL1-FGSG_09025

ATGGACACCGACTCGACCGACAGCGAAGATGATCGCGTTCAGTATCGCCTGACCGTGAGGCCTTCGAAGCATCGAAAGAATACAGAGAAGAAGCGCCTGAACAAGCAGGTTTTGAAA
CAATACATGATAGAACACGACAGAGAAGCCTATGCCAAAGATTCTGAGAAAAAGAAGCGCGGCCCCTTCGCTGAAGCTTCCACCGACATTACACCGCGAGAATATCAGATAGAACTCT
TCGAAGCCGCCAAGGAGAAGAATCTCATTGTGGTTTTACCTACAGGTATTTTCTTGTCCCTTTCTGACTCTACTCTGGACATTCTAATAGGCACAGGTTCTGGTAAAACACTCATCTCCAT
CTTATTGCTAAAATACTACATTCGAATCGAAGTGGAATCTCGCGCTCTTGGAAATCCGAGGAAGGTGGCCTTTTTCTTGGTGGAAAAAGTAGCCCTCTGTGAGCAGCAATACCGATTTC
TTAAGGACCAGATTTTCGGCCACAACATTGTCATGTTCACAGGCGATAACCGCGGCGTGACCAAGGACAAGAAGTACTGGGATGATCAGTTTTCCTCAAACAAGGTTGTGGTCTGCAC
TGCTCACATTTTGCTCGACTGTCTGAACAACGGCTTCATTACAATGGACCAGATCAACCTCCTCATCTTCGACGAAGCCCATCATGCAAAGAAGAAGCATGATTACGCGCAAATTGT
CCGACGATATTATTATTCTACCGAAAAGAACAAGAGACCTCGCATTCTAGGAATGACCGCTTCCCCTGTGGATTCCAAGGCTGGAGATGTTGCAGAACTGGCACTTGAACTTGAGA
AAACCCTTGACAGCGAGATCGCAACACTCTCCGACAAGATGATGCGACAGGCGACTGATTTCCAAGTTCATGTTGAAGAGACAGTCAAATACAACACACTTGGACTACCAGACGAG
ACCAAGACACAGCTTTGGGACTCGATCTCTAAGCTAGTATCGCGAAACAAGGAATTCAAGGCGTCTCTCGACTTCACAAAAGAGGCCTCCACAATCCTAGGACCCTGGTGTGCGGA
CCGATACTGGCAAGTCTTGATCGACGATACAGAGATCAAGCGACTCGCCGACAGGACTCGCATGGCTTTTTCGGGGGTGGAGAGAAGTTGTTGGCAAGAGGAGACCAAGCAGA
AGAGGCTGTCAGGGAGGTTCAAAAGGTCGTCGCAGCCCACGAGTTTAGGGCGATCAGTCCTCAATCGCAGGAATTGTCAGCTAAAGTGAAATGTCTACATGAAATCCTGGTTCAT
GCCTTCACAGTCGATAACACAAAGCGCTGCATCGTTTTTGTTGATCAGAGACACACAGCTTGCCTCCTTTCGGACCTTTACGACCAAGTTTCAATGGCAATTCCCGGTATGAATGCTT
CGTATATGGTAAGTTGAGTCCCATTTCCAACAGCAGTAACTAACCACAATAGATTGGTCAACAATCTAGCAGCAGCACCCTTGGCAATATGTCTCTGCGAAAGCAATGTTCAACGCT
CAAGAACTTTAGGGACGGCGTGATAAACTGTCTCTTTGCAACATCAGTGGCAGAGGAGGGAATTGACATTCCGAGTTGTGATCTTGTTATCCGATTTGATCTCTATACTTCTGTTATTCA
GTATGTTCAATCCAAAGGGCGTGCGAGACACGAATCTTCACGGTATATCACCATGCTGGAAGACGGCAACATGAGACAGATTCGCAGTCTGAAACAAGCAGCGAGAGATGCAACAGC
CCTTCGAGAGTTCTGTCTAAGAATACCTGCCGATCGAAAACTTCAAGACGATGTATTTGATGAGGAGACGGAAAGTCAGATCAAGCAAATACGTTTTAACGTGTACAAAATAGAATCA
ACGGGCGCACAACTTACATTCCCCTCAAGCCTCGAGATACTAGCTCGATTCGTTGCATCCTTGGGTACAGCAGAGAGCAGCCATAGCAAGGCTGAATATCACGTCTACAAGGTGGGAA
CATATTTCACAGCCGCCGTCAATCTACCGTCCAGTTCCCCCATCGTCTCCCAAACAGGCTATCCACAACGAAGCAAGCTTCTCGCAAAATGCTCAGCGGCTTTTGAGGTTTGCAAGAAG
CTCATCAATGGCAAACACATTGATGATCATCTTCAGCCTACTTTCAAGAAACATTTCCACAAAATGCGCAATGCTCGTGTGGGAATAAGCCCTAACAAGAAGGGTGAGCATGACATGC
GCCTGAGGCCCAACGTTTGGAGTATCCGTGGAGAATGGACACACTTCTTCCCAACAAGAATTACTCTTGACAGGGATTGTGGAGAGAAAAACAGGTCGTTGATTCTTCTTTCGCGAAG
TCCACTTCCAGGACTACCTTCAATCCCTCTATTCTTCGGCAATGGACGCTCAGCCATCGTTGAAGTGACATGTTCTCAAGAACCTTTACCCATCACGACCGAGGAAGCTGGGGGTTTGAC
TGCTTTCACACTCAAAATCTTTGCCGACGTTTTCAGTAAAGAGTTTGAGGCCACTTGCGACCAGTTTCCTTACCTTCTTGCCCCCTTGGCAAAAGACACCAATCTAAACGAAATATCGCG
AATCGACTGGGATACTGTCAACCTTGTCAGAGACCATGACAGTCTCGAATGGGAGAATGCGCCCGACGATTTCTTTTTCGACAAGCTTGTTGTAGATCCATATGATGGAGGGCGCAAG
CTTATAATCAAAGGCATTGACAAATCCAAGAAGCCTTCTGATCCTACACCGGAGGGAGTGCCTGAGTCGAGAAGTCGTGCTTATAGGTCTGCGGAACAAAACATTAAGCAGTACAGCA
ACAGTCTGTTTTCCAAGTCTCGACTAACGGCCCAGTGGCGAGACGATCAACCGGTTGTCAAAGCTGAGCTTCTCTCATTGCGACGCAATCTGTTGGACGAGTTTCAAGTAAACGAGGA
AATCAACAAGGATTGCTTCGTCATTTTAGAACCCCTCAACGTGTCACCTGTAAGTGAAAGACTCTTCTGTAAAACGTATCTAACATGCCCAGCTGCCAATTGACGTCGTTTCCATGGCAC
TCAAGTTCCCGGCAATCATCCACAGAATCGATTCTGCTCTGATCGCTCTTGATGCATGCGAACTATTCGACCTCTCTATTCCGCCAGCGCTGGCACTCGAGGCAATGACCAAAGACAGC
GACAACACTGAGGATCATGGCAAGCAACAAATCAATTTCCAAGCTGGCATGGGTTCCAACTATGAAAGGTTGGAATTTCTTGGAGACTCGTTTCTCAAAATGGCCACCACAATCTCCAT
TTTTGTACTCAAACCCAAGAGCAACGAATGTTTGTACCATGTAGAGCGCATGCTGCTCATCTGCAACAACAATCTGTTCAACACGGCCGTAGATTGCAAGCTCCCAGAGTACATACG
ATCCTTGGCATTCGACAGGCGAACTTGGTACCCTGATCTTACACTCAGAAAAGGCAAAGCTTTCAAGGCAACAGCGCGACAGCGCTTAGCCGACAAAAGTATTGCGGATGTCTGTG
AAGCTCTCATTGGTGCTGCATACCTCTCAAGCAAGGATGACAATTTGAACATGGCCGTCAAAGCTGTGTCACAGATGTGCAAAGCAAAGTACCATACCATGATGGCTTACGATGAGTA
CTACGCATCTTTCAAGGTTCCAGATTGGCAGAAAGCCAGTCCAAACGCCAACCAGCGTAGACTTGTGCAGAAAGTGGCAGACGCTACCGGGTACCACTTCAAGTCTGCGCCGCTGCTC
CAGAGTGCATTCACACACCCTTCTTACGCGTATTCAGGGAACGTTCCAAACTATCAACGCCTCGAGTTTCTAGGCGATGCCCTCATCGACATGACCATCGTCGAATATCTCTATCGCAAC
TTTCCCCTCGCAGACCCTCAGTGGTTGACGGAGCACAAGATGGCAATGGCCTCGAACCAATTTCTCGGTTGTCTGTGTGTTAAGCTCAATCTGCACCACCATCTTCTGTTCAACACGTCG
CAGTTCATCAGCAAAATTCGTGACTATGTGGCCGAACTTGAGTTGGCTGAAGAGACTGCGCGCCAAGAGGCAGAAGAAGACGGGACTCCAATGCGCATGGACTTTTGGCTCAATGCG
ACAACGCCTCCAAAAGCGTACGCAGATTCAATCGAGGCTCTTATGGGGGCCATGTTTGTGGATTCTGAATTCGACTATTCTGTTGTTGAGGATTTCTTTACCAAGTTCATCTTCCCGTAC
TTTAAAGACATGTCTCTGTACGATACCTTTGCAAACAAGCATCCTTACACATTTCTCACCAAGAAGATGCAACAGGAGATCGGGTGCATGAAATTCTGTATGATTTCAGACACCCGCGTT
CCTGATGCAGAGCGTGGCATGGAAGTTATGAAAGAGTACGACATATATTCAGCCTTTCAAGTGCACGAAAGAGTCATCACATGTCACGTATCAAAGAGTGGAAGGTACGGTAAGATT
GCTGCTGCAAAGGGGGCACTCGAGTTGTTGGAGCCGTATGGCGGTGATGTGGTCGCGATGAAGAAGCTGTTGGGCTGCGACTGCGACTCTGTAACAGCAGCCATGGCGGAGATGGA
CCATGGAACAGCTGTCTAA

Fig. S3: CDS of *FgDCL1* with the sequences of the dsRNAs marked

Coding sequences (CDS) of the respective Fg target gene with the sequences of the dsRNA marked (blue, tool-designed; red, manually designed).

FgDCL2-FGSG_04408

ATGTCCTCAAGCGATAAGGTCATGGCGGACGCCTCTTCCATACCAGACTCCGAGGTCAAAACAATAGCGTCGTCCTCGGTCGTCGAGATCTCTGCTACAGGCGAGAAGGAGATAACGA
CTCATATACCTGTCGCAGATACACCAATGTGCTCAGATGACCAGGCCAATGTGCAAGAGCAAGACGAAGAAGTTAAGCCTCAGAAAGTGACGCCCAATCCAGAGGTGGTAAATCCCC
GCGGTTACCAGCGAGAGATGCTGGAACAAAGCATCAAAAGGAATGTCATCGTTGCAGTAAGTTATTCCAAGTACCCCATTCAATCTGCATTCGGTGACCTGATTAGATGGACACGGGA
AGTGGTAAAACTCAAGTGTATGTCACTTCCATACCATCGAAAAAGAGAGAGACTAATTATAACTCGTAGGGCCGTGATGCGCATCCAACATGAACTCGATACATGTGCACCAGACAAG
GTTGGTGAACAAAGAAACATAATATCGCGGTCAAAACTAACCAATATAGATTATCTGGTTCTTAGGCAAGACAGTATCGCTATGTGAACAGCAATACAGCGTTGTCCAAAGGCAAATG
CCGTCGGTATCGATGAAACTGCTAACGGGGCAATTGAACATCGATGCATGGTCCGAGGACGTCTGGCCCCGTATCCTTAATGGGACTCGTATCATTGTCTCGACCTTTGATATCCTGCG
AGATGCTTTGGACCATGCATTTGTCAAGATGAACATGCTGTCCCTTATCGTCTTCGATGAAGGTGAGACATCGCCAACACTTACAATATCATTACTGACTTTTTACAGTTCATAATTGTGT
AAAGAATAGCTCTGGTCGAAAGGTTATGGTGAATTTCTATCACGAACACAAGAACGCCGGCATGCCCGTGCCTGCTATCCTGGGTTTAACAGCCAGCCCGATACAGTCGAAGTCAATC
CACGACGAAATCCTTGAGCTCGAGGTCACCATGGATGCTGTATGCATCACTCCAACAATTAACCGGAAAGAACTCCTCCAGCACGTCAACAAGCCCAATCTTTCCCGAGTATTGTATG
ATGTGGAAGAGCATCCGACTCGAACCCCCCTAATGCAGACTCTGCAGTCTGAGTACTCGGCGATGGACATCACCCAGGACCCAAGTATTATAAAGGCCAAGCAACTTATCGCTAAG
GGCGAGAAGACTGGACCTGAAATACTAAGTATGTTGATGAAACACAGGACCTTCTCTCAGAAGCAGTTAAAGTCCTTATGGAACAAAAGCAAAGACATTCTTGATGAACTCGGGC
CTTGGGCTGCTGACAAGTACATCTCCGAGTTGGTCAGTCTGTTTCTCAAGAGAATCGACTCGCCAATGACGTTTAACGAGTCCTGGAGCAATGAGGATAGGACCTACCTCGCAGGT
CATTTGAGACAGATCGCTGCCAGTCCCCATCAGCCCAAACTACCAGACAGACACAACTTGGCCGACAAGACGAATAAACTAATCCAGGAACTACTTGCAGCGGATGAAGATGTGGT
CGGCATTATATTCGTCAGATCAAGGGCTGCTGCCAACGTCCTTTGTGCTCTTTTGAGGGAGCACCCCGAGATTCGACAGCGATATCGAGTCGGCTCTGTAGTAGGATCCGCAGCCAC
CAAGATTCGAAAGCAAAACATCTACGAGTATCTGCCCGGCGCGACTGCCGATACATTACGCGATTTCAAAACAGGCGCCATCAACCTTTTGGTCTCGACTAGTGTTCTTGAAGAGG
GTATTGATGTCGCAGTGTGCAACCTCGTCATATGTTTCGATGAGACAACGACACTCAAGTCCCATATCCAACGCCGCGGACGAGCTCGCAAACAAAAATCAAAGATGATAGTACTT
GCTAGATCTTCATCCGACGCTCGGGAATGGGATTCCCTAGAAAGAGACATGAAGAGTCGTTATGAGCAGGAAAGGGGAGAGTTGGACGCTTTAGAGATAGAGGCTCGCACTGAAGC
GACGTCCTCTTTTTCTTATACTGTGAAAAACTCAGGGGCTAGATTGGACCTCGAGAATTCTCGCCAGCATCTGGAACATTTTTGTAACAAGGTTTTCCAGCGAGATTACGTTGATCCGAG
ACCCGTCTACATTTTCCACAAGACCGAACTGGGATCAGCACCGCCGACTTTCAGCGCAACGGTGACTCTTCCCTCGGGTCTGCCTAAGCACCTCCGAAGGTGCCAAGGTGGAGGTGGA
TGGAGATCAGAAAAGAATGCGATGAAGGAAGCGGCTTTTCGTGCATTCGTCATGCTGCACCAAGAAGGTTTGGTTAGCGACCACCTTCTTCCCCTAAATGCAGATTCGAAAGAAGCAG
AAGAAGAGGTGCAGCTAACTGCGCCCGAGCTTCTATTTGACCCATGGAAAGACATTGCACAGCGGTGGGAGACCACGGCTGAGAAATGGCTCTATGCTTACGAGTTCGCCGATCACG
AGTATGTTACTCCTCTTCATTTCGAGATTGCCTTGCCTGTGTGTCTTCCACGACCCCGCGACATCACCTTTCATCCTGAAGAGGGACTTAAATGGCATGTCAAATGCACCTCAATCAAGA
GGATCTCCAATGATGAATGCTTGGGCTTGCCAGATCATACGTCAACCCTATTGGCGATGCATTATGGCCACCGCTGGAACGTGGAAGATCGTGACCATGTGATCAAATTCATATATGA
GAACAAGAATCTCACCCGAGATCAAATTGGATCGGTACCCTTCGGCGAAAGCATTGATGCTCTATTGGAAAAGAGAGTCCTGGTTCGGGACCCCAAAAATACTCCCTTCCACTACGTCA
AAATGATCCCATCAAAGCCTCCAAAAGAGCAAGTTCAGCACCCATTTAATGAATACGAGGAAGCGCCAGAAGAACAGTATCTAGTTGTGGATCAATGGACACGCAGGTCGGACCTGTT
GCATGAGATAAAACCCGGTCAGGGGAAGAGCTCTTGCACCAAACCCTACCGCTGGGTTCTCCCGATTTCCAGAGCGACTGTTGATGAGGTTCCTCGGCGTGCCGCTAAGTGCGGTATG
CTTATCCCTTCCATCATTCACGAATTGGAGGTTCAGCTCATCGCGAATGAACTGTCCTCGACACTTTTGGCGCCAGTTGGTATCACAGATCTGCAATTGGTGATTGAAGCCATCAGCTCG
CGTAGCGCTGCAGAGCCTGTTGACTATGAACGTATTGAATTTTTGGGCGATTCGGTTTTGAAGTATTGCACTGTTATTCAAGCCTACTCTGAACGTAAGTCTTCCGCATCCCTCTATCGT
CACTTTCACTGATCATTGTCACAGATCCCTTTTGGCCCGAAGGTCTACTCAACCATTTCAAAGACCGACTAGTCTCCAATACCCGTTTGACTCGCATGTGCCTTGAGACAGGCCTTTCCAA
GTTCATTTTTTCCAAAACATTTACTGGAATCAAGTGGAGACCGCTATATCGAGACGAATTCCTAGATAAGAAGCCAGTCGATGGTGTATCAAGGTTTGTTGGTCCAAAGACTCTTGCTG
ATGTGGTCGAGGCACTTGTTGGAGCCTCCTACCAGGATGGAGGAATCAGCAAAGCTCTGGAGTGCATCAAGGTTTTCTTGGGCACCAAGTGCAATTGGCATGATGACAAAGTCGCCA
GAGACATACTCTTCCGAGCAGCAATTAGCGACGTACCGTTGCCCCCCACGATGGAGCCTTTGGAAGAGCTCATCGGGTACACATTTCAGAAGAAGTCTCTACTCATTGAGGCAATG
ACTCACGGGTCGTATGCGGCTGATGGGCAGCAGCGATCTTATGAACAACTCGAGTTTCTTGGAGATGCGGTTCTTGACTACATTGTCGTAACCCGAATGTTCCAATCTGACCCCCCAG
TGCCCAATGGACGCTTACACATGGTCAAGACTGCCATGGCCAACGCTGATTTCCTTGCTTTTACAAACATGCAACATGGACTACGCCGGCCTGAAGTTGAAATAAATGAGAACGGCGA
ACCAGTGCCTACAGAAGTTTCACTGCCGATATGGAAATTCATGCGTCATAGCTCTCCAGAGATGGGTAGAATCATGAATGAGACCCAGGCCCGATTTGAGAGCCTTCAAGAGGAAATC
AATGAGGCTAGGACGAATGGTAAACACTACCCCTGGACACTTCTCGCTCGTCTTCACCCGAAGAAGTTCTACTCCGATATTTTCGAGGCTACCCTAGGTGCCATTTGGGTTGATTCAGG
AGATATCGAAGTATGCACAGCCTTTCTTCACAAGTTCGGCGTCTTGCCGTATCTTGACCGAATTCTCAGCGATAATATTCATGTTCAACATCCTAAAGAGGAACTCGCCAAACTAGCAAT
CGACCAGAAAATGACGTATGATTATACGGCTGTTGATGGGCCTATAAAGGAGTACCTCTGCACGGCCAAGGTTGGAGATCGCGTCGTGGGAGTCGTGTCAGGGGCACTCAATAAGGC
TGAGGCAATGACCAAGGCTGCCGAAGAGGGCGTGAATTTTTTGAATGGGGAGCAGAAACGTGCAGAGAAGGCGGCTCAGGATGAAATGGCGCGATTTCTTGTTGCCATGGAACTCA
TTTAG

Fig. S4: CDS of *FgDCL2* with the sequences of the dsRNAs marked

Coding sequences (CDS) of the respective Fg target gene with the sequences of the dsRNA marked (blue, tool-designed; red, manually designed).

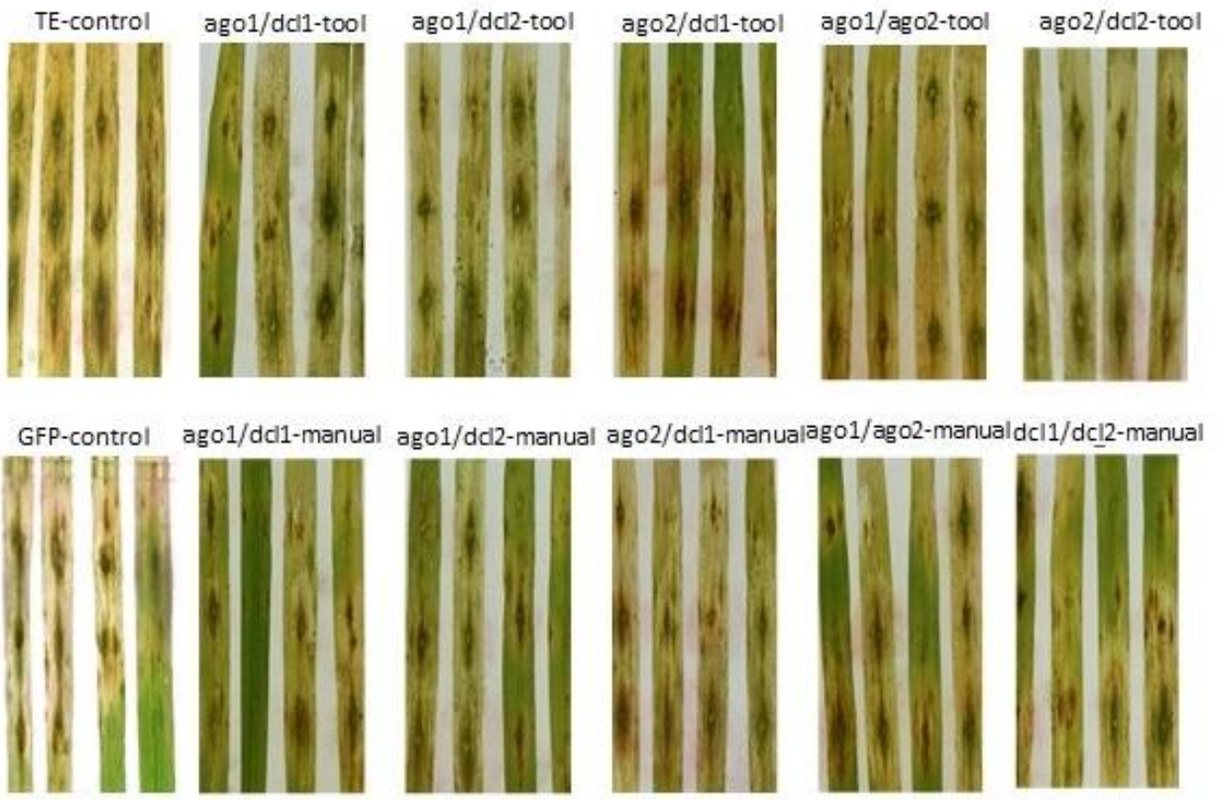

Fig. S5: Representative pictures of barley leaves 5 dpi

Representative pictures of barley (cv. Golden Promise) leaves sprayed with 10 µg (20ng/µl) of respective dsRNA in TE Buffer and the control without dsRNA. DsRNA was applied on the upper half of 10 leaves and 2 days after spraying the leaves were inoculated with three 20 µl droplets of Fg (50,000 spores/ml). Pictures were taken 5 dpi.

Tab. S1: Primer sequences

Name	Sequence
FgAGO1_F	TCCTCTCCAATTTCTTCCCCG
FgAGO1_R	TGACTTCGACAGAACCGGAC
FgAGO2_F	GGGATGGTGGCAAGTTCCTA
FgAGO2_R	CTCCCTTTTGGATGTCGGCT
FgDCL1_F	TGGTCTGCACTGCTCACATT
FgDCL1_R	ATATTGCCAAGGGTGCTGCT
FgDCL2_F	ACAAGCCCAATCTTTCCCGA
FgDCL2_R	ATTCCCGAGCGTCGGATGA
FgAGO1+NotI_F	CTGCGGCCGCTCCTCTCCAATTTCTTCCCCG
FgAGO1+NdeI _RC	CTCATATGTGACTTCGACAGAACCGGAC
FgAGO2+NotI _F	CTGCGGCCGCGGGATGGTGGCAAGTTCCTA
FgAGO2+NdeI_R	CCTCATATGCTCCCTTTTGGATGTCGGCT
FgDCL1+NotI _F	CTGCGGCCGCTGGTCTGCACTGCTCACATT
FgDCL1+NedI _R	CCTCATATGATATTGCCAAGGGTGCTGCT
FgDCL2+NotI _F	CTGCGGCCGCACAAGCCCAATCTTTCCCGA
FgDCL2+SalI _RC	CTGTCGACATTCCCGAGCGTCGGATGA
FgDCL2+NotI _F	CTGCGGCCGCACAAGCCCAATCTTTCCCGA
FgDCL2+BstxI _R	CCAGAGAGGTGGATTCCCGAGCGTCGGATGA
Fg.AGO1(PGEMT*)F	CAACCGACAGCAGCTGCCTG
Fg.AGO1(PGEMT*)R	GATGTCGCTTGACGGAAACG
Fg.AGO2 (PGEMT*)F	ACCCCAATGCCACTCGATAC
Fg.AGO2 (PGEMT*)R	ATACATGAGCGAACTGGCCT
Fg.DCL1 (PGEMT*)F	ATGTTTGTACCATGTAGAGC
Fg.DCL1 (PGEMT*)R	CGGCTAAGCGCTGTCGCGCT
Fg.DCL2 (PGEMT*)F	TTCTTGGGCACCAAGTGCAA
Fg.DCL2 (PGEMT*)R	GCTGCTGCCCATCAGCCGCA
Fg.AGO1*F NotI	GTGCGGCCGCCAACCGACAGCAGCTGCCTG
Fg.AGO1*R SalI	CCGGTCGACGATGTCGCTTGACGGAAACG
Fg.AGO2 *F NotI	GTGCGGCCGCACCCCAATGCCACTCGATAC
Fg.AGO2*R SalI	CCGGTCGACATACATGAGCGAACTGGCCT
Fg.DCL1*F NotI	GTGCGGCCGCATGTTTGTACCATGTAGAGC
Fg.DCL1*R SalI	CCGGTCGACCGGCTAAGCGCTGTCGCGCT
Fg.DCL2*F NotI	GTGCGGCCGCTTCTTGGGCACCAAGTGCAA
Fg.DCL2*R SalI	CCGGTCGACGCTGCTGCCCATCAGCCGCA
FgAGO1_F+T7	TAATACGACTCACTATAGGGTCCTCTCCAATTTCTTCCCCG
FgAGO1_R+T7	TAATACGACTCACTATAGGGTGACTTCGACAGAACCGGAC
FgAGO2_F+T7	TAATACGACTCACTATAGGGGGGATGGTGGCAAGTTCCTA
FgAGO2_R+T7	TAATACGACTCACTATAGGGCTCCCTTTTGGATGTCGGCT
FgDCL1_F+T7	TAATACGACTCACTATAGGGTGGTCTGCACTGCTCACATT
FgDCL1_R+T7	TAATACGACTCACTATAGGGATATTGCCAAGGGTGCTGCT

FgDCL2_F+T7	TAATACGACTCACTATAGGGACAAGCCCAATCTTTCCCGA
FgDCL2_R+T7	TAATACGACTCACTATAGGGATTCCCGAGCGTCGGATGA
Fg.AGO1*+T7F	TAATACGACTCACTATAGGGCAACCGACAGCAGCTGCCTG
Fg.AGO1*+T7R	TAATACGACTCACTATAGGGGATGTCGCTTGACGGAAACG
Fg.AGO2 *+T7F	TAATACGACTCACTATAGGGACCCCAATGCCACTCGATAC
Fg.AGO2*+T7R	TAATACGACTCACTATAGGGATACATGAGCGAACTGGCCT
Fg.DCL1*+T7F	TAATACGACTCACTATAGGGATGTTTGTACCATGTAGAGC
Fg.DCL1*+T7R	TAATACGACTCACTATAGGGCGGCTAAGCGCTGTCGCGCT
Fg.DCL2*+T7F	TAATACGACTCACTATAGGGTTCTTGGGCACCAAGTGCAA
Fg.DCL2*+T7R	TAATACGACTCACTATAGGGGCTGCTGCCCATCAGCCGCA

Chapter I: Discussion

The earlier approaches to assess the importance of *FgAGO*s and *FgDCL*s during *Fg* pathogenesis were conducted with KO-mutants (Chen et al. 2015; Gaffar et al. 2019). This gene KO influences several different processes by disrupting one component of the RNAi machinery over long periods of time, possibly spanning several fungal generations. During this time these changes can be compensated, in the case of *FgDCL1* KO e.g. by an increased *FgDCL2* expression (Yu et al. 2018).

Interestingly, nearly all knock-down events resulted in significantly reduced disease symptoms, except for the combined knock-down of *FgAGO1*/*FgDCL2* confirming their role in ascospore formation (Son et al. 2017).

This study avoided the prolonged gene disruption before the experiment by the application of SIGS, and demonstrated the importance of AGOs and DCLs during pathogenesis.

Chapter II: *Fusarium graminearum* DICER-like-dependent sRNAs are required for the suppression of host immune genes and full virulence

This chapter is published in the journal PLoS ONE, in Volume 16(8), Article e0252365, on the August 5th 2021. DOI: https://doi.org/10.1101/2021.05.17.444440

Chapter II: Introduction

Following confirmation of the importance of RNAi during *Fg* pathogenesis, the hypothesis is developed that *Fg* utilizes ckRNAi to silence specific host genes as an explanation for the importance of *Fg*DCLs, due to their role in sRNA biogenesis.

PLOS ONE

RESEARCH ARTICLE

Fusarium graminearum DICER-like-dependent sRNAs are required for the suppression of host immune genes and full virulence

Bernhard Timo Werner[1], Aline Koch[2], Ena Šečić[1], Jonas Engelhardt[1], Lukas Jelonek[3], Jens Steinbrenner[1], Karl-Heinz Kogel[1]*

1 Institute of Phytopathology, Centre for BioSystems, Land Use and Nutrition, Justus Liebig University, Giessen, Germany, **2** Institute for Phytomedicine, University of Hohenheim, Stuttgart, Germany, **3** Institute of Bioinformatics and Systems Biology, Justus Liebig University, Giessen, Germany

* Karl-Heinz.Kogel@agrar.uni-giessen.de

Citation: Werner BT, Koch A, Šečić E, Engelhardt J, Jelonek L, Steinbrenner J, et al. (2021) *Fusarium graminearum* DICER-like-dependent sRNAs are required for the suppression of host immune genes and full virulence. PLoS ONE 16(8): e0252365. https://doi.org/10.1371/journal.pone.0252365

Editor: Richard A Wilson, University of Nebraska-Lincoln, UNITED STATES

Received: May 11, 2021

Accepted: July 19, 2021

Published: August 5, 2021

Data Availability Statement: Data used in this study are available from the NCBI (Bioproject) repository at accession number: PRJNA749737 (https://www.ncbi.nlm.nih.gov/bioproject/PRJNA749737).

Funding: This work was supported by the Deutsche Forschungsgemeinschaft (www.dfg.de; Research Unit FOR5116) to KHK. BTW, AK, ES, JE, LJ and JS received no specific funding for this work. The funders had no role in study design, data

Abstract

In filamentous fungi, gene silencing by RNA interference (RNAi) shapes many biological processes, including pathogenicity. Recently, fungal small RNAs (sRNAs) have been shown to act as effectors that disrupt gene activity in interacting plant hosts, thereby undermining their defence responses. We show here that the devastating mycotoxin-producing ascomycete *Fusarium graminearum* (*Fg*) utilizes DICER-like (DCL)-dependent sRNAs to target defence genes in two Poaceae hosts, barley (*Hordeum vulgare*, *Hv*) and *Brachypodium distachyon* (*Bd*). We identified 104 *Fg*-sRNAs with sequence homology to host genes that were repressed during interactions of *Fg* and *Hv*, while they accumulated in plants infected by the DCL double knock-out (dKO) mutant PH1-*dcl1/2*. The strength of target gene expression correlated with the abundance of the corresponding *Fg*-sRNA. Specifically, the abundance of three tRNA-derived fragments (tRFs) targeting immunity-related *Ethylene overproducer 1-like 1* (*HvEOL1)* and three Poaceae orthologues of *Arabidopsis thaliana BRI1-associated receptor kinase 1* (*HvBAK1*, *HvSERK2* and *BdSERK2*) was dependent on fungal DCL. Additionally, RNA-ligase-mediated Rapid Amplification of cDNA Ends (RLM-RACE) identified infection-specific degradation products for the three barley gene transcripts, consistent with the possibility that tRFs contribute to fungal virulence via targeted gene silencing.

Introduction

RNA interference (RNAi) is a biological process in which small RNA (sRNA) molecules mediate gene silencing at the transcriptional or post-transcriptional level. In agriculture, RNAi-mediated silencing strategies have the potential to protect crops from pests and microbial pathogens [1–5]. Expression of non-coding double-stranded (ds) RNA targeting essential genes in a pest, a pathogen or a virus can render host plants more resistant by a process known as host-induced gene silencing (HIGS) [6–9]. Alternatively, plants can be protected by foliar application of dsRNA to plants [10–16]. While these RNAi-based crop protection strategies are

collection and analysis, decision to publish, or preparation of the manuscript.

Competing interests: The authors have declared that no competing interests exist.

proving to be efficient and agronomically practical in the control of insects [17] and viruses [18], many questions remain unanswered with regard to the control of fungi.

The blueprint for using RNA to fight disease comes from nature [7]. During infection of *Arabidopsis thaliana* (*At*), the necrotrophic ascomycete *Botrytis cinerea* (*Bc*) secretes DICER-like (DCL)-dependent sRNAs that are taken up into plant cells to interact with the Arabidopsis ARGONAUTE protein *At*AGO1 and initiate silencing of plant immune genes [19, 20]. For instance, sRNA *Bc*-siR3.2 targets mitogen-activated protein kinases, including *MPK2* and *MPK1* in *At*, and *MAPKKK4* in tomato (*Solanum lycopersicum*), while *Bc*-siR37 targets several immune-related transcription factors including *WRKY7*, *PMR6* and *FEI2* [21]. Likewise, the oomycete *Hyaloperonospora arabidopsidis* produces 133 AGO1-bound sRNAs, which are crucial for virulence [22], and microRNA-like RNA1 (*Pst*-milR1) from the yellow rust causing biotrophic basidiomycete *Puccinia striiformis* f.sp. *tritici* (*Pst*) reduced expression of the defence gene *Pathogenesis-related* 2 (*PR2*) in wheat (*Triticum aestivum*) [23]. Notably, when comparing sRNA in the leaf rust fungus *Puccinia triticina* (*Pt*), 38 *Pt*-sRNAs were homologous to sRNAs previously identified in *Pst* [24, 25], hinting to the possibility that sRNA effectors are conserved among related fungal species as it is known for plant miRNAs [26, 27]. One group of conserved sRNAs with putative effector function are transfer RNA (tRNA)-derived fragments (tRFs). Bacterial tRFs play a role in the symbiotic interaction between soybean (*Glycine max*) and its nitrogen fixing symbiont *Bradyrhizobium japonicum* during root nodulation [28]. Similarly, the protozoan pathogen *Trypanosoma cruzi* secretes tRF-containing microvesicles resulting in gene expression changes in mammalian host cells [29].

Fungal species of the genus *Fusarium* belong to the most devastating pathogens of cereals causing Fusarium head blight and crown rot [30], and contaminate the grain with mycotoxins such as the B group trichothecenes deoxynivalenol (DON), nivalenol (NIV), and their acetylated derivatives (3A-DON, 15A-DON, and 4A-NIV) [31–33]. Viability, aggressiveness, and virulence of Fusaria are under control of the RNAi machinery [8, 34, 35]. In tomato, a *Fol-milR1* produced by *F. oxysporum* f.sp. *lycopersici* (Fol) was shown to target the protein kinase *SlyFRG4* via AGO4a [36]. Moreover, in wheat, *Fg-sRNA1* produced by *Fg* targets and silences the pattern recognition receptor gene *TaCEBiP* (*Chitin Elicitor Binding Protein*) [37].

To further test the possibility of *Fg* producing sRNAs that exert effector function and promote pathogenesis, we predicted *Fg*-sRNA targets in two Poaceae hosts, *Hordeum vulgare* (*Hv*) and *Brachypodium distachyon* (*Bd*). Among the many predicted plant targets of fungal sRNA, three fungal tRFs had sequence similarity to *BRI1-associated receptor kinase 1* (*BAK1*) homologs and *EOL1* (*Ethylene overproducer 1-like 1*) in *Hv* and *Bd*. Upon infection with the wild type *Fg* strain, transcripts of genes were strongly reduced, while in contrast they were increased upon infection with *Fg* strains compromised for DCL activity. Degradation products of target mRNAs were detected by RNA-ligase-mediated Rapid Amplification of cDNA Ends (RLM-RACE), supporting the possibility that DCL-dependent sRNAs play a critical role in the interaction of *Fg* with cereal hosts.

Results

Fusarium graminearum DCL mutants are less virulent on barley and *Brachypodium* leaves

The *Fusarium* mutant IFA65-*dcl1* is partially impaired in infecting wheat ears and causing Fusarium Head Blight [8]. We extended this earlier study to examine the effects of impaired DCL activity on the plant defence response. To this end, two to three-week-old detached second leaves of barley cv. Golden Promise (GP) were drop-inoculated with 3 μl of a solution containing 150,000 conidia per ml of *Fg* isolate PH1 or the double knock-out (dKO) mutant

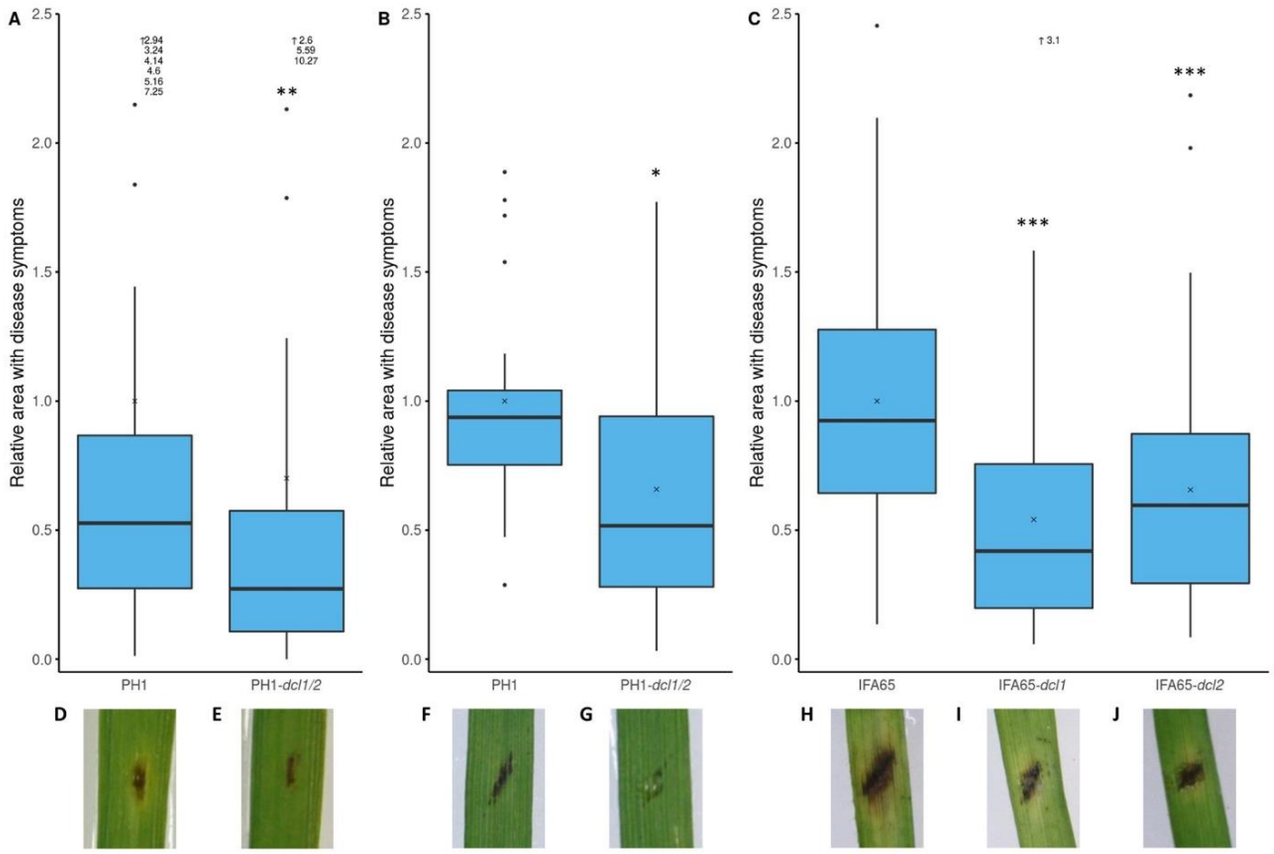

Fig 1. Virulence of *Fusarium graminearum* DCL single and dKO mutants on barley and *Brachypodium*. A: Relative infected area on leaves of barley cv. Golden Promise (GP) at 5 dpi. Detached leaves were inoculated with 3 μl of a solution containing 150,000 conidia per mL. The area with leaf necrosis was measured with the free image analysis software package PlantCV. Boxplots represent the median and quartiles of three independent biological experiments (n = 56). (Wilcoxon Rank Sum Test, $P = 7.1^{*}10^{-3}$, x = mean). B and C: Relative infected leaf area on leaves of *Brachypodium distachyon* Bd21-3 at 4 dpi (B) or 5 dpi (C). Detached leaves were inoculated with 10 μl of a solution containing 10,000 conidia per mL. The area with leaf necrosis was measured with ImageJ. Boxplots represent the median and quartiles of three (B) or nine (C) independent biological experiments (n = 21 (B), n = 63 (C)). (B: Wilcoxon Rank Sum Test, P = 0.013; C: Pairwise Wilcoxon Rank Sum Test, Bonferroni corrected, $P_{dcl1} = 4.9^{*}10^{-8}$, $P_{dcl2} = 2.6^{*}10^{-4}$; x = mean). Outliers (>2.5) are not shown but indicated as written values next to the upward arrow (↑). D-J: Representative pictures of disease symptoms of PH1 (D and F), PH1-*dcl1/2* (E and G), IFA65 (H), IFA65-*dcl1* (I) and IFA65-*dcl2* (J) on barley (D and E) and Bd (F-J).

https://doi.org/10.1371/journal.pone.0252365.g001

PH1-*dcl1/2*. At five days post inoculation (dpi), the dKO mutant produced significantly smaller necrotic lesions (30%; median (MED) (27%); interquartile range (IQR) (47%) Wilcoxon rank sum test, p = 0.007) than the wild type (wt) strain, confirming that DCL activity is required for full *Fg* virulence (Fig 1A).

Next, we determined the virulence of *DCL* mutants on *Brachypodium distachyon* Bd21-3. Flag leaves of three-week-old plants were inoculated with 10 μl (10,000 conidia ml^{-1}) of fungal inoculum. Single mutants IFA65-*dcl1* and IFA65-*dcl2* and dKO mutant PH1-*dcl1/2* produced significantly smaller lesions than the wt (PH1-*dcl1/2*, 66%; MED (52%); IQR (66%); Wilcoxon rank sum test; p = 0.013, IFA65-*dcl1*, 54%; MED (42%); IQR (56%) and IFA65-*dcl2*, 66%; MED (60%); IQR (58%); pairwise Wilcoxon rank sum test; Bonferroni corrected; $p<0.005$) (Fig 1B and 1C). These results substantiate the earlier findings [8] that fungal DCL activity is required for *Fusarium* virulence on graminaceous plants.

Selection of sRNAs with sequence homology to plant genes

We looked for interaction-related fungal sRNAs that potentially could interfere with plant gene expression by sequence-specific silencing. To this end, a previously published sRNA sequencing data set of *Fg* sRNAs from an axenic IFA65 culture [10] was analysed for sRNAs with sequence complementarity to barley genes. In order to identify a wide range of potential targets, we applied only two selection criteria, namely *i*. size (21–24 nt) and *ii*. a minimal number of reads (at least 400 reads in the dataset). From a total of 35,997,924 raw reads, 5,462,596 (comprising 589,943 unique sequences) had a length of 21–24 nt. From the unique sequences, 1,987 had at least 400 reads. Since the IFA65 genome has not been sequenced, we used the published genome information of *Fg* strain PH1 (genome assembly ASM24013v3 from International Gibberella zeae Genomics Consortium: GCA_000240135.3) for further analysis. The majority of the 1,987 unique sRNAs mapped to rRNA (64.4%) and intergenic regions (21.6%), while 3.7% and 2.4% mapped to protein coding genes and tRNAs, respectively, and 7.8% did not perfectly match the reference genome (S1 Fig). According to the TAPIR algorithm, the 1,987 sequences overall matched mRNAs of 2,492 genes (Hordeum vulgare IBSC PGSB v2 reference genome; [38]) sufficiently close according to the refined target prediction criteria suggested by Srivastava et al. [39]. GO-enrichment analysis revealed an enrichment in functions of nucleotide binding, motor activity and kinase activity and processes such as transport and localization (S2 Fig). Most of the 14,156 transcripts of the 2,492 target genes, which we nominated as potential sRNA targets, showed partially homologous sequences to more than one sRNA accounting for a total of 17,275 unique pairs of potential target gene—sRNA combinations. Target prediction results are presented with only one transcript (splice variant) for every combination (S1 Table). Of note, merely 101 out of the 1,987 sRNAs had no predicted target among the total number of 248,391 plant mRNAs in the IBSC_PGSB_v2 annotation.

Barley immune genes accumulate to higher levels in PH1-dcl1/2-infected leaves

From the set of 2,492 barley genes with partial sequence homology to *Fg* sRNAs, we selected 16 genes for further analysis, based on an educated guess that they are potentially involved in biotic stress reactions during plant-fungal interaction (Table 1). When tested with RT-qPCR, we found eight genes, being targeted by a total of 104 unique *Fg* sRNAs, significantly higher expressed (Student's *t*-test, paired, $^{*}p<0.1$, $^{**}p<0.05$, $^{***}p<0.01$) in leaves infected with PH1-*dcl1/2* vs. PH1 (Fig 2). Among these genes are three that encode proteins involved in the regulation of either ethylene (ET) (Ethylene overproducer 1-like 1, *Hv*EOL1) or auxin responses (Auxin response transcription factors *Hv*ARF10 and *Hv*ARF19) and three kinases, of which Somatic embryogenesis receptor-like kinase 2 (*Hv*SERK2) and BRI1-associated receptor kinase 1 (*Hv*BAK1) are likely involved in recognition of microbe-associated molecular patterns (MAMPs). Moreover, genes encoding the plastid kinase 2-Phosphoglycolate phosphatase 2 (*Hv*PGLP2), Resurrection 1 (*Hv*RST1, with a rather elusive function in cuticle formation and embryo development), and the histone-lysine N-methyltransferase Su(var)3-9-related protein 5 (*Hv*SUVR5, involved in transcriptional gene silencing) were also strongly expressed.

The first column gives the name of the respective gene abbreviated as in Fig 1 and in full. The second column shows the respective accession. In the third column selected GO terms are shown. The fourth and fifth columns give the accession and abbreviated name of the closest homologue in *At*.

Table 1. Selected GO-terms of tested genes and closest homologs in *A. thaliana*.

Name	ensembl_gene_id	GO_term	*A.thaliana* Homolog	Abbr.
HvARF3	HORVU1Hr1G076690	auxin-activated signaling pathway	AT2G33860	*ARF3*
Auxin response transcription factor 3		regulation of transcription, DNA-templated		
		nucleus		
HvSUB1	HORVU2Hr1G028070	Golgi apparatus	AT4G08810	*SUB1*
Short under blue light 1		transferase activity, transferring glycosyl groups		
		fucose metabolic process		
HvPPR	HORVU2Hr1G078260	protein binding	AT2G06000	
Pentatricopeptide repeat superfamily protein				
HvSERK2	HORVU2Hr1G080020	integral component of membrane	AT1G34210	*SERK2*
Somatic embryogenesis receptor-like kinase 2_1		positive regulation of innate immune response		
		regulation of defense response to fungus		
HvARF10	HORVU2Hr1G089670	auxin-activated signaling pathway	AT2G28350	*ARF10*
Auxin response transcription factor 10		regulation of transcription, DNA-templated		
		nucleus		
HvEOL1	HORVU2Hr1G119180	regulation of ethylene biosynthetic process	AT4G02680	*EOL1*
ETO1-like 1		protein binding		
HvRST1	HORVU3Hr1G016630	integral component of membrane	AT3G27670	*RST1*
Resurrection 1		membrane		
HvPIX7	HORVU3Hr1G051080	protein serine/threonine kinase activity	AT5G15080	*PIX7*
Putative interactor of XopAC 7		ATP binding		
		protein kinase activity		
Hvemb2726	HORVU5Hr1G024470	translation elongation factor activity	AT4G29060	*emb2726*
Embryo defective 2726		mitochondrion		
		intracellular		
HvPGLP2	HORVU5Hr1G052320	chloroplast	AT5G47760	*PGLP2*
2-Phosphoglycolate phosphatase 2		phosphoglycolate phosphatase activity		
		hydrolase activity		
HvATG2	HORVU6Hr1G034660	autophagy of peroxisome	AT3G19190	*ATG2*
Autophagy-related 2		autophagy		
HvSUVR5	HORVU6Hr1G069350	histone-lysine N-methyltransferase activity	AT2G23740	*SUVR5*
Su(var)3-9-related protein 5		chromosome		
		methyltransferase activity		
HvRDR1	HORVU6Hr1G074180	RNA-directed 5'-3' RNA polymerase activity	AT1G14790	*RDR1*
RNA-dependent RNA polymerase 1		RNA binding		
		gene silencing by RNA		
HvGDH	HORVU6Hr1G076880	glycine decarboxylation via glycine cleavage system	AT2G35370	*GDH1*
Glycine decarboxylase complex H		glycine cleavage complex		
		mitochondrion		
HvBAK1	HORVU7Hr1G068990	integral component of membrane	AT1G34210	*SERK2*
Somatic embryogenesis receptor-like kinase 2_2		transmembrane receptor protein serine/threonine kinase signaling pathway		
HvARF19	HORVU7Hr1G096460	auxin-activated signaling pathway		
Auxin response transcription factor 19		regulation of transcription, DNA-templated		
		nucleus		
BdSERK2	BRADI_5g12227v3	integral component of membrane	AT1G34210	*SERK2*
Somatic embryogenesis receptor-like kinase 2		positive regulation of innate immune response		
		regulation of defense response to fungus		

https://doi.org/10.1371/journal.pone.0252365.t001

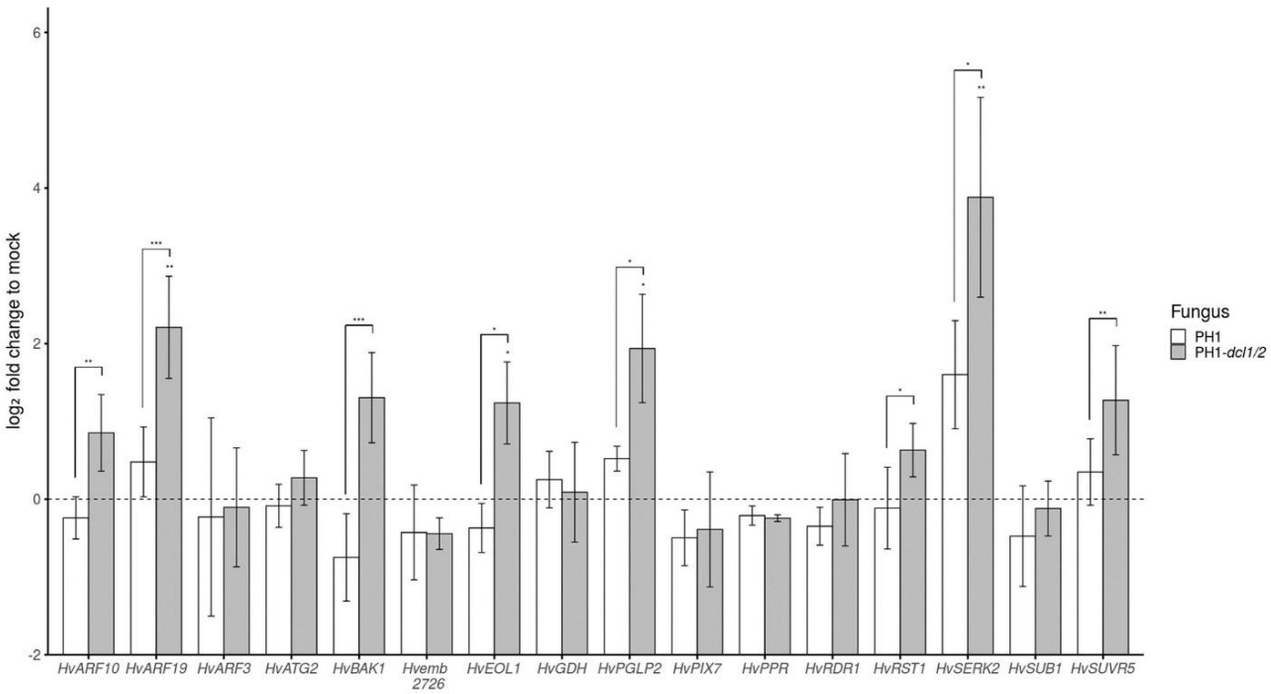

Fig 2. Relative expression (log2 fold) of potential barley target genes for fungal sRNAs in leaves infected with *Fusarium graminearum* wt strain PH1 vs. PH1-dcl1/2. Expression was normalized against barley *Ubiquitin* (*HvUBQ*) and subsequently against the Δct of the uninfected control (mock treatment). Bars represent the mean±SE of three independent biological replicates. Significant differences were calculated for the expression of a respective gene in PH1 vs. PH1-*dcl1/2*-infected samples and PH1 vs. controls. The dotted line shows the expression level of mock treatment. (Student's *t*-test, (paired) one sided, $^{*}P<0.1$, $^{**}P<0.05$, $^{***}P<0.01$).

https://doi.org/10.1371/journal.pone.0252365.g002

HvEOL1 transcripts also accumulate to higher levels upon DCL knock-down via spray induced gene silencing (SIGS)

We selected *HvEOL1* (*HORVU2Hr1G119180*), which is a homologue of *At Ethylene overproducer1* (*AtETO1*; *AT4GO2680.1*), for further analysis. The alignment of the respective protein sequences of *Hv*EOL1 and *At*ETO1 is shown in S3 Fig. *At*ETO1 negatively regulates ethylene synthesis in *At* by ubiquitination of type-2 1-Aminocyclopropane-1-carboxylate synthases (ACSs), which produce the direct precursor of ET [40] (S4 Fig). Upon inoculation with PH1, *HvEOL1* expression was reduced by 23% as compared to non-inoculated barley leaves. In contrast, *HvEOL1* was strongly expressed in PH1-*dcl1/2*-infected leaves well above the levels measured either in PH1- or mock-inoculated leaves. To further substantiate that *HvEOL1* expression is under the control of fungal DCL activity, we used a SIGS strategy [10] to partially inactivate DCL function in *Fg*. Two-week-old detached leaves were sprayed with 20 ng μl^{-1} of dsRNA-*dcl1/2*, a 1,782 nt long dsRNA derived from the sequences of IFA65-*DCL1* and IFA65-*DCL2* (S5A and S5B Fig). 48 h later, leaves were drop inoculated with conidia and harvested at 5 dpi. Consistent with the expectation that exogenous dsRNA-*dcl1/2* mediates silencing of their *DCL* gene targets, RT-qPCR analysis confirmed that the transcript levels of IFA65-*DCL1* and IFA65-*DCL2* were reduced to 22% and 42%, respectively, as compared with the Tris-EDTA (TE) buffer control (Fig 3A). In accordance with the results obtained with strain PH1, *HvEOL1* was also significantly ($p = 0.029$, Student's *t*-test (Δct), one sided, paired) downregulated in response to IFA65 infection compared to mock controls treated with 0.02% Tween20 (Fig 3B). In contrast, however, when leaves were sprayed with dsRNA-*dcl1/2* prior to

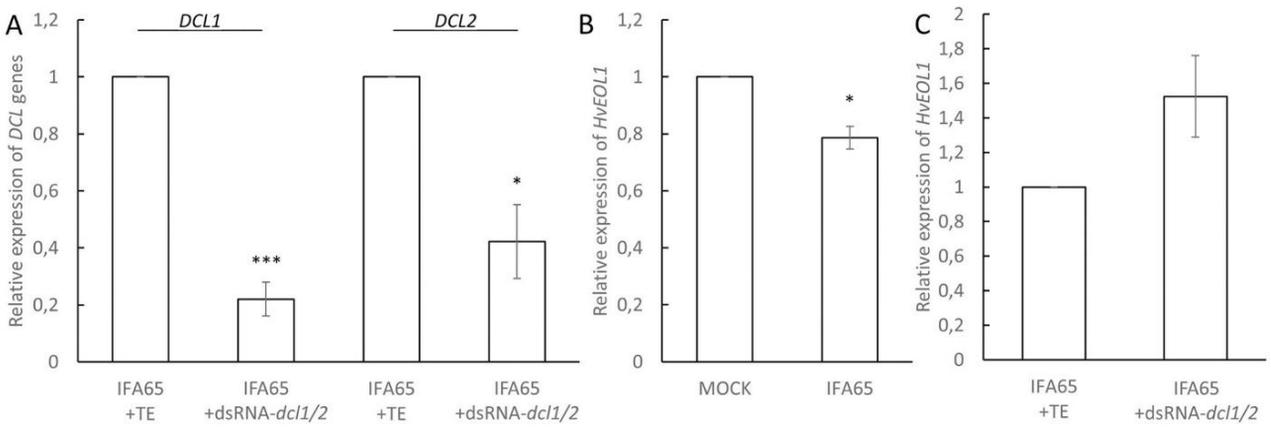

Fig 3. Relative expression of HvEOL1 in response to inoculation of barley leaves with *Fusarium graminearum*. **A,** Relative expression of *FgDCL1* and *FgDCL2* on detached barley cv. Golden Promise leaves at 5 dpi in wt strain IFA65 and 7 days post spray application of the 1,782 nt long dsRNA construct dsRNA-*dcl1/2* vs. TE buffer. **B**, Relative expression of *HvEOL1* at 5 dpi with IFA65 vs. mock control. **C**, Relative expression of *HvEOL1* 5 dpi with wt strain IFA65 and 7 days post spray application of dsRNA-*dcl1/2* vs. TE buffer. Gene expression was first normalized against the reference gene *HvUBQ (HORVU1Hr1G023660)* and subsequently against the Δct of the respective control for B (mock = 0.002% Tween20) and for A,C (IFA65 / TE). Bars represent the mean ± SE of three (B) and four (A, C) independent biological replicates. (Student's *t*-test, $^{*}P<0.05$, $^{***}P<0,005$).

https://doi.org/10.1371/journal.pone.0252365.g003

inoculation with IFA65, *HvEOL1* transcripts accumulated (p = 0.055, Student's *t*-test (Δct), one sided, paired) in comparison with the inoculated leaves sprayed with TE buffer (Fig 3C).

Fungal sRNAs targeting HvBAK1, HvEOL1, and HvSERK2 mRNAs are less abundant in PH1-dcl1/2 vs. PH1

To detect the abundance of specific *Fg*-sRNAs, originally identified by sequencing of axenic IFA65 mycelium, in PH1-infected plant tissue, we performed reverse transcription stem-loop qPCR [41]. From the above defined pool of 1,987 *Fg*-sRNAs (axenic, 21–24 nt length, > = 400 reads) 22 unique sRNAs matched partial sequences of *HvEOL1*, 10 matched *HvBAK1* and five matched *HvSERK2*. *Fg*-sRNA-1921 matched all three genes and *Fg*-sRNA-321 matched both *HvEOL1* and *HvBAK1* (Table 2 and S2 Table). These two sRNAs show high sequence similarities among each other. To identify their origin, they were aligned to the genomic sequence of strain PH1 (GCA_900044135.1). We found that they match the gene *Fg_CS3005_tRNA-Gly-GCC-1-9* encoding tRNA-Gly for the anticodon GCC. Of note, a larger cluster of 27 overlapping tRNA-derived fragments (tRFs) with more than 50 reads matching the tRNA-Gly gene sequence were detected (S6 Fig). To assess differential accumulation of tRFs from the *Fg_CS3005_tRNA-Gly-GCC-1-9* cluster in leaves infected with PH1 *vs.* PH1-*dcl1/2*, sRNAs were reverse transcribed using hairpin-priming followed by qPCR amplification [41]. For this analysis, we chose *Fg*-sRNA-321, the most abundant tRF from this cluster, along with *Fg*-sRNA-1921, which targets all three GOIs and an additional tRF (*Fg*-sRNA-6717), which targets *HvEOL1* and *HvBAK1* (see Table 2) to assess the sensitivity of the assay. In the initial IFA65 dataset the *Fg*-sRNA-321 had a read count of 2,106, *Fg*-sRNA-1921 had 416 and *Fg*-sRNA-6717 had 86 from a total of more than 5 million reads (S7 Fig). This equals 386 reads per million (rpm) for *Fg*-sRNA-321, while in average unique reads had only 1.7 rpm. Using TAPIR [42], we also calculated the target score values for all three tRFs, which is a measure for the similarity between sRNA and target. A high value refers to more dissimilarities. Mismatches (MMs) increase the score by one point and G-U pairs by 0.5 points. These values are doubled if the respective MMs and G-U pairs are located between the second and 12th nt of the sRNA

Table 2. Target prediction results of *Fg*-sRNAs with more than 400 reads in IFA65 axenic culture.

sRNA-Name	Reads	Score	Alignment			Length
Fg-sRNA-321	2106	4.5	3'	GCUUGGGUCCCGAGGGGCUACC	5'	22
				..|.o||||||||||o|||		
HvEOL1			5'	GAAUUCCAGGGCUCCCCGGUGG	3'	
Fg-sRNA-1921	416	3.5	3'	CUUGGGUCCCGAGGGGCUACC	5'	21
				.|.o||||||||||o|||		
HvEOL1			5'	AAUUCCAGGGCUCCCCGGUGG	3'	
Fg-sRNA-6717	86	4.5	3'	UAGCUUGGGUCCCGAGGGGCUAC	5'	23
				||..|.o||||||||||o||		
HvEOL1			5'	AUGAAUUCCAGGGCUCCCCGGUG	3'	
Fg-sRNA-1921	416	6	3'	CUUGGGUCCCGAGGGGCUACC	5'	21
				|.||.||||.||.||||||		
HvSERK2			5'	GCACGCAGGGGUCACCGAUGG	3'	
Fg-sRNA-321	2106	4.5	3'	GCUUGGGUCCCGAGGGGCUACC	5'	22
				o|.||.|||||||||.|||		
HvBAK1			5'	UGCACACAGGGCUCCCCCAUGG	3'	
Fg-sRNA-1921	416	4	3'	CUUGGGUCCCGAGGGGCUACC	5'	21
				|.||.|||||||||.|||		
HvBAK1			5'	GCACACAGGGCUCCCCCAUGG	3'	
Fg-sRNA-6717	86	5.5	3'	UAGCUUGGGUCCCGAGGGGCUAC	5'	23
				.|o|.||.|||||||||.|||		
HvBAK1			5'	UUUGCACACAGGGCUCCCCCAUG	3'	
Fg-sRNA-321	2106	5.5	3'	GCUUGGGUCCCGAGGGGCUACC	5'	22
				..|.o||||||||o|||o|||		
BdEOL1			5'	GAAUUCCAGGGCUCUCCGGUGG	3'	
Fg-sRNA-1921	416	4.5	3'	CUUGGGUCCCGAGGGGCUACC	5'	21
				.|.o||||||||o|||o|||		
BdEOL1			5'	AAUUCCAGGGCUCUCCGGUGG	3'	
Fg-sRNA-6717	86	5.5	3'	UAGCUUGGGUCCCGAGGGGCUAC	5'	23
				||..|.o||||||||o|||o||		
BEOL1			5'	AUGAAUUCCAGGGCUCUCCGGUG	3'	
Fg-sRNA-321	2106	3.5	3'	GCUUGGGUCCCGAGGGGCUACC	5'	22
				o|.||.||.|||||||||||		
BdSERK2			5'	UGCACGCAAGGCUCCCCGAUGG	3'	
Fg-sRNA-1921	416	3	3'	CUUGGGUCCCGAGGGGCUACC	5'	21
				|.||.||.|||||||||||		
BdSERK2			5'	GCACGCAAGGCUCCCCGAUGG	3'	
Fg-sRNA-6717	86	5.5	3'	UAGCUUGGGUCCCGAGGGGCUAC	5'	23
				..o|.||.||.||||||||||		
BdSERK2			5'	UCUGCACGCAAGGCUCCCCGAUG	3'	

Mismatches (MMs) between mRNA and sRNA are marked as ".", while G-U pairs are marked as "o".

https://doi.org/10.1371/journal.pone.0252365.t002

(5'-3') because a high similarity in the seed region of the sRNA is especially important for RNAi [43]. *Fg*-sRNA-321 has a score of 4.5 for *HvBAK1* and *HvEOL1*, *Fg*-sRNA-1921 has a score of 4, 3.5 and 6 for *HvBAK1*, *HvEOL1* and *HvSERK2*, respectively and *Fg*-sRNA-6717 has a score of 5.5 and 4.5 with *HvBAK1* and *HvEOL1*. In plants other than Arabidopsis, such as

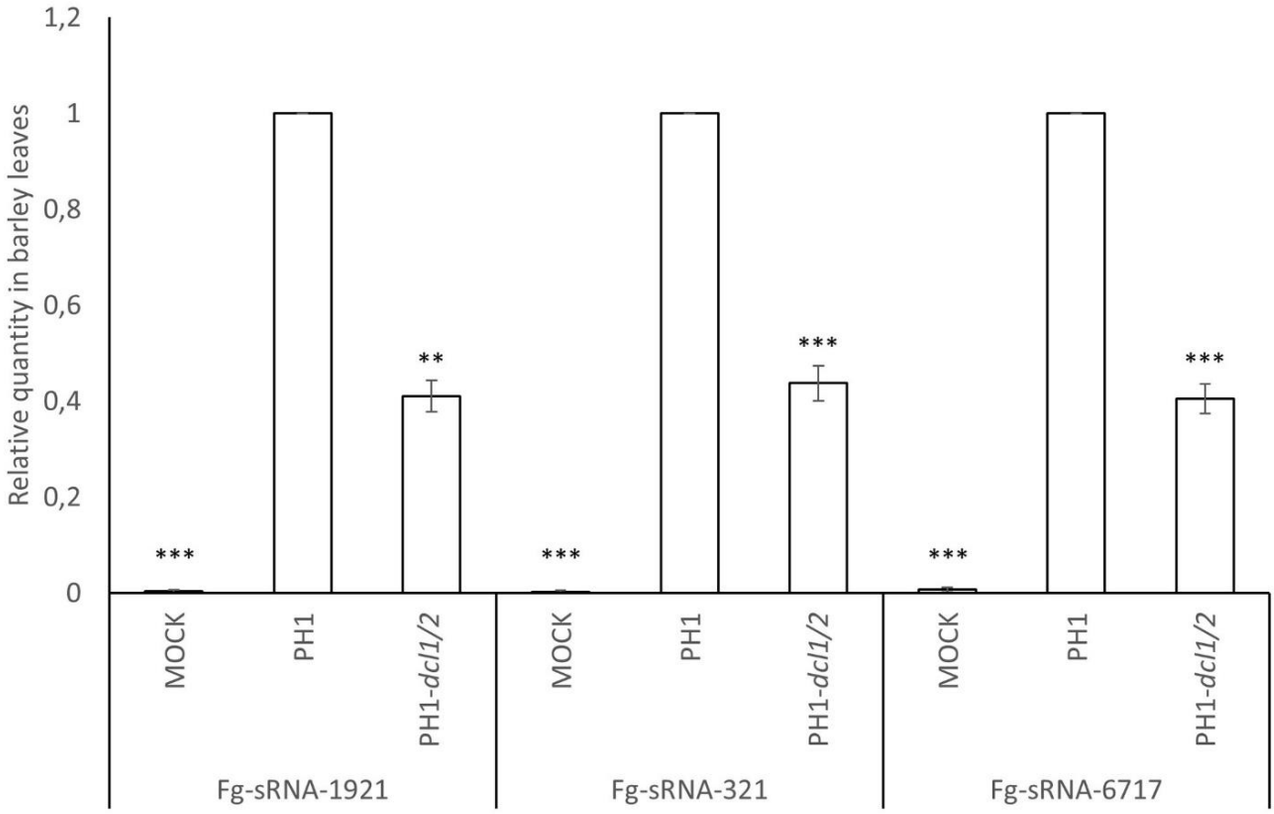

Fig 4. Relative amount of different fungal tRFs with homology to *HvEOL1* mRNA. Relative amount of different fungal tRFs with homology to *HvEOL1* mRNA during infection of barley leaves with PH1 and PH1-*dcl1/2* normalized to fungal biomass and relative quantity of sRNAs normalized to wt PH1 measured by qPCR. *Fg*-sRNA-1921, *Fg*-sRNA-321 and *Fg*-sRNA-6717 quantity was normalized to *Hvu*-miR159 and *Hvu*-miR168 and fungal biomass as determined by *FgEF1α* expression was normalized to *HvUBQ*. Subsequently the amount of sRNAs was normalized with fungal biomass. The amount of sRNA in PH1-infected leaves was set to 1. Values and error bars represent the mean ± SE of three independent biological replicates. Significance was calculated via a one-sample *t*-test. (**P<0.01, ***P<0.005).

https://doi.org/10.1371/journal.pone.0252365.g004

wheat and rice, a score cut off at 4 or 6 points lead to a precision of 82% or 62% and a recall of known interactions of 39% or 58% respectively according to Srivastava et al. [39].

All three fungal tRFs were detected in infected leaves, while they could not be found in uninfected leaves (Fig 4). Significantly lower amounts of *Fg*-sRNA-1921 (59%), *Fg*-sRNA-321 (56%), and *Fg*-sRNA-6717 (60%) were detected in PH1-*dcl1/2 vs*. PH1-infected leaves (Fig 4), showing that their biogenesis is DCL-dependent.

Fg-sRNA-321 and *Fg*-sRNA-1921 also match *SERK2* in *Brachypodium distachyon* Bd21-3

Next, we assessed the possibility that *Fg*-sRNA-321, *Fg*-sRNA-1921 and *Fg*-sRNA-6717 also have sequence homologies in *At* and the model grass *Bd*. Target prediction with the TAPIR algorithm using the optimised parameters for *At* (score = 4; mfe = 0.7), could not detect potential targets in *At* ecotype Col-0. In contrast, these three tRFs matched the sequence of *Brachypodium somatic embryogenesis receptor-like kinase 2* (*BdSERK2*) in Bd21-3 with a score of 3.5, 3 and 5.5, respectively (Table 2). We examined the expression pattern of *BdSERK2* in response to leaf infection: *BdSERK2* is relatively weakly expressed in uninfected plants and is not further suppressed after inoculation with PH1, whereas it strongly accumulated in PH1-*dcl1/2 vs*.

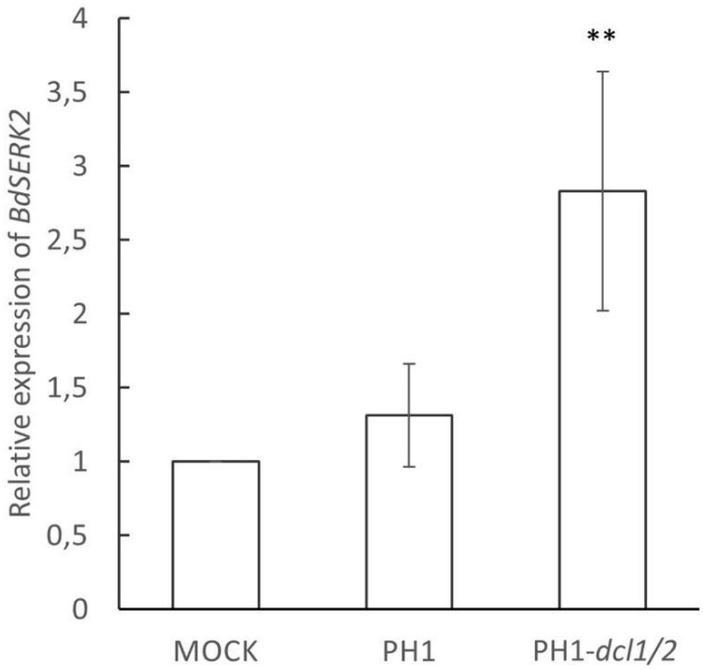

Fig 5. Relative expression of BdSERK2 in response to inoculation of *Brachypodium distachyon* leaves with *Fusarium graminearum*. Relative expression of *BdSERK2* in detached Bd21-3 leaves at 4 dpi with PH1 vs. PH1-*dcl1/2*. The gene expression was first normalized against the reference gene *BdUBI4* and subsequently against the Δct of the mock treated control. Values and error bars represent the mean ± SE of three independent biological replicates. (Student's t-test, paired, one sided, $^{**}P<0,01$).

https://doi.org/10.1371/journal.pone.0252365.g005

PH1-infected Bd21-3 (Fig 5). This finding further supports the possibility that the control of *SERK2* expression via RNAi pathways by *Fg* is evolutionary conserved in cereals.

RLM-RACE shows infection specific degradation products of *HvBAK1*, *HvEOL1* and *HvSERK2*

We assessed the sRNA-mediated cleavage of *HvBAK1*, *HvEOL1*, and *HvSERK2* mRNAs, using a modified RNA-ligase-mediated Rapid Amplification of cDNA Ends (RLM-RACE) assay. Control samples were prepared both from uninfected tissue and from infected tissue without the reverse transcription step (no-RT control) and PCR products were visualized on an EtBr-Agarose gel. In these no-RT controls no amplification was visible.

For each gene more than one infection-specific product was amplified (blue and red arrows), which could not be amplified from the uninfected sample (Fig 6D–6F). We excised three bands (red arrows) of the expected size for a *Fg*-sRNA-1921 guided cleavage of *HvBAK1* (Fig 6D) and one band for *HvEOL1* (Fig 6E) and *HvSERK2* (Fig 6F) and cloned them into the pGEM-T easy vector system. According to the IBSC_PGSB_v2 assembly, *HvBAK1* has splice variants, which could produce cleavage products of different lengths while for *HvSERK2* and *HvEOL1* there are no introns between sRNA target site and primer. From each band, five colonies were picked and for 23 of these extracted plasmids sequences were obtained. 16 sequences perfectly matched the reference genome, four with one MM and one with four MMs. Two sequences did not match the reference sufficiently enough to be aligned over the full length. The observed cleavage products are close to but do not match the canonical slice site between the 10^{th} and 11^{th} nt of *Fg*-sRNA-1921 and *Fg*-sRNA-321 (Fig 6A–6C).

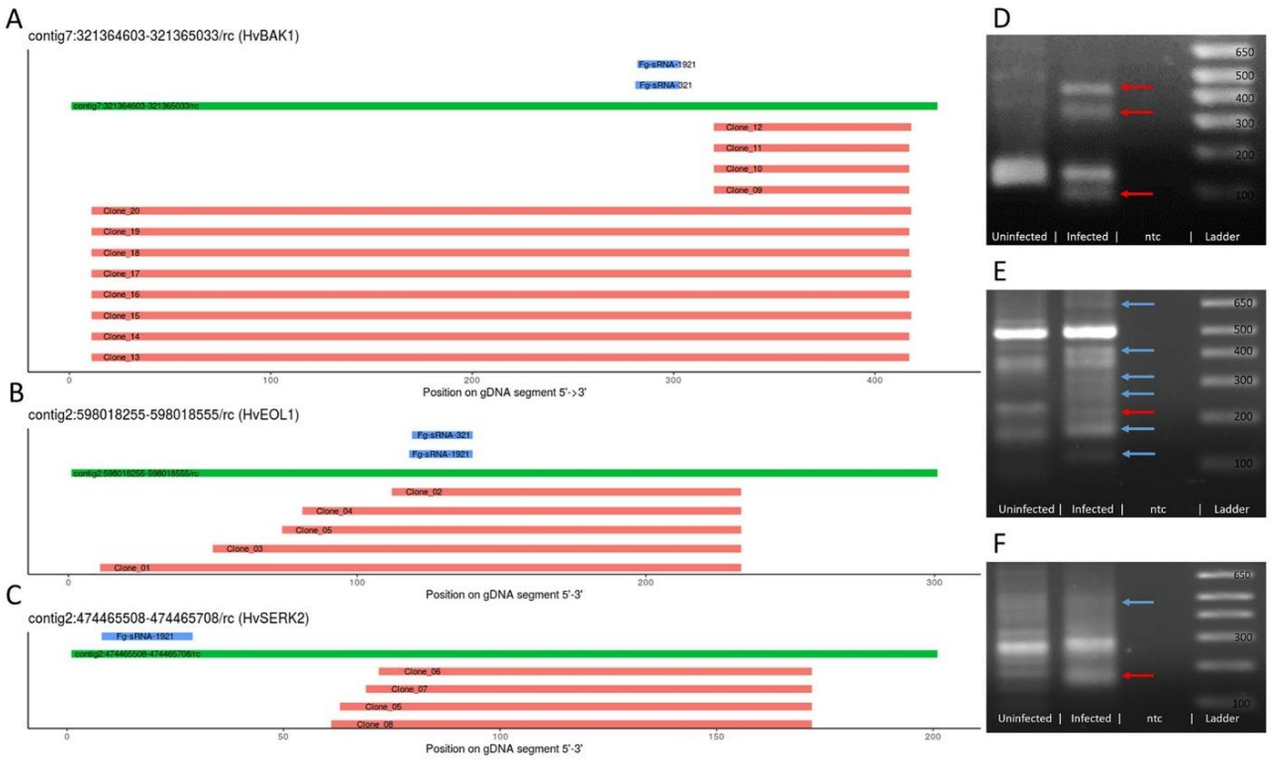

Fig 6. Analysis of potential target sites of *Fg*-sRNAs as determined by RLM-RACE products. A,B,C Potential target sites of *Fg*-sRNA-321 and *Fg*-sRNA-1921 predicted by TAPIR (blue), genomic DNA (GPv1, GCA_902500625.1, A: contig7:321364603–321365033, B: contig2:598018255–598018555, C: contig2:474465508–474465708) of barley cv. Golden Promise (green), and the alignment of sequences derived from the RLM-RACE PCR (red) relative to the *Hv*-gDNA and *Fg*-sRNAs. **D,E,F** PCR-products of the second nested RLM-RACE-PCR visualized in an EtBr-Agarose gel. Red arrows indicate excised bands and blue arrows indicate infection specific products.

https://doi.org/10.1371/journal.pone.0252365.g006

Total sRNAs predicted to target a gene in barley are correlated with the de-repression strength

Not all potential targets of *Fg*-sRNAs are downregulated nor do all potential targets show a re-accumulation upon infection with PH1-*dcl1/2* (see Fig 3). To address this bias we conducted a more focused target prediction exclusively for the 16 genes already tested by RT-qPCR. This allowed a much more thorough search, where targets for all sRNAs with at least two reads were predicted. From these 136,825 unique sRNAs (axenic, 21–24 nt length, > = 2 reads) representing 4,997,312 reads of the total of 5,439,472 reads 21–24 nt in length, 5,052 have potential target sequences in the 16 mRNA sequences selected for further investigation in the *Hordeum vulgare* cv. GP assembly GCA_902500625. An additional filter step was employed to select for sRNAs with a maximum of one MM to the PH1 assemblies GCA_000240135.3 and GCA_900044135.1. Subsequently, sRNAs with up to one MM to *Fg*-rRNAs were removed leaving a total of 1,212 sRNAs with 1,311 potential sRNA-mRNA interactions representing 85,531 reads in the analysis.

To establish a correlation of the observed resurgence of potential target genes and targeting sRNAs, we analysed the *DCL*-dependent expression change using ΔΔΔct values. To compare the expression of a GOI in two samples, the difference between the ct-values for a reference gene and the GOI can be determined (Δct) and to calculate the expression difference between the control and treated sample the difference between the Δct values (ΔΔct) is calculated. We

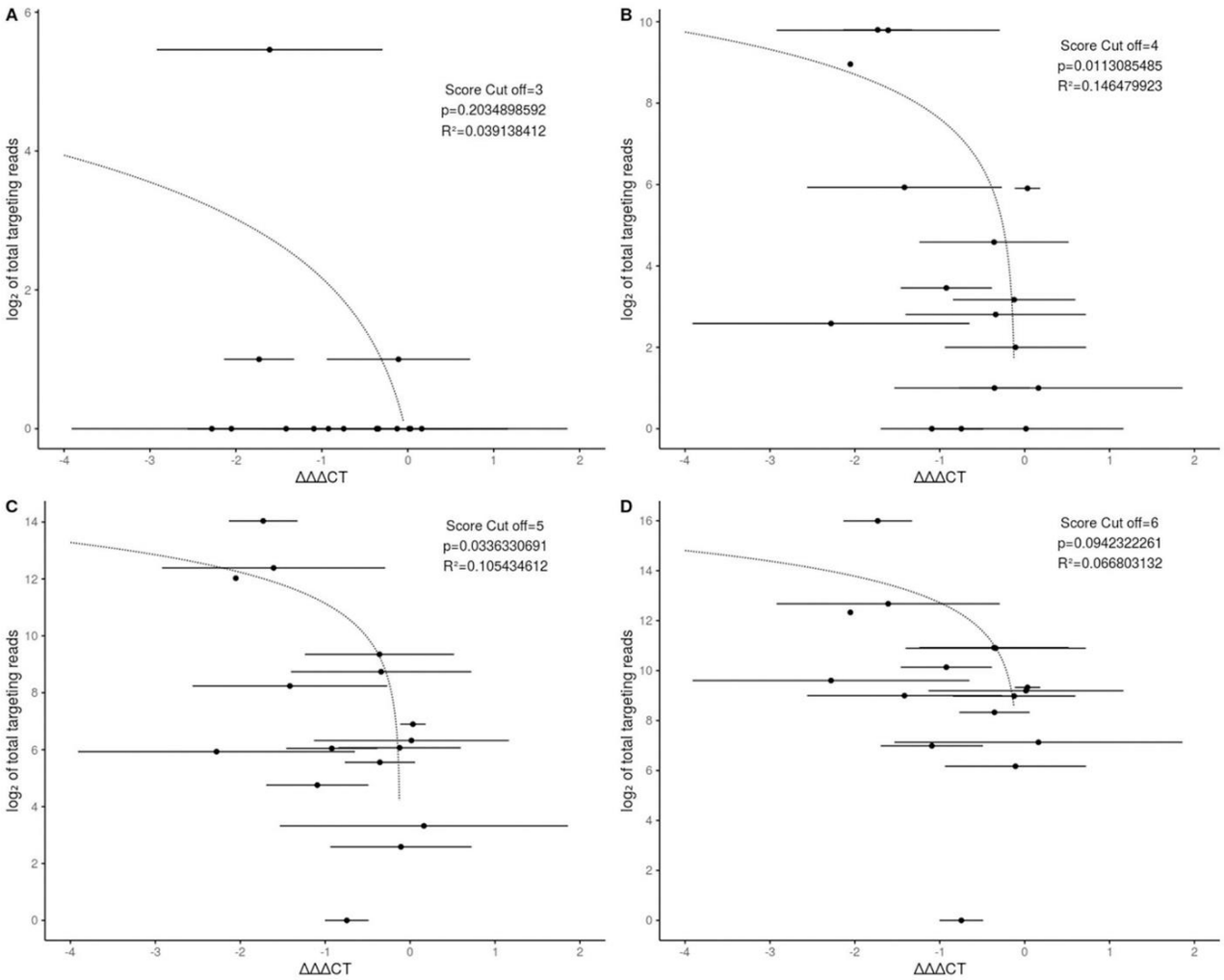

Fig 7. The degree of DCL-dependent gene silencing is correlated with the number of homologous fungal sRNAs. Each dot represents a predicted target gene of *Fg*-sRNAs. On the x-axis the ΔΔΔct-value is shown with bars representing SD. On the y-axis the $\log_2$ of the number of total sRNAs potentially targeting each gene are shown. The dotted line represents a linear regression model. P indicates the significance (t-test) of the model and the score cut-off indicates the score limit used during the target prediction. Plot A, B, C and D are the calculations for a score cut off of 3, 4, 5 and 6 respectively.

https://doi.org/10.1371/journal.pone.0252365.g007

further defined the ΔΔΔct value as the difference between the ΔΔct values for a GOI in PH1 and PH1-*dcl1/2*-infected samples. From this follows a gene with a negative ΔΔΔct value shows a higher transcript accumulation during the infection with a fungal strain with compromised DCL function and the stronger the accumulation the lower this ΔΔΔct value is. We found a negative correlation between the ΔΔΔct value and the number of total sRNAs targeting a GOI (Fig 7). This correlation becomes more significant if a lower score cut-off for the target prediction is chosen until the cut-off of four. The most significant correlation is for all predicted interactions with a score equal or below four with a p-value of 0.011 (t-test) (Fig 7B). The p-value for a correlation with a cut-off of five (Fig 7C) is 0.033 (t-test) and six (Fig 7D) is 0.094 (t-test), while a score cut-off of 3 leads to a situation, where there are no predicted sRNA interactions for all genes except for three (Fig 7A).

Discussion

We show here that full virulence of the ascomycete fungus *Fusarium graminearum* on graminaceous leaves depends on the activity of fungal DCLs. The dKO mutant PH1-*dcl1/2* is less virulent on barley and the two single KO mutants IFA65-*dcl1* and IFA65-*dcl2* also are less virulent on *Brachypodium*. These results are consistent with our previous studies showing that knock-down or SIGS-mediated silencing of *Fusarium DCLs* and other components of the RNAi machinery reduced the virulence of the fungus on barley [8, 44]. DCL enzymes are key components of the fungal RNAi machinery required for the biogenesis of sRNAs directing silencing of sequence-complementary endogenous and foreign genes [45]. The latter case involves DCL-dependent pathogen-derived sRNAs that target plant defense genes to increase virulence as shown for *Botrytis cinerea* [19, 21], *Puccinia striiformis* [23] and *Magnaporthe oryzae* [46].

In the present work we found potential host target genes for fungal small RNAs (*Fg*-sRNAs) that were differentially regulated in response to plant infection with *Fg* wt *vs*. *Fg* DCL KO mutants, and the same effect was confirmed when DCLs were silenced by SIGS. This suggests a scenario in which impaired DCL function resulting in reduced fungal RNAi activity ultimately leads to de-repression of host target genes. Of note, target gene de-repression was also observed when the transcript was not significantly downregulated by the wt fungus during infection. This could be explained by a mutually neutralizing effect in which *Fg*-sRNAs continuously target genes for silencing, while concurrent plant immune responses are a trigger for up-regulation. Thus, one can speculate that these described effects reflect an abrogation of host-favouring upregulation by host immunity *vs*. pathogen-favouring downregulation by sRNA effectors.

We identified three tRFs predicted to target *BdSERK2*, *HvBAK1*, *HvEOL1* and *HvSERK2*. Unexpectedly, these tRFs are partially DCL-dependent, with a reduced abundance by more than 50% during infections with the dKO mutant PH1-*dcl1/2 vs*. wt PH1 based on fungal biomass. Current knowledge of tRFs in fungi and oomycetes suggests that their silencing activity is independent of DCL, as shown for *Sclerotinia sclerotiorum* [47] and *Phytophthora infestans*, where the production is partially dependent on AGO [48]. Furthermore, analysis of tRFs in Cryptococcus spp. revealed a RNAi-independent generation of tRFs and possible compensatory effects in an RNAi-deficient genotype [49]. Interestingly however, the tRFs *Fg*-sRNA-321, *Fg*-sRNA-1921 and *Fg*-sRNA-6717 are neither 5'- or 3' tRNA halves nor do they belong to any of the described tRF-1, tRF-2, tRF-4 or tRF-5 classes [50] applied by the tRFtarget database for animals, yeast (*Schizosaccharomyces pombe*) and the bacterium *Rhodobacter sphaeroides* [51]. When following the classification of the tsRBase used for all eukaryotic kingdoms and bacteria [52], the three tRFs are classified as internal tRFs based on the origin within the mature tRNA. Interestingly, there are tRFs found in *Phytophthora sojae* starting in the anticodon loop and ending in the T loop of mature tRNAs [53], which resembles the Fg-sRNA tRFs (S8 Fig).

We observed several infection-specific degradation products of the predicted host target genes *HvBAK1*, *HvEOL1* and *HvSERK2* for tRFs *Fg*-sRNA-321, *Fg*-sRNA-1921 and *Fg*-sRNA-6717. However, cleavage occurred outside the canonical miRNA cleavage site as defined by Mallory et al. [43], though these genes are partially silenced during infection and silencing is apparently abolished upon infection with the DCL dKO mutant. While the canonical cleavage site for miRNA-directed cleavage in *At* is well defined, the tRF-directed cleavage observed by 5' RACE of transposable elements in *At* [54] and of defence-related genes during the infection of black pepper (*Piper nigrum*) with *Phytophthora capsici* [55] was found outside of the canonical cleavage site. Additionally, the identification of sRNA-directed cleavage sites in barley often leads to divergent findings. Ferdous et al. [56] predicted ~400 target genes for 11

presumably drought responsive miRNAs and found cleavage products for 15 targets overlapping the respective miRNAs alignment through degradome sequencing in the two barley cultivars Golden Promise (GP) and Pallas. From these confirmed targets, 13 were cleaved at the canonical 10^{th}-11^{th} nt site, one was cleaved at 19^{th}-20^{th} nt, and one at the 5^{th}-6^{th} nt. Hackenberg et al. [57] predicted 97 target genes of drought responsive miRNAs in GP and identified eight targets through degradome sequencing, which were all cleaved outside of the 10^{th}-11^{th} nt site. Thus, both studies suggest the presence of non-canonical miRNA directed cleavage. Of note, both studies relied on the same degradome sequencing dataset from GP, while Ferdous et al. also observed non-canonical cleavage in an independent Pallas dataset. Moreover, in a study performed by Curaba et al. [58] 96 target genes of GP for miRNAs involved in seed development and germination were identified by degradome sequencing and only 16 targets were cleaved exclusively at the 10^{th}-11^{th} nt site, while the other targets were sporadically cleaved with an offset (24) and 56 were cleaved in majority in a non-canonical site. Finally, Deng et al. [59] identify in the barley cultivar Morex 65 target genes of 39 miRNAs, and for only 32% of the identified targets the canonical 10^{th}-11^{th} nt cleavage product was the major degradome product. Together these studies highlight the challenges in the identification of cleavage sites of sRNAs in barley and cleavage sites of tRFs in plants. The absence of canonical cleavage products for tRFs does therefore not exclude the tRF-directed cleavage of *HvBAK1*, *HvEOL1* and *HvSERK2*.

We found that 22 *Fg*-sRNAs target *HvEOL1*, a putative negative regulator of ET biosynthesis in barley. In *Arabidopsis thaliana* the EOL1 homolog *At*ETO1 acts together with *At*EOL1 and *At*ETO1-like 2 (EOL2) in directing the ubiquitination and subsequent degradation of type-2 1-aminocyclopropane-1-carboxylate synthase (ACS) proteins (e.g. ET overproducer 2 (ETO2)) [40, 60]. ET is a gaseous plant hormone that plays an important role in regulating plant growth and development, and is critical for pathogen interaction and abiotic stresses [61]. Generally, ET acts synergistically with jasmonate (JA) in the defence response against necrotrophic pathogens and this ET/JA response has antagonistic effects on salicylic acid (SA) signalling against biotrophic pathogens. Yet in low amounts JA and SA act synergistically [62, 63]. Therefore, controlling both ET biosynthesis and ET signalling is crucial for plants. Towards this, plants have evolved complex mechanisms that allow tight regulation of ET pathways e.g. at the level of (i) ET production mainly by regulating ACS gene family members, (ii) ET perception through constitutive triple response 1 (CTR1)-mediated inhibition of positive regulator ET insensitive 2 (EIN2) [64, 65], and (iii) expression of ET-responsive TFs (e.g. ET response factor 1 (ERF1)) via EBF-mediated degradation of ET insensitive 3 (EIN3) [66] (S4 Fig). According to the anticipated role of ET in the plant response to necrotrophic pathogens, such as *Fg*, targeting negative regulators of ET synthesis such as *HvEOL1* would be detrimental to *Fg* colonization. Of note, our findings are consistent with previous results demonstrating that *Fg* exploits ET signalling to enhance colonization of Arabidopsis, wheat and barley [67], supposedly through an increase in DON-induced cell death through ET. These findings further challenge the role of ET in defence against necrotrophic pathogens. Strikingly, the authors showed that in Arabidopsis ET overproducing mutants (ETO1 and ETO2) and a negative regulator of ET signalling (CTR1) are more susceptible to *Fg*, while *At* mutants in ET perception (ETR1) and signalling (EIN2 and EIN3) are resistant. These findings were confirmed by the direct application of ET during the infection of wheat and barley, which lead to increased susceptibility to *Fg*. Based on these findings, we suggest that negative regulators of ET are efficient targets for sRNA-directed manipulation of host immunity by *Fg*.

The bacterial pathogen *Pseudomonas syringae* secretes two effector molecules, AvrPto and AvrPtoB, into host plants. These effectors interact with the receptor-like kinase BRI1-associated receptor kinase 1 (BAK1), also known as SERK3, thereby preventing the recognition of

various MAMPs through the association of BAK1 with pattern recognition receptors (PRRs) such as flagellin-sensitive 2 (FLS2) and Ef-Tu receptor (EFR) [68]. We observed *FgDCL*-dependent silencing of the cereal BAK1 homologs *HvBAK1*, *HvSERK2* and *BdSERK2*. While these genes have a higher similarity to *AtSERK2* than to *AtSERK3* (*AtBAK1*), they still are among the closest homologs to *AtBAK1* found in cereals (S9 Fig). It is tempting to speculate that further experiments will uncover additional hubs that are targeted both by protein and sRNA effectors.

Conclusion

Our data show that in the necrotrophic ascomycete *Fusarium graminearum* gene silencing by RNAi shapes its ability to cause disease, which is consistent with earlier results on the significance of the RNAi machinery in *Fg* [8, 35]. Pathogenicity relies on DICER-like (DCL)-dependent sRNAs that were identified as potential candidates for fungal effectors targeting defence genes in two Poaceae hosts, barley and *Brachypodium*. We identified *Fg*-sRNAs with sequence homology to host genes that were down-regulated by *Fg* during plant colonisation, while they were expressed above their level in healthy plants after infection with a DCL dKO mutant. In PH1-*dcl1/2 vs.* PH1 the strength of target gene accumulation correlated with the abundance of the corresponding *Fg*-sRNA. Our data hint to the possibility that three DCL-dependent tRFs with sequence homology to immunity-related *Ethylene overproducer 1-like 1* (*HvEOL1)* and three Poaceae orthologues of *Arabidopsis thaliana BRI1-associated receptor kinase 1* (*HvBAK1*, *HvSERK2* and *BdSERK2*) contribute to fungal virulence via targeted gene silencing.

Experimental procedures

Plants, fungi and plant infection

Fusarium graminearum (*Fg*) strain PH1, the double knock-out (dKO) PH1-*dcl1/2* (Dr. Martin Urban, Rothamsted Research, England), strain IFA65 (IFA, Department for Agrobiotechnology, Tulln, Austria) and single mutants IFA65-*dcl1* and IFA65-*dcl2* [8] were cultured on synthetic nutrient poor agar (SNA). Preparation of fungal inoculum was performed as described [69]. *Arabidopsis thaliana* ecotype Col-0 and *Atago1-27* ([70]; Polymorphism:3510706481) were grown in 8 h photoperiod at 22˚C with 60% relative humidity in a soil—sand mixture (4:1) (Fruhstorfer Type T, Hawita, Germany). For infection, 15 rosette leaves were detached and transferred in square Petri plates containing 1% water-agar. Drop-inoculation of *At* leaves was done with 5 μl of a suspension of 5×10^4 *Fg* conidia ml^{-1} at two spots per leaf. Infection strength was recorded as infection area (size of chlorotic lesions relative to total leaf area) using the ImageJ software (https://imagej.nih.gov/ij/).

For infection of barley (*Hordeum vulgare* cv. Golden Promise, GP) and *Brachypodium distachyon* (Bd21-3), plants were grown in a 16 h photoperiod at 20˚C/18˚C day/night and 60% relative humidity in soil (Fruhstorfer Type LD80, Hawita). Ten detached second leaves were transferred into square Petri plates containing 1% water-agar. GP leaves were drop-inoculated with 3 μl of 1.5×10^5 conidia ml^{-1} conidia suspension. Bd21-3 leaves were drop-inoculated on two spots with 10 μl of 1×10^4 conidia ml^{-1} conidia suspension. Infection strength was measured with the PlantCV v2 software package (https://plantcv.danforthcenter.org/) (*Hv*) by training a machine learning algorithm to recognize necrotic lesions or by ImageJ (*Bd*). For gene expression analysis, a suspension of 5×10^4 *Fg* conidia ml^{-1} was used and leaves were either inoculated on 3 spots with 20 μl (*Hv*) or on 2 spots with 10 μl (*Bd*), respectively and experiments were evaluated 5 dpi or 4 dpi for strain PH1 on *Bd*.

Fungal transcript analysis

Gene expression analysis was performed using reverse transcription quantitative PCR (RT-qPCR). RNA extraction was performed with GENEzol reagent (Geneaid) following the manufacturer's instructions. DNA was digested with DNAse I (Thermo Scientific) according to manufacturer protocol and remaining RNA was used for cDNA synthesis using qScript™ cDNA kit (Quantabio). For RT-qPCR, 10 ng of cDNA was used as template in the QuantStudio 5 Real-Time PCR system (Applied Biosystems). Amplifications were performed with 5 μl of SYBR® green JumpStart Taq ReadyMix (Sigma-Aldrich) with 5 pmol oligonucleotides. Each sample had three technical repetitions. After an initial activation step at 95˚C for 5 min, 40 cycles (95˚C for 30 sec, 60˚C for 30 sec, 72˚C for 30 sec) were performed followed by a melt curve analysis (60˚C-95˚C, 0.075˚C/s). Ct values were determined with the QuantStudio design and analysis software supplied with the instrument. Transcript levels were determined via the $2^{-\Delta\Delta Ct}$ method [71] by normalizing the amount of target transcript to the amount of the reference transcript *Elongation factor 1-alpha* (*EF1-a*, FGSG_08811) gene (S2 Table).

Plant transcript analysis

Leaves were shock frozen at 5 dpi and RT-qPCR was performed as for fungal transcript analysis. Reference genes were *Ubiquitin-40S ribosomal protein S27a-3* (HORVU1Hr1G023660) for GP and *Ubi4* (Bradi3g04730) for Bd21-3 according to Chambers et al. [72] (S1 Table). Primers were designed using Primer3 v2.4.0 [73].

Spray application of dsRNA

Second leaves of 2 to 3-week-old GP were detached and transferred to square Petri plates containing 1% water agar. dsRNA was diluted in 500 μl water to a final concentration of 20 ng μl^{-1}. As control, Tris-EDTA (TE) buffer was diluted in 500 μl water corresponding to the amount used for dilution of the dsRNA. Typical RNA concentration after elution was 500 ng μl^{-1}, with 400 μM Tris-HCL and 40 μM EDTA in the final dilution. Each plate containing 10 detached leaves was evenly sprayed with either dsRNAs or TE buffer with 500 μl, and subsequently kept at room temperature [10]. Two days after spraying, leaves were drop-inoculated with three 20 μl drops of *Fg* suspension containing 5×10^4 conidia ml^{-1}. After inoculation, plates were closed and incubated for five days at room temperature.

Target prediction for sRNAs

RNA was purified and enriched for sRNAs from fungal axenic culture (PRJNA749737) using the mirVana miRNA Isolation Kit (Life Technologies). Indexed sRNA libraries were constructed from these sRNA fractions with the NEBNext Multiplex Small RNA Library Prep Set for Illumina (New England Biolabs) according to the manufacturer's instructions. Reads were trimmed with the cutadapt tool v2.1 [74] by removing adapters and retaining reads with a length of 21–24 nt and quality checked with the fastQC tool v0.11.9 (http://www.bioinformatics.babraham.ac.uk/projects/fastqc/). For S1 Fig reads were aligned to the *Fg* reference genome (GCF_000240135.3_ASM24013v3) with bowtie2 [75] following a sensitive alignment policy (-D 100, -R 10, -L 19). The aligned reads were assigned to the additional attribute "gene_biotype" with htseq-count [76] according to the latest assembly (ftp://ftp.ensemblgenomes.org/pub/release-44/fungi/gff3/fungi_ascomycota3_collection/fusarium_graminearum_gca_000240135). Remaining reads were collapsed with the fastx toolkit v0.0.14 [77] and reads with at least 400 reads were targeted against the IBSC_PGSB_v2 cDNA annotation with the plant miRNA target prediction algorithm TAPIR [42], following the optimized

parameters according to Srivastava et al. [39]. The results of the target prediction were further analysed with RStudio [78] and the package biomaRt [79] to find targets associated with stress and immunity associated Gene ontology (GO) terms in the database "plants_mart" from plants.ensembl.org hosted by the EBI (European Bioinformatics Institute) and the Wellcome Trust Sanger Institute. The same method was used for the identification of target genes in *B. distachyon* (GCA_000005505.4) and *A. thaliana* (Araport11).

Stemloop-RT-qPCR of sRNAs

RNA was extracted and genomic DNA was digested as described for the transcript analyses. The sequences of sRNAs found in axenic fungal culture were used to design specific stem loop (SL) primers matching the sRNA over 6 nt at the 3'end. For the primer design, the tool of Adhikari et al. [80] was used. SL-primers were diluted to 10 pM and folded in a cycler (95˚C for 15 min, 90˚C 5 min, 85˚C 5 min, 80˚C 5 min, 75˚C 1 h, 68˚C 1 h, 65˚C 1 h, 62˚C 1 h, 60˚C 3 h). These primers were used for cDNA synthesis (Thermo Scientific RevertAid RT Reverse Transcription Kit) according to manufacturer's instruction with an annealing step at 16˚C instead of 25˚C and were used in multiplex to target respective fungal sRNAs and barley miRNAs *Hvu*-mir159 and *Hvu*-mir168 as references. To obtain amplification efficiencies, a mix from all RNAs was diluted in a four step dilution series with a factor of ten and reverse transcribed. Reactions were set up with the highest concentration of 15 ng μl^{-1} and the lowest of 15 pg μl^{-1} cDNA. All sRNA amplifications showed an efficiency of 80–82% and an R^2 between 1 and 0.997 except for Fg-sRNA-6717 with an efficiency of 66.4%. For RT-qPCR, 1.5 μl of 3 ng μl^{-1} cDNA was used as template in the QuantStudio 5 Real-Time PCR system (Applied Biosystems). Amplifications were performed with 5 μl of SYBR® green JumpStart Taq ReadyMix (Sigma-Aldrich) with 1.5 pmol or 3 pmol oligonucleotides. Each sample had three technical repetitions. As forward primer the unused nucleotides of the remaining sequence of the sRNA were used, which were extended to achieve optimal melting temperature, and as reverse primer the universal stem loop primer developed by Chen et al. [41] was used. Relative abundance of the sRNAs was calculated with the ΔΔct-method with incorporation of amplification efficiencies. sRNAs were normalized against the reference miRNAs Hvu-mir-159a and 168-5p and after this against the fungal biomass measured as *EF1-α* against *HvUBQ* (*HORVU1Hr1G023660*).

Statistics

To assess the differential expression of genes via RT-qPCRs the Δct values were compared via a one or two sided paired Students *t*-test. Disease symptoms were either compared via Students *t*-test if the data showed a normal distribution in Shapiro-Wilk test or via a Wilcoxon rank sum test.

RLM-RACE

RNA from GP barley infected with *Fg*-IFA65 at 5 dpi and an uninfected control was extracted with the Isolate II plant miRNA kit (Bioline). 1 μg of RNA (>200 nt) of infected, uninfected and a mix of both samples for a–RT-control were assembled. 1 μl of the 5'RACE Adapter [0.3 μg/μl], 1 μl of the 10x Reaction Buffer, 1 μl of 1mg/μl BSA, 0.5 μl of T4 RNA Ligase [10U/μl] (Thermo Scientific) and DEPC-treated water up to 10 μl were prepared and incubated at 37˚C for 60 min. Subsequently, the whole reaction was used for reverse transcription (RevertAid Reverse Transcriptase, Thermo Scientific). 10 μl ligation reaction, 1 μl Random Hexamer [100pmol/μl], 4 μl 5x Reaction Buffer, 0.5 μl RiboLock RNase Inhibitor (Thermo Scientific), 2 μl dNTP Mix [10 mM] and 1 μl RevertAid Reverse Transcriptase (or water (–RT control))

and 1.5 μl water were mixed and run for 10 min at 25˚C, 60 min at 42˚C and 10 min at 70˚C. Then, a nested hot-start touch-down PCR for each target gene was performed. The primer sequences for the outer (first) and inner (second) PCR are shown in S1 Table. 5 μl of 10x Buffer B, 1 μl of a dNTP Mix [10 mM], 2 μl $MgCl_2$ [25 mM], 1μl Adapter specific Primer [10 pmol μl^{-1}] and 1 μl gene specific primer (GSP) [10 pmol μl^{-1}], 0.6 μl DCS DNA Polymerase (DNA Cloning Service) [5 U/μl] and 2 μl cDNA or outer PCR reaction and 37.4 μl water were mixed and run at 95˚C for 5 min, (95˚for 30 s, 68˚C-0.5˚C/cycle for 30 s, 72˚C for 30 s)*15, (95˚C for 30 s, 60˚C for 30 s, 72˚C for 30 s)*18 and 72˚C for 5 min. PCR products were evaluated in a 1.5% agarose gel and bands of the expected size, which were present in the infected but not uninfected samples, were excised. Products were cleaned with the Wizard SV Gel and PCR Clean-Up System (Promega) and cloned with the pGEM-T easy Vector Systems (Promega). For each band, five clones were picked for sequencing. Plasmids from O/N cultures were extracted with the Monarch Plasmid Miniprep Kit (New England Biolabs) and sent for sequencing to LGC genomics.

Analysis of target genes and targeting sRNAs

After the initial target prediction an additional target prediction for the newly released cultivar specific genome (GCA_902500625) of barley cv. Golden Promise (GP) was conducted. Adapters were removed and reads were collapsed as described before for the target prediction. All sRNA sequences were read with SeqinR v3.6–1 [81] and stored in a list of SeqFastadna objects. To identify the homologous genes to the already identified targets in GP, the cDNA library was blasted with the command-line blast application (Nucleotide-Nucleotide BLAST 2.6.0+) [82] against the identified target sequences from the IBSC_PGSB_v2 cDNA library with percent identity of 90 and a query coverage of 55% as cut-off values. All sRNAs with at least two reads were written to a file in chunks of 2000 each and ran against each individual target gene with TAPIR via the system2 function in R [83] in the RStudio software. Results were collected, stored in a data.frame, and further analysed with R. sRNAs identified to target a gene of interest (GOI) were written to a fasta file with SeqinR and blasted against the rRNAs from the assemblies GCA_900044135.1 (*Fg*-PH1), GCA_000240135.3 (*Fg*-PH1) and the *Fusarium* rRNAs from the RNAcentral fungal ncRNA dataset (ftp://ftp.ebi.ac.uk/pub/databases/RNAcentral/current_release/sequences/by-database/ensembl_fungi.fasta (12/Sep/2020)) with the options wordsize = 4, perc_identity = 95, qcov_hsp_perc = 95. All sRNAs matching rRNAs were removed. Thereafter, sRNAs were compared to the *Fg* assemblies GCA_900044135.1 (*Fg*-PH1) and GCA_000240135.3 (*Fg*-PH1) with the same blast strategy and only perfectly matching sRNAs were retained.

To derive the relative expression of a GOI between two samples the following formula is used.

$$Relativeexpression_{GOI} = 2^{-\Delta\Delta ct_{GOI}}$$

We further defined the ΔΔΔct value as the difference between the ΔΔct values for a GOI in PH1 and PH1-*dcl1/2*-infected samples.

$$\Delta\Delta\Delta\text{ct} = \Delta\Delta ct_{PH1-dcl1/2} - \Delta\Delta ct_{PH1}$$

This enables the calculation of the re-accumulation between the two samples as follows.

$$DCL-dependent\ \ resurgence\ \ factor = \frac{Relativeexpression_{PH1-dcl1/2}}{Relativeexpression_{PH1}} = 2^{-\Delta\Delta\Delta ct_{GOI}}$$

The sum of all reads and the corresponding ΔΔΔct-value were plotted with ggplot2 [84] and

a linear regression was added to the plot. To allow a log2-transformation of the plots genes with zero targeting reads were set to one targeting read. The plots were arranged using ggpubr v.0.4.0 [85].

GO enrichment analysis

Gene ontology (GO) enrichment analysis was performed via the AgriGO v.2.0 analysis toolkit [86] with the standard parameters singular enrichment analysis (SEA).

Phylogenetic analysis of SERK homologs

Homologs of *HvBAK1* and *HvSERK2* were searched in *At*, *Hv* and *Bd* with biomaRt v.2.40.5 [79] and downloaded from the EMBL's European Bioinformatics Institute plants genome page (plants.ensembl.org) in the plants_mart dataset hvulgare_eg_gene (Ensembl Plants Genes v. 50). For these homologs the CDS of all homologs within the respective datasets athaliana_eg_gene, hvulgare_eg_gene and bdistachyon_eg_gene were downloaded. The CDS were subsequently aligned with the muscle algorithm in MEGA7 [87] and a phylogenetic tree was constructed via a bootstrap method with 200 iterations.

Supporting information

S1 Fig. Feature mapping of *Fg*-sRNAs with a read length of 21–24 nt. Reads were trimmed as described earlier and aligned to the PH1 reference genome (GCF_000240135.3_ASM24013v3) with bowtie2 [75].
(TIF)

S2 Fig. GO-enrichment analysis of all potential targets of *Fg*-sRNAs with more than 400 reads. The plot shows all significantly enriched GO-terms in the target gene set for (A) molecular function and (B) biological process. The analysis was done using agriGo v2.0. Each box contains information regarding one term. GO: indicates the GO accession, in brackets the p-value is stated (Fisher; Yekutieli (FDR)). After the bracket the GO-term description is written followed by the number of genes associated with said term 1. in the gene set and 2. In the background.
(TIF)

S3 Fig. Alignment of AtETO1 and HvEOL1. Identical amino acids are marked blue and similar amino acids are marked red. The alignment and visualization was done with the msa package for R [88].
(TIF)

S4 Fig. Regulation of ET synthesis in At. *At*ETO1 negatively regulates ethylene **(ET)** synthesis in *At*. *At*ETO1 acts together with *At*EOL1 and *At*ETO1-like 2 (EOL2) in directing the ubiquitination and subsequent degradation of type-2 1-aminocyclopropane-1-carboxylate synthase (ACS) proteins (e.g. ET overproducer 2 (ETO2)), which produce the direct precursor of ET.
(TIF)

S5 Fig. Sequences of dsRNA-dcl1/2. Coding Sequences (CDS) of the respective *FgDCL* genes with the sequences comprising the dsRNAs marked in red. A. FgDCL1-FGSG_09025 (912 nt long dsRNA-FgDCL1). B. FgDCL2-FGSG_04408 (870 nt long dsRNA-FgDCL2).
(TIF)

S6 Fig. Position and read count of all tRFs from *Fg*-tRNA-Gly(GCC). Alignment position of all *Fg*-sRNAs from axenic culture with more than 50 reads perfectly matching the *Fg*-tRNA-Gly(GCC)-9 gene (Fusarium_graminearum_CS3005-tRNA-Gly-GCC-1-9) colored by read count.
(TIF)

S7 Fig. Abundance of unique *Fg*-sRNAs in axenic culture of IFA65. A: Histogram of the read count of every unique sRNA. The plot is truncated to make abundances recognizable. Most sRNAs have very low read counts and very few sRNAs have more reads than 3,000. Maximum read count per sRNA is 42,866. B: Violin plot of log2-transformed reads counts untruncated.
(TIF)

S8 Fig. Origin of tRFs in *Fg*-tRNA-Gly(GCC). The centroid secondary structure of the *Fg*-tRNA-Gly(GCC) generated on the RNAfold web server (http://rna.tbi.univie.ac.at/cgi-bin/RNAWebSuite/RNAfold.cgi) with the origin and alignment of *Fg*-sRNA-321, *Fg*-sRNA-1921 and *Fg*-sRNA-6717. The colors of bases indicate the base pair probabilities.
(TIF)

S9 Fig. Molecular Phylogenetic analysis by maximum likelihood method. The evolutionary history was inferred by using the Maximum Likelihood method based on the General Time Reversible model [89]. The tree with the highest log likelihood (-25430.37) is shown. Initial tree(s) for the heuristic search were obtained automatically by applying Neighbor-Join and BioNJ algorithms to a matrix of pairwise distances estimated using the Maximum Composite Likelihood (MCL) approach, and then selecting the topology with superior log likelihood value. The tree is drawn to scale, with branch lengths measured in the number of substitutions per site. The analysis involved 77 nucleotide sequences. Codon positions included were 1st +2nd+3rd. There were a total of 2427 positions in the final dataset. Evolutionary analyses were conducted in MEGA7 [87].
(TIF)

S10 Fig. Unedited gel images from Fig 6.
(PDF)

S1 Table. Primer sequences.
(DOCX)

S2 Table. Target prediction results. Results of the target prediction with the TAPIR algorithm for all *Fg*-sRNAs with more than 400 reads.
(XLSX)

Acknowledgments

We thank the Salk Institute Genomic Analysis Laboratory for providing the sequence-indexed Arabidopsis TDNA insertion mutants.

Author Contributions

Conceptualization: Bernhard Timo Werner, Aline Koch, Karl-Heinz Kogel.

Data curation: Bernhard Timo Werner, Aline Koch, Lukas Jelonek.

Formal analysis: Bernhard Timo Werner, Ena Šečić, Jonas Engelhardt, Lukas Jelonek.

Funding acquisition: Aline Koch, Jens Steinbrenner, Karl-Heinz Kogel.

Investigation: Aline Koch, Ena Šečić, Karl-Heinz Kogel.

Methodology: Bernhard Timo Werner, Aline Koch, Ena Šečić, Jonas Engelhardt, Jens Steinbrenner.

Project administration: Aline Koch, Jens Steinbrenner, Karl-Heinz Kogel.

Resources: Bernhard Timo Werner.

Software: Bernhard Timo Werner, Ena Šečić, Jonas Engelhardt, Lukas Jelonek.

Supervision: Aline Koch, Jens Steinbrenner, Karl-Heinz Kogel.

Validation: Bernhard Timo Werner.

Visualization: Bernhard Timo Werner.

Writing – original draft: Bernhard Timo Werner, Aline Koch, Karl-Heinz Kogel.

Writing – review & editing: Bernhard Timo Werner, Aline Koch, Ena Šečić, Lukas Jelonek, Jens Steinbrenner, Karl-Heinz Kogel.

References

1. Koch A., & Kogel K. H. (2014). New wind in the sails: improving the agronomic value of crop plants through RNA i-mediated gene silencing. *Plant biotechnology journal*, 12(7), 821–831. https://doi.org/10.1111/pbi.12226 PMID: 25040343
2. Guo Q., Liu Q., Smith N.A., Liang G., & Wang M.B. (2016). RNA Silencing in plants: mechanisms, technologies and applications in horticultural crops. *Current Genomics*, 17, 476–489. https://doi.org/10.2174/1389202917666160520103117 PMID: 28217004
3. Liu S., Jaouannet M., Dempsey D. M. A., Imani J., Coustau C., & Kogel K. H. (2020). RNA-based technologies for insect control in plant production. *Biotechnology advances*, 39, 107463. https://doi.org/10.1016/j.biotechadv.2019.107463 PMID: 31678220
4. Šečić E and Kogel KH (2021). Requirements for fungal uptake of dsRNA and gene silencing in RNAi-based crop protection strategies. *Current Opinion in Biotechnology*, COBIOT-D-21-00048. https://doi.org/10.1016/j.copbio.2021.04.001 PMID: 34000482
5. Koch A., & Wassenegger M. (2021). Host-induced gene silencing–mechanisms and applications. *New Phytologist*, 231(1), 54–59. https://doi.org/10.1111/nph.17364 PMID: 33774815
6. Rosa C., Kuo Y. W., Wuriyanghan H., & Falk B. W. (2018). RNA interference mechanisms and applications in plant pathology. *Annual review of phytopathology*, 56, 581–610. https://doi.org/10.1146/annurev-phyto-080417-050044 PMID: 29979927
7. Cai Q., He B., Kogel K. H., & Jin H. (2018). Cross-kingdom RNA trafficking and environmental RNAi—nature's blueprint for modern crop protection strategies. *Current opinion in microbiology*, 46, 58–64. https://doi.org/10.1016/j.mib.2018.02.003 PMID: 29549797
8. Gaffar F. Y., Imani J., Karlovsky P., Koch A., & Kogel K.-H. (2019). Different components of the RNA interference machinery are required for conidiation, ascosporogenesis, virulence, deoxynivalenol production, and fungal inhibition by exogenous double-stranded RNA in the Head Blight pathogen *Fusarium graminearum*. *Frontiers in Microbiology*, 10, 1662. https://doi.org/10.3389/fmicb.2019.01662 PMID: 31616385
9. Niehl A., & Heinlein M. (2019). Perception of double-stranded RNA in plant antiviral immunity. *Molecular plant pathology*, 20(9), 1203–1210. https://doi.org/10.1111/mpp.12798 PMID: 30942534
10. Koch A., Biedenkopf D., Furch A., Weber L., Rossbach O., Abdellatef E., et al. (2016). An RNAi-based control of *Fusarium graminearum* infections through spraying of long dsRNAs involves a plant passage and is controlled by the fungal silencing machinery. *PLoS pathogens*, 12(10), e1005901. https://doi.org/10.1371/journal.ppat.1005901 PMID: 27737019
11. Wang M., Weiberg A., Lin F.-M., Thomma B. P. H. J., Huang H.D., & Jin H. (2016). Bidirectional cross-kingdom RNAi and fungal uptake of external RNAs confer plant protection. *Nature Plants*, 2, 16151. https://doi.org/10.1038/nplants.2016.151 PMID: 27643635
12. Konakalla N. C., Kaldis A., Berbati M., Masarapu H., & Voloudakis A. E. (2016). Exogenous application of double-stranded RNA molecules from TMV p126 and CP genes confers resistance against

TMV in tobacco. *Planta*, 244(4), 961–969. https://doi.org/10.1007/s00425-016-2567-6 PMID: 27456838

13. Mitter N., Worrall E. A., Robinson K. E., Li P., Jain R. G., Taochy C., et al. (2017). Clay nanosheets for topical delivery of RNAi for sustained protection against plant viruses. *Nature plants*, 3(2), 1–10. https://doi.org/10.1038/nplants.2016.207 PMID: 28067898

14. Kaldis A., Berbati M., Melita O., Reppa C., Holeva M., Otten P., et al. (2018). Exogenously applied dsRNA molecules deriving from the Zucchini yellow mosaic virus (ZYMV) genome move systemically and protect cucurbits against ZYMV. *Molecular plant pathology*, 19(4), 883–895. https://doi.org/10.1111/mpp.12572 PMID: 28621835

15. McLoughlin A. G., Wytinck N., Walker P. L., Girard I. J., Rashid K. Y., de Kievit T., et al. (2018). Identification and application of exogenous dsRNA confers plant protection against Sclerotinia sclerotiorum and Botrytis cinerea. *Scientific Reports*, 8(1), 1–14. https://doi.org/10.1038/s41598-017-17765-5 PMID: 29311619

16. Sang H., & Kim J. I. (2020). Advanced strategies to control plant pathogenic fungi by host-induced gene silencing (HIGS) and spray-induced gene silencing (SIGS). *Plant Biotechnology Reports*, 14(1), 1–8.

17. Head G. P., Carroll M. W., Evans S. P., Rule D. M., Willse A. R., Clark T. L., et al. (2017). Evaluation of SmartStax and SmartStax PRO maize against western corn rootworm and northern corn rootworm: efficacy and resistance management. *Pest management science*, 73(9), 1883–1899. https://doi.org/10.1002/ps.4554 PMID: 28195683

18. Niehl A., Soininen M., Poranen M. M., & Heinlein M. (2018). Synthetic biology approach for plant protection using ds RNA. *Plant biotechnology journal*, 16(9), 1679–1687.

19. Weiberg A., Wang M., Lin F. M., Zhao H., Zhang Z., Kaloshian I., et al. (2013). Fungal small RNAs suppress plant immunity by hijacking host RNA interference pathways. *Science*, 342(6154), 118–123. https://doi.org/10.1126/science.1239705 PMID: 24092744

20. Cai Q., Qiao L., Wang M., He B., Lin F. M., Palmquist J., et al. (2018). Plants send small RNAs in extracellular vesicles to fungal pathogen to silence virulence genes. *Science*, 360(6393), 1126–1129. https://doi.org/10.1126/science.aar4142 PMID: 29773668

21. Wang M., Weiberg A., Dellota E. Jr, Yamane D, & Jin H. (2017). Botrytis small RNA Bc-siR37 suppresses plant defense genes by cross-kingdom RNAi. *RNA Biology*, 14, 421–428. https://doi.org/10.1080/15476286.2017.1291112 PMID: 28267415

22. Dunker F., Trutzenberg A., Rothenpieler J. S., Kuhn S., Pröls R., Schreiber T., et al. (2020). Oomycete small RNAs bind to the plant RNA-induced silencing complex for virulence. *Elife*, 9, e56096. https://doi.org/10.7554/eLife.56096 PMID: 32441255

23. Wang B., Sun Y.F., Song N., Zhao M.X., Liu R., Feng H., et al. (2017). *Puccinia striiformis f. sp tritici* microRNA-like RNA 1 (Pst-milR1), an important pathogenicity factor of Pst, impairs wheat resistance to Pst by suppressing the wheat pathogenesis-related 2 gene. *New Phytologist*, 215, 338–350.

24. Dubey H., Kiran K., Jaswal R., Jain P., Kayastha A. M., Bhardwaj S. C., et al. (2019). Discovery and profiling of small RNAs from Puccinia triticina by deep sequencing and identification of their potential targets in wheat. *Functional & integrative genomics*, 19(3), 391–407. https://doi.org/10.1007/s10142-018-00652-1 PMID: 30618015

25. Mueth N. A., Ramachandran S. R., & Hulbert S. H. (2015). Small RNAs from the wheat stripe rust fungus (Puccinia striiformis f. sp. tritici). *Bmc Genomics*, 16(1), 1–16.

26. Reinhart B. J., Weinstein E. G., Rhoades M. W., Bartel B., & Bartel D. P. (2002). MicroRNAs in plants. *Genes & development*, 16(13), 1616–1626. https://doi.org/10.1101/gad.1004402 PMID: 12101121

27. Ren B., Wang X., Duan J., & Ma J. (2019). Rhizobial tRNA-derived small RNAs are signal molecules regulating plant nodulation. *Science*, 365(6456), 919–922. https://doi.org/10.1126/science.aav8907 PMID: 31346137

28. Jones-Rhoades M. W. (2012). Conservation and divergence in plant microRNAs. *Plant molecular biology*, 80(1), 3–16. https://doi.org/10.1007/s11103-011-9829-2 PMID: 21996939

29. Garcia-Silva M. R., Cabrera-Cabrera F., Cura das Neves R. F., Souto-Padrón T., de Souza W., & Cayota A. (2014). Gene expression changes induced by *Trypanosoma cruzi* shed microvesicles in mammalian host cells: relevance of trna-derived halves. *BioMed Research International*, 2014, 1–11. https://doi.org/10.1155/2014/305239 PMID: 24812611

30. Dean R., Van Kan J. A., Pretorius Z. A., Hammond-Kosack K. E., Di Pietro A., Spanu P. D., et al. (2012). The Top 10 fungal pathogens in molecular plant pathology. *Molecular plant pathology*, 13(4), 414–430. https://doi.org/10.1111/j.1364-3703.2011.00783.x PMID: 22471698

31. Desjardins A. E., Hohn T. M., & McCORMICK S. P. (1993). Trichothecene biosynthesis in *Fusarium* species: chemistry, genetics, and significance. *Microbiology and Molecular Biology Reviews*, 57(3), 595–604.

32. Jansen C., Von Wettstein D., Schäfer W., Kogel K. H., Felk A., & Maier F. J. (2005). Infection patterns in barley and wheat spikes inoculated with wild-type and trichodiene synthase gene disrupted *Fusarium graminearum*. *Proceedings of the National Academy of Sciences*, 102(46), 16892–16897. https://doi.org/10.1073/pnas.0508467102 PMID: 16263921

33. Ilgen P., Hadeler B., Maier F. J., & Schäfer W. (2009). Developing kernel and rachis node induce the trichothecene pathway of *Fusarium graminearum* during wheat head infection. *Molecular plant-microbe interactions*, 22(8), 899–908. https://doi.org/10.1094/MPMI-22-8-0899 PMID: 19589066

34. Kim H. K., Jo S. M., Kim G. Y., Kim D. W., Kim Y. K., & Yun S. H. (2015). A large-scale functional analysis of putative target genes of mating-type loci provides insight into the regulation of sexual development of the cereal pathogen *Fusarium graminearum*. *PLoS Genet*, 11(9), e1005486. https://doi.org/10.1371/journal.pgen.1005486 PMID: 26334536

35. Son H, Park AR, Lim JY, Shin C, Lee Y-W (2017) Genome-wide exonic small interference RNA-mediated gene silencing regulates sexual reproduction in the homothallic fungus *Fusarium graminearum*. PLoS Genet 13(2): e1006595. https://doi.org/10.1371/journal.pgen.1006595 PMID: 28146558

36. Ji H., Mao H., Li S., Feng T., Zhang Z., Cheng L., et al. (2021). *Fol*-milR1, a pathogenicity factor of *Fusarium oxysporum*, confers tomato wilt disease resistance by impairing host immune responses. *New Phytologist*, nph.17436. https://doi.org/10.1111/nph.17436 PMID: 33960431

37. Jian J., & Liang X. (2019). One small RNA of *Fusarium graminearum* targets and silences CEBiP gene in common wheat. *Microorganisms*, 7(10), 425. https://doi.org/10.3390/microorganisms7100425 PMID: 31600909

38. Mascher M., Gundlach H., Himmelbach A., Beier S., Twardziok S. O., Wicker T., et al. (2017). A chromosome conformation capture ordered sequence of the barley genome. *Nature*, 544(7651), 427–433. https://doi.org/10.1038/nature22043 PMID: 28447635

39. Srivastava P. K., Moturu T. R., Pandey P., Baldwin I. T., & Pandey S. P. (2014). A comparison of performance of plant miRNA target prediction tools and the characterization of features for genome-wide target prediction. *BMC genomics*, 15(1), 1–15. https://doi.org/10.1186/1471-2164-15-348 PMID: 24885295

40. Christians M. J., Gingerich D. J., Hansen M., Binder B. M., Kieber J. J., & Vierstra R. D. (2009). The BTB ubiquitin ligases ETO1, EOL1 and EOL2 act collectively to regulate ethylene biosynthesis in Arabidopsis by controlling type-2 ACC synthase levels. *The Plant Journal*, 57(2), 332–345. https://doi.org/10.1111/j.1365-313X.2008.03693.x PMID: 18808454

41. Chen C., Ridzon D. A., Broomer A. J., Zhou Z., Lee D. H., Nguyen J. T., et al. (2005). Real-time quantification of microRNAs by stem–loop RT–PCR. *Nucleic acids research*, 33(20), e179–e179. https://doi.org/10.1093/nar/gni178 PMID: 16314309

42. Bonnet E., He Y., Billiau K., & Van de Peer Y. (2010). TAPIR, a web server for the prediction of plant microRNA targets, including target mimics. *Bioinformatics*, 26(12), 1566–1568. https://doi.org/10.1093/bioinformatics/btq233 PMID: 20430753

43. Mallory A. C., Reinhart B. J., Jones-Rhoades M. W., Tang G., Zamore P. D., Barton M. K., et al. (2004). MicroRNA control of PHABULOSA in leaf development: importance of pairing to the microRNA 5′ region. *The EMBO journal*, 23(16), 3356–3364. https://doi.org/10.1038/sj.emboj.7600340 PMID: 15282547

44. Werner B. T., Gaffar F. Y., Schuemann J., Biedenkopf D., & Koch A. M. (2020). RNA-spray-mediated silencing of *Fusarium graminearum* AGO and DCL genes improve barley disease resistance. *Frontiers in Plant Science*, 11, 476. https://doi.org/10.3389/fpls.2020.00476 PMID: 32411160

45. Lax C., Tahiri G., Patiño-Medina J. A., Cánovas-Márquez J. T., Pérez-Ruiz J. A., Osorio-Concepción M., et al. (2020). The Evolutionary Significance of RNAi in the Fungal Kingdom. *International Journal of Molecular Sciences*, 21(24), 9348. https://doi.org/10.3390/ijms21249348 PMID: 33302447

46. Zanini S., Šečić E., Busche T., Galli M., Zheng Y., Kalinowski J., et al. (2021). Comparative Analysis of Transcriptome and sRNAs Expression Patterns in the *Brachypodium distachyon—Magnaporthe oryzae* Pathosystems. *International Journal of Molecular Sciences*, 22(2), 650. https://doi.org/10.3390/ijms22020650 PMID: 33440747

47. Lee Marzano S. Y., Neupane A., Mochama P., Feng C., & Saleem H. (2019). Roles of argonautes and dicers on Sclerotinia sclerotiorum antiviral RNA silencing. *Frontiers in Plant Science*, 10, 976. https://doi.org/10.3389/fpls.2019.00976 PMID: 31440265

48. Åsman A. K., Vetukuri R. R., Jahan S. N., Fogelqvist J., Corcoran P., Avrova A. O., et al. (2014). Fragmentation of tRNA in Phytophthora infestans asexual life cycle stages and during host plant infection. *BMC microbiology*, 14(1), 308. https://doi.org/10.1186/s12866-014-0308-1 PMID: 25492044

49. Streit R. S. A., Ferrareze P. A. G., Vainstein M. H., & Staats C. C. (2021). Analysis of tRNA-derived RNA fragments (tRFs) in *Cryptococcus* spp.: RNAi-independent generation and possible compensatory

effects in a RNAi-deficient genotype. *Fungal Biology*, 125(5), 389–399. https://doi.org/10.1016/j.funbio.2020.12.003 PMID: 33910680

50. Kumar P., Kuscu C., & Dutta A. (2016). Biogenesis and function of transfer RNA-related fragments (tRFs). *Trends in biochemical sciences*, 41(8), 679–689. https://doi.org/10.1016/j.tibs.2016.05.004 PMID: 27263052

51. Li N., Shan N., Lu L., & Wang Z. (2021). tRFtarget: a database for transfer RNA-derived fragment targets. *Nucleic Acids Research*, 49(D1), D254–D260. https://doi.org/10.1093/nar/gkaa831 PMID: 33035346

52. Zuo Y., Zhu L., Guo Z., Liu W., Zhang J., Zeng Z., et al. (2021). tsRBase: a comprehensive database for expression and function of tsRNAs in multiple species. *Nucleic Acids Research*, 49(D1), D1038–D1045. https://doi.org/10.1093/nar/gkaa888 PMID: 33068436

53. Wang Q., Li T., Xu K., Zhang W., Wang X., Quan J., et al. (2016b). The tRNA-derived small RNAs regulate gene expression through triggering sequence-specific degradation of target transcripts in the oomycete pathogen Phytophthora sojae. *Frontiers in plant science*, 7, 1938.

54. Martinez G., Choudury S. G., & Slotkin R. K. (2017). tRNA-derived small RNAs target transposable element transcripts. *Nucleic acids research*, 45(9), 5142–5152. https://doi.org/10.1093/nar/gkx103 PMID: 28335016

55. Asha S., & Soniya E. V. (2016). Transfer RNA derived small RNAs targeting defense responsive genes are induced during Phytophthora capsici infection in black pepper (Piper nigrum L.). *Frontiers in plant science*, 7, 767. https://doi.org/10.3389/fpls.2016.00767 PMID: 27313593

56. Ferdous J., Sanchez-Ferrero J. C., Langridge P., Milne L., Chowdhury J., Brien C., et al. (2017). Differential expression of microRNAs and potential targets under drought stress in barley. *Plant, cell & environment*, 40(1), 11–24. https://doi.org/10.1111/pce.12764 PMID: 27155357

57. Hackenberg M., Gustafson P., Langridge P., & Shi B. J. (2015). Differential expression of micro RNA s and other small RNA s in barley between water and drought conditions. *Plant biotechnology journal*, 13(1), 2–13. https://doi.org/10.1111/pbi.12220 PMID: 24975557

58. Curaba J., Spriggs A., Taylor J., Li Z., & Helliwell C. (2012). miRNA regulation in the early development of barley seed. *BMC plant biology*, 12(1), 1–16. https://doi.org/10.1186/1471-2229-12-120 PMID: 22838835

59. Deng P., Wang L., Cui L., Feng K., Liu F., Du X., et al. (2015). Global identification of microRNAs and their targets in barley under salinity stress. *PLoS One*, 10(9), e0137990. https://doi.org/10.1371/journal.pone.0137990 PMID: 26372557

60. Yoshida H., Wang K.L., Chang C.M., Mori K., Uchida E., Ecker J.R. (2006). The ACC synthase TOE sequence is required for interaction with ETO1 family proteins and destabilization of target proteins. Plant Mol Biol. 62(3):427–37. https://doi.org/10.1007/s11103-006-9029-7 PMID: 16897471

61. Abeles F. B., Morgan P. W., & Saltveit M. E. (1992). CHAPTER 5—Roles and Physiological Effects of Ethylene in Plant Physiology: Dormancy, Growth, and Development. In *Ethylene in Plant Biology* (2nd ed., pp. 120–181)., Academic Press.

62. Glazebrook J. (2005). Contrasting mechanisms of defense against biotrophic and necrotrophic pathogens. *Annu. Rev. Phytopathol.*, 43, 205–227. https://doi.org/10.1146/annurev.phyto.43.040204.135923 PMID: 16078883

63. Li N., Han X., Feng D., Yuan D., & Huang L. J. (2019). Signaling crosstalk between salicylic acid and ethylene/jasmonate in plant defense: do we understand what they are whispering?. *International Journal of Molecular Sciences*, 20(3), 671. https://doi.org/10.3390/ijms20030671 PMID: 30720746

64. Kieber J. J., Rothenberg M., Roman G., Feldmann K. A., & Ecker J. R. (1993). CTR1, a negative regulator of the ethylene response pathway in Arabidopsis, encodes a member of the raf family of protein kinases. *Cell*, 72(3), 427–441. https://doi.org/10.1016/0092-8674(93)90119-b PMID: 8431946

65. Alonso J. M., Hirayama T., Roman G., Nourizadeh S., & Ecker J. R. (1999). EIN2, a bifunctional transducer of ethylene and stress responses in Arabidopsis. *Science*, 284(5423), 2148–2152. https://doi.org/10.1126/science.284.5423.2148 PMID: 10381874

66. Potuschak T., Lechner E., Parmentier Y., Yanagisawa S., Grava S., Koncz C., et al. (2003). EIN3-dependent regulation of plant ethylene hormone signaling by two Arabidopsis F box proteins: EBF1 and EBF2. *Cell*, 115(6), 679–689. https://doi.org/10.1016/s0092-8674(03)00968-1 PMID: 14675533

67. Chen X., Steed A., Travella S., Keller B., & Nicholson P. (2009). *Fusarium graminearum* exploits ethylene signalling to colonize dicotyledonous and monocotyledonous plants. *New Phytologist*, 182(4), 975–983. https://doi.org/10.1111/j.1469-8137.2009.02821.x PMID: 19383094

68. Shan L., He P., Li J., Heese A., Peck S. C., Nürnberger T., et al. (2008). Bacterial effectors target the common signaling partner BAK1 to disrupt multiple MAMP receptor-signaling complexes and impede

plant immunity. *Cell host & microbe*, 4(1), 17–27. https://doi.org/10.1016/j.chom.2008.05.017 PMID: 18621007

69. Koch A., Kumar N., Weber L., Keller H., Imani J., & Kogel K. H. (2013). Host-induced gene silencing of cytochrome P450 lanosterol C14α-demethylase–encoding genes confers strong resistance to *Fusarium* species. *Proceedings of the National Academy of Sciences*, 110(48), 19324–19329. https://doi.org/10.1073/pnas.1306373110 PMID: 24218613

70. Morel J. B., Godon C., Mourrain P., Béclin C., Boutet S., Feuerbach F., et al. (2002). Fertile hypomorphic ARGONAUTE (ago1) mutants impaired in post-transcriptional gene silencing and virus resistance. *The Plant Cell*, 14(3), 629–639. https://doi.org/10.1105/tpc.010358 PMID: 11910010

71. Livak K. J., & Schmittgen T. D. (2001). Analysis of relative gene expression data using real-time quantitative PCR and the 2− ΔΔCT method. *methods*, 25(4), 402–408. https://doi.org/10.1006/meth.2001.1262 PMID: 11846609

72. Chambers J. P., Behpouri A., Bird A., & Ng C. K. (2012). Evaluation of the use of the Polyubiquitin Genes, Ubi4 and Ubi10 as reference genes for expression studies in *Brachypodium distachyon*. *PLoS One*, 7(11), e49372. https://doi.org/10.1371/journal.pone.0049372 PMID: 23166649

73. Untergasser A., Cutcutache I., Koressaar T., Ye J., Faircloth B. C., Remm M., et al. (2012). Primer3—new capabilities and interfaces. *Nucleic acids research*, 40(15), e115–e115. https://doi.org/10.1093/nar/gks596 PMID: 22730293

74. Martin M. (2011). Cutadapt removes adapter sequences from high-throughput sequencing reads. *EMBnet. journal*, 17(1), 10–12.

75. Langmead B., & Salzberg S. L. (2012). Fast gapped-read alignment with Bowtie 2. *Nature methods*, 9(4), 357. https://doi.org/10.1038/nmeth.1923 PMID: 22388286

76. Anders S., Pyl P. T., & Huber W. (2015). HTSeq—a Python framework to work with high-throughput sequencing data. *Bioinformatics*, 31(2), 166–169. https://doi.org/10.1093/bioinformatics/btu638 PMID: 25260700

77. Hannon, G. "Fastx-toolkit." FASTQ/A Short-reads Preprocessing Tools (2010)

78. RStudio Team (2016). RStudio: Integrated Development for R. RStudioInc., Boston, MA URL http://www.rstudio.com/.

79. Durinck S., Moreau Y., Kasprzyk A., Davis S., De Moor B., Brazma A., et al. (2005). BioMart and Bioconductor: a powerful link between biological databases and microarray data analysis. *Bioinformatics*, 21(16), 3439–3440. https://doi.org/10.1093/bioinformatics/bti525 PMID: 16082012

80. Adhikari S., Turner M., & Subramanian S. (2013). Hairpin priming is better suited than in vitro polyadenylation to generate cDNA for plant miRNA qPCR. *Molecular plant*, 6(1), 229–231. https://doi.org/10.1093/mp/sss106 PMID: 23024207

81. Charif D., & Lobry J. R. (2007). SeqinR 1.0–2: a contributed package to the R project for statistical computing devoted to biological sequences retrieval and analysis. In *Structural approaches to sequence evolution* (pp. 207–232). Springer, Berlin, Heidelberg.

82. Camacho C., Coulouris G., Avagyan V., Ma N., Papadopoulos J., Bealer K., et al. (2009). BLAST+: architecture and applications. *BMC bioinformatics*, 10(1), 1–9. https://doi.org/10.1186/1471-2105-10-421 PMID: 20003500

83. R Core Team, R. (2019). R: A language and environment for statistical computing.

84. Wickham, H. (2016). ggplot2: elegant graphics for data analysis. springer.

85. Kassambara, A. (2017). ggpubr: "ggplot2" based publication ready plots. R package version 0.1. 6.

86. Tian T., Liu Y., Yan H., You Q., Yi X., Du Z., et al. (2017). agriGO v2. 0: a GO analysis toolkit for the agricultural community, 2017 update. *Nucleic acids research*, 45(W1), W122–W129. https://doi.org/10.1093/nar/gkx382 PMID: 28472432

87. Kumar S., Stecher G., & Tamura K. (2016). MEGA7: molecular evolutionary genetics analysis version 7.0 for bigger datasets. *Molecular biology and evolution*, 33(7), 1870–1874. https://doi.org/10.1093/molbev/msw054 PMID: 27004904

88. Bodenhofer U., Bonatesta E., Horejš-Kainrath C., & Hochreiter S. (2015). msa: an R package for multiple sequence alignment. *Bioinformatics*, 31(24), 3997–3999. https://doi.org/10.1093/bioinformatics/btv494 PMID: 26315911

89. Nei M., & Kumar S. (2000). Molecular evolution and phylogenetics. Oxford university press.

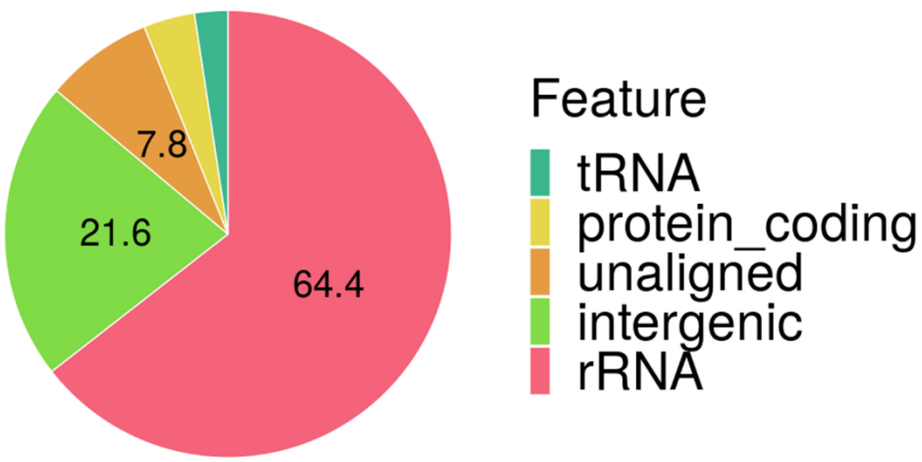

Feature	Counts	%
rRNA	3517854	64.4
intergenic	1181441	21.6
unaligned	423796	7.8
protein_coding	204681	3.7
tRNA	132329	2.4

Fig. S1: Feature mapping of Fg-sRNAs with a read length of 21-24 nt

Reads were trimmed as described earlier and aligned to the PH1 reference genome (GCF_000240135.3_ASM24013v3) with bowtie2 (Langmead & Salzberg 2012).

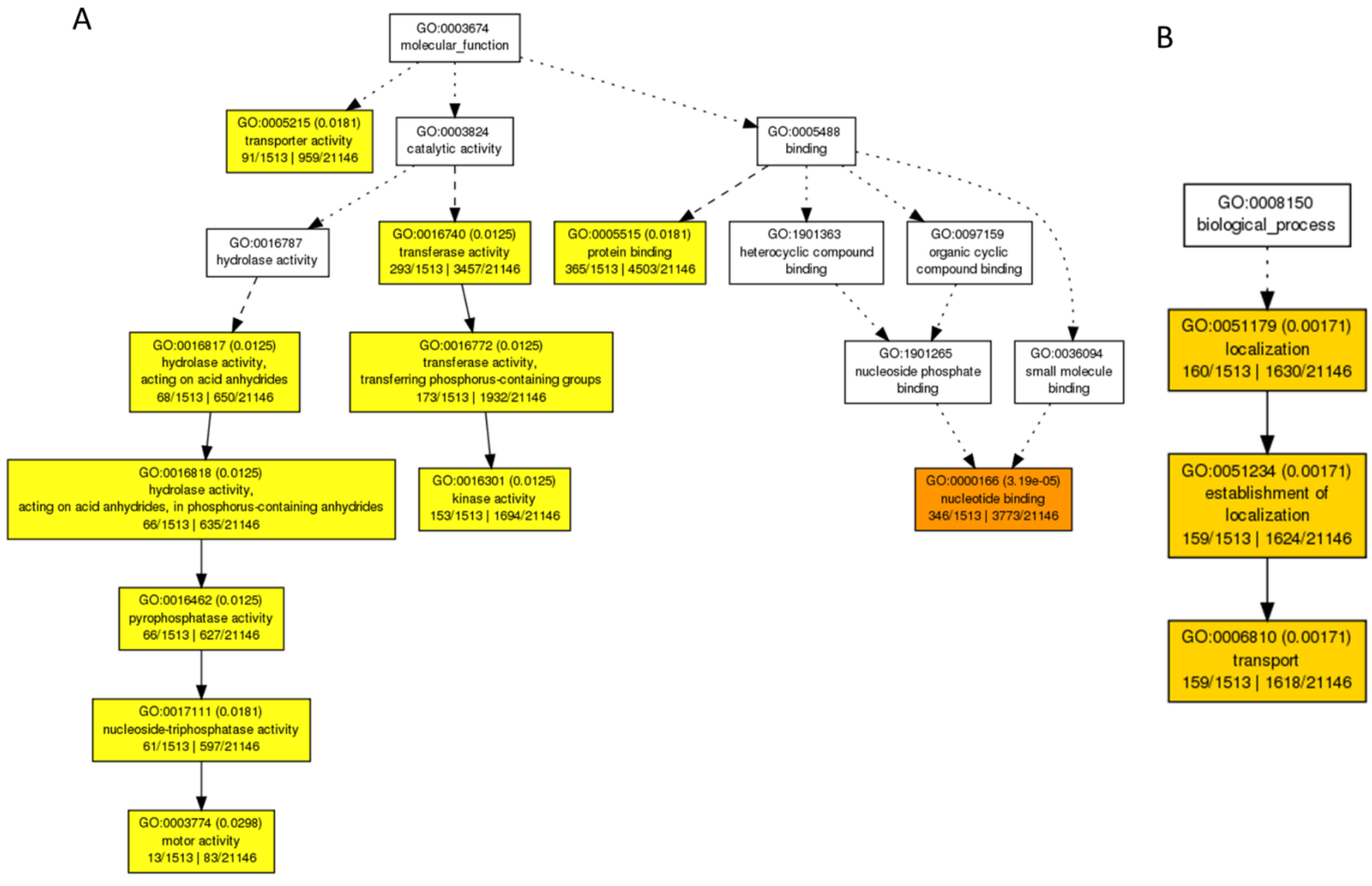

Fig. S2: GO-enrichment analysis of all potential targets of *Fg*-sRNAs with more than 400 reads

The plot shows all significantly enriched GO-terms in the target gene set for (A) molecular function and (B) biological process. The analysis was done using agriGo v2.0. Each box contains information regarding one term. GO: indicates the GO accession, in brackets the p-value is stated (Fisher; Yekutieli (FDR)). After the bracket the GO-term description is written followed by the number of genes associated with said term 1. in the gene set and 2. In the background.

Fig. S3: Alignment of *At*ETO1 and *Hv*EOL1

Identical amino acids are marked blue and similar amino acids are marked red. The alignment and visualization was done with the msa package for R (Bodenhofer et al. 2015).

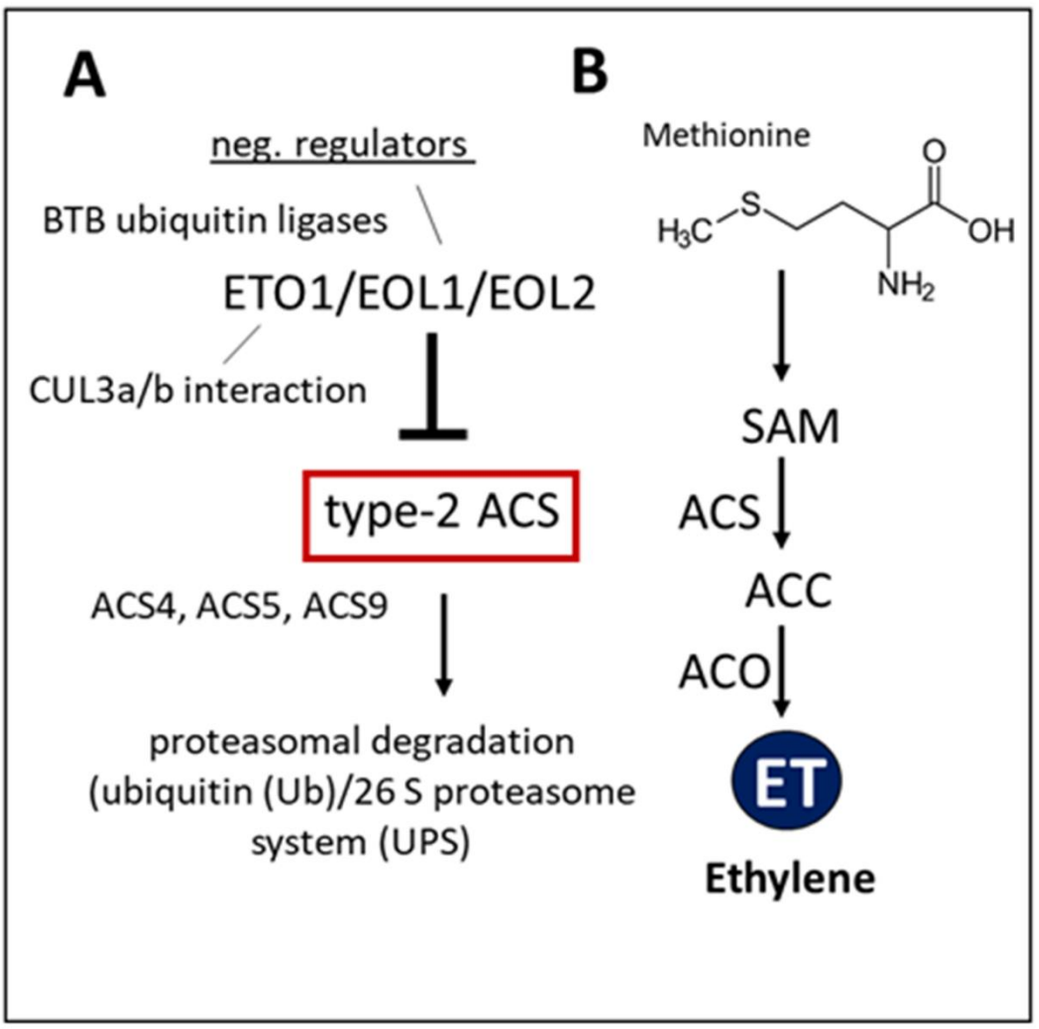

Fig. S4: Regulation of ET synthesis in At

*At*ETO1 negatively regulates ethylene **(ET)** synthesis in *At***.** *At*ETO1 acts together with *At*EOL1 and *At*ETO1-like 2 (EOL2) in directing the ubiquitination and subsequent degradation of type-2 1-aminocyclopropane-1-carboxylate synthase (ACS) proteins (e.g. ET overproducer 2 (ETO2)), which produce the direct precursor of ET.

FgDCL1-FGSG_09025

ATGGACACCGACTCGACCGACAGCGAAGATGATCGCGTTCAGTATCGCCTGACCGTGAGGCCTTCGAAGCATCGAAAGAATACAGAGAAGAAGCGCCTG
AACAAGCAGGTTTTGAAACAATACATGATAGAACACGACAGAGAAGCCTATGCCAAAGATTCTGAGAAAAAGAAGCGCGGCCCCTTCGCTGAAGCTTCCA
CCGACATTACACCGCGAGAATATCAGATAGAACTCTTCGAAGCCGCCAAGGAGAAGAATCTCATTGTGGTTTTACCTACAGGTATTTTCTTGTCCCTTTCTG
ACTCTACTCTGGACATTCTAATAGGCACAGGTTCTGGTAAAACACTCATCTCCATCTTATTGCTAAAATACTACATTCGAATCGAAGTGGAATCTCGCGCTCT
TGGAAATCCGAGGAAGGTGGCCTTTTTCTTGGTGGAAAAAGTAGCCCTCTGTGAGCAGCAATACCGATTTCTTAAGGACCAGATTTTCGGCCACAACATTG
TCATGTTCACAGGCGATAACCGCGGCGTGACCAAGGACAAGAAGTACTGGGATGATCAGTTTTCCTCAAACAAGGTTG<u>TGGTCTGCACTGCTCACATTTTG
CTCGACTGTCTGAACAACGGCTTCATTACAATGGACCAGATCAACCTCCTCATCTTCGACGAAGCCCATCATGCAAAGAAGAAGCATGATTACGCGCAAATT
GTCCGACGATATTATTATTCTACCGAAAAGAACAAGAGACCTCGCATTCTAGGAATGACCGCTTCCCCTGTGGATTCCAAGGCTGGAGATGTTGCAGAACT
GGCACTTGAACTTGAGAAAACCCTTGACAGCGAGATCGCAACACTCTCCGACAAGATGATGCGACAGGCGACTGATTTCCAAGTTCATGTTGAAGAGACA
GTCAAATACAACACACTTGGACTACCAGACGAGACCAAGACACAGCTTTGGGACTCGATCTCTAAGCTAGTATCGCGAAACAAGGAATTCAAGGCGTCTCT
CGACTTCACAAAAGAGGCCTCCACAATCCTAGGACCCTGGTGTGCGGACCGATACTGGCAAGTCTTGATCGACGATACAGAGATCAAGCGACTCGCCGAC
AGGACTCGCATGGCTTTTTTCGGGGGTGGAGAGAAGTTGTTGGCAAGAGGAGACCAAGCAGAAGAGGCTGTCAGGGAGGTTCAAAAGGTCGTCGCAGC
CCACGAGTTTAGGGCGATCAGTCCTCAATCGCAGGAATTGTCAGCTAAAGTGAAATGTCTACATGAAATCCTGGTTCATGCCTTCACAGTCGATAACACAA
AGCGCTGCATCGTTTTTGTTGATCAGAGACACACAGCTTGCCTCCTTTCGGACCTTTACGACCAAGTTTCAATGGCAATTCCCGGTATGAATGCTTCGTATAT
GGTAAGTTGAGTCCCATTTCCAACAGCAGTAACTAACCACAATAGATTGGTCAACAATCTAGCAGCAGCACCCTTGGCAATAT</u>GTCTCTGCGAAAGCAATG
TTCAACGCTCAAGAACTTTAGGGACGGCGTGATAAACTGTCTCTTTGCAACATCAGTGGCAGAGGAGGGAATTGACATTCCGAGTTGTGATCTTGTTATCC
GATTTGATCTCTATACTTCTGTTATTCAGTATGTTCAATCCAAAGGGCGTGCGAGACACGAATCTTCACGGTATATCACCATGCTGGAAGACGGCAACATGA
GACAGATTCGCAGTCTGAAACAAGCAGCGAGAGATGCAACAGCCCTTCGAGAGTTCTGTCTAAGAATACCTGCCGATCGAAAACTTCAAGACGATGTATTT
GATGAGGAGACGGAAAGTCAGATCAAGCAAATACGTTTTAACGTGTACAAAATAGAATCAACGGGCGCACAACTTACATTCCCCTCAAGCCTCGAGATAC
TAGCTCGATTCGTTGCATCCTTGGGTACAGCAGAGAGCAGCCATAGCAAGGCTGAATATCACGTCTACAAGGTGGGAACATATTTCACAGCCGCCGTCAAT
CTACCGTCCAGTTCCCCCATCGTCTCCCAAACAGGCTATCCACAACGAAGCAAGCTTCTCGCAAAATGCTCAGCGGCTTTTGAGGTTTGCAAGAAGCTCATC
AATGGCAAACACATTGATGATCATCTTCAGCCTACTTTCAAGAAACATTTCCACAAAATGCGCAATGCTCGTGTGGGAATAAGCCCTAACAAGAAGGGTGA
GCATGACATGCGCCTGAGGCCCAACGTTTGGAGTATCCGTGGAGAATGGACACACTTCTTCCCAACAAGAATTACTCTTGACAGGGATTGTGGAGAGAAA
AACAGGTCGTTGATTCTTCTTTCGCGAAGTCCACTTCCAGGACTACCTTCAACCCTCTATTCTTCGGCAATGGACGCTCAGCCATCGTTGAAGTGACATGTTC
TCAAGAACCTTTACCCATCACGACCGAGGAAGCTGGGGGTTTGACTGCTTTCACACTCAAAATCTTTGCCGACGTTTTCAGTAAAGAGTTTGAGGCCACTTG
CGACCAGTTTCCTTACCTTCTTGCCCCCTTGGCAAAAGACACCAATCTAAACGAAATATCGCGAATCGACTGGGATACTGTCAACCTTGTCAGAGACCATGA
CAGTCTCGAATGGGAGAATGCGCCCGACGATTTCTTTTTCGACAAGCTTGTTGTAGATCCATATGATGGAGGGCGCAAGCTTATAATCAAAGGCATTGACA
AATCCAAGAAGCCTTCTGATCCTACACCGGAGGGAGTGCCTGAGTCGAGAAGTCGTGCTTATAGGTCTGCGGAACAAAACATTAAGCAGTACAGCAACAG
TCTGTTTTCCAAGTCTCGACTAACGGCCCAGTGGCGAGACGATCAACCGGTTGTCAAAGCTGAGCTTCTCTCATTGCGACGCAATCTGTTGGACGAGTTTCA
AGTAAACGAGGAAATCAACAAGGATTGCTTCGTCATTTTAGAACCCCTCAACGTGTCACCTGTAAGTGAAAGACTCTTCTGTAAAACGTATCTAACATGCCC
AGCTGCCAATTGACGTCGTTTCCATGGCACTCAAGTTCCCGGCAATCATCCACAGAATCGATTCTGCTCTGATCGCTCTTGATGCATGCGAACTATTCGACCT
CTCTATTCCGCCAGCGCTGGCACTCGAGGCAATGACCAAAGACAGCGACAACACTGAGGATCATGGCAAGCAACAAATCAATTTCCAAGCTGGCATGGGT
TCCAACTATGAAAGGTTGGAATTTCTTGGAGACTCGTTTCTCAAAATGGCCACCACAATCTCCATTTTTGTACTCAAACCCAAGAGCAACGAATGTTTGTACC
ATGTAGAGCGCATGCTGCTCATCTGCAACAACAATCTGTTCAACACGGCCGTAGATTGCAAGCTCCCAGAGTACATACGATCCTTGGCATTCGACAGGCGA
ACTTGGTACCCTGATCTTACACTCAGAAAAGGCAAAGCTTTCAAGGCAACAGCGCGACAGCGCTTAGCCGACAAAAGTATTGCGGATGTCTGTGAAGCTCT
CATTGGTGCTGCATACCTCTCAAGCAAGGATGACAATTTGAACATGGCCGTCAAAGCTGTGTCACAGATGTGCAAAGCAAAGTACCATACCATGATGGCTT
ACGATGAGTACTACGCATCTTTCAAGGTTCCAGATTGGCAGAAAGCCAGTCCAAACGCCAACCAGCGTAGACTTGTGCAGAAAGTGGCAGACGCTACCGG
GTACCACTTCAAGTCTGCGCCGCTGCTCCAGAGTGCATTCACACACCCTTCTTACGCGTATTCAGGGAACGTTCCAAACTATCAACGCCTCGAGTTTCTAGG
CGATGCCCTCATCGACATGACCATCGTCGAATATCTCTATCGCAACTTTCCCCTCGCAGACCCTCAGTGGTTGACGGAGCACAAGATGGCAATGGCCTCGAA
CCAATTTCTCGGTTGTCTGTGTGTTAAGCTCAATCTGCACCACCATCTTCTGTTCAACACGTCGCAGTTCATCAGCAAAATTCGTGACTATGTGGCCGAACTT
GAGTTGGCTGAAGAGACTGCGCGCCAAGAGGCAGAAGAAGACGGGACTCCAATGCGCATGGACTTTTGGCTCAATGCGACAACGCCTCCAAAAGCGTAC
GCAGATTCAATCGAGGCTCTTATGGGGGCCATGTTTGTGGATTCTGAATTCGACTATTCTGTTGTTGAGGATTTCTTTACCAAGTTCATCTTCCCGTACTTTA
AAGACATGTCTCTGTACGATACCTTTGCAAACAAGCATCCTTACACATTTCTCACCAAGAAGATGCAACAGGAGATCGGGTGCATGAAATTCTGTATGATTT
CAGACACCCGCGTTCCTGATGCAGAGCGTGGCATGGAAGTTATGAAAGAGTACGACATATATTCAGCCTTTCAAGTGCACGAAAGAGTCATCACATGTCAC
GTATCAAAGAGTGGAAGGTACGGTAAGATTGCTGCTGCAAAGGGGGCACTCGAGTTGTTGGAGCCGTATGGCGGTGATGTGGTCGCGATGAAGAAGCT
GTTGGGCTGCGACTGCGACTCTGTAACAGCAGCCATGGCGGAGATGGACCATGGAACAGCTGTCTAA

Fig. S5A: Sequence of *FgDCL1*-FGSG_09025 (912 nt long dsRNA-*FgDCL1*)

Coding Sequence (CDS) of the respective *FgDCL* gene with the sequences comprising the dsRNAs marked in red.

FgDCL2-FGSG_04408

ATGTCCTCAAGCGATAAGGTCATGGCGGACGCCTCTTCCATACCAGACTCCGAGGTCAAAACAATAGCGTCGTCCTCGGTCGTCGAGATCTCTGCTACAGG
CGAGAAGGAGATAACGACTCATATACCTGTCGCAGATACACCAATGTGCTCAGATGACCAGGCCAATGTGCAAGAGCAAGACGAAGAAGTTAAGCCTCAG
AAAGTGACGCCCAATCCAGAGGTGGTAAATCCCCGCGGTTACCAGCGAGAGATGCTGGAACAAAGCATCAAAAGGAATGTCATCGTTGCAGTAAGTTATT
CCAAGTACCCCATTCAATCTGCATTCGGTGACCTGATTAGATGGACACGGGAAGTGGTAAAACTCAAGTGTATGTCACTTCCATACCATCGAAAAAGAGAG
AGACTAATTATAACTCGTAGGGCCGTGATGCGCATCCAACATGAACTCGATACATGTGCACCAGACAAGGTTGGTGAACAAAGAAACATAATATCGCGGT
CAAAACTAACCAATATAGATTATCTGGTTCTTAGGCAAGACAGTATCGCTATGTGAACAGCAATACAGCGTTGTCCAAAGGCAAATGCCGTCGGTATCGAT
GAAACTGCTAACGGGGCAATTGAACATCGATGCATGGTCCGAGGACGTCTGGCCCCGTATCCTTAATGGGACTCGTATCATTGTCTCGACCTTTGATATCCT
GCGAGATGCTTTGGACCATGCATTTGTCAAGATGAACATGCTGTCCCTTATCGTCTTCGATGAAGGTGAGACATCGCCAACACTTACAATATCATTACTGAC
TTTTTACAGTTCATAATTGTGTAAAGAATAGCTCTGGTCGAAAGGTTATGGTGAATTTCTATCACGAACACAAGAACGCCGGCATGCCCGTGCCTGCTATCC
TGGGTTTAACAGCCAGCCCGATACAGTCGAAGTCAATCCACGACGAAATCCTTGAGCTCGAGGTCACCATGGATGCTGTATGCATCACTCCAACAATTAAC
CGGAAAGAACTCCTCCAGCACGTCAACAAGCCCAATCTTTCCCGAGTATTGTATGATGTGGAAGAGCATCCGACTCGAACCCCCCTAATGCAGACTCTGCA
GTCTGAGTACTCGGCGATGGACATCACCCAGGACCCAAGTATTATAAAGGCCAAGCAACTTATCGCTAAGGGCGAGAAGACTGGACCTGAAATACTAAGT
ATGTTGATGAAACACAGGACCTTCTCTCAGAAGCAGTTAAAGTCCTTATGGAACAAAAGCAAAGACATTCTTGATGAACTCGGGCCTTGGGCTGCTGACAA
GTACATCTCCGAGTTGGTCAGTCTGTTTCTCAAGAGAATCGACTCGCCAATGACGTTTAACGAGTCCTGGAGCAATGAGGATAGGACCTACCTCGCAGGTC
ATTTGAGACAGATCGCTGCCAGTCCCCATCAGCCCAAACTACCAGACAGACACAACTTGGCCGACAAGACGAATAAACTAATCCAGGAACTACTTGCAGCG
GATGAAGATGTGGTCGGCATTATATTCGTCAGATCAAGGGCTGCTGCCAACGTCCTTTGTGCTCTTTTGAGGGAGCACCCCGAGATTCGACAGCGATATCG
AGTCGGCTCTGTAGTAGGATCCGCAGCCACCAAGATTCGAAAGCAAAACATCTACGAGTATCTGCCCGGCGCGACTGCCGATACATTACGCGATTTCAAAA
CAGGCGCCATCAACCTTTTGGTCTCGACTAGTGTTCTTGAAGAGGGTATTGATGTCGCAGTGTGCAACCTCGTCATATGTTTCGATGAGACAACGACACTCA
AGTCCCATATCCAACGCCGCGGACGAGCTCGCAAACAAAAATCAAAGATGATAGTACTTGCTAGATCTTCATCCGACGCTCGGGAATGGGATTCCCTAGAA
AGAGACATGAAGAGTCGTTATGAGCAGGAAAGGGGAGAGTTGGACGCTTTAGAGATAGAGGCTCGCACTGAAGCGACGTCCTCTTTTTCTTATACTGTGA
AAAACTCAGGGGCTAGATTGGACCTCGAGAATTCTCGCCAGCATCTGGAACATTTTTGTAACAAGGTTTTCCAGCGAGATTACGTTGATCCGAGACCCGTC
TACATTTTCCACAAGACCGAACTGGGATCAGCACCGCCGACTTTCAGCGCAACGGTGACTCTTCCCTCGGGTCTGCCTAAGCACCTCCGAAGGTGCCAAGG
TGGAGGTGGATGGAGATCAGAAAAGAATGCGATGAAGGAAGCGGCTTTTCGTGCATTCGTCATGCTGCACCAAGAAGGTTTGGTTAGCGACCACCTTCTT
CCCCTAAATGCAGATTCGAAAGAAGCAGAAGAAGAGGTGCAGCTAACTGCGCCCGAGCTTCTATTTGACCCATGGAAAGACATTGCACAGCGGTGGGAG
ACCACGGCTGAGAAATGGCTCTATGCTTACGAGTTCGCCGATCACGAGTATGTTACTCCTCTTCATTTCGAGATTGCCTTGCCTGTGTGTCTTCCACGACCCC
GCGACATCACCTTTCATCCTGAAGAGGGACTTAAATGGCATGTCAAATGCACCTCAATCAAGAGGATCTCCAATGATGAATGCTTGGGCTTGCCAGATCAT
ACGTCAACCCTATTGGCGATGCATTATGGCCACCGCTGGAACGTGGAAGATCGTGACCATGTGATCAAATTCATATATGAGAACAAGAATCTCACCCGAGA
TCAAATTGGATCGGTACCCTTCGGCGAAAGCATTGATGCTCTATTGGAAAAGAGAGTCCTGGTTCGGGACCCCAAAAATACTCCCTTCCACTACGTCAAAAT
GATCCCATCAAAGCCTCCAAAAGAGCAAGTTCAGCACCCATTTAATGAATACGAGGAAGCGCCAGAAGAACAGTATCTAGTTGTGGATCAATGGACACGC
AGGTCGGACCTGTTGCATGAGATAAAACCCGGTCAGGGGAAGAGCTCTTGCACCAAACCCTACCGCTGGGTTCTCCCGATTTCCAGAGCGACTGTTGATGA
GGTTCCTCGGCGTGCCGCTAAGTGCGGTATGCTTATCCCTTCCATCATTCACGAATTGGAGGTTCAGCTCATCGCGAATGAACTGTCCTCGACACTTTTGGC
GCCAGTTGGTATCACAGATCTGCAATTGGTGATTGAAGCCATCAGCTCGCGTAGCGCTGCAGAGCCTGTTGACTATGAACGTATTGAATTTTTGGGCGATT
CGGTTTTGAAGTATTGCACTGTTATTCAAGCCTACTCTGAACGTAAGTCTTCCGCATCCCTCTATCGTCACTTTCACTGATCATTGTCACAGATCCCTTTTGGC
CCGAAGGTCTACTCAACCATTTCAAAGACCGACTAGTCTCCAATACCCGTTTGACTCGCATGTGCCTTGAGACAGGCCTTTCCAAGTTCATTTTTTCCAAAAC
ATTTACTGGAATCAAGTGGAGACCGCTATATCGAGACGAATTCCTAGATAAGAAGCCAGTCGATGGTGTATCAAGGTTTGTTGGTCCAAAGACTCTTGCTG
ATGTGGTCGAGGCACTTGTTGGAGCCTCCTACCAGGATGGAGGAATCAGCAAAGCTCTGGAGTGCATCAAGGTTTTCTTGGGCACCAAGTGCAATTGGCA
TGATGACAAAGTCGCCAGAGACATACTCTTCCGAGCAGCAATTAGCGACGTACCGTTGCCCCCCACGATGGAGCCTTTGGAAGAGCTCATCGGGTACACAT
TTCAGAAGAAGTCTCTACTCATTGAGGCAATGACTCACGGGTCGTATGCGGCTGATGGGCAGCAGCGATCTTATGAACAACTCGAGTTTCTTGGAGATGCG
GTTCTTGACTACATTGTCGTAACCCGAATGTTCCAATCTGACCCCCCAGTGCCCAATGGACGCTTACACATGGTCAAGACTGCCATGGCCAACGCTGATTTC
CTTGCTTTTACAAACATGCAACATGGACTACGCCGGCCTGAAGTTGAAATAAATGAGAACGGCGAACCAGTGCCTACAGAAGTTTCACTGCCGATATGGAA
ATTCATGCGTCATAGCTCTCCAGAGATGGGTAGAATCATGAATGAGACCCAGGCCCGATTTGAGAGCCTTCAAGAGGAAATCAATGAGGCTAGGACGAAT
GGTAAACACTACCCCTGGACACTTCTCGCTCGTCTTCACCCGAAGAAGTTCTACTCCGATATTTTCGAGGCTACCCTAGGTGCCATTTGGGTTGATTCAGGA
GATATCGAAGTATGCACAGCCTTTCTTCACAAGTTCGGCGTCTTGCCGTATCTTGACCGAATTCTCAGCGATAATATTCATGTTCAACATCCTAAAGAGGAA
CTCGCCAAACTAGCAATCGACCAGAAAATGACGTATGATTATACGGCTGTTGATGGGCCTATAAAGGAGTACCTCTGCACGGCCAAGGTTGGAGATCGCG
TCGTGGGAGTCGTGTCAGGGGCACTCAATAAGGCTGAGGCAATGACCAAGGCTGCCGAAGAGGGCGTGAATTTTTTGAATGGGGAGCAGAAACGTGCA
GAGAAGGCGGCTCAGGATGAAATGGCGCGATTTCTTGTTGCCATGGAACTCATTTAG

Fig. S5B: Sequence of *FgDCL2*-FGSG_04408 (870 nt long dsRNA-*FgDCL2*)

Coding Sequence (CDS) of the respective *FgDCL* gene with the sequences comprising the dsRNAs marked in red.

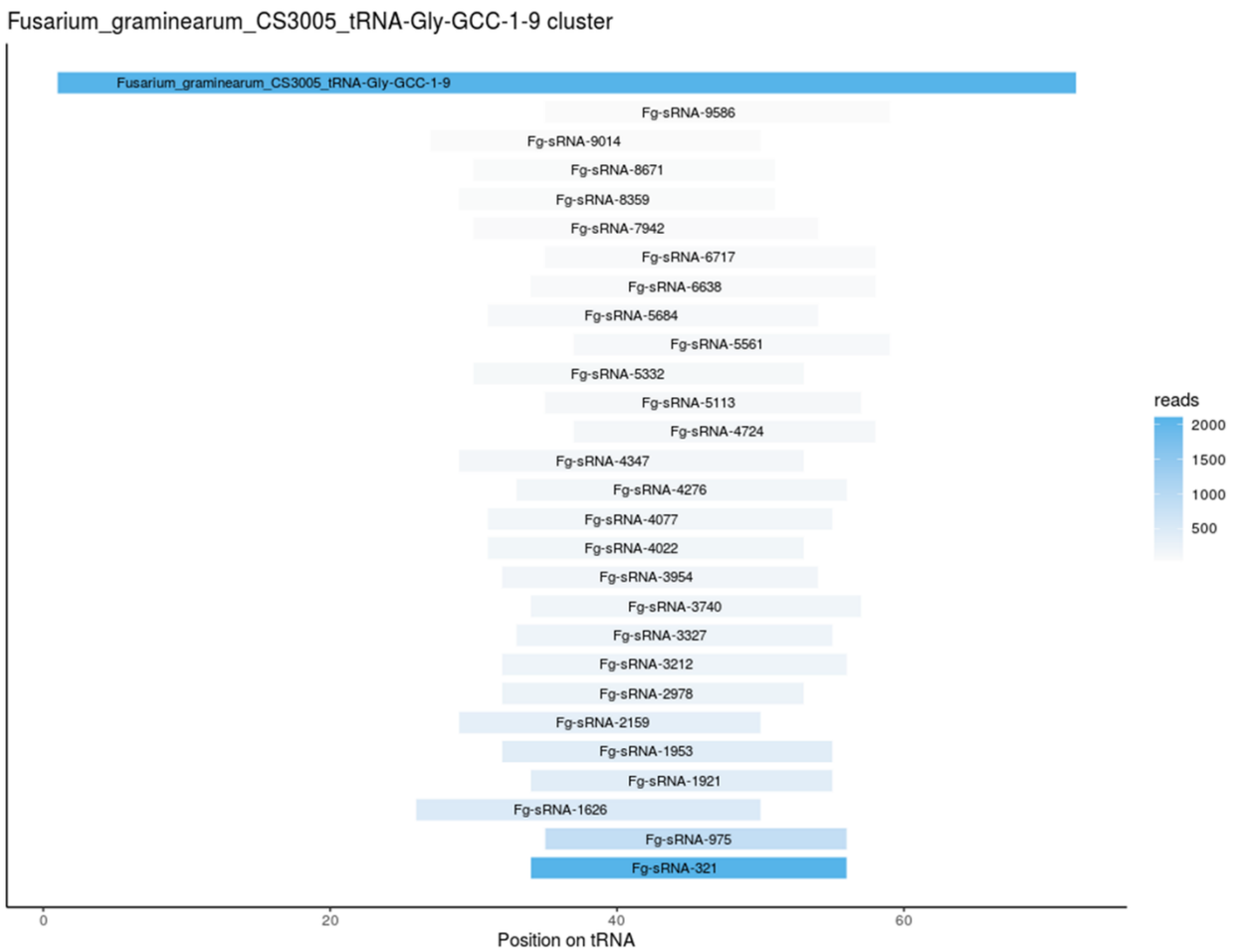

Fig. S6: Position and read count of all tRFs from Fg-tRNA-Gly(GCC)

Alignment position of all *Fg*-sRNAs from axenic culture with more than 50 reads perfectly matching the *Fg*-tRNA-Gly(GCC)-9 gene (Fusarium_graminearum_CS3005-tRNA-Gly-GCC-1-9) colored by read count.

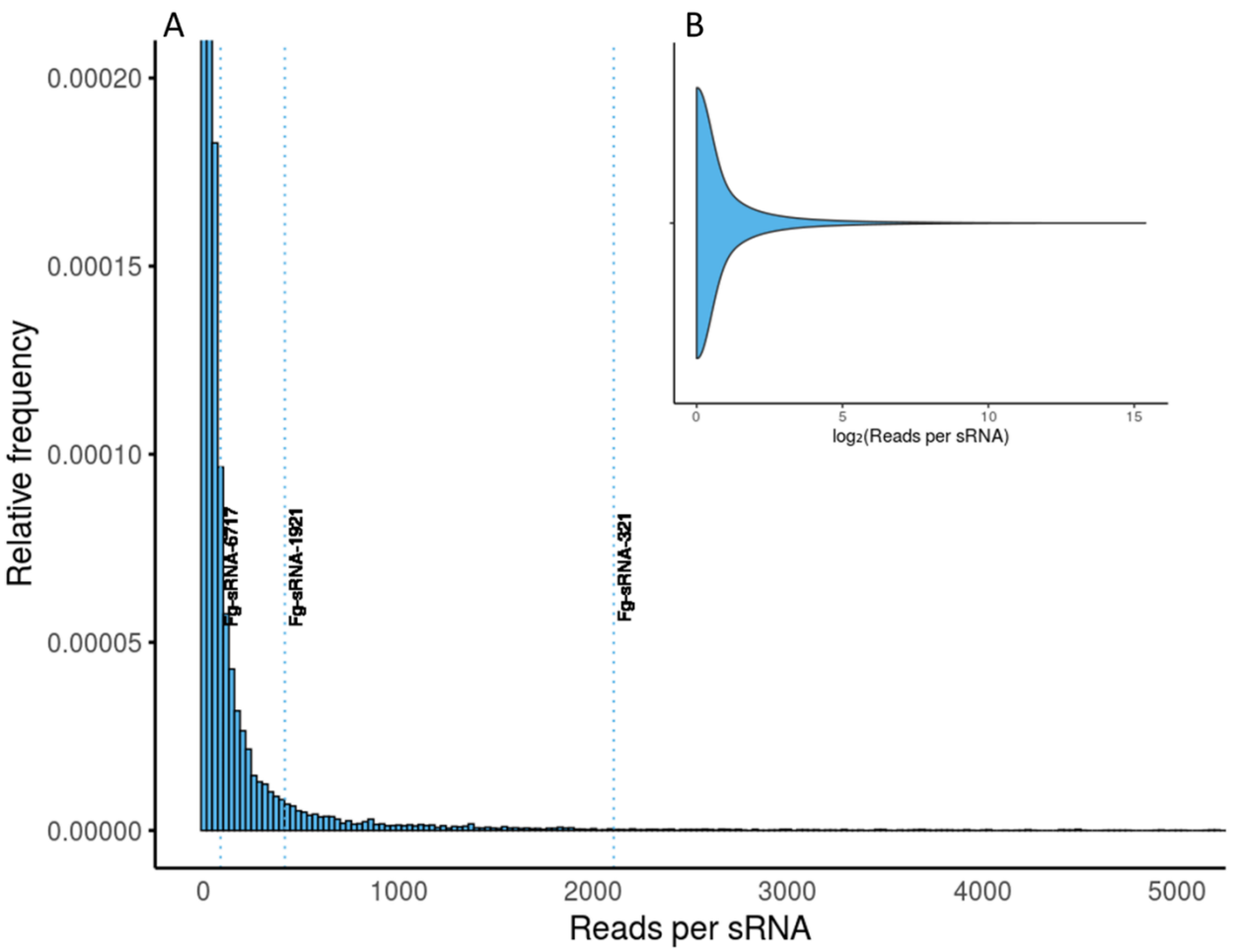

Fig. S7: Abundance of unique Fg-sRNAs in axenic culture of IFA65

A: Histogram of the read count of every unique sRNA. The plot is truncated to make abundances recognizable. Most sRNAs have very low read counts and very few sRNAs have more reads than 3,000. Maximum read count per sRNA is 42,866. B: Violin plot of log2-transformed reads counts untruncated.

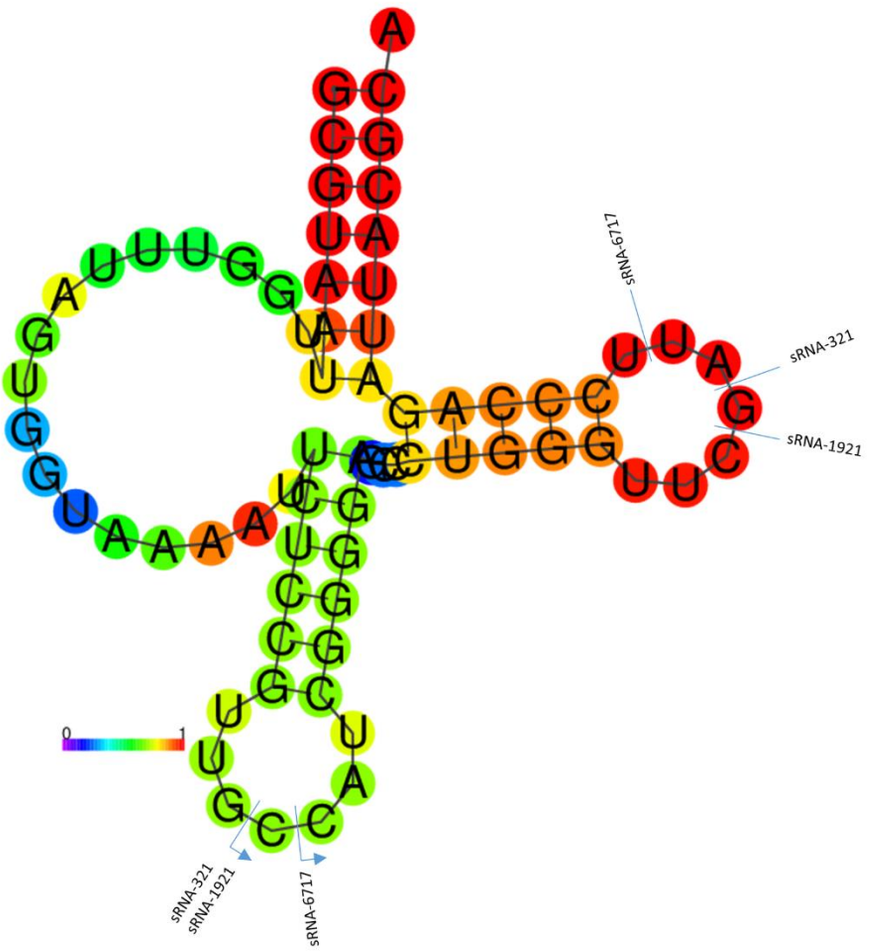


```
>Fg-sRNA-321                                                                    CCAUCGGGGAGCCCUGGGUUCG
>Fg-sRNA-1921                                                                   CCAUCGGGGAGCCCUGGGUUC
>Fg-sRNA-6717                                                                    CAUCGGGGAGCCCUGGGUUCGAU
>lcl|Query_57046 Fusarium_graminearum_CS3005_tRNA-Gly-GCC-1-9 GCGUAAUUGGUUUAGUGGUAAAAUUCUCCGUUGCCAUCGGGGAGCCCUGGGUUCGAUUCCCAGAUUACGCA
 centroid secondary structure                                 (((((((.................((((((.......))))))...((((((.......)))))))))))).
```

Fig. S8: Origin of tRFs in Fg-tRNA-Gly(GCC)

The centroid secondary structure of the *Fg*-tRNA-Gly(GCC) generated on the RNAfold web server (http://rna.tbi.univie.ac.at/cgi-bin/RNAWebSuite/RNAfold.cgi) with the origin and alignment of *Fg*-sRNA-321, *Fg*-sRNA-1921 and *Fg*-sRNA-6717. The colors of bases indicate the base pair probabilities.

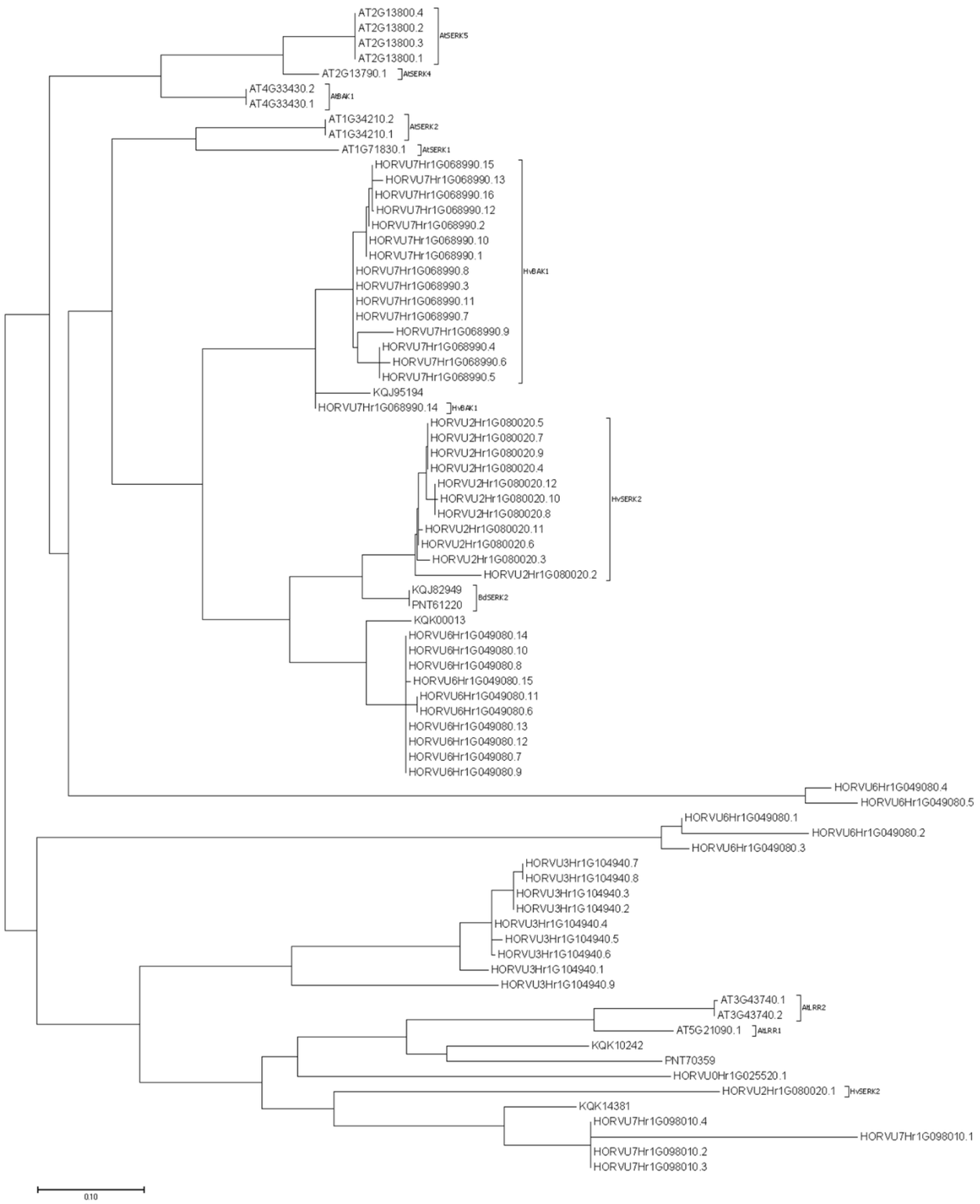

Fig. S9: Molecular Phylogenetic analysis by Maximum Likelihood method

Fig. S9: Molecular Phylogenetic analysis by Maximum Likelihood method

The evolutionary history was inferred by using the Maximum Likelihood method based on the General Time Reversible model (Nei & Kumar, 2000). The tree with the highest log likelihood (-25430.37) is shown. Initial tree(s) for the heuristic search were obtained automatically by applying Neighbor-Join and BioNJ algorithms to a matrix of pairwise distances estimated using the Maximum Composite Likelihood (MCL) approach, and then selecting the topology with superior log likelihood value. The tree is drawn to scale, with branch lengths measured in the number of substitutions per site. The analysis involved 77 nucleotide sequences. Codon positions included were 1st+2nd+3rd. There were a total of 2427 positions in the final dataset. Evolutionary analyses were conducted in MEGA7 (Kumar et al. 2016b).

Tab. S1: Primer sequences

Sequences and target accessions for all primers used in the study

Gene	Accession	Primer Name	Sequence
HvARF3	HORVU1Hr1G076690	HORVU1Hr1G076690_F	GGTTCAGCTCAGAAACGAAGC
		HORVU1Hr1G076690_R	ATTCTGACGCTCCACTCCTTG
HvPPR	HORVU2Hr1G078260	HORVU2Hr1G078260_F	GGGTGCTTCATCGAGTTGGAA
		HORVU2Hr1G078260_R	CTGCAAAACCACAGAGCTTGT
HvSERK2	HORVU2Hr1G080020	HORVU2Hr1G080020.6_F	GATGACAGACAGAGTCCTGCT
		HORVU2Hr1G080020.6_R	AGCACTACTACCAGCACCGA
HvARF10	HORVU2Hr1G089670	HORVU2Hr1G089670_F	CACATCGGCGATGAACCTTTC
		HORVU2Hr1G089670_R	TCGGCTCAAGATCGATGGATG
HvPGLP2	HORVU5Hr1G052320	HORVU5Hr1G052320_F	CTCCTTGTTCTGTCAGGTGTGA
		HORVU5Hr1G052320_R	ATTGCTGGTGCTGTATTCGGA
HvATG2	HORVU6Hr1G034660	HORVU6Hr1G034660_F	TTCTTATCTCGGGGCTTGGTG
		HORVU6Hr1G034660_R	TCGTAGCAGCCAAGAACCATT
HvGDH	HORVU6Hr1G076880	HORVU6Hr1G076880_F	GGCAACGTGGAGAGTGTGAA
		HORVU6Hr1G076880_R	GTACGGGCTCGAGTTGATCAG
HvARF19	HORVU7Hr1G096460	HORVU7Hr1G096460_F	GGGCCGGTCTATCGACATTAG
		HORVU7Hr1G096460_R	TTGACAAACTCCTCCCAAGGG
HvSUB1	HORVU2Hr1G028070	MLOC_12796.1_F	CAGAGTTCAGGAGGGGCAAG
		MLOC_12796.1_R	GACAAACGTCCGGTTGAGGA
HvSUVR5	HORVU6Hr1G069350	MLOC_14605.1_F	TGCATTTTGTTGACCGCAGG
		MLOC_14605.1_R	AGGCTTGTCTGGGAACGATG
Hvemb2726	HORVU5Hr1G024470	MLOC_58105.1_F	AGACTGATGTTGCGGTGGAG
		MLOC_58105.1_R	GGTTGCGACCTAACTTGGGA
HvPIX7	HORVU3Hr1G051080	MLOC_5991.1_F	GATGGGCTTCAGGGGCATAA
		MLOC_5991.1_R	ATGGGAGCGGAAATGACCTC
HvRDR1	HORVU6Hr1G074180	MLOC_75294.1_F	TATCTGAAGGTTCGGCCTGC
		MLOC_75294.1_R	GTTCCGCTCCACAGAACAGA
HvRST1	HORVU3Hr1G016630	MLOC_75306.1_F	TTGCGGGACTTGTTCTTGGT
		MLOC_75306.1_R	TGACAGATGGCAGAGCAAGG
HvEOL1	HORVU2Hr1G119180	MLOC_8741_F	CACTTCAAGCCCGCTGACTA
		MLOC_8741_R	CTCATGTATCGTGCTCGCCT
BdSERK2	BRADI_5g12227v3	PNT61220_F	AGTTGCGTTTCCTCCGTCTT
		PNT61220_R	ACCAGTTGATGGAACCTCTCC
HvUBI	HORVU1Hr1G023660	Ubideg60_F	ACCCTCGCCGACTACAACAT
		Ubideg60_R	CAGTAGTGGCGGTCGAAGTG
FgEF1a	FGSG_08811	EF1a_F	CAAGGCCGTCGAGAAGTCCAC
		EF1a_R	TGCCAACATGATCATTTCGTCGTA

Name	Sequence (RNA)	Primer	Sequence (Primer)
***Hvu*-miRNA-159a**	UUUGGAUUGAAGGGAGCUCUG	hvu-mir159a_F	TGGCTCGCTtttggattgaaggga
		hvu-mir159a_RT	GTCGTATCCAGTGCAGGGTCCGAGGTATTCGCACTGGATACGACcagagc
***Hvu*-miRNA-168**	UCGCUUGGUGCAGAUCGGGAC	hvu-mir168-5p_F	GTTCGCTtcgcttggtgcagat
		hvu-mir168-5p_RT	GTCGTATCCAGTGCAGGGTCCGAGGTATTCGCACTGGATACGACgtcccg
***Fg*-sRNA-321**	GCUUGGGUCCCGAGGGGCUACC	Fg-sRNA_321-2106_F	TCGCTccatcggggagccctg
		Fg-sRNA_321-2106_RT	GTCGTATCCAGTGCAGGGTCCGAGGTATTCGCACTGGATACGACcgaacc
***Fg*-sRNA-1921**	CUUGGGUCCCGAGGGGCUACC	Fg-sRNA_1921-416_F	TCGCTccatcggggagccct
		Fg-sRNA_1921-416_RT	GTCGTATCCAGTGCAGGGTCCGAGGTATTCGCACTGGATACGACgaaccc
***Fg*-sRNA-6717**	UAGCUUGGGUCCCGAGGGGCUAC	Fg-sRNA_6717-86_F	TCGCTcatcggggagccctggg
		Fg-sRNA_6717-86_RT	GTCGTATCCAGTGCAGGGTCCGAGGTATTCGCACTGGATACGACatcgaa
Universal SL Reverse		UniSL_R	CCAGTGCAGGGTCCGAGGTA
Target	**Accession**	**Name**	**Sequence**
RLM-adapter		RLM_Adapter	GCUGAUGGCGAUGAAUGAACACUGCGUUUGCUGGCUUUGAUGAAA
RLM outer adapter Primer		RLM_Uni_O1	GCTGATGGCGATGAATGAACACTG
RLM inner adapter primer		RLM_Uni_I1	GAACACTGCGTTTGCTGGCTTTGATG
HvEOL1	HORVU2Hr1G119180	HvEOL1_outer	GAATTTACTGATGGCCCGCAT
	HORVU2Hr1G119180	HvEOL1_inner	ACCCACCATTAAGCATCGCA
HvSERK2	HORVU2Hr1G080020	HvSERK2_1_outer	GAGCCTCAGGAGACGGTTTT
	HORVU2Hr1G080020	HvSERK2_1_inner	AGTGGAGTCGACGATCCAGT
HvBAK1	HORVU7Hr1G068990	HvSERK2_2_outer	GGGTTTGCACATGCTCGTAC
	HORVU7Hr1G068990	HvSERK2_2_inner	TGAGGACCCAGCTCTACCTC

Tab. S2: Target prediction results

Results of the target prediction with the TAPIR algorithm for all *Fg*-sRNAs with more than 400 reads

Table S2 can be found via: https://doi.org/10.1371/journal.pone.0252365.s012

Chapter II: Discussion

While the presence of infection specific degradation products of *Fg*-sRNA target genes, the infection specific repression and derepression in the absence of functioning FgDCLs shows the presence of ckRNAi during the pathogenesis of *Fg* a proof for its biological significance is lacking.

The disruption of DCL-function in several systems could show a dependence of *Fg* infection on *DCL*s, but due to the many possible functions of RNAi in endogenous processes in *Fg* this alone does not provide a proof for a significant role of ckRNAi for pathogenesis.

Methods to address this in other pathosystems were the expression of specific fungal sRNAs in planta (Wang et al. 2017a), or the postulated usage of so called “miRNA sponges” (Kluiver et al. 2012). While being less obstructive in general these methods still remain prone to criticism, the first for its strong expression and the second for its potential off-target effects. These trans genic based approaches also focus on a single sRNA and fail to account for the many potential sRNAs involved in cross-kingdom communication.

Chapter III: The impact on codon-usage emphasizes the biological significance and points to the double-edged nature of cross-kingdom RNAi

Chapter III: Introduction

As priorly described, the methods used to establish the presence of ckRNAi fail to show clear proof for its biological significance. To address this problem described as the fourth (iv) research question a look at the codon-usage in RNAi targeted regions could reveal a selective pressure of sRNAs on the host plant.

This pressure would be conclusive proof for the biological significance of RNAi and could also indicate the role and contribution of specific sRNAs.

In a recent publication (Dunker et al. 2020) a publically available dataset of sRNAs associated with *At*AGO1 during the infection with *Hyaloperonospora arabidopsidis* was generated. This data shows the clear presence of pathogen derived sRNAs within the plant cell and enables the search for changes in codon usage for sRNAs actually associated with ckRNAi and also enables working on a well-researched model species.

The impact on codon-usage emphasizes the biological significance and points to the double-edged nature of cross-kingdom RNAi

Bernhard T. Werner*[1], Annette Kopp-Schneider[2] and Karl-Heinz Kogel[1]

Institute of Phytopathology, Centre for BioSystems, Land Use and Nutrition, Justus Liebig University, Heinrich-Buff-Ring 26-32, D-35392, Giessen, Germany[1]

Division of Biostatistics, German Cancer Research Center, Im Neuenheimer Feld 280, D-69120, Heidelberg, Germany[2]

Email addresses

Bernhard.T.Werner@online.de

kopp@dkfz-heidelberg.de

Karl-Heinz.Kogel@agrar.uni-giessen.de

*Corresponding author

Abstract

Cross-kingdom (ck)RNAi describes the phenomenon in host-pathogen systems in which small (s)RNAs are exchanged to silence corresponding target genes associated with defence function in the host and virulence function in the pathogen, respectively. We hypothesised that a consequence of the ckRNAi model should be that target regions of sRNA-targeted plant genes have a bias in codon use to avoid recognition. *Hyaloperonospora arabidopsidis* (Ha) and *Fusarium graminearum* (Fg) are examples of plant pathogens that use sRNAs as effector molecules to silence specific genes in their respective host plants *Arabidopsis thaliana* (At) and *Hordeum vulgare* (Hv). We calculated the probability (P_{CHS}) that synonymous host plant codons in a predicted sRNA target region would show the same or stronger complementarity as actually observed and compared this probability to the probability of sets of virtual analogous sRNAs. To test our hypothesis, we first calculated this probability for a set of Arabidopsis micro (mi)RNAs that have an endogenous target in the plant. There was significantly different codon usage in the target regions of these miRNAs (P_{CHS} 36.5% higher than in the virtual sets). Also for the sets of Ha (P_{CHS} 24.9% lower than in the virtual sets) and Fg (P_{CHS} 19.3% lower than in the virtual sets) sRNAs, there was a significant difference in codon usage in their target regions in plant genes, but unexpectedly for both sets of microbial sRNA we found a tendency towards codons with an unexpectedly high complementarity. This bias in host plants suggests an evolutionary pressure to facilitate silencing by exogenous microbial sRNAs, which is not consistent with the anticipated biological role of pathogen sRNAs as effectors in cross-kingdom RNAi. To resolve this conflict, we propose an extended model in which microbial sRNAs are perceived by plants via RNA interference and, via coevolution, primarily help to fine-tune plant gene expression.

Summary

While the standard genetic code is used nearly universally among eukaryotic organisms, the usage of synonymous codons differs greatly. Different forces such as differences in translational efficiency and mutation bias influence the usage of synonymous codons, which leads to the establishment of an equilibrium state of the codon usage bias in each species. We hypothesised that a consequence of the ckRNAi model should be that target regions of sRNA-targeted plant genes have a bias in codon use to avoid recognition. To this end, we analysed codon usage bias in gene regions of *Arabidopsis thaliana* (At) predicted to be targeted by either endogenous miRNAs or a set of infection-related AtAGO-bound sRNAs of the oomycete pathogen *Hyaloperonospora arabidopsidis* (Ha). To this end, we calculated the probability P_{CHS} of a codon in a predicted miRNA or sRNA target region to have the same or stronger complementarity with the respective RNA under the assumption i. the amino acid (aa) sequence of each gene is conserved and ii. the codon usage is consistent over all genes. To account for the codon usage bias introduced by the target prediction algorithm we generated virtual random sets of sRNAs of the same size and following the same base compositions as the actual sRNA set (rsRNAs). As a negative control we applied the same methodology to a set of *Gorilla gorilla* (Gg) miRNA target regions in At. We found that At-miRNAs and Ha-sRNAs show a significantly different codon usage in target regions of both endogenous miRNAs and cross-kingdom-associated sRNAs, while no change in codon usage was detected in target calculated regions for miRNAs of Gg, strongly supporting our hypothesis. Unexpectedly, however, the codon usage in Ha-sRNAs target regions is biased towards codons with an unexpectedly high complementarity to the pathogen sRNAs. We extended our analysis to the agronomically important crop plant – microbe system of *Fusarium graminearum* (Fg) and barley (*Hordeum vulgare*, Hv). For Fg-sRNA, like for Ha-sRNAs, we found a codon bias in predicted Hv target regions of Fg-sRNA in barley towards codons with an unexpectedly high complementarity to the pathogen sRNAs. This bias in host plants suggests an evolutionary pressure to facilitate silencing by exogenous RNAs which challenges the conjectured role of pathogen sRNAs as primarily effector-like. To resolve this contradiction, we propose an extended model, in which microbial sRNAs are perceived by plants via RNA interference, and predominately aid in the fine tuning of plant gene expression, while the role of sRNAs as effector is an exception.

Main Body

Cross-kingdom RNA interference (ckRNAi) is a process in which small RNAs (sRNAs) are transferred from one organism to one from a different kingdom of life, where they cause gene silencing of complementary genes in the receiving organism (Baulcombe 2013). In the field of plant – microbe interactions, ckRNAi first came into focus through work by Hailing Jin's group, Riverside. In a game changing work, they showed that the ascomycete fungal pathogen *Botrytis cinerea* (Bc) delivers 21 nucleotide (nt) sRNAs into its host plants *Arabidopsis thaliana* (At) and tomato (Weiberg et al. 2013; Wang et al. 2017b). Fungal sRNAs were shown to operate as RNA effector molecules that interfere with and silence plant defense genes such as mitogen-activated protein kinases *MPK1* and *MPK2*. This added another mosaic to our understanding of plant - pathogen interactions, as in the past effectors have typically been defined as mostly smaller, microbe-derived proteins that interfere with components of the plant immune system (He et al. 2020). According to the new understanding, sRNAs, like protein effectors, are the product of an evolutionary arms race between host and microbe (Jones and Dangl 2006).

In 2016, Hui-Shan Guo's group also demonstrated the transfer of plant sRNAs into interacting fungi: cotton plants export micro (mi)RNAs into the pathogenic ascomycete fungus *Verticillium dahliae*, and some of these miRNAs target fungal virulence genes (Zhang et al. 2016). Further work has shown that this exchange takes place via extracellular vesicles, which, in addition to other cellular components, also carry sRNAs as cargo (Cai et al. 2018a; Rutter and Innes 2018; Cai et al. 2021). Proof in principle of the transfer of sRNA from the host plant to the fungus has already been provided in 2010 by the discovery of the process of host-induced gene silencing (HIGS; Nowara et al. 2010). The latter authors showed that transgenic barley plants producing double-stranded (ds)RNA export corresponding sRNAs into the powdery mildew fungus, where they subsequently silence target genes. Many reports have confirmed that HIGS can mediate strong resistance against target organisms including fungi, oomycetes and insects thereby demonstrating the great agronomic potential of artificial sRNAs (Knip et al. 2014; Cai et al. 2018b; Liu et al. 2020; Šečić and Kogel 2021).

In recent years many more sRNA effectors have been discovered in plant pathogenic fungi (Wang et al. 2017a; Dubey et al. 2019; Werner et al. 2021), oomycetes (Dunker et al. 2020), beneficial fungal endophytes (Šečić et al. 2021), and bacteria (Ren et al. 2019). Their importance as effectors is often experimentally supported by knock-out (KO) of *Dicer-like* (*DCLs*) genes in

the microbe and/or *Argonaute* (*AGO*) genes in the host, as loss-of-function mutations correspondingly impair either the microbe's ability to produce sRNAs or the host's ability to recognize silencing signals (Weiberg et al. 2013; Cai et al. 2021), while arguably DCLs and AGOs play important roles in virulence and immunity both in plants (Fang et al. 2016) and fungi (Nicolás et al. 2013, Gaffar et al. 2019), independent of ckRNAi. Further experimental evidence for specific fungal sRNA effectors can be provided by detecting corresponding degraded target host mRNAs fragments using degradome sequencing, also referred to as parallel analysis of RNA ends (PARE, German et al. 2008), and/or through recording their effect on pathogenicity upon artificial overexpression in the host (Weiberg et al. 2013). An elegant strategy to detect ckRNAi is the introduction of short tandem target mimics (STTM) that provides RNA target sequences such that an exogenous sRNA rather forms a complex with the mimic and is degraded than with AGO, thus preventing the silencing activity of the fungal sRNA effector (Yan et al. 2012; Zhang et al. 2016; Dunker et al. 2020). The latter authors examined *At*AGO1-linked sRNAs of the oomycete pathogen *Hyaloperonospora arabidopsidis* (Ha) after infection of Arabidopsis. Three of these sRNAs were confirmed as enhancing the pathogenicity of the oomycete by employing the STTM technique (Dunker et al. 2020). Above all, these recent discoveries have one key aspect in common: Plants and microbes can take up exogenous dsRNA. This is at the first glance puzzling because as shown by the above examples uptake of dsRNA can have detrimental effects on the survival of the receiving organism.

Based on the current knowledge about HIGS and ckRNAi, we speculated that in ckRNAi during evolutionary arms race between a plant and a pathogen plants could acquire synonymous mutations to abolish silencing with a relatively low fitness cost. Such an assumed evolutionary strategy was mimicked and shown to be feasible by Dunker et al. (2020), demonstrating that sRNA-resistant versions of plant targeted genes, when generated by artificially introducing synonymous mutations, rendered host plants more resistant to Ha. Synonymous mutations occur due to the degenerative nature of the genetic code which enables organisms to encode the 20 possible amino acids (aa) with 64 three base long codons in mRNA (Crick et al. 1961). Even if these codons code for the same aa, there is an evolutionary cost attached to it and therefore these synonymous mutations are often non-silent. For example, At and other organisms prefer certain codons over others, especially in highly expressed genes, due in part to differences in translational efficiency, ultimately leading to a codon bias (Duret & Mouchiroud 1999).

Avoiding the formation of sRNA-mRNA complexes and gene silencing of defence genes is an advantage for the plant in ckRNAi systems. We hypothesised that codon usage in target regions of sRNA effectors should differ from other coding regions in a plant genome if ckRNAi is evolutionarily significant. To reveal the difference in codon usage between sRNA target and non-target regions, we compared the observed bias in codon usage of sRNA complementary regions, which is predicted by the target prediction algorithm TAPIR (Bonnet et al. 2010), with the bias created by natural selection in response to ckRNAi. To achieve this, we compared the codon usage of published sets of At-miRNAs or microbial sRNAs from Ha and the plant pathogenic ascomycete *Fusarium graminearum*, respectively, to virtual sets of sRNAs (random (r)sRNAs). These rsRNAs were generated randomly by using the relative abundance of nucleotides (nts) in the respective published RNA set, to generate analogous sRNAs with the same length, size (Tab. S1 & S2) and base composition (Tab. S3) as the respective set of miRNAs or microbial sRNAs. Figure S1 gives an overview of our workflow.

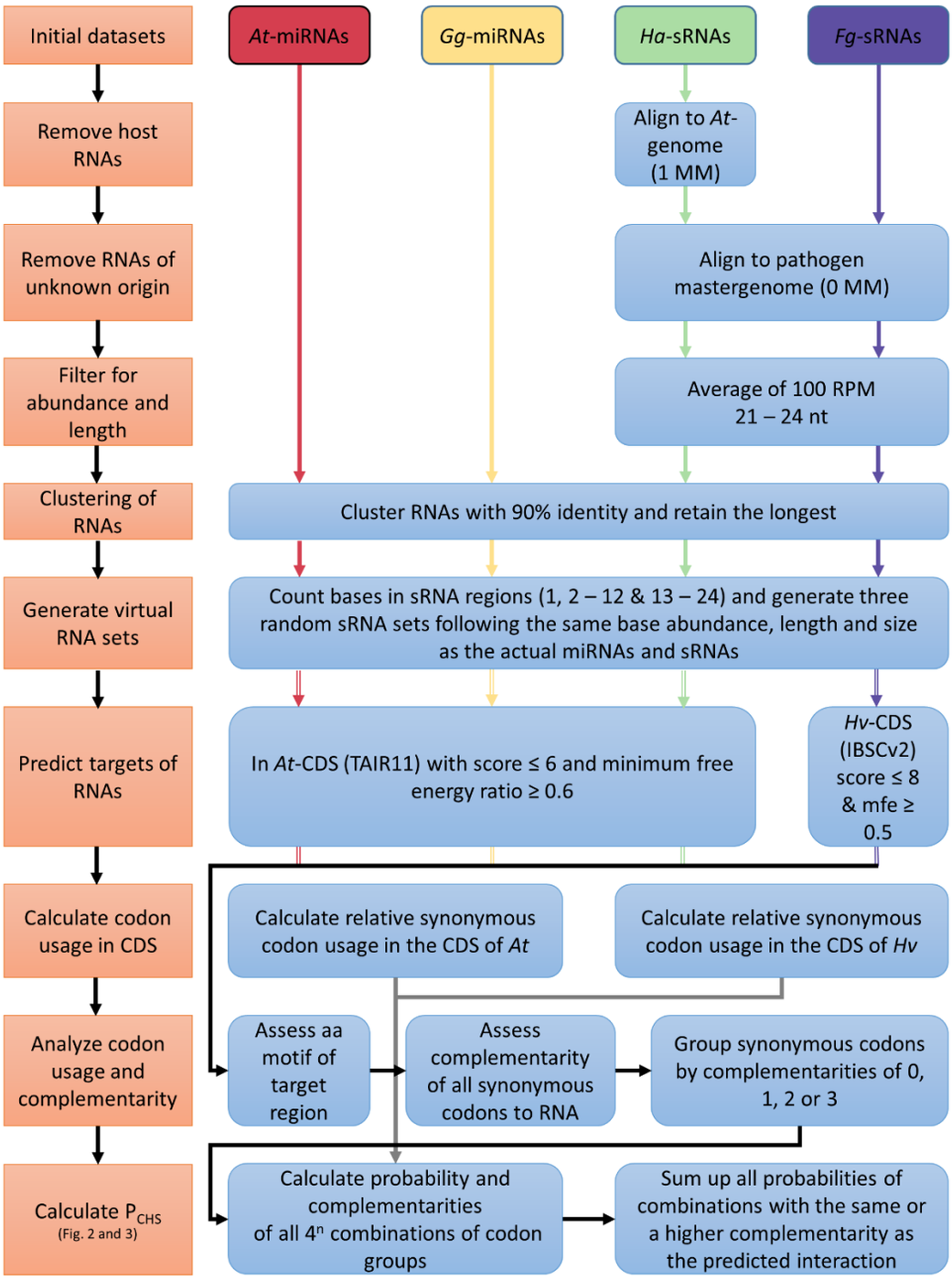

Figure S1: Workflow of the computational analysis of codon usage in RNAi targeted mRNA regions.

The left column (orange) gives an overview of the overall workflow. More detailed steps are depicted in blue. The colored arrows (red: At, *Arabidopsis thaliana*; yellow: Gg, *Gorilla gorilla*; green: Ha, *Hyaloperonospora arabidopsidis*; purple: Fg, *Fusarium graminearum*) indicate each set of small RNAs by organism of origin and visualize the detailed steps applied to each set, while black and gray arrows apply to all sets. In 4^n, n refers to the number of codons covered fully or partially by the respective sRNA, which leads to a maximum of 4^9 combinations for each interaction, in the case of a not in frame 24 nt long sRNA covering 7 codons completely and 2 partly. For further details, please refer to the supplementary methods.

For comparing the codon usage in the target regions of sRNAs and rsRNAs we calculated the probability P_{CHS} of each sRNA's and rsRNA's interaction with a coding sequence (CDS) having the same or a higher complementarity, under the assumptions that i. the aa sequence is conserved and ii. synonymous codons are chosen randomly, following the overall codon usage of the CDS of the host organism (Tab. S4 & S5). The procedure is pictured for At-miRNA400 as an example (Fig. 1). At-miRNA400 targets several pentatricopeptide repeat (PPR) proteins and is involved in biotic stress responses (Park et al. 2014). In Figure 1A the alignment of At-miRNA400 and two *PPR* genes is shown. The miRNA is perfectly complementary to *PPR1* (AT1G06580), while there are four mismatches (MM) to its homolog *T8K14.4* (AT1G79540). Remarkably, the underlying aa sequence of both PPRs is identical in the miRNA target site VTYNTLI.

The relative abundance for all synonymous codons for this aa motif is shown in Figure 1B, with the nts complementary to At-miRNA400 marked in bold. This data enables the calculation of the probability of different number of target site nts being complementary to the miRNA under assumptions i & ii (Fig.1C) using the distribution of synonymous codons given in Fig.1B. For instance, the respective value for the 21 nts target site being fully complementary to At-miRNA400 is p = 0.25·0.35·0.54·0.54·0.35·0.16·0.26 = 0.0004, and the respective value for 17 nts is p = 0.2236, summing all probabilities for combining 4 MM in the 21 positions. To predict an interaction between sRNA and mRNA leading to silencing the TAPIR algorithm (Bonnet et al. 2010) applies a target score cutoff. This score is calculated by increasing the score for each mismatch by 1 and for each G-U alignment by 0.5 with doubled values in the seed region (nt 2-12). The four MM with one MM in the seed region between At-miRNA400 and *T8K14.4* lead to a target score of 5 which is above the typical threshold (target score ≤ 4) for silencing to occur in At (Bonnet et al. 2010). The probability (P_{CHS}) for the same or a higher complementarity between miRNA400 is 0.0004 for *PPR1* and $\sum_{k=17}^{21} P(k) = 0.3686$ for *T8K14.4*. These P_{CHS} are consistent with the view that some PPR proteins being silenced during the expression of At-miRNA400 are beneficial for At, while the silencing of other PPR's would be detrimental, and that for the beneficial case synonymous mutations were positively selected to enable this selective silencing of proteins carrying the same motif.

A

```
AT1G06580 (PPR1)        5' GUGACUUAUAAUACUCUCAUA 3'
                           |||||||||||||||||||||
At-miR400               3' CACUGAAUAUUAUGAGAGUAU 5'
                           ||.||||||.||.|||||||||.
AT1G79540 (T8K14.4)     5' GUCACUUACAACACUCUCAUC 3'
```

B

Val	Thr	Tyr	Asn	Thr	Leu	Ile
GUA	**AC**A	**UA**C	**AA**C	**AC**A	**CU**A	**AUA**
0.16	0.33	0.46	0.46	0.33	0.11	0.26
GUC	**AC**C	**UAU**	**AAU**	**AC**C	**CUC**	**AU**C
0.18	0.19	0.54	0.54	0.19	0.16	0.33
GUG	**AC**G			**AC**G	**CU**G	**AU**U
0.25	0.14			0.14	0.11	0.42
GUU	**ACU**			**ACU**	**CU**U	
0.41	0.35			0.35	0.26	
					U**U**A	
					0.14	
					U**U**G	
					0.23	

C

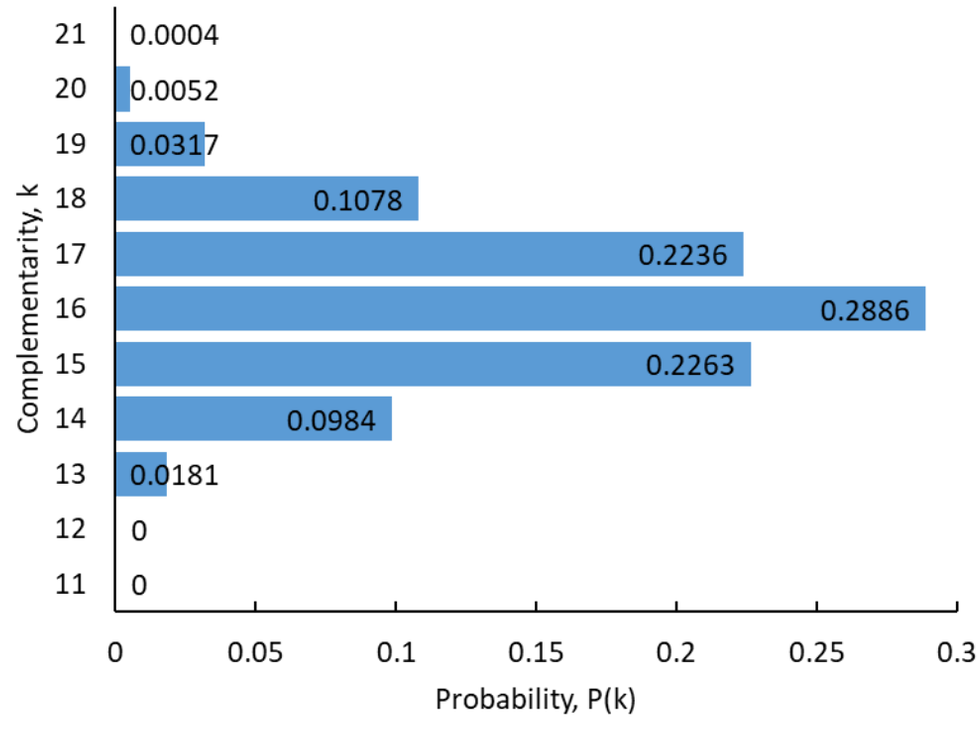

Figure 1: Exemplary calculation of the probability of a given complementarity between At-miRNA400 and the aa motif VTYNTLI present in PPR1 (AT1G06580) and T8K14.4 (AT1G79540).

A: The alignment of AT1G06580 and AT1G79540 to At-miRNA400 is shown, with MM annotated as "." and complementary bases as "|". B: The distribution of synonymous codons for the aa present in the aa motif VTYNTLI in the At-CDS. Bases complementary to the miRNA in the respective position are marked in bold. C: By calculating the probability of all combinations of codons and the respective number of complementary bases the total probability for each number of complementary bases is shown.

While this selection can be obvious in the case of PPR proteins, other genes with less family members should still be subject to the same kind of selective pressure where either silencing is beneficial or detrimental in the absence of another protein with an identical aa motif present in the genome. This pressure would persist until mutations lead to the abolishment of silencing. To establish a baseline probability, we predicted via TAPIR (Bonnet et al. 2010) all possible interactions and interactions one seed MM above the default threshold (target score ≤ 6) (Tab. S6) of all known At-miRNAs from miRBase (Griffiths-Jones et al. 2006) and a set of rsRNAs with the same size and nt abundances as the published At-miRNAs and calculated the P_{CHS} for all interactions in R. We repeated the simulation experiment three times for three different sets of rsRNAs (Fig. 2A). The P_{CHS} of the At-miRNAs is significantly higher than the P_{CHS} of the rsRNA sets (estimated ratio of P_{CHS} and [95%-CI]: 1.204 [1.12, 1.295]; 1.112 [1.035, 1.194]; 1.226 [1.14, 1.319]). This could be the consequence of an adaptation of miRNAs to target-specific motifs consisting of the most common codons. Interestingly however, some interactions of the At-miRNAs have a very low P_{CHS}, suggesting a change in codon usage to enable silencing as shown for the At-miRNA400 - *PPR1* interaction. To further substantiate our calculation, we repeated this experiment three times for the total set of *Gorilla gorilla* (Gg) miRNAs as a negative control (Fig. 2B). Consistent with the obvious lack of biological significance for Gg-miRNAs in the At-genome we did not see significant differences in the P_{CHS} for any set (estimated ratio of P_{CHS} and [95%-CI]: 1.034 [0.948, 1.127]; 1.058 [0.974, 1.15]; 1.039 [0.954, 1.131]).

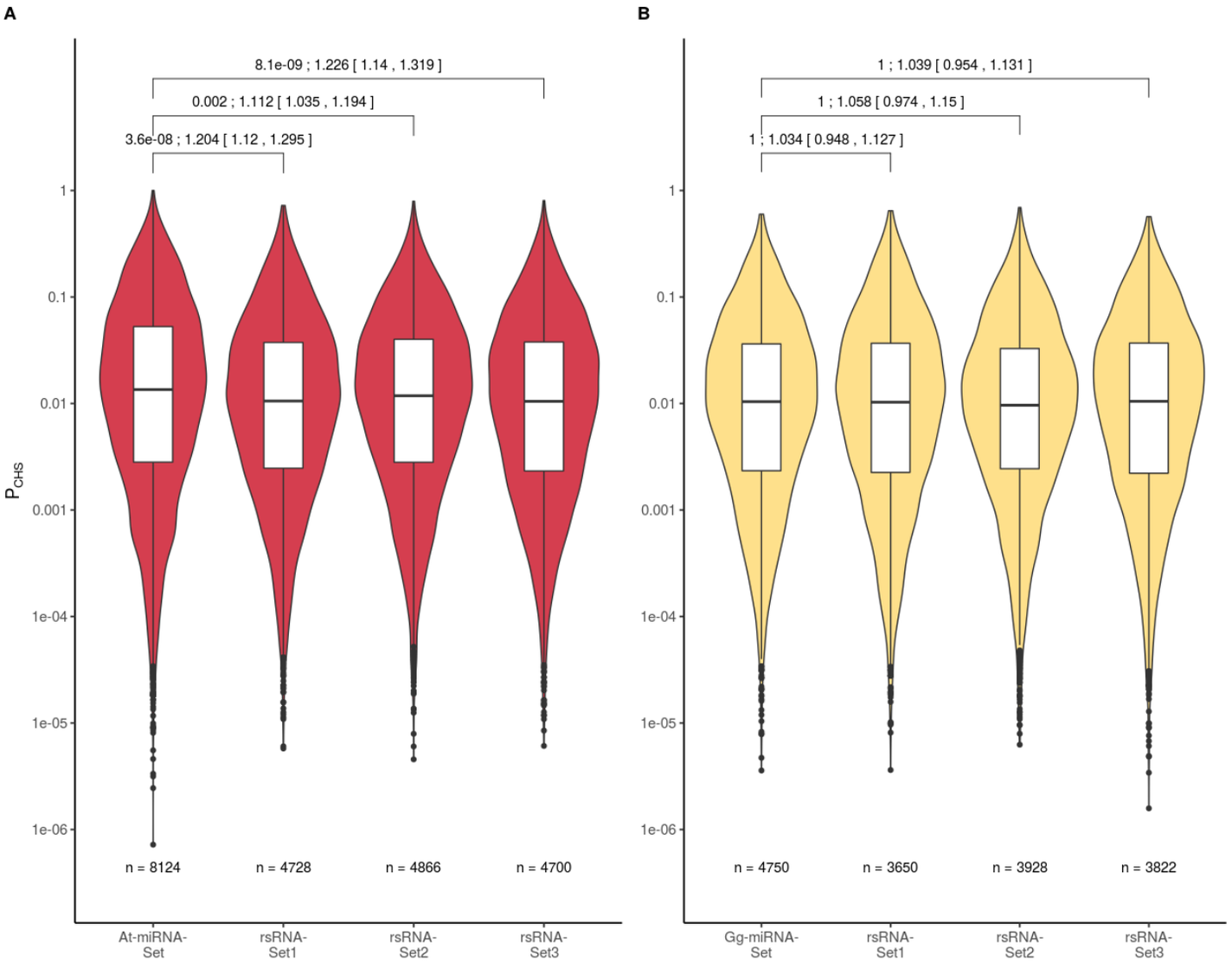

Figure 2: Calculated P_{CHS} values for the predicted mRNA-sRNA interactions in the At-CDS by At- and Gg-miRNAs.

The violin plots with internal boxplots show the distribution of P_{CHS} values of the computationally predicted mRNA-sRNA interactions. The P_{CHS} is the probability of a random selection of synonymous codons based on the relative frequency of codons in the At-CDS to have the same complementarity or a higher complementarity as the actual complementarity. The values are shown for different sRNA sets taken from miRBase, A: At-miRNAs; B: Gg-miRNAs as a negative control, and three analogous random sets of sRNAs (rsRNA-sets, see methods). p-values were calculated with a Kruskal-Wallis test adjusted for multiple testing after Benjamini & Yekutieli (2001). Only p values for comparisons between published and rsRNA sets are shown. There were no significant differences between individual rsRNA-sets. To achieve normality, P_{CHS} values were $\log_{10}$-transformed. The 95% confidence interval (95%-CI) for the difference of mean $\log_{10}(P_{CHS})$ was calculated via a two-sample Welch t-test and subsequently retransformed and is shown as relative difference to the respective rsRNA-set. n refers to the total number of predicted

interactions. The results of the statistical tests are shown as: p-value; arithmetic mean [upper and lower bounds of 95%-CI]

In a next step, we applied the same methodology established for At-miRNA to the microbial Ha-sRNA set provided by Dunker et al. (2020). We analyzed all sRNAs with at least an average of 100 reads per million in the published datasets (Fig. 3A & Tab. S1). In all three repetitions, the median P_{CHS} was lower for the Ha-sRNAs compared to the respective rsRNA-sets, showing that target sites in the At-genome for Ha-sRNAs, like At-miRNAs, evolved a significantly different codon usage, supporting our hypothesis. Unexpectedly, however, the codon usage in Ha-sRNAs target regions was biased towards codons with a surprisingly high complementarity to the pathogen sRNAs, reflected in a lower P_{CHS} (estimated ratio of P_{CHS} and [95%-CI]: 0.62 [0.472, 0.814]; 0.758 [0.576, 0.998]; 0.595 [0.447, 0.793]). Next, we analyzed a published sRNA dataset from *Fusarium graminearum* (Werner et al. 2021) in combination with the CDS from its host plant barley (*Hordeum vulgare*). Fg is an important plant pathogen with identified sRNA-effectors (Werner et al. 2021; Jian & Liang 2019). Again, we found that the Fg-sRNAs targeted regions were composed of codons with an unlikely high complementarity to the respective sRNA, compared to the rsRNAs (estimated ratio of P_{CHS} and [95%-CI]: 0.711 [0.639, 0.791]; 0.732 [0.66, 0.813]; 0.801 [0.721, 0.89]) (Fig. 3B). This bias in host plants suggests an evolutionary pressure to facilitate silencing by exogenous RNAs, which challenges the conjectured role of pathogen sRNAs as primarily effector-like. To resolve this contradiction, we propose an extended model, in which microbial sRNAs are perceived by plants via RNA interference, and predominately aid in the fine-tuning of plant gene expression, while the role of sRNAs as effector is an exception.

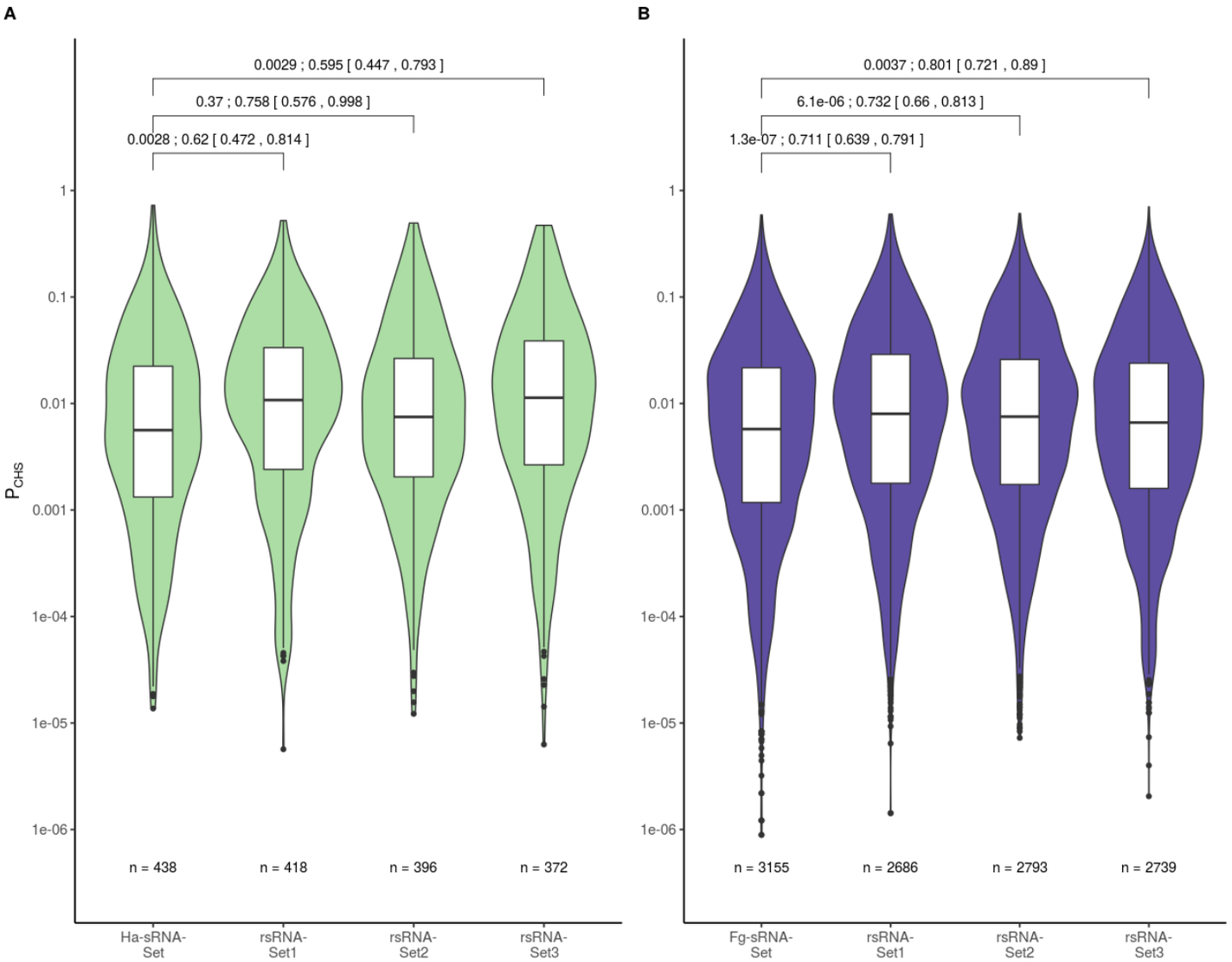

Figure 3: Calculated P_{CHS} values for the predicted mRNA-sRNA interactions in the At-CDS with Ha-sRNAs and barley-CDS with Fg-sRNAs.

The violin plots with internal boxplots show the distribution of P_{CHS} values of the computationally predicted mRNA-sRNA interactions. The P_{CHS} is the probability of a random selection of synonymous codons based on the relative frequency of codons in the At- or Hv-CDS to have the same complementarity or a higher complementarity as the actual complementarity. The values are shown for sRNA-sets from two organisms A: Ha-sRNAs from an At-AGO1 co-IP experiment (Dunker et al. 2020) and B: Fg-sRNAs from axenic culture (Werner et al. 2021) and three virtual analogous random sets of sRNAs (rsRNA-sets). p-values were calculated with a Kruskal-Wallis test adjusted for multiple testing after Benjamini & Yekutieli (2001). Only p values for comparisons between published and rsRNA sets are shown. There were no significant differences between individual rsRNA-sets. To achieve normality, P_{CHS} values were $\log_{10}$-transformed. The 95% confidence interval (95%-CI) for the difference of mean $\log_{10}(P_{CHS})$ was calculated via a two-sample Welch t-test and subsequently retransformed and is shown as relative difference to the

respective rsRNA-set. n refers to the total number of predicted interactions. The results of the statistical tests are shown as: p-value; arithmetic mean [upper and lower bounds of 95%-CI]

Since P_{CHS} ($=\sum_k^n P(k)$) is increasing monotonously with decreasing complementarity k, i.e. with increasing number of mismatches between sRNA and mRNA, we wanted to exclude the possibility that an evolution of pathogen sRNAs leads to a lower number of mismatches between sRNA and target causing the observed lower P_{CHS} for interactions of pathogen sRNAs in contrast to rsRNAs. Therefore, we restricted the focus exclusively on interactions with the best fitting mRNA codons to the respective sRNA, i.e. for complementarity k such that $P(k) > 0$ but $P(l) = 0$ for $l > k$. In this restricted subset the same trends as for the whole set persist, yet only significant for At-miRNAs, most likely due to the lower number of interactions in this reduced set (Fig. S2).

Unlike interaction prediction methods of protein effectors (Rao et al. 2014), the interactions of sRNA effectors with host genes can be predicted with less effort and higher reliability (Srivastava et al. 2014). In combination with the analysis of codon usage this untapped potential reveals a coevolution within the hosts CDS. There is no reason why this co-evolution could not also take place outside the CDS, and our results therefore only give an incomplete picture.

Thus, according to current understanding, the natural occurrence of ckRNAi is harmful to the ingesting organism, but many organisms nevertheless ingest free exogenous dsRNA species (Qiang et al. 2021; Šečić and Kogel 2021). To solve these apparent conflicts, we propose an extended ckRNAi model in which organisms gather information about the microbiome of their habitat by taking up RNA from their environment to adapt to the microbial environment, which mechanistically occurs via the RNAi pathway. This mechanism would benefit an organism by fine-tuning gene expression according to the presence of specific groups of pathogens, symbionts or commensalists. The extended model is not inconsistent with the current notion that certain pathogens "highjack" this mechanism (Weiberg et al. 2013), by delivering sRNA effectors. However, according to the extended model, this parasitic role of sRNAs is the exception and the uptake of environmental RNAs in general benefits organisms by providing a tool of microbiome perception.

Acknowledgments

This work was funded in the cooperative program of the Deutsche Forschungsgemeinschaft (DFG) FOR5116 to KHK.

Competing financial interests

The authors declare no competing financial interests.

Supplementary Methods

sRNA-Dataset selection

Sequences for At-miRNAs and Gg-miRNAs were obtained from miRBase release 22.1 (miRBase.org; Kozomara et al. 2019). The whole dataset of miRNAs was read with the R package SeqinR v.3.6-1 (Charif & Lobry 2007) in the RStudio environment v.1.1.463 (RStudio Team 2020). Sequence names of miRNAs were selected with the R Base v.3.6.3 (R Core Team 2021) grep function and written to a different file for each organism.

For Ha-sRNAs the AtAGO1-co-IP datasets generated by Dunker et al. (2020) (SRR11810702, SRR5852210) were downloaded from the NCBI SRA with the sra toolkit function fastq-dump v.2.8.2 (Sherry et al. 2012) using the system2 package. Details for the Fg-sRNAs dataset from axenic culture are published in Werner et al. (2021).

Filtering of sRNAs

The Ha co-IP sequencing runs were treated similarly as described by Dunker et al. (2020). After downloading the already trimmed runs with fastq-dump the runs were transcribed to fasta with fastq_to_fasta and collapsed using the fastx_collapser from the fastx toolkit v0.0.14 (Gordon & Hannon 2010). The collapsed reads were first aligned to the At-TAIR10 (GCA_000001735) genome release (Lamesch et al. 2012) with the bowtie aligner v.1.2.1.1 (Langmead et al. 2009) with one allowed mismatch. Fg-sRNAs were not filtered to a plant genome due to their origin from axenic culture. Reads which did not align were kept and aligned to a Ha-mastergenome which consisted of the assemblies of the Ha-strains Emoy2, Cala2 and Noks1 (GCA_000173235.2, GCA_001414265.1, GCA_001414525.1) or the Fg-mastergenome which consisted of all 110 Fg genome assemblies from the NCBI database (see Table S7) and only perfect matches were kept. Remaining reads were further filtered with SeqinR and R Base for reads with at least a total sum of reads in both co-IP datasets of 200 a length between 21 and 24 nt and at least 1 RPM (reads per million) in each dataset for Ha, or 100 RPM for Fg.

sRNA clustering and generation of analogous random sRNA sets

sRNA-datasets were clustered with the CD-HIT v.4.8.1 (Fu et al. 2012) function cd-hit-est with a similarity threshold of 90%. The nucleotide frequency of clustered reads for position 1 (5'->3'), position 2-12 and the remaining nucleotides was calculated. These frequencies were used to generate three sets of analogous random sRNAs (rsRNAs) with the same number of sequences,

the same frequency of nucleotides for each section and the same length distribution using SeqinR, the package stringr v.1.4.0 and the sample function from R Base with the relative frequencies as probabilities.

Preparation of At and barley coding sequences and calculation of codon usage indices

The CDS of the Araport11 annotation (Cheng et al. 2017) and *Hordeum vulgare IBSC PGSB v2* reference genome annotation (Mascher et al. 2017) were filtered and only CDS staring with a start codon (ATG) and ending with a stop codon (TAG, TAA, TGA) were retained. Additionally, sequences were filtered for a length of a multiple of three nt's using the function is.whole from the package sfsmisc v.1.1-7. Codon usage was calculated for the filtered sequences with the function uco from the SeqinR package.

Target prediction

For each set of sRNAs and its respective sets of analogous random sRNAs a target prediction was conducted with the TAPIR algorithm v.1.1 with a score cut-off of 6 (default=4) and a mfe-ratio of 0.6 (default=0.7) for At and a score cut-off of 8 and a mfe-ratio of 0.5 for barley according to the optimized parameters suggested by Srivastava et al. (2014) to obtain predicted likely interactions and those one mutation outside the default parameters.

P_{CHS} calculation

Target prediction results were read and saved to a R data frame and duplicated target regions of a specific sRNA in the same gene were removed with the duplicated function. The in frame CDS from the first sRNA overlapping codon was saved as a vector. The sRNA sequence was also saved in 3'-5' direction in a character vector. Bulges in the mRNA or sRNA were accounted for by either removing the sRNA base overlapping the bulge in the sRNA sequence or by adding an unmatching character in the sRNA sequence for a bulge in the mRNA. After this preparation for each codon in the mRNA all synonymous codons were analyzed for their complementarity to the sRNA sequence with SeqinR and base functions and the probability of codons with 0, 1, 2 or 3 complementary bases to the sRNA were calculated based on the codon frequency calculated before. All possible 4 to the power of overlapping codons permutations were written to a data frame with the expand.grid function and the row sums were saved as a vector. The prior calculated probabilities of complementarities were used to replace the values in the permutations data frame and the prod function was applied to each row with the apply

function giving the probabilities to each row sum of complementarities. The sum of probabilities for each row sum with i. the same complementarity as the actual interaction and ii. a higher complementarity were added to the data frame containing the target prediction results. The probabilities i. and ii. were added to calculate the P_{CHS} for each interaction. P_{CHS} values were plotted on $\log_{10}$-scale with the package ggplot2 v.3.3.2 (Wickham 2016) and ggpubr v.0.4.0 (Kassambara 2020). P-values were calculated via a Kruskal-Wallis test and adjusted for multiple testing (Benjamini & Yekutieli 2001) with the function compare_means. To calculate the 95% confidence intervals (CIs) the function t.test was applied with default parameters (two.sided, var.equal=F, paired=F, conf.level=0.95) on the approximately normally distributed $\log_{10}(P_{CHS})$ values. These CIs were retransformed via 10^CI to obtain the relative difference between sRNA and rsRNA-sets.

Supplementary Figures

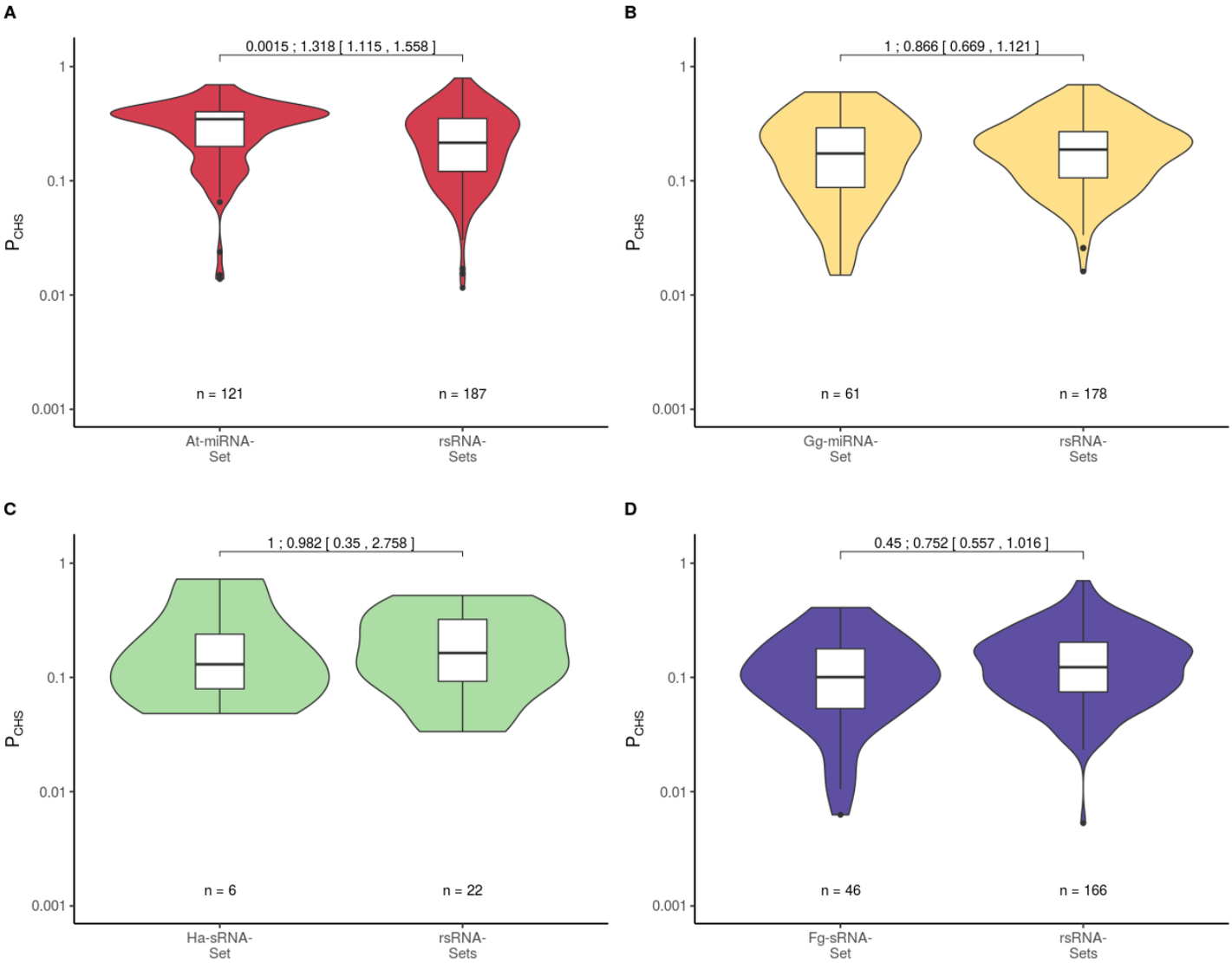

Figure S2: Calculated P_{CHS} values for the predicted mRNA-sRNA interactions with maximum complementarity.

The violin plots with internal boxplots show the distribution of P_{CHS} values of the computationally predicted mRNA-sRNA interactions with best fitting codons exclusively. The P_{CHS} is the probability of a random selection of synonymous codons based on the relative frequency of codons in the CDS to have the same complementarity or a higher complementarity as the actual complementarity. This figure shows a subset of interactions from Figures 2 and 3 that have the maximum number of complementary bases possible. The values are shown for small RNA-sets from four organisms A: At-miRNAs (miRBase), B: Gg-miRNAs (miRBase), C: Ha-sRNAs from an At-AGO1 co-IP experiment (Dunker et al. 2020) and D: Fg-sRNAs from axenic culture (Werner et al. 2021) and the respective virtual analogous random sets of sRNAs (rsRNA-sets). p-values were calculated with a Kruskal-Wallis test adjusted for

multiple testing after Benjamini & Yekutieli (2001). To achieve normality, P_{CHS} values were $\log_{10}$-transformed. The 95% confidence interval (95%-CI) for the difference of mean $\log_{10}(P_{CHS})$ was calculated via a two-sample Welch t-test and subsequently retransformed and is shown as relative difference to the respective rsRNA-set. n refers to the total number of predicted interactions. The results of the statistical tests are shown as: p-value; arithmetic mean [upper and lower bounds of 95%-CI]

Supplementary Tables

Tab. S1: Summary of sRNA datasets

This table gives the number of reads or sequences (total and unique) before and after each filtering step with the number of sequences kept for further analysis in bold.

	Name	At-miRNAs	Gg-miRNAs	Ha-sRNAs		Fg-sRNAs
				3 dpi	4 dpi	
	Source	miRBase	miRBase	NCBI SRA		NCBI SRA
				SRR5852210	SRR11810702	SRR15248620
Before filtering	Unique	38,589	38,589	7,572,861	2,341,954	568,558
	Total	-	-	132,130,456	51,089,216	5,425,987
Removal of plant-derived reads	Unique	-	-	1,610,177	1,254,381	
	Total	-	-	5,872,565	3,399,779	
Perfect matches to pathogen	Unique	-	-	13,580	258,387	139,910
	Total	-	-	22,790	381,200	4,340,933
Sequences for final analysis	Unique	**428**	**369**		**108**	**1,745**
	Total	-	-	1,142	1,157	3,029,961

Tab. S2: Summary of sRNA clustering

This table shows the number of sequences after the filtering (shown in Tab. S1) and the reduction of reads or sequences after clustering of similar RNAs.

RNA set	At-miRNAs	Gg-miRNAs	Ha-sRNAs	Fg-sRNAs
No of sequences	428	369	108	1,745
No of clusters	**335**	**351**	**66**	**457**
Mean cluster size	1.278	1.051	1.636	3.818

Tab. S3: Nucleotide composition of sRNA sets in different sections

This table gives the base composition in the clustered sRNA-sets used for the generation of the random analogous RNA-sets.

RNA set	At-miRNAs	Gg-miRNAs	Ha-sRNAs	Fg-sRNAs
1st nt				
A	24.8%	30.5%	30.3%	23.9%
C	9.3%	14.2%	21.2%	23.2%
G	10.7%	8.8%	22.7%	20.4%
U	55.2%	46.4%	25.8%	32.6%
Seed (2nd-12th nt)				
A	26.6%	26.1%	28.5%	24.1%
C	18.2%	23.0%	19.4%	21.1%
G	26.1%	26.6%	26.7%	29.2%
U	29.1%	24.3%	25.3%	25.6%
End (13th-last nt)				
A	27.3%	23.0%	24.0%	23.2%
C	19.4%	21.0%	18.9%	23.4%
G	24.2%	27.9%	30.5%	28.4%
U	29.1%	28.1%	26.7%	25.1%
Total				
A	26.8%	25.0%	26.5%	23.6%
C	18.3%	21.7%	19.2%	22.3%
G	24.5%	26.3%	28.3%	28.4%
U	30.3%	27.0%	26.0%	25.7%

Tab. S4: Occurrences and relative frequencies of synonymous codons in the Araport11 annotation

Amino Acid	Codon	Occurrences	Relative Frequency
Lysine	AAA	659,375	49.59%
	AAG	670,179	50.41%
Asparagine	AAC	418,657	45.77%
	AAT	496,098	54.23%
Threonine	ACA	342,305	32.50%
	ACC	199,360	18.93%
	ACG	147,692	14.02%
	ACT	363,987	34.56%
Arginine	AGA	408,475	36.28%
	AGG	231,221	20.53%
	CGA	131,881	11.71%
	CGC	76,766	6.82%
	CGG	100,347	8.91%
	CGT	177,310	15.75%
Serine	AGC	242,457	12.64%
	AGT	315,625	16.46%
	TCA	408,100	21.28%
	TCC	226,420	11.81%
	TCG	184,065	9.60%
	TCT	540,891	28.21%
Isoleucine	ATA	284,518	25.85%
	ATC	358,653	32.58%
	ATT	457,619	41.57%
Methionine	ATG	509,709	100.00%
Glutamine	CAA	420,938	56.37%
	CAG	325,843	43.63%
Histidine	CAC	173,590	36.58%
	CAT	300,965	63.42%
Proline	CCA	340,804	34.32%
	CCC	106,564	10.73%
	CCG	158,588	15.97%
	CCT	387,002	38.97%
Leucine	CTA	215,166	10.82%
	CTC	311,189	15.65%
	CTG	219,166	11.02%
	CTT	513,875	25.84%
	TTA	280,005	14.08%
	TTG	449,182	22.59%

Glutamic Acid	GAA	753,248	53.03%
	GAG	667,114	46.97%
Aspartic Acid	GAC	345,908	30.60%
	GAT	784,565	69.40%
Alanine	GCA	377,962	28.88%
	GCC	195,418	14.93%
	GCG	167,370	12.79%
	GCT	567,989	43.40%
Glycine	GGA	486,845	36.76%
	GGC	183,090	13.82%
	GGG	211,801	15.99%
	GGT	442,665	33.42%
Valine	GTA	220,305	15.96%
	GTC	248,294	17.99%
	GTG	349,466	25.32%
	GTT	562,053	40.72%
Stop codon	TAA	17,577	36.44%
	TAG	9,898	20.52%
	TGA	20,757	43.04%
Tyrosine	TAC	265,603	45.56%
	TAT	317,324	54.44%
Cysteine	TGC	153,423	40.25%
	TGT	227,727	59.75%
Tryptophan	TGG	254,759	100.00%
Phenylalanine	TTC	403,565	46.05%
	TTT	472,797	53.95%

Tab. S5: Occurrences and relative frequencies of synonymous codons in the barley IBSCv2 annotation

Amino Acid	Codon	Occurrences	Relative Frequency
Lysine	AAA	931,360	37.85%
	AAG	1,529,125	62.15%
Asparagine	AAC	886,774	49.86%
	AAT	891,820	50.14%
Threonine	ACA	692,223	30.38%
	ACC	607,873	26.68%
	ACG	392,499	17.23%
	ACT	585,985	25.72%
Arginine	AGA	577,809	21.47%
	AGG	704,744	26.19%
	CGA	235,490	8.75%
	CGC	443,708	16.49%
	CGG	413,389	15.36%
	CGT	315,934	11.74%
Serine	AGC	755,547	18.90%
	AGT	550,365	13.77%
	TCA	783,348	19.59%
	TCC	681,459	17.04%
	TCG	446,272	11.16%
	TCT	781,049	19.54%
Isoleucine	ATA	567,069	25.17%
	ATC	870,434	38.63%
	ATT	815,806	36.20%
Methionine	ATG	1,209,257	100.00%
Glutamine	CAA	716,645	41.25%
	CAG	1,020,702	58.75%
Histidine	CAC	549,041	46.03%
	CAT	643,733	53.97%
Proline	CCA	718,205	30.34%
	CCC	457,329	19.32%
	CCG	515,556	21.78%
	CCT	675,991	28.56%
Leucine	CTA	434,057	9.50%
	CTC	965,930	21.14%
	CTG	1,045,193	22.88%
	CTT	918,147	20.10%
	TTA	390,168	8.54%

	TTG	815,116	17.84%
Glutamic Acid	GAA	1,203,764	42.61%
	GAG	1,621,566	57.39%
Aspartic Acid	GAC	1,136,016	45.29%
	GAT	1,372,440	54.71%
Alanine	GCA	959,211	26.26%
	GCC	1,004,024	27.49%
	GCG	684,449	18.74%
	GCT	1,004,609	27.51%
Glycine	GGA	747,093	23.57%
	GGC	1,002,984	31.65%
	GGG	666,870	21.04%
	GGT	752,150	23.73%
Valine	GTA	417,867	13.49%
	GTC	777,749	25.11%
	GTG	1,004,162	32.42%
	GTT	897,389	28.97%
Stop codon	TAA	30,806	24.20%
	TAG	36,006	28.29%
	TGA	60,444	47.49%
Tyrosine	TAC	691,781	54.49%
	TAT	577,788	45.51%
Cysteine	TGC	540,108	59.38%
	TGT	369,471	40.62%
Tryptophan	TGG	593,276	100.00%
Phenylalanine	TTC	997,261	55.90%
	TTT	786,642	44.10%

Tab. S6: Summary of target prediction results

This table gives an overview of the target prediction results and the subsequent filtering with the last column giving the remaining interactions for statistics and plotting

Organism	RNA set	Interactions	sRNAs targeting	Targeted genes	Unique gene-sRNA interactions
At	actual	14,524	335	6,318	8,124
	analogous 1	8,936	333	4,195	4,728
	analogous 2	9,069	329	4,279	4,866
	analogous 3	8,586	333	4,156	4,700
Gg	actual	8,762	348	4,023	4,750
	analogous 1	6,767	338	3,323	3,650
	analogous 2	7,244	342	3,538	3,928
	analogous 3	6,980	339	3,450	3,822
Ha	actual	783	59	421	438
	analogous 1	739	57	410	418
	analogous 2	645	59	392	396
	analogous 3	701	54	366	372
Fg	actual	12,649	452	2,322	3,155
	analogous 1	11,183	447	2,458	2,686
	analogous 2	12,038	448	2,546	2,793
	analogous 3	11,676	449	2,476	2,739

Tab. S7: List of Fg-assembly's accessions used for alignment of Fg-reads

GCA_000240135.3
GCA_900044135.1
GCA_000599445.1
GCA_018346015.1
GCA_018346495.1
GCA_018345745.1
GCA_018345515.1
GCA_018219515.1
GCA_018346565.1
GCA_018346265.1
GCA_018346165.1
GCA_018346045.1
GCA_018219745.1
GCA_018345395.1
GCA_018346705.1
GCA_018345735.1
GCA_018346005.1
GCA_018346585.1
GCA_018346715.1
GCA_018346155.1
GCA_018345975.1
GCA_018346625.1
GCA_018345585.1
GCA_018346455.1
GCA_018346685.1
GCA_018346425.1
GCA_018345645.1
GCA_018345945.1
GCA_018345885.1
GCA_018345845.1
GCA_018345715.1
GCA_018346095.1
GCA_018346355.1
GCA_018346405.1
GCA_018346635.1
GCA_018346505.1
GCA_018346765.1
GCA_018345485.1
GCA_018346245.1
GCA_018346695.1
GCA_018345675.1
GCA_018346485.1
GCA_018346805.1
GCA_018219565.1
GCA_018345295.1
GCA_018346445.1
GCA_018345545.1
GCA_018345365.1
GCA_018346255.1
GCA_018345725.1
GCA_018346575.1
GCA_018345925.1
GCA_018219705.1
GCA_018345915.1
GCA_018346145.1
GCA_018345815.1
GCA_018346035.1
GCA_018346665.1
GCA_018346815.1
GCA_018219635.1
GCA_018346325.1
GCA_018346305.1
GCA_900492705.1
GCA_018219645.1
GCA_018219675.1
GCA_018345865.1
GCA_018345335.1
GCA_018346225.1
GCA_018219625.1
GCA_018346545.1
GCA_018345995.1
GCA_018346365.1
GCA_018346345.1
GCA_018219525.1
GCA_018345325.1
GCA_018345415.1
GCA_018345575.1
GCA_018219575.1
GCA_018345475.1
GCA_002352725.1
GCA_018345455.1
GCA_018345435.1
GCA_018345795.1
GCA_018345655.1
GCA_018345615.1
GCA_905359455.1
GCA_012959185.1
GCA_018346185.1
GCA_018219555.1
GCA_018219715.1
GCA_018219795.1
GCA_006942295.1
GCA_900476405.1
GCA_905359475.1
GCA_901446245.1
GCA_018346115.1
GCA_018345635.1
GCA_018219765.1
GCA_001717905.1
GCA_018219485.1
GCA_018219475.1
GCA_018345835.1
GCA_018219615.1
GCA_001717915.1
GCA_000966645.1
GCA_018346775.1
GCA_000966635.1
GCA_018346795.1
GCA_018345315.1
GCA_900073075.1

Chapter III: Discussion

The presented method as discussed above shows the significant impact of ckRNAi on the codon usage of At and Hv. Therefore, we can conclude that ckRNAi has a significant biological impact on pathogenesis. Furthermore, it shows the double-edged nature of ckRNAi by showing a change in codon usage facilitating silencing by Ha and Fg derived sRNA. This challenges the predominant assumption that ckRNAi has a purely effector-like role during pathogenesis.

This method provides a tool, if broadly applied, to disentangle the different roles of pathogen derived sRNAs and to identify the presence of RNA communication between different organisms.

References

Abeles, F. W. (1992). Roles and physiological effects of ethylene in plant physiology: dormancy, growth, and development. *Ethylene in plant biology*.

Adams, E., Leeb, C., Roodt, A. P., & Brühl, C. A. (2021). Interspecific sensitivity of European amphibians towards two pesticides and comparison to standard test species. *Environmental Sciences Europe*, *33*(1), 1-7.

Adhikari, S., Turner, M., & Subramanian, S. (2013). Hairpin priming is better suited than in vitro polyadenylation to generate cDNA for plant miRNA qPCR. *Molecular plant*, *6*(1), 229-231.

Ahmed, F., Senthil-Kumar, M., Dai, X., Ramu, V. S., Lee, S., Mysore, K. S., & Zhao, P. X. (2020). pssRNAit: A Web Server for Designing Effective and Specific Plant siRNAs with Genome-Wide Off-Target Assessment. *Plant Physiology*, *184*(1), 65-81.

Akond, Z., Rahman, H., Ahsan, M. A., Mosharaf, M. P., Alam, M., & Mollah, M. N. H. (2020). Bioinformatic analysis based genome-wide identification, characterization, diversification and regulatory transcription components of RNA silencing machinery genes in wheat (Triticum aestivum L.). *bioRxiv*.

Alexa, A., & Rahnenführer, J. (2009). Gene set enrichment analysis with topGO. *Bioconductor Improv*, *27*, 1-26.

Alonso, J. M., Hirayama, T., Roman, G., Nourizadeh, S., & Ecker, J. R. (1999). EIN2, a bifunctional transducer of ethylene and stress responses in Arabidopsis. *Science*, *284*(5423), 2148-2152.

Amarasinghe, C., Sharanowski, B., & Fernando, W. G. (2019). Molecular phylogenetic relationships, trichothecene chemotype diversity and aggressiveness of strains in a global collection of Fusarium graminearum species. *Toxins*, *11*(5), 263.

Anders, S., Pyl, P. T., & Huber, W. (2015). HTSeq—a Python framework to work with high-throughput sequencing data. *Bioinformatics*, *31*(2), 166-169.

Anderson, N. R., Freije, A. N., Bergstrom, G. C., Bradley, C. A., Cowger, C., Faske, T., ... & Wise, K. A. (2020). Sensitivity of Fusarium graminearum to metconazole and tebuconazole fungicides

before and after widespread use in wheat in the United States. *Plant Health Progress*, *21*(2), 85-90.

Appels, R., Eversole, K., Stein, N., Feuillet, C., Keller, B., Rogers, J., ... & Khurana, J. P. (2018). Shifting the limits in wheat research and breeding using a fully annotated reference genome. *Science*, *361*(6403).

Asha, S., & Soniya, E. V. (2016). Transfer RNA derived small RNAs targeting defense responsive genes are induced during Phytophthora capsici infection in black pepper (Piper nigrum L.). *Frontiers in plant science*, *7*, 767.

Åsman, A. K., Vetukuri, R. R., Jahan, S. N., Fogelqvist, J., Corcoran, P., Avrova, A. O., ... & Dixelius, C. (2014). Fragmentation of tRNA in Phytophthora infestans asexual life cycle stages and during host plant infection. *BMC microbiology*, *14*(1), 308.

Baibakova, E. V., Nefedjeva, E. E., Suska-Malawska, M., Wilk, M., Sevriukova, G. A., & Zheltobriukhov, V. F. (2019). Modern fungicides: mechanisms of action, fungal resistance and phytotoxic effects. *Annual Research & Review in Biology*, 1-16.

Baldwin, T., Islamovic, E., Klos, K., Schwartz, P., Gillespie, J., Hunter, S., & Bregitzer, P. (2018). Silencing efficiency of dsRNA fragments targeting Fusarium graminearum TRI6 and patterns of small interfering RNA associated with reduced virulence and mycotoxin production. *PloS one*, *13*(8), e0202798.

Bao, Z., Yang, H., & Hua, J. (2013). Perturbation of cell cycle regulation triggers plant immune response via activation of disease resistance genes. *Proceedings of the National Academy of Sciences*, 110(6), 2407-2412.

Baulcombe, D. (2004). RNA silencing in plants. *Nature*, *431*(7006), 356-363.

Baulcombe, D. (2013). Small RNA—The secret of noble rot. *Science*, *342*(6154), 45-46.

Belsky, J., & Joshi, N. K. (2020). Effects of fungicide and herbicide chemical exposure on Apis and non-Apis bees in agricultural landscape. *Frontiers in Environmental Science*.

Benjamini, Y., & Yekutieli, D. (2001). The control of the false discovery rate in multiple testing under dependency. *Annals of statistics*, 1165-1188.

Bethke, G., Grundman, R. E., Sreekanta, S., Truman, W., Katagiri, F., & Glazebrook, J. (2014). Arabidopsis PECTIN METHYLESTERASEs contribute to immunity against Pseudomonas syringae. *Plant Physiology*, *164*(2), 1093-1107.

Bharti, P., Jyoti, P., Kapoor, P., Sharma, V., Shanmugam, V., & Yadav, S. K. (2017). Host-induced silencing of pathogenicity genes enhances resistance to Fusarium oxysporum wilt in tomato. *Molecular biotechnology*, *59*(8), 343-352.

Bilir, Ö., Telli, O., Norman, C., Budak, H., Hong, Y., & Tör, M. (2019). Small RNA inhibits infection by downy mildew pathogen Hyaloperonospora arabidopsidis. *Molecular plant pathology*, *20*(11), 1523-1534.

Bodenhofer, U., Bonatesta, E., Horejš-Kainrath, C., & Hochreiter, S. (2015). msa: an R package for multiple sequence alignment. *Bioinformatics*, *31*(24), 3997-3999.

Bollmann, S. R., Fang, Y., Press, C. M., Tyler, B. M., & Grünwald, N. J. (2016). Diverse evolutionary trajectories for small RNA biogenesis genes in the oomycete genus Phytophthora. *Frontiers in plant science*, *7*, 284.

Bollmann, S. R., Press, C. M., Tyler, B. M., & Grünwald, N. J. (2018). Expansion and divergence of argonaute genes in the oomycete genus phytophthora. *Frontiers in microbiology*, *9*, 2841.

Bonnet, E., He, Y., Billiau, K., & Van de Peer, Y. (2010). TAPIR, a web server for the prediction of plant microRNA targets, including target mimics. *Bioinformatics*, *26*(12), 1566-1568.

Borges, F., & Martienssen, R. A. (2015). The expanding world of small RNAs in plants. *Nature reviews Molecular cell biology*, *16*(12), 727-741.

Bowyer, P., & Denning, D. W. (2014). Environmental fungicides and triazole resistance in Aspergillus. *Pest management science*, *70*(2), 173-178.

Buck, A. H., Coakley, G., Simbari, F., McSorley, H. J., Quintana, J. F., Le Bihan, T., ... & Maizels, R. M. (2014). Exosomes secreted by nematode parasites transfer small RNAs to mammalian cells and modulate innate immunity. *Nature communications*, *5*(1), 1-12.

Buermans, H. P. J., & Den Dunnen, J. T. (2014). Next generation sequencing technology: advances and applications. *Biochimica et Biophysica Acta (BBA)-Molecular Basis of Disease*, *1842*(10), 1932-1941.

Cai, Q., He, B., Kogel, K. H., & Jin, H. (2018b). Cross-kingdom RNA trafficking and environmental RNAi—nature's blueprint for modern crop protection strategies. *Current opinion in microbiology*, *46*, 58-64.

Cai, Q., He, B., Wang, S., Fletcher, S., Niu, D., Mitter, N., Birch, P.R.J., Jin, H. (2021) Message in a Bubble: Shuttling Small RNAs and Proteins Between Cells and Interacting Organisms Using Extracellular Vesicles. *Annual Review of Plant Biology*, *72*(1), 497-524.

Cai, Q., Qiao, L., Wang, M., He, B., Lin, F. M., Palmquist, J., ... & Jin, H. (2018a). Plants send small RNAs in extracellular vesicles to fungal pathogen to silence virulence genes. *Science*, *360*(6393), 1126-1129.

Camacho, C., Coulouris, G., Avagyan, V., Ma, N., Papadopoulos, J., Bealer, K., & Madden, T. L. (2009). BLAST+: architecture and applications. *BMC bioinformatics*, *10*(1), 1-9.

Carlsbecker, A., Lee, J. Y., Roberts, C. J., Dettmer, J., Lehesranta, S., Zhou, J., ... & Benfey, P. N. (2010). Cell signalling by microRNA165/6 directs gene dose-dependent root cell fate. *Nature*, *465*(7296), 316-321.

Chambers, J. P., Behpouri, A., Bird, A., & Ng, C. K. (2012). Evaluation of the use of the Polyubiquitin Genes, Ubi4 and Ubi10 as reference genes for expression studies in Brachypodium distachyon. *PLoS One*, *7*(11), e49372.

Charif, D., & Lobry, J. R. (2007). SeqinR 1.0-2: a contributed package to the R project for statistical computing devoted to biological sequences retrieval and analysis. In *Structural approaches to sequence evolution* (pp. 207-232). Springer, Berlin, Heidelberg.

Chen, Y., Gao, Q., Huang, M., Liu, Y., Liu, Z., Liu, X., & Ma, Z. (2015). Characterization of RNA silencing components in the plant pathogenic fungus Fusarium graminearum. *Scientific reports*, *5*(1), 1-13.

Chen, W., Kastner, C., Nowara, D., Oliveira-Garcia, E., Rutten, T., Zhao, Y., ... & Schweizer, P. (2016). Host-induced silencing of Fusarium culmorum genes protects wheat from infection. *Journal of experimental botany*, *67*(17), 4979-4991.

Chen, C., Ridzon, D. A., Broomer, A. J., Zhou, Z., Lee, D. H., Nguyen, J. T., ... & Guegler, K. J. (2005). Real-time quantification of microRNAs by stem–loop RT–PCR. *Nucleic acids research*, *33*(20), e179-e179.

Chen, X., Steed, A., Travella, S., Keller, B., & Nicholson, P. (2009). Fusarium graminearum exploits ethylene signalling to colonize dicotyledonous and monocotyledonous plants. *New Phytologist*, *182*(4), 975-983.

Cheng, C. Y., Krishnakumar, V., Chan, A. P., Thibaud-Nissen, F., Schobel, S., & Town, C. D. (2017). Araport11: a complete reannotation of the Arabidopsis thaliana reference genome. *The Plant Journal*, *89*(4), 789-804.

Cheng, W., Song, X. S., Li, H. P., Cao, L. H., Sun, K., Qiu, X. L., ... & Liao, Y. C. (2015). Host-induced gene silencing of an essential chitin synthase gene confers durable resistance to F usarium head blight and seedling blight in wheat. *Plant biotechnology journal*, *13*(9), 1335-1345.

Cho, C. H., Jang, S., Choi, B. Y., Hong, D., Choi, D. S., Choi, S., ... & Lee, Y. (2019). Phylogenetic analysis of ABCG subfamily proteins in plants: functional clustering and coevolution with ABCGs of pathogens. *Physiologia plantarum*.

Christians, M. J., Gingerich, D. J., Hansen, M., Binder, B. M., Kieber, J. J., & Vierstra, R. D. (2009). The BTB ubiquitin ligases ETO1, EOL1 and EOL2 act collectively to regulate ethylene biosynthesis in Arabidopsis by controlling type-2 ACC synthase levels. *The Plant Journal*, *57*(2), 332-345.

Chung, B. Y., Deery, M. J., Groen, A. J., Howard, J., & Baulcombe, D. C. (2017). Endogenous miRNA in the green alga Chlamydomonas regulates gene expression through CDS-targeting. *Nature plants*, *3*(10), 787-794.

Coates, M. E., & Beynon, J. L. (2010). Hyaloperonospora arabidopsidis as a pathogen model. *Annual review of phytopathology*, *48*, 329-345.

Crick, F. H., Barnett, L., Brenner, S., & Watts-Tobin, R. J. (1961). General nature of the genetic code for proteins. *Nature*, *192*(4809), 1227-1232.

Curaba, J., Spriggs, A., Taylor, J., Li, Z., & Helliwell, C. (2012). miRNA regulation in the early development of barley seed. *BMC plant biology*, *12*(1), 1-16.

Dai, X., Zhuang, Z., & Zhao, P. X. (2018). psRNATarget: a plant small RNA target analysis server (2017 release). *Nucleic acids research*, *46*(W1), W49-W54.

Dalakouras, A., Wassenegger, M., Dadami, E., Ganopoulos, I., Pappas, M. L., & Papadopoulou, K. (2020). Genetically modified organism-free RNA interference: exogenous application of RNA molecules in plants. *Plant physiology*, *182*(1), 38-50.

Dalakouras, A., Wassenegger, M., McMillan, J. N., Cardoza, V., Maegele, I., Dadami, E., ... & Wassenegger, M. (2016). Induction of silencing in plants by high-pressure spraying of in vitro-synthesized small RNAs. *Frontiers in plant science*, *7*, 1327.

Das, S., Swetha, C., Pachamuthu, K., Nair, A., & Shivaprasad, P. V. (2020). Loss of function of Oryza sativa Argonaute 18 induces male sterility and reduction in phased small RNAs. *Plant reproduction*, 1-15.

Dean, R., Van Kan, J. A., Pretorius, Z. A., Hammond-Kosack, K. E., Di Pietro, A., Spanu, P. D., ... & Foster, G. D. (2012). The Top 10 fungal pathogens in molecular plant pathology. *Molecular plant pathology*, *13*(4), 414-430.

Denancé, N., Ranocha, P., Oria, N., Barlet, X., Rivière, M. P., Yadeta, K. A., ... & Goffner, D. (2013). Arabidopsis wat1 (walls are thin1)-mediated resistance to the bacterial vascular pathogen, Ralstonia solanacearum, is accompanied by cross-regulation of salicylic acid and tryptophan metabolism. *The Plant Journal*, *73*(2), 225-239.

Deng, P., Wang, L., Cui, L., Feng, K., Liu, F., Du, X., ... & Weining, S. (2015). Global identification of microRNAs and their targets in barley under salinity stress. *PLoS One*, *10*(9), e0137990.

Desjardins, A. E., Hohn, T. M., & McCORMICK, S. P. (1993). Trichothecene biosynthesis in Fusarium species: chemistry, genetics, and significance. *Microbiology and Molecular Biology Reviews*, *57*(3), 595-604.

Dubey, H., Kiran, K., Jaswal, R., Jain, P., Kayastha, A. M., Bhardwaj, S. C., ... & Sharma, T. R. (2019). Discovery and profiling of small RNAs from Puccinia triticina by deep sequencing and identification of their potential targets in wheat. *Functional & integrative genomics*, *19*(3), 391-407.

Dubrovina, A. S., & Kiselev, K. V. (2019). Exogenous RNAs for gene regulation and plant resistance. *International journal of molecular sciences*, *20*(9), 2282.

Dunker, F., Trutzenberg, A., Rothenpieler, J. S., Kuhn, S., Pröls, R., Schreiber, T., ... & Weiberg, A. (2020). Oomycete small RNAs bind to the plant RNA-induced silencing complex for virulence. *Elife*, *9*, e56096.

Duret, L., & Mouchiroud, D. (1999). Expression pattern and, surprisingly, gene length shape codon usage in Caenorhabditis, Drosophila, and Arabidopsis. *Proceedings of the National Academy of Sciences*, *96*(8), 4482-4487.

Durinck, S., Moreau, Y., Kasprzyk, A., Davis, S., De Moor, B., Brazma, A., & Huber, W. (2005). BioMart and Bioconductor: a powerful link between biological databases and microarray data analysis. *Bioinformatics*, *21*(16), 3439-3440.

Durinck, S., Spellman, P. T., Birney, E., & Huber, W. (2009). Mapping identifiers for the integration of genomic datasets with the R/Bioconductor package biomaRt. *Nature protocols*, *4*(8), 1184.

Eulalio, A., Huntzinger, E., & Izaurralde, E. (2008). Getting to the root of miRNA-mediated gene silencing. *Cell*, *132*(1), 9-14.

Fang, X., & Qi, Y. (2016). RNAi in plants: an argonaute-centered view. *The Plant Cell*, *28*(2), 272-285.

Ferdous, J., Sanchez-Ferrero, J. C., Langridge, P., Milne, L., Chowdhury, J., Brien, C., & Gaffar, F. Y., & Koch, A. (2019). Catch me if you can! RNA silencing-based improvement of antiviral plant immunity. *Viruses*, *11*(7), 673.

Ferrari, S., Galletti, R., Vairo, D., Cervone, F., & De Lorenzo, G. (2006). Antisense expression of the Arabidopsis thaliana AtPGIP1 gene reduces polygalacturonase-inhibiting protein accumulation and enhances susceptibility to Botrytis cinerea. *Molecular Plant-Microbe Interactions*, *19*(8), 931-936.

Fisher, M. C., Hawkins, N. J., Sanglard, D., & Gurr, S. J. (2018). Worldwide emergence of resistance to antifungal drugs challenges human health and food security. *Science*, *360*(6390), 739-742.

Forman, J. J., Legesse-Miller, A., & Coller, H. A. (2008). A search for conserved sequences in coding regions reveals that the let-7 microRNA targets Dicer within its coding sequence. *Proceedings of the National Academy of Sciences*, *105*(39), 14879-14884.

Fu, L., Niu, B., Zhu, Z., Wu, S., & Li, W. (2012). CD-HIT: accelerated for clustering the next-generation sequencing data. *Bioinformatics*, *28*(23), 3150-3152.

Fukudome, A., & Fukuhara, T. (2017). Plant dicer-like proteins: double-stranded RNA-cleaving enzymes for small RNA biogenesis. *Journal of plant research*, *130*(1), 33-44.

Gaffar, F. Y., Imani, J., Karlovsky, P., Koch, A., & Kogel, K. H. (2019). Different components of the RNA interference machinery are required for conidiation, ascosporogenesis, virulence, deoxynivalenol production, and fungal inhibition by exogenous double-stranded RNA in the head blight pathogen Fusarium graminearum. *Frontiers in microbiology*, *10*, 1662.

Gaffar, F. Y., & Koch, A. (2019). Catch me if you can! RNA silencing-based improvement of antiviral plant immunity. *Viruses*, *11*(7), 673.

Galiana, E., Bonnet, P., Conrod, S., Keller, H., Panabières, F., Ponchet, M., ... & Ricci, P. (1997). RNase activity prevents the growth of a fungal pathogen in tobacco leaves and increases upon induction of systemic acquired resistance with elicitin. *Plant Physiology*, *115*(4), 1557-1567.

Garcia-Ruiz, H., Takeda, A., Chapman, E. J., Sullivan, C. M., Fahlgren, N., Brempelis, K. J., & Carrington, J. C. (2010). Arabidopsis RNA-dependent RNA polymerases and dicer-like proteins in antiviral defense and small interfering RNA biogenesis during Turnip Mosaic Virus infection. *The Plant Cell*, *22*(2), 481-496.

Garcia-Silva, M. R., Cabrera-Cabrera, F., Cura das Neves, R. F., Souto-Padrón, T., de Souza, W., & Cayota, A. (2014). Gene expression changes induced by Trypanosoma cruzi shed microvesicles in mammalian host cells: relevance of tRNA-derived halves. *BioMed research international*, *2014*.

Gareis, M. (2003). Collection of occurrence data of Fusarium toxins in food and assessment of dietary intake by the population of EU member states. *Report of Experts Participating in SCOOP Task 3.2. 10-Final Report*, 5-10.

Garnier, S. (2018). viridis: Default Color Maps from "matplotlib." 2018. *R package version 0.5.1*.

Gasciolli, V., Mallory, A. C., Bartel, D. P., & Vaucheret, H. (2005). Partially redundant functions of Arabidopsis DICER-like enzymes and a role for DCL4 in producing trans-acting siRNAs. *Current Biology*, *15*(16), 1494-1500.

German, M. A., Pillay, M., Jeong, D. H., Hetawal, A., Luo, S., Janardhanan, P., ... & Green, P. J. (2008). Global identification of microRNA–target RNA pairs by parallel analysis of RNA ends. *Nature biotechnology*, *26*(8), 941-946.

Ghag, S. B., Shekhawat, U. K., & Ganapathi, T. R. (2014). Host-induced post-transcriptional hairpin RNA-mediated gene silencing of vital fungal genes confers efficient resistance against Fusarium wilt in banana. *Plant biotechnology journal*, *12*(5), 541-553.

Ghelfenstein-Ferreira, T., Saade, A., Alanio, A., Bretagne, S., de Castro, R. A., Hamane, S., ... & Dellière, S. (2021). Recovery of a triazole-resistant Aspergillus fumigatus in respiratory specimen of COVID-19 patient in ICU–A case report. *Medical Mycology Case Reports*, *31*, 15-18.

Glazebrook, J. (2005). Contrasting mechanisms of defense against biotrophic and necrotrophic pathogens. *Annu. Rev. Phytopathol.*, *43*, 205-227.

Gordon, A., & Hannon, G. J. (2010). Fastx-toolkit. FASTQ/A short-reads preprocessing tools 433.

Goswami, R. S., & Kistler, H. C. (2004). Heading for disaster: Fusarium graminearum on cereal crops. *Molecular plant pathology*, *5*(6), 515-525.

Griffiths-Jones, S., Grocock, R. J., Van Dongen, S., Bateman, A., & Enright, A. J. (2006). miRBase: microRNA sequences, targets and gene nomenclature. *Nucleic acids research*, *34*(suppl_1), D140-D144.

Gu, W., Wang, X., Zhai, C., Xie, X., & Zhou, T. (2012). Selection on synonymous sites for increased accessibility around miRNA binding sites in plants. *Molecular biology and evolution*, *29*(10), 3037-3044.

Guo, Q., Liu, Q., A Smith, N., Liang, G., & Wang, M. B. (2016). RNA silencing in plants: mechanisms, technologies and applications in horticultural crops. *Current Genomics*, *17*(6), 476-489.

Guo, H., Song, X., Wang, G., Yang, K., Wang, Y., Niu, L., ... & Fang, R. (2014). Plant-generated artificial small RNAs mediated aphid resistance. *PLoS One*, *9*(5), e97410.

Haas, B. J., Kamoun, S., Zody, M. C., Jiang, R. H., Handsaker, R. E., Cano, L. M., ... & Nusbaum, C. (2009). Genome sequence and analysis of the Irish potato famine pathogen Phytophthora infestans. *Nature*, *461*(7262), 393-398.

Hackenberg, M., Gustafson, P., Langridge, P., & Shi, B. J. (2015). Differential expression of micro RNA s and other small RNA s in barley between water and drought conditions. *Plant biotechnology journal*, *13*(1), 2-13.

Hamar, É., Szaker, H. M., Kis, A., Dalmadi, Á., Miloro, F., Szittya, G., ... & Havelda, Z. (2020). Genome-wide identification of RNA silencing-related genes and their expressional analysis in response to heat stress in barley (Hordeum vulgare l.). *Biomolecules*, *10*(6), 929.

Hannon, G. "Fastx-toolkit." FASTQ/A Short-reads Preprocessing Tools (2010)

Harvey, S., Kumari, P., Lapin, D., Griebel, T., Hickman, R., Guo, W., ... & Steinbrenner, J. (2020). Downy Mildew effector HaRxL21 interacts with the transcriptional repressor TOPLESS to promote pathogen susceptibility. *PLoS Pathogens*, 16(8), e1008835.

He, Q., McLellan, H., Boevink, P. C., & Birch, P. R. (2020). All roads lead to susceptibility: the many modes of action of fungal and oomycete intracellular effectors. *Plant Communications*, *1*(4), 100050.

Head, G. P., Carroll, M. W., Evans, S. P., Rule, D. M., Willse, A. R., Clark, T. L., ... & Meinke, L. J. (2017). Evaluation of SmartStax and SmartStax PRO maize against western corn rootworm and northern corn rootworm: efficacy and resistance management. *Pest management science*, *73*(9), 1883-1899.

Höfle, L., Biedenkopf, D., Werner, B. T., Shrestha, A., Jelonek, L., & Koch, A. (2020). Study on the efficiency of dsRNAs with increasing length in RNA-based silencing of the Fusarium CYP51 genes. *RNA biology*, *17*(4), 463-473.

Hu, W., Luo, H., Yang, Y., Wang, Q., Hong, N., Wang, G., ... & Wang, L. (2019). Comprehensive analysis of full genome sequence and Bd-milRNA/target mRNAs to discover the mechanism of hypovirulence in Botryosphaeria dothidea strains on pear infection with BdCV1 and BdPV1. *IMA fungus*, *10*(1), 1-25.

Hu, Z., Parekh, U., Maruta, N., Trusov, Y., & Botella, J. R. (2015). Down-regulation of Fusarium oxysporum endogenous genes by host-delivered RNA interference enhances disease resistance. *Frontiers in chemistry*, *3*, 1.

Huang, G., Allen, R., Davis, E. L., Baum, T. J., & Hussey, R. S. (2006). Engineering broad root-knot resistance in transgenic plants by RNAi silencing of a conserved and essential root-knot nematode parasitism gene. *Proceedings of the National Academy of Sciences*, *103*(39), 14302-14306.

Huibers, R. P., De Jong, M., Dekter, R. W., & Van den Ackerveken, G. (2009). Disease-specific expression of host genes during downy mildew infection of Arabidopsis. *Molecular plant-microbe interactions*, 22(9), 1104-1115.

Ilgen, P., Hadeler, B., Maier, F. J., & Schäfer, W. (2009). Developing kernel and rachis node induce the trichothecene pathway of Fusarium graminearum during wheat head infection. *Molecular plant-microbe interactions*, *22*(8), 899-908.

Ismaiel, A. A., & Papenbrock, J. (2015). Mycotoxins: producing fungi and mechanisms of phytotoxicity. *Agriculture*, *5*(3), 492-537.

Jansen, C., Von Wettstein, D., Schäfer, W., Kogel, K. H., Felk, A., & Maier, F. J. (2005). Infection patterns in barley and wheat spikes inoculated with wild-type and trichodiene synthase gene disrupted Fusarium graminearum. *Proceedings of the National Academy of Sciences*, *102*(46), 16892-16897.

Jayakodi, M., Padmarasu, S., Haberer, G., Bonthala, V. S., Gundlach, H., Monat, C., ... & Stein, N. (2020). The barley pan-genome reveals the hidden legacy of mutation breeding. *Nature*, *588*(7837), 284-289.

Jay, F., Renou, J. P., Voinnet, O., & Navarro, L. (2010). Biotic stress-associated microRNAs: identification, detection, regulation, and functional analysis. In *Plant MicroRNAs* (pp. 183-202). Humana Press.

Jian, J., & Liang, X. (2019). One small RNA of *Fusarium graminearum* targets and silences CEBiP gene in common wheat. *Microorganisms*, *7*(10), 425.

Jiménez, R. R., Alvarado, G., Ruepert, C., Ballestero, E., & Sommer, S. (2021). The Fungicide Chlorothalonil Changes the Amphibian Skin Microbiome: A Potential Factor Disrupting a Host Disease-Protective Trait. *Applied Microbiology*, *1*(1), 26-37.

Jin, B. J., Chun, H. J., & Kim, M. C. (2013, July). Development of antifungal transgenic plant by using host induced gene silencing. In *2013 한국육종학회-차세대BG21 사업단 공동심포지엄* (pp. 102-102).

Jin, Y., Zhao, J. H., Zhao, P., Zhang, T., Wang, S., & Guo, H. S. (2019). A fungal milRNA mediates epigenetic repression of a virulence gene in Verticillium dahliae. *Philosophical Transactions of the Royal Society B*, *374*(1767), 20180309.

Jones, J. D., & Dangl, J. L. (2006). The plant immune system. *nature*, *444*(7117), 323-329.

Jones-Rhoades, M. W. (2012). Conservation and divergence in plant microRNAs. *Plant molecular biology*, *80*(1), 3-16.

Kaldis, A., Berbati, M., Melita, O., Reppa, C., Holeva, M., Otten, P., & Voloudakis, A. (2018). Exogenously applied dsRNA molecules deriving from the Zucchini yellow mosaic virus (ZYMV) genome move systemically and protect cucurbits against ZYMV. *Molecular plant pathology*, *19*(4), 883-895.

Kassambara, A. (2017). ggpubr: "ggplot2" based publication ready plots. R package version 0.1. 6.

Kassambara, A. (2020). ggpubr:"ggplot2" based publication ready plots. *R package version 0.4.0*.

Kapoor, M., Arora, R., Lama, T., Nijhawan, A., Khurana, J. P., Tyagi, A. K., & Kapoor, S. (2008). Genome-wide identification, organization and phylogenetic analysis of Dicer-like, Argonaute and RNA-dependent RNA Polymerase gene families and their expression analysis during reproductive development and stress in rice. *BMC genomics*, *9*(1), 1-17.

Kawabe, A., & Miyashita, N. T. (2003). Patterns of codon usage bias in three dicot and four monocot plant species. *Genes & genetic systems*, *78*(5), 343-352.

Kazan, K., Gardiner, D. M., & Manners, J. M. (2012). On the trail of a cereal killer: recent advances in Fusarium graminearum pathogenomics and host resistance. *Molecular plant pathology*, *13*(4), 399-413.

Kehr, J., & Kragler, F. (2018). Long distance RNA movement. *New Phytologist*, *218*(1), 29-40.

Ketting, R. F. (2011). The many faces of RNAi. *Developmental cell*, *20*(2), 148-161.

Khoury, C. K., Bjorkman, A. D., Dempewolf, H., Ramirez-Villegas, J., Guarino, L., Jarvis, A., ... & Struik, P. C. (2014). Increasing homogeneity in global food supplies and the implications for food security. *Proceedings of the National Academy of Sciences*, *111*(11), 4001-4006.

Kieber, J. J., Rothenberg, M., Roman, G., Feldmann, K. A., & Ecker, J. R. (1993). CTR1, a negative regulator of the ethylene response pathway in Arabidopsis, encodes a member of the raf family of protein kinases. *Cell*, *72*(3), 427-441.

Kim, H. K., Jo, S. M., Kim, G. Y., Kim, D. W., Kim, Y. K., & Yun, S. H. (2015). A large-scale functional analysis of putative target genes of mating-type loci provides insight into the regulation of sexual development of the cereal pathogen Fusarium graminearum. *PLoS Genet*, *11*(9), e1005486.

Kloek, A. P., Verbsky, M. L., Sharma, S. B., Schoelz, J. E., Vogel, J., Klessig, D. F., & Kunkel, B. N. (2001). Resistance to Pseudomonas syringae conferred by an Arabidopsis thaliana coronatine-insensitive (coi1) mutation occurs through two distinct mechanisms. *The Plant Journal*, *26*(5), 509-522.

Knip M, Constantin ME, Thordal-Christensen H: Trans-kingdom cross-talk: small RNAs on the move. *PLoS Genet* 2014, 10.

Koch, A., Biedenkopf, D., Furch, A., Weber, L., Rossbach, O., Abdellatef, E., ... & Kogel, K. H. (2016). An RNAi-based control of Fusarium graminearum infections through spraying of long dsRNAs involves a plant passage and is controlled by the fungal silencing machinery. *PLoS pathogens*, *12*(10), e1005901.

Koch, A., Höfle, L., Werner, B. T., Imani, J., Schmidt, A., Jelonek, L., & Kogel, K. H. (2019). SIGS vs HIGS: a study on the efficacy of two dsRNA delivery strategies to silence Fusarium FgCYP51 genes in infected host and non-host plants. *Molecular plant pathology*, *20*(12), 1636-1644.

Koch, A., & Kogel, K. H. (2014). New wind in the sails: improving the agronomic value of crop plants through RNA i-mediated gene silencing. *Plant biotechnology journal*, *12*(7), 821-831.

Koch, A., Kumar, N., Weber, L., Keller, H., Imani, J., & Kogel, K. H. (2013). Host-induced gene silencing of cytochrome P450 lanosterol C14α-demethylase–encoding genes confers strong resistance to Fusarium species. *Proceedings of the National Academy of Sciences*, *110*(48), 19324-19329.

Koch, A., Schlemmer, T., Hoefle, L., Werner, B., Preusser, C., Hardt, M., ... & Kogel, K. H. (2020). Host-induced gene silencing involves transfer of dsRNA-derived siRNA via extracellular vesicles. *bioRxiv*.

Koch, A., Stein, E., & Kogel, K. H. (2018). RNA-based disease control as a complementary measure to fight Fusarium fungi through silencing of the azole target Cytochrome P450 Lanosterol C-14 α-Demethylase. *European journal of plant pathology*, *152*(4), 1003-1010.

Koch, A., & Wassenegger, M. (2021). Host-induced gene silencing–mechanisms and applications. *New Phytologist* doi: 10.1111/nph.17364.

Koczera, P., Martin, L., Marx, G., & Schuerholz, T. (2016). The ribonuclease a superfamily in humans: canonical RNases as the buttress of innate immunity. *International journal of molecular sciences*, *17*(8), 1278.

Konakalla, N. C., Kaldis, A., Berbati, M., Masarapu, H., & Voloudakis, A. E. (2016). Exogenous application of double-stranded RNA molecules from TMV p126 and CP genes confers resistance against TMV in tobacco. *Planta*, *244*(4), 961-969.

Kozomara, A., Birgaoanu, M., & Griffiths-Jones, S. (2019). miRBase: from microRNA sequences to function. *Nucleic acids research*, *47*(D1), D155-D162.

Kozomara, A., & Griffiths-Jones, S. (2010). miRBase: integrating microRNA annotation and deep-sequencing data. *Nucleic acids research*, *39*(suppl_1), D152-D157.

Kluiver, J., Slezak-Prochazka, I., Smigielska-Czepiel, K., Halsema, N., Kroesen, B. J., & van den Berg, A. (2012). Generation of miRNA sponge constructs. *Methods*, *58*(2), 113-117.

Kuck, K. H., Stenzel, K., & Vors, J. P. (2012). Sterol biosynthesis inhibitors modern crop protection compounds (pp. 761–805).

Kumar, P., Kuscu, C., & Dutta, A. (2016a). Biogenesis and function of transfer RNA-related fragments (tRFs). *Trends in biochemical sciences*, *41*(8), 679-689.

Kumar, S., Stecher, G., & Tamura, K. (2016b). MEGA7: molecular evolutionary genetics analysis version 7.0 for bigger datasets. *Molecular biology and evolution*, *33*(7), 1870-1874.

Kuzmenko, A., Oguienko, A., Esyunina, D., Yudin, D., Petrova, M., Kudinova, A., ... & Kulbachinskiy, A. (2020). DNA targeting and interference by a bacterial Argonaute nuclease. *Nature*, *587*(7835), 632-637.

Laday, M., Bagi, F., Mesterhazy, A., & Szecsi, A. (2000). Isozyme evidence for two groups of Fusarium graminearum. *Mycological Research*, *104*(7), 788-793.

Lamesch, P., Berardini, T. Z., Li, D., Swarbreck, D., Wilks, C., Sasidharan, R., ... & Huala, E. (2012). The Arabidopsis Information Resource (TAIR): improved gene annotation and new tools. *Nucleic acids research*, *40*(D1), D1202-D1210.

Lamour, K., & Kamoun, S. (2009). *Oomycete genetics and genomics: diversity, interactions and research tools*. John Wiley & Sons.

Langmead, B. (2010). Aligning short sequencing reads with Bowtie. *Current protocols in bioinformatics*, *32*(1), 11-7.

Langmead, B., & Salzberg, S. L. (2012). Fast gapped-read alignment with Bowtie 2. *Nature methods*, *9*(4), 357.

Langmead, B., Trapnell, C., Pop, M., & Salzberg, S. L. (2009). Ultrafast and memory-efficient alignment of short DNA sequences to the human genome. *Genome biology*, *10*(3), R25.

Laurie-Berry, N., Joardar, V., Street, I. H., & Kunkel, B. N. (2006). The Arabidopsis thaliana JASMONATE INSENSITIVE 1 gene is required for suppression of salicylic acid-dependent defenses during infection by Pseudomonas syringae. *Molecular Plant-Microbe Interactions*, *19*(7), 789-800.

Lax, C., Tahiri, G., Patiño-Medina, J. A., Cánovas-Márquez, J. T., Pérez-Ruiz, J. A., Osorio-Concepción, M., ... & Calo, S. (2020). The Evolutionary Significance of RNAi in the Fungal Kingdom. *International Journal of Molecular Sciences*, *21*(24), 9348.

Lee Marzano, S. Y., Neupane, A., Mochama, P., Feng, C., & Saleem, H. (2019). Roles of argonautes and dicers on Sclerotinia sclerotiorum antiviral RNA silencing. *Frontiers in Plant Science*, *10*, 976.

Li, N., Han, X., Feng, D., Yuan, D., & Huang, L. J. (2019). Signaling crosstalk between salicylic acid and ethylene/jasmonate in plant defense: do we understand what they are whispering?. *International Journal of Molecular Sciences*, *20*(3), 671.

Li, Y., Kabbage, M., Liu, W., & Dickman, M. B. (2016). Aspartyl protease-mediated cleavage of BAG6 is necessary for autophagy and fungal resistance in plants. *The Plant Cell*, *28*(1), 233-247.

Li, N., Shan, N., Lu, L., & Wang, Z. (2021). tRFtarget: a database for transfer RNA-derived fragment targets. *Nucleic Acids Research, 49*(D1), D254-D260.

Liang, G., He, H., Li, Y., & Yu, D. (2012). A new strategy for construction of artificial miRNA vectors in Arabidopsis. *Planta*, *235*(6), 1421-1429.

Liu, S., Jaouannet, M., Dempsey, D. M. A., Imani, J., Coustau, C., & Kogel, K. H. (2020). RNA-based technologies for insect control in plant production. *Biotechnology advances*, *39*, 107463.

Liu, S., Ladera-Carmona, M. J., Poranen, M. M., van Bel, A. J., Kogel, K. H., & Imani, J. (2021). Evaluation of dsRNA delivery methods for targeting macrophage migration inhibitory factor MIF in RNAi-based aphid control. *Journal of Plant Diseases and Protection*, 1-12.

Liu, W. W., Meng, J., Cui, J., & Luan, Y. S. (2017). Characterization and function of MicroRNA∗ s in Plants. *Frontiers in plant science*, *8*, 2200.

Livak, K. J., & Schmittgen, T. D. (2001). Analysis of relative gene expression data using real-time quantitative PCR and the 2− ΔΔCT method. *methods*, *25*(4), 402-408.

Lorenz, R., Bernhart, S. H., Zu Siederdissen, C. H., Tafer, H., Flamm, C., Stadler, P. F., & Hofacker, I. L. (2011). ViennaRNA Package 2.0. *Algorithms for molecular biology*, *6*(1), 1-14.

Lucas, W. J., Bouché-Pillon, S., Jackson, D. P., Nguyen, L., Baker, L., Ding, B., & Hake, S. (1995). Selective trafficking of KNOTTED1 homeodomain protein and its mRNA through plasmodesmata. *Science*, *270*(5244), 1980-1983.

Lück, S., Kreszies, T., Strickert, M., Schweizer, P., Kuhlmann, M., & Douchkov, D. (2019). siRNA-Finder (si-Fi) software for RNAi-target design and off-target prediction. *Frontiers in plant science*, *10*, 1023.

Machado, A. K., Brown, N. A., Urban, M., Kanyuka, K., & Hammond-Kosack, K. E. (2018). RNAi as an emerging approach to control Fusarium head blight disease and mycotoxin contamination in cereals. *Pest management science*, *74*(4), 790-799.

Majumdar, R., Rajasekaran, K., & Cary, J. W. (2017). RNA interference (RNAi) as a potential tool for control of mycotoxin contamination in crop plants: concepts and considerations. *Frontiers in plant science*, *8*, 200.

Mallory, A. C., Reinhart, B. J., Jones-Rhoades, M. W., Tang, G., Zamore, P. D., Barton, M. K., & Bartel, D. P. (2004). MicroRNA control of PHABULOSA in leaf development: importance of pairing to the microRNA 5' region. *The EMBO journal*, *23*(16), 3356-3364.

Marshall, R. E., Caskey, C. T., & Nirenberg, M. (1967). Fine structure of RNA codewords recognized by bacterial, amphibian, and mammalian transfer RNA. *Science*, *155*(3764), 820-826.

Martin, M. (2011). Cutadapt removes adapter sequences from high-throughput sequencing reads. *EMBnet. journal*, *17*(1), 10-12.

Martinez, G., Choudury, S. G., & Slotkin, R. K. (2017). tRNA-derived small RNAs target transposable element transcripts. *Nucleic acids research*, *45*(9), 5142-5152.

Mascher, M., Gundlach, H., Himmelbach, A., Beier, S., Twardziok, S. O., Wicker, T., ... & Stein, N. (2017). A chromosome conformation capture ordered sequence of the barley genome. *Nature*, *544*(7651), 427-433.

McEwan, D. L., Weisman, A. S., & Hunter, C. P. (2012). Uptake of extracellular double-stranded RNA by SID-2. *Molecular cell*, *47*(5), 746-754.

McLoughlin, A. G., Wytinck, N., Walker, P. L., Girard, I. J., Rashid, K. Y., de Kievit, T., ... & Belmonte, M. F. (2018). Identification and application of exogenous dsRNA confers plant protection against Sclerotinia sclerotiorum and Botrytis cinerea. *Scientific Reports*, *8*(1), 1-14.

McMullen, M., Jones, R., & Gallenberg, D. (1997). Scab of wheat and barley: a re-emerging disease of devastating impact. *Plant disease*, *81*(12), 1340-1348.

McMullen, M., Bergstrom, G., De Wolf, E., Dill-Macky, R., Hershman, D., Shaner, G., & Van Sanford, D. (2012). A unified effort to fight an enemy of wheat and barley: Fusarium head blight. *Plant Disease*, *96*(12), 1712-1728.

Meyer, M., Diehl, D., Schaumann, G. E., & Muñoz, K. (2021). Agricultural mulching and fungicides—impacts on fungal biomass, mycotoxin occurrence, and soil organic matter decomposition. *Environmental Science and Pollution Research*, 1-16.

Mi, S., Cai, T., Hu, Y., Chen, Y., Hodges, E., Ni, F., ... & Qi, Y. (2008). Sorting of small RNAs into Arabidopsis argonaute complexes is directed by the 5′ terminal nucleotide. *Cell*, *133*(1), 116-127.

Millar, A. A., Lohe, A., & Wong, G. (2019). Biology and Function of miR159 in Plants. *Plants*, *8*(8), 255.

Mittelbrunn, M., Gutiérrez-Vázquez, C., Villarroya-Beltri, C., González, S., Sánchez-Cabo, F., González, M. Á., ... & Sánchez-Madrid, F. (2011). Unidirectional transfer of microRNA-loaded exosomes from T cells to antigen-presenting cells. *Nature communications*, *2*(1), 1-10.

Mitter, N., Worrall, E. A., Robinson, K. E., Li, P., Jain, R. G., Taochy, C., ... & Xu, Z. P. (2017). Clay nanosheets for topical delivery of RNAi for sustained protection against plant viruses. *Nature plants*, *3*(2), 1-10.

More, P., Agarwal, P., Anand, A., Sanan-Mishra, N., & Agarwal, P. K. (2021). Artificial miRNA mediated resistance in tobacco against Jatropha leaf curl Gujarat virus by targeting RNA silencing suppressors. *Scientific reports*, *11*(1), 1-16.

Morel, J. B., Godon, C., Mourrain, P., Béclin, C., Boutet, S., Feuerbach, F., ... & Vaucheret, H. (2002). Fertile hypomorphic ARGONAUTE (ago1) mutants impaired in post-transcriptional gene silencing and virus resistance. *The Plant Cell*, *14*(3), 629-639.

Moriyama, E. N., & Powell, J. R. (1997). Codon usage bias and tRNA abundance in Drosophila. *Journal of molecular evolution*, *45*(5), 514-523.

Mueth, N. A., Ramachandran, S. R., & Hulbert, S. H. (2015). Small RNAs from the wheat stripe rust fungus (Puccinia striiformis f. sp. tritici). *Bmc Genomics*, *16*(1), 1-16.

Murray, E. E., Lotzer, J., & Eberle, M. (1989). Codon usage in plant genes. *Nucleic Acids Research*, *17*(2), 477-498.

Nei, M., & Kumar, S. (2000). *Molecular evolution and phylogenetics*. Oxford university press.

Nicholson, A. W. (1997). Escherichia coli ribonucleases: paradigms for understanding cellular RNA metabolism and regulation. In *Ribonucleases* (pp. 1-49). Academic Press.

Nicolas, F. E., Torres-Martinez, S., & Ruiz-Vazquez, R. M. (2013). Loss and retention of RNA interference in fungi and parasites. *PLoS pathogens*, *9*(1), e1003089.

Niehl, A., & Heinlein, M. (2019). Perception of double-stranded RNA in plant antiviral immunity. *Molecular plant pathology*, *20*(9), 1203-1210.

Niehl, A., Soininen, M., Poranen, M. M., & Heinlein, M. (2018). Synthetic biology approach for plant protection using ds RNA. *Plant biotechnology journal*, *16*(9), 1679-1687.

Nirenberg, H. I. (1981). A simplified method for identifying Fusarium spp. occurring on wheat. *Canadian Journal of Botany*, *59*(9), 1599-1609.

Nowara, D., Gay, A., Lacomme, C., Shaw, J., Ridout, C., Douchkov, D., ... & Schweizer, P. (2010). HIGS: host-induced gene silencing in the obligate biotrophic fungal pathogen Blumeria graminis. *The Plant Cell*, *22*(9), 3130-3141.

Olombrada, M., Martínez-del-Pozo, Á., Medina, P., Budia, F., Gavilanes, J. G., & García-Ortega, L. (2014). Fungal ribotoxins: Natural protein-based weapons against insects. *Toxicon*, *83*, 69-74.

Ossowski, S., Schwab, R., & Weigel, D. (2008). Gene silencing in plants using artificial microRNAs and other small RNAs. *The Plant Journal*, *53*(4), 674-690.

Pareek, M., & Rajam, M. V. (2017). RNAi-mediated silencing of MAP kinase signalling genes (Fmk1, Hog1, and Pbs2) in Fusarium oxysporum reduces pathogenesis on tomato plants. *Fungal biology*, *121*(9), 775-784.

Park, Y. J., Lee, H. J., Kwak, K. J., Lee, K., Hong, S. W., & Kang, H. (2014). MicroRNA400-guided cleavage of pentatricopeptide repeat protein mRNAs renders Arabidopsis thaliana more susceptible to pathogenic bacteria and fungi. *Plant and Cell Physiology*, *55*(9), 1660-1668.

Pestka, J. J. (2010). Deoxynivalenol: mechanisms of action, human exposure, and toxicological relevance. *Archives of toxicology*, *84*(9), 663-679.

Plotkin, J. B., & Kudla, G. (2011). Synonymous but not the same: the causes and consequences of codon bias. *Nature Reviews Genetics*, *12*(1), 32-42.

Potuschak, T., Lechner, E., Parmentier, Y., Yanagisawa, S., Grava, S., Koncz, C., & Genschik, P. (2003). EIN3-dependent regulation of plant ethylene hormone signaling by two Arabidopsis F box proteins: EBF1 and EBF2. *Cell*, *115*(6), 679-689.

Pozo, M. J., Van Der Ent, S., Van Loon, L. C., & Pieterse, C. M. (2008). Transcription factor MYC2 is involved in priming for enhanced defense during rhizobacteria-induced systemic resistance in Arabidopsis thaliana. *New Phytologist*, *180*(2), 511-523.

Price, C. L., Parker, J. E., Warrilow, A. G., Kelly, D. E., & Kelly, S. L. (2015). Azole fungicides–understanding resistance mechanisms in agricultural fungal pathogens. *Pest management science*, *71*(8), 1054-1058.

Qi, T., Guo, J., Peng, H., Liu, P., Kang, Z., & Guo, J. (2019). Host-induced gene silencing: a powerful strategy to control diseases of wheat and barley. *International journal of molecular sciences*, *20*(1), 206.

Qiao, L., Lan, C., Capriotti, L., Ah-Fong, A., Nino Sanchez, J., Hamby, R., Heller, J., Zhao, H., Glass, N. L., Judelson, H. S., Mezzetti, B., Niu, D. and Jin, H. (2021) Spray-induced gene silencing for disease control is dependent on the efficiency of pathogen RNA uptake. *Plant Biotechnol. J.*, https://doi.org/10.1111/pbi.13589

Qu, J., Ye, J., & Fang, R. (2007). Artificial microRNA-mediated virus resistance in plants. *Journal of virology*, *81*(12), 6690-6699.

R Core Team, R. (2013). R: A language and environment for statistical computing.

R Core Team, R. (2019). R: A language and environment for statistical computing.

Rao, V. S., Srinivas, K., Sujini, G. N., & Kumar, G. N. (2014). Protein-protein interaction detection: methods and analysis. *International journal of proteomics*, *2014*.

Rehmsmeier, M., Steffen, P., Höchsmann, M., & Giegerich, R. (2004). Fast and effective prediction of microRNA/target duplexes. *Rna*, *10*(10), 1507-1517.

Reinhart, B. J., Weinstein, E. G., Rhoades, M. W., Bartel, B., & Bartel, D. P. (2002). MicroRNAs in plants. *Genes & development*, *16*(13), 1616-1626.

Ren, B., Wang, X., Duan, J., & Ma, J. (2019). Rhizobial tRNA-derived small RNAs are signal molecules regulating plant nodulation. *Science*, *365*(6456), 919-922.

Reynolds, A., Leake, D., Boese, Q., Scaringe, S., Marshall, W. S., & Khvorova, A. (2004). Rational siRNA design for RNA interference. *Nature biotechnology*, *22*(3), 326-330.

Roberts, A. F., Devos, Y., Lemgo, G. N., & Zhou, X. (2015). Biosafety research for non-target organism risk assessment of RNAi-based GE plants. *Frontiers in plant science*, *6*, 958.

Rosa, C., Kuo, Y. W., Wuriyanghan, H., & Falk, B. W. (2018). RNA interference mechanisms and applications in plant pathology. *Annual review of phytopathology*, *56*, 581-610.

RStudio Team (2016). RStudio: Integrated Development for R. RStudioInc., Boston, MA URL http://www.rstudio.com/.

RStudio Team (2020). RStudio: Integrated Development for R. RStudio, PBC, Boston, MA URL http://www.rstudio.com/.

Rutter, B.D., Innes, R.W. (2018) Extracellular vesicles as key mediators of plant-microbe interactions. *Curr Opin Plant Biol*, 44:16-22. doi: 10.1016/j.pbi.2018.01.008. Epub 2018 Feb 14. PMID: 29452903.

Samad, A. F., Sajad, M., Nazaruddin, N., Fauzi, I. A., Murad, A., Zainal, Z., & Ismail, I. (2017). MicroRNA and transcription factor: key players in plant regulatory network. *Frontiers in plant science*, *8*, 565.

Sang, H., & Kim, J. I. (2020). Advanced strategies to control plant pathogenic fungi by host-induced gene silencing (HIGS) and spray-induced gene silencing (SIGS). *Plant Biotechnology Reports*, *14*(1), 1-8.

Schneider, C. A., Rasband, W. S., & Eliceiri, K. W. (2012). NIH Image to ImageJ: 25 years of image analysis. *Nature methods*, *9*(7), 671-675.

Scholthof, K. B. G., Irigoyen, S., Catalan, P., & Mandadi, K. K. (2018). Brachypodium: a monocot grass model genus for plant biology. *The Plant Cell*, *30*(8), 1673-1694.

Šečić, E., & Kogel, K. H. (2021). Requirements for fungal uptake of dsRNA and gene silencing in RNAi-based crop protection strategies. *Current Opinion in Biotechnology*, *70*, 136-142.

Šečić, E., Zanini, S., & Kogel, K. H. (2019). Further elucidation of the ARGONAUTE and DICER protein families in the model grass species Brachypodium distachyon. *Frontiers in plant science*, *10*, 1332.

Šečić, E., Zanini, S., Wibberg, D., Jelonek, L., Busche, T., Kalinowski, J., ... & Kogel, K. H. (2021). A novel plant-fungal association reveals fundamental sRNA and gene expression reprogramming at the onset of symbiosis. *BMC biology*, *19*(1), 1-22.

Shan, L., He, P., Li, J., Heese, A., Peck, S. C., Nürnberger, T., ... & Sheen, J. (2008). Bacterial effectors target the common signaling partner BAK1 to disrupt multiple MAMP receptor-signaling complexes and impede plant immunity. *Cell host & microbe*, *4*(1), 17-27.

Sharp, P. M., & Li, W. H. (1986). An evolutionary perspective on synonymous codon usage in unicellular organisms. *Journal of molecular evolution*, *24*(1-2), 28-38.

Sharp, P. M., & Li, W. H. (1987). The codon adaptation index-a measure of directional synonymous codon usage bias, and its potential applications. *Nucleic acids research*, *15*(3), 1281-1295.

Sherry, S., Xiao, C., Durbrow, K., Kimelman, M., Rodarmer, K., Shumway, M., & Yaschenko, E. (2012, January). Ncbi sra toolkit technology for next generation sequence data. In *Plant and Animal Genome XX Conference (January 14-18, 2012). Plant and Animal Genome*.

Singh, R. K., Gase, K., Baldwin, I. T., & Pandey, S. P. (2015). Molecular evolution and diversification of the Argonaute family of proteins in plants. *BMC plant biology*, *15*(1), 1-16.

Singh, J., Mishra, V., Wang, F., Huang, H. Y., & Pikaard, C. S. (2019). Reaction mechanisms of Pol IV, RDR2, and DCL3 drive RNA channeling in the siRNA-directed DNA methylation pathway. *Molecular cell*, *75*(3), 576-589.

Shahid, S., Kim, G., Johnson, N. R., Wafula, E., Wang, F., Coruh, C., ... & Axtell, M. J. (2018). MicroRNAs from the parasitic plant Cuscuta campestris target host messenger RNAs. *Nature*, *553*(7686), 82-85.

Shao, Y., Chan, C. Y., Maliyekkel, A., Lawrence, C. E., Roninson, I. B., & Ding, Y. (2007). Effect of target secondary structure on RNAi efficiency. *Rna*, *13*(10), 1631-1640.

Sharp, P. M., & Matassi, G. (1994). Codon usage and genome evolution. *Current opinion in genetics & development*, *4*(6), 851-860.

Son, H., Park, A. R., Lim, J. Y., Shin, C., & Lee, Y. W. (2017). Genome-wide exonic small interference RNA-mediated gene silencing regulates sexual reproduction in the homothallic fungus Fusarium graminearum. *PLoS genetics*, *13*(2), e1006595.

Song, J. J., Smith, S. K., Hannon, G. J., & Joshua-Tor, L. (2004). Crystal structure of Argonaute and its implications for RISC slicer activity. *science*, *305*(5689), 1434-1437.

Soto-Suárez, M., Baldrich, P., Weigel, D., Rubio-Somoza, I., & San Segundo, B. (2017). The Arabidopsis miR396 mediates pathogen-associated molecular pattern-triggered immune responses against fungal pathogens. *Scientific reports*, *7*(1), 1-14.

Spolti, P., Del Ponte, E. M., Dong, Y., Cummings, J. A., & Bergstrom, G. C. (2014). Triazole sensitivity in a contemporary population of Fusarium graminearum from New York wheat and competitiveness of a tebuconazole-resistant isolate. *Plant disease*, *98*(5), 607-613.

Srivastava, P. K., Moturu, T. R., Pandey, P., Baldwin, I. T., & Pandey, S. P. (2014). A comparison of performance of plant miRNA target prediction tools and the characterization of features for genome-wide target prediction. *BMC genomics*, *15*(1), 1-15.

Streit, R. S. A., Ferrareze, P. A. G., Vainstein, M. H., & Staats, C. C. (2021). Analysis of tRNA-derived RNA fragments (tRFs) in Cryptococcus spp.: RNAi-independent generation and possible compensatory effects in a RNAi-deficient genotype. *Fungal Biology*.

Stenico, M., Lloyd, A. T., & Sharp, P. M. (1994). Codon usage in Caenorhabditis elegans: delineation of translational selection and mutational biases. *Nucleic acids research*, *22*(13), 2437-2446.

Sunkar, R., & Zhu, J. K. (2004). Novel and stress-regulated microRNAs and other small RNAs from Arabidopsis. *The Plant Cell*, *16*(8), 2001-2019.

Talas, F., & McDonald, B. A. (2015). Significant variation in sensitivity to a DMI fungicide in field populations of Fusarium graminearum. *Plant Pathology*, *64*(3), 664-670.

Team, R. C. (2021). R: A language and environment for statistical computing.

Thole, V., Peraldi, A., Worland, B., Nicholson, P., Doonan, J. H., & Vain, P. (2012). T-DNA mutagenesis in Brachypodium distachyon. *Journal of experimental botany*, *63*(2), 567-576.

Tian, T., Liu, Y., Yan, H., You, Q., Yi, X., Du, Z., ... & Su, Z. (2017). agriGO v2. 0: a GO analysis toolkit for the agricultural community, 2017 update. *Nucleic acids research*, *45*(W1), W122-W129.

Tijsterman, M., May, R. C., Simmer, F., Okihara, K. L., & Plasterk, R. H. (2004). Genes required for systemic RNA interference in Caenorhabditis elegans. *Current Biology*, *14*(2), 111-116.

Ulvila, J., Parikka, M., Kleino, A., Sormunen, R., Ezekowitz, R. A., Kocks, C., & Rämet, M. (2006). Double-stranded RNA is internalized by scavenger receptor-mediated endocytosis in Drosophila S2 cells. *Journal of Biological Chemistry*, *281*(20), 14370-14375.

Untergasser, A., Cutcutache, I., Koressaar, T., Ye, J., Faircloth, B. C., Remm, M., & Rozen, S. G. (2012). Primer3—new capabilities and interfaces. *Nucleic acids research, 40*(15), e115-e115.

Vaucheret, H., Vazquez, F., Crété, P., & Bartel, D. P. (2004). The action of ARGONAUTE1 in the miRNA pathway and its regulation by the miRNA pathway are crucial for plant development. *Genes & development*, *18*(10), 1187-1197.

Vazquez, F., Gasciolli, V., Crété, P., & Vaucheret, H. (2004). The nuclear dsRNA binding protein HYL1 is required for microRNA accumulation and plant development, but not posttranscriptional transgene silencing. *Current Biology*, *14*(4), 346-351.

Wagaba, H., Patil, B. L., Mukasa, S., Alicai, T., Fauquet, C. M., & Taylor, N. J. (2016). Artificial microRNA-derived resistance to Cassava brown streak disease. *Journal of virological methods*, *231*, 38-43.

Wang, W., Mauleon, R., Hu, Z., Chebotarov, D., Tai, S., Wu, Z., ... & Leung, H. (2018). Genomic variation in 3,010 diverse accessions of Asian cultivated rice. *Nature*, *557*(7703), 43-49.

Wang, J., Mei, J., & Ren, G. (2019). Plant microRNAs: biogenesis, homeostasis, and degradation. *Frontiers in plant science*, *10*, 360.

Wang, Q., Li, T., Xu, K., Zhang, W., Wang, X., Quan, J., ... & Shan, W. (2016b). The tRNA-derived small RNAs regulate gene expression through triggering sequence-specific degradation of target transcripts in the oomycete pathogen Phytophthora sojae. *Frontiers in plant science*, *7*, 1938.

Wang, B., Sun, Y., Song, N., Zhao, M., Liu, R., Feng, H., ... & Kang, Z. (2017a). Puccinia striiformis f. sp. tritici mi croRNA-like RNA 1 (Pst-milR1), an important pathogenicity factor of Pst, impairs wheat resistance to Pst by suppressing the wheat pathogenesis-related 2 gene. *New Phytologist*, *215*(1), 338-350.

Wang, M., Weiberg, A., Dellota Jr, E., Yamane, D., & Jin, H. (2017b). Botrytis small RNA Bc-siR37 suppresses plant defense genes by cross-kingdom RNAi. *RNA biology*, *14*(4), 421-428.

Wang, M., Weiberg, A., Lin, F.-M., Thomma, B. P. H. J., Huang, H.D., & Jin, H. (2016a). Bidirectional cross-kingdom RNAi and fungal uptake of external RNAs confer plant protection. *Nature Plants, 2*, 16151.

Weiberg, A., Bellinger, M., & Jin, H. (2015). Conversations between kingdoms: small RNAs. *Current opinion in biotechnology*, *32*, 207-215.

Weiberg, A., Wang, M., Lin, F. M., Zhao, H., Zhang, Z., Kaloshian, I., ... & Jin, H. (2013). Fungal small RNAs suppress plant immunity by hijacking host RNA interference pathways. *Science*, *342*(6154), 118-123.

Werner, B. T., Gaffar, F. Y., Schuemann, J., Biedenkopf, D., & Koch, A. M. (2020). RNA-spray-mediated silencing of Fusarium graminearum AGO and DCL genes improve barley disease resistance. *Frontiers in Plant Science*, *11*, 476.

Werner, B. T., Koch, A., Šečić, E., Engelhardt, J., Jelonek, L., Steinbrenner, J., & Kogel, K. H. (2021) *Fusarium graminearum* DICER-like-dependent sRNAs are required for the suppression of host immune genes and full virulence. *PLoS ONE*, 16(8), e0252365.

Whangbo, J. S., & Hunter, C. P. (2008). Environmental RNA interference. *Trends in genetics*, *24*(6), 297-305.

Wickham, H. (2016). GGPLOT2: Elegant Graphics for Data Analysis 2016 Springer-Verlag, New York.

Winston, W. M., Sutherlin, M., Wright, A. J., Feinberg, E. H., & Hunter, C. P. (2007). Caenorhabditis elegans SID-2 is required for environmental RNA interference. *Proceedings of the National Academy of Sciences*, *104*(25), 10565-10570.

World Health Organization. (2009). Global and regional food consumption patterns and trends. *WHO Technical Report Series*, *916*, 1-17.

Wu, Z., Huang, S., Zhang, X., Wu, D., Xia, S., & Li, X. (2017). Regulation of plant immune receptor accumulation through translational repression by a glycine-tyrosine-phenylalanine (GYF) domain protein. *Elife*, *6*, e23684.

Wright, F. (1990). The 'effective number of codons' used in a gene. *Gene*, *87*(1), 23-29.

Wytinck, N., Sullivan, D. S., Biggar, K. T., Crisostomo, L., Pelka, P., Belmonte, M. F., & Whyard, S. (2020). Clathrin mediated endocytosis is involved in the uptake of exogenous double-stranded RNA in the white mold phytopathogen Sclerotinia sclerotiorum. *Scientific reports*, *10*(1), 1-12.

Xoconostle-Cázares, B., Xiang, Y., Ruiz-Medrano, R., Wang, H. L., Monzer, J., Yoo, B. C., ... & Lucas, W. J. (1999). Plant paralog to viral movement protein that potentiates transport of mRNA into the phloem. *Science*, *283*(5398), 94-98.

Xue, T., Liu, Z., Dai, X., & Xiang, F. (2017). Primary root growth in Arabidopsis thaliana is inhibited by the miR159 mediated repression of MYB33, MYB65 and MYB101. *Plant Science*, *262*, 182-189.

Yadav, C. B., Muthamilarasan, M., Pandey, G., & Prasad, M. (2015). Identification, characterization and expression profiling of Dicer-like, Argonaute and RNA-dependent RNA polymerase gene families in foxtail millet. *Plant molecular biology reporter*, *33*(1), 43-55.

Yan J, Gu Y, Jia X, Kang W, Pan S, Tang X, Chen X, Tang G, (2012) Effective Small RNA Destruction by the Expression of a Short Tandem Target Mimic in *Arabidopsis. The Plant Cell*, Volume 24, Issue 2, Pages 415–427, https://doi.org/10.1105/tpc.111.094144

Yang, C., Hamel, C., Vujanovic, V., & Gan, Y. (2011). Fungicide: modes of action and possible impact on nontarget microorganisms. *International Scholarly Research Notices*, *2011*.

Yang, Y., Jittayasothorn, Y., Chronis, D., Wang, X., Cousins, P., & Zhong, G. Y. (2013). Molecular characteristics and efficacy of 16D10 siRNAs in inhibiting root-knot nematode infection in transgenic grape hairy roots. *PloS one*, *8*(7), e69463.

Yin, C., & Hulbert, S. (2015). Host induced gene silencing (HIGS), a promising strategy for developing disease resistant crops. *Gene Technol*, *4*(130), 10-4172.

Yin, Y., Liu, X., Li, B., & Ma, Z. (2009). Characterization of sterol demethylation inhibitor-resistant isolates of Fusarium asiaticum and F. graminearum collected from wheat in China. *Phytopathology*, *99*(5), 487-497.

Yogindran, S., & Rajam, M. V. (2021). Host-derived artificial miRNA-mediated silencing of ecdysone receptor gene provides enhanced resistance to Helicoverpa armigera in tomato. *Genomics*, *113*(1), 736-747.

Yoshida, H., Wang, K.L., Chang, C.M., Mori, K., Uchida, E., Ecker, J.R. (2006). The ACC synthase TOE sequence is required for interaction with ETO1 family proteins and destabilization of target proteins. Plant Mol Biol. 62(3):427-37.

Yu, J., Lee, K. M., Cho, W. K., Park, J. Y., & Kim, K. H. (2018). Differential contribution of RNA interference components in response to distinct Fusarium graminearum virus infections. *Journal of virology*, *92*(9).

Yuan, Y. R., Pei, Y., Chen, H. Y., Tuschl, T., & Patel, D. J. (2006). A potential protein-RNA recognition event along the RISC-loading pathway from the structure of A. aeolicus Argonaute with externally bound siRNA. *Structure*, *14*(10), 1557-1565.

Zanini, S., Šečić, E., Busche, T., Galli, M., Zheng, Y., Kalinowski, J., & Kogel, K. H. (2021). Comparative Analysis of Transcriptome and sRNAs Expression Patterns in the Brachypodium distachyon—Magnaporthe oryzae Pathosystems. *International Journal of Molecular Sciences*, *22*(2), 650.

Zeng, W., Wang, J., Wang, Y., Lin, J., Fu, Y., Xie, J., ... & Cheng, J. (2018). Dicer-like proteins regulate sexual development via the biogenesis of perithecium-specific microRNAs in a plant pathogenic fungus Fusarium graminearum. *Frontiers in microbiology*, *9*, 818.

Zhang, L., Hou, D., Chen, X., Li, D., Zhu, L., Zhang, Y., ... & Zhang, C. Y. (2012). Exogenous plant MIR168a specifically targets mammalian LDLRAP1: evidence of cross-kingdom regulation by microRNA. *Cell research*, *22*(1), 107-126.

Zhang, J., Khan, S. A., Heckel, D. G., & Bock, R. (2017). Next-generation insect-resistant plants: RNAi-mediated crop protection. *Trends in biotechnology*, *35*(9), 871-882.

Zhang, X., Niu, D., Carbonell, A., Wang, A., Lee, A., Tun, V., ... & Jin, H. (2014). ARGONAUTE PIWI domain and microRNA duplex structure regulate small RNA sorting in Arabidopsis. *Nature communications*, *5*(1), 1-11.

Zhang, H., Xia, R., Meyers, B. C., & Walbot, V. (2015). Evolution, functions, and mysteries of plant ARGONAUTE proteins. *Current opinion in plant biology*, *27*, 84-90.

Zhang, T., Zhao, Y. L., Zhao, J. H., Wang, S., Jin, Y., Chen, Z. Q., ... & Guo, H. S. (2016). Cotton plants export microRNAs to inhibit virulence gene expression in a fungal pathogen. *Nature plants*, *2*(10), 1-6.

Zhao, H., Li, Q., Li, J., Zeng, C., Hu, S., & Yu, J. (2006). The study of neighboring nucleotide composition and transition/transversion bias. *Science in China Series C: Life Sciences*, *49*(4), 395-402.

Zhao, J. H., Zhang, T., Liu, Q. Y., & Guo, H. S. (2021). Trans-kingdom RNAs and their fates in recipient cells: advances, utilization and perspectives. *Plant Communications*, 100167.

Zheng, Z., Reichel, M., Deveson, I., Wong, G., Li, J., & Millar, A. A. (2017). Target RNA secondary structure is a major determinant of miR159 efficacy. *Plant Physiology*, *174*(3), 1764-1778.

Zhu, K., Liu, M., Fu, Z., Zhou, Z., Kong, Y., Liang, H., ... & Chen, X. (2017). Plant microRNAs in larval food regulate honeybee caste development. *PLoS genetics*, *13*(8), e1006946.

Zuo, Y., Zhu, L., Guo, Z., Liu, W., Zhang, J., Zeng, Z., ... & Peng, Y. (2021). tsRBase: a comprehensive database for expression and function of tsRNAs in multiple species. *Nucleic Acids Research, 49*(D1), D1038-D1045.

Acknowledgements

I would like to thank my supervisor Prof. Dr. Karl-Heinz Kogel for his ongoing support, teaching and compassion, for providing financial support and a wonderful work environment at his institute, his door always open, and for being a role model in his unlimited determination and dedication to the improvement of food security and sustainability.

I would like to thank Dr. Aline Koch for her direct support and academic input, her constant motivation and stimulation throughout the recent years and for providing the foundation of this research.

I would like to thank Dr. Jens Steinbrenner and Dr. Jafargholi Imani for their wise advice and support, Dagmar Biedenkopf, Christina Birkenstock**,** Elke Stein, Martina Claar for technical guidance and assistance in my experiments, as well as all technical assistance provided by our lab members, it was essential to the execution of all experiments.

I would also like to thank all my peers I had the pleasure to meet over the years for countless interesting discussions, foremost Ena Šečić for the regular and fruitful exchange of ideas on the topics of ckRNAi.

I would also like to thank my parents for their ongoing support throughout my whole life, for without neither this work nor I would exist, Theresa, Tobi, Lautaro and Carina for always being there for me, and Sonja for all the above and even more.

Thanks to family and friends, and for all the fish.